University of Alberta

Evaluation of Canadian Long-Term Pavement performance (C-LTPP) Project

by

Ali Sadri Khanloo ©

A thesis submitted to the Faculty of Graduate Studies and Research in partial fulfillment of the requirements for the degree of Master of Science

in

Construction Engineering and Project Management
Department of Civil and Environmental Engineering

Edmonton, Alberta
Fall 2003

National Library
of Canada

Acquisitions and
Bibliographic Services

395 Wellington Street
Ottawa ON K1A 0N4
Canada

Bibliothèque nationale
du Canada

Acquisisitons et
services bibliographiques

395, rue Wellington
Ottawa ON K1A 0N4
Canada

Your file Votre référence
ISBN: 0-612-87873-2
Our file Notre référence
ISBN: 0-612-87873-2

The author has granted a non-exclusive licence allowing the National Library of Canada to reproduce, loan, distribute or sell copies of this thesis in microform, paper or electronic formats.

The author retains ownership of the copyright in this thesis. Neither the thesis nor substantial extracts from it may be printed or otherwise reproduced without the author's permission.

L'auteur a accordé une licence non exclusive permettant à la Bibliothèque nationale du Canada de reproduire, prêter, distribuer ou vendre des copies de cette thèse sous la forme de microfiche/film, de reproduction sur papier ou sur format électronique.

L'auteur conserve la propriété du droit d'auteur qui protège cette thèse. Ni la thèse ni des extraits substantiels de celle-ci ne doivent être imprimés ou aturement reproduits sans son autorisation.

Canada

University of Alberta

Library Release Form

Name of Author: *Ali Sadri Khanloo*

Title of Thesis: *Evaluation of Canadian Long-Term Pavement Performance (C-LTPP) Project*

Degree: *Master of Science*

Year this Degree Granted: *2003*

Permission is hereby granted to the University of Alberta Library to reproduce single copies of this thesis and to lend or sell such copies for private, scholarly or scientific research purposes only.

The author reserves all other publication and other rights in association with the copyright in the thesis, and except as herein before provided, neither the thesis nor any substantial portion thereof may be printed or otherwise reproduced in any material form whatever without the author's prior written permission.

24.09.2003

University of Alberta

Faculty of Graduate Studies and Research

The undersigned certify that they have read, and recommend to the Faculty of Graduate Studies and Research for acceptance, a thesis entitled **Evaluation of Pavement Performance in the C-LTPP Project** submitted by **Ali Sadri Khanloo** in partial fulfillment of the requirements for the degree of **Master of Science**. in Construction Engineering and Project Management.

24.09.2003

Abstract

Highway agencies' limited budgets have resulted in the preservation of pavement infrastructures through the implementation of timely maintenance and rehabilitation. Overlaying with asphalt concrete is one of the most common methods for rehabilitating an old pavement. It is thus crucial for highway agencies to find the most efficient overlay design to extend the serviceability of pavements. The Canadian Long-Term Pavement Performance (C-LTPP) project was initiated under the supervision of the Canadian Strategic Highway Research Program (C-SHRP) in 1989, with the overall goal of evaluating and improving the overlaid pavements. The C-LTPP program monitors the performance of 65 in-service overlaid pavement sections in Canada.

This research is a network level analysis of available data from the C-LTPP program until year 2002. The main objectives of this study are to evaluate the performance of C-LTPP sections and to investigate the effect of different factors on overlay performance for Canadian traffic and climate conditions.

To my dear wife,

Nazanin,

who, with loving patience, accepted every challenge during my graduate studies.

I can see her love for me in the very pages of this report.

Without her support, I could never have completed the requirements for the M.Sc. program.

ACKNOWLEDGMENTS

I would like to express my gratitude to the individuals and organizations who helped me to complete this research project:

Dr. Hamid. R. Soleymani, my supervisor, for his guidance and help through out this thesis. During all its stages, his supervision and directions to me were vital. As well, he helped me with the kind of challenges that generally occur for a newly married couple like me and my wife, far from their home country; **The Natural Sciences and Engineering Research Council of Canada (NSERC) and The Department of Civil and Environmental Engineering at University of Alberta** for their financial support during this research project; **Mr. S.Goodman,** former program manager at the C-SHRP, and later, **Mr. Tom Christison** for providing access to the C-LTPP data; **Dr. S. Nazarian at Texas University in El Paso** for kindly providing the REPP2000 program for use in this study; **The EBA Consultants Engineering, Ltd. (Edmonton)** for their help with the backcalculation of FWD data; **The Statistical Consultants Student Center at University of Alberta** for helping me with the statistical analysis of the C-LTPP data; and finally, **Mr. P. Klovan**, freelance editor and writer, who helped me with the editorial requirements of this thesis report.

Table of Contents

CHAPTER 1: INTRODUCTION 1

1.1. Background 1

1.2. Problem definition 2

1.3. Objectives and scope of the study 3

1.4. Methodology and thesis organization 3

CHAPTER 2: THE C-LTPP PROJECT AND A LITERATURE REVIEW 7

2.1. Introduction 7

2.2. The C-LTPP database and the data collection program 13

2.3. Literature review about the C-LTPP Project 17

CHAPTER 3: EVALUATION OF PAVEMENT PERFORMANCE IN THE C-LTPP PROJECT 32

3.1. Introduction 32

3.2. Evaluation of the C-LTPP sections, based on the AASHTO design method 33

3.2.1. FWD data and backcalculation 34

3.2.1.1. AASHTO backcalculation method 36

3.2.1.2. EVERCALC backcalculation computer program 42

3.2.1.3. MICHBACK backcalculation computer program 48

3.2.1.4. Comparison between backcalculation results 51

3.2.2. Service lives of the C-LTPP sections, based on the AASHTO method 54

3.2.3. Comparison of results from this study with those from EBA study 58

3.3. Roughness and its importance in pavement evaluation 60

3.3.1. Roughness measurement 61

3.3.2. Roughness evaluation of the C-LTPP sections 63

3.3.3. Analysis of the roughness trends for the C-LTPP sections 64

3.3.4. Prediction of future roughness in the C-LTPP project 65

3.3.4.1. Roughness-prediction model 1 66

3.3.4.2. Roughness-prediction model 2 67
3.3.4.3. Roughness-prediction model 3 68
3.3.5. Service lives of the C-LTPP sections based on roughness 70
3.4. Rutting evaluation of the C-LTPP sections 76
3.4.1. Rut definition, its importance, and measurement 76
3.4.2. Rut progression in asphalt pavement 81
3.4.3. Analysis of rutting for the C-LTPP sections 82
3.4.4. Service lives of the C-LTPP sections, based on rut 83
3.5. Evaluation of the C-LTPP sections, based on a Mechanistic-Empirical (M-E) approach 89
3.5.1. Pavement analysis of the C-LTPP sections 91
3.5.2. Service lives of the C-LTPP sections, based on M-E models for rut... 94
3.5.3. Service lives of the C-LTPP sections, based on M-E models for fatigue cracking 98
3.6. Evaluation of the C-LTPP sections, based on the REPP2000 program 102
3.6.1. Service lives of the C-LTPP sections, based on the REPP2000 Program... 104
3.7. Comparison of the service lives of the C-LTPP sections, from different methods 107
CHAPTER 4: FACTORS AFFECTING THE PERFORMANCE OF THE C-LTPP TEST SECTIONS 112
4.1. Introduction 112
4.2. Factors affecting roughness in the C-LTPP sections 113
4.2.1. Effect of climate 118
4.2.2. Effect of traffic 123
4.2.3. Effect of overlay thickness 125
4.2.4. Effect of overlay material 128
4.2.5. Effect of subgrade material 130

4.2.6. Effect of milling 132
4.3. Summary of the factors affecting roughness in the C-LTPP project 134
4.4. Evaluation of design practices for roughness of the C-LTPP sections 137
4.5. Factors affecting pavement rutting 141
4.5.1. Effect of climate 144
4.5.2. Effect of traffic 147
4.5.3. Effect of overlay thickness 150
4.5.4. Effect of overlay material 152
4.5.5. Effect of subgrade material 154
4.5.6. Effect of milling 156
4.6. Summary for factors affecting pavement rutting in the C-LTPP project. 158
4.7. Evaluation of design practices for rutting of the C-LTPP sections 159
4.8. Artificial Neural Network (ANN) approach 163
4.8.1. Using the ANN 166
4.8.2. The ANN for roughness in the C-LTPP sections 168
4.8.3. The ANN for rutting in the C-LTPP sections 170
4.9. Summary of the ANN application to the C-LTPP project 172
CHAPTER 5: CONCLUSION 174
5.1. Recommendations for future studies 180
REFERENCES 182

List of Tables

Table 2-1: The experimental design of the C-LTPP project 10

Table 2-2: The outline of the specific experiments under study in the C-LTPP program 11

Table 2-3: Location and the experiment code of the C-LTPP test sections 12

Table 2-4: The eleven main modules in the C-LTPP database 14

Table 2-5: The frequency of data collection in the C-LTPP project and the organizations responsible for it 15

Table 3-1: Results of AASHTO backcalculation procedure for moduli of pavement layers and SN for the C-LTPP sections 40

Table 3-2: The general ranges and the typical values for Poisson ratio 45

Table 3-3: Results of EVERCALC program for moduli of pavement layers in the C-LTPP sections 47

Table 3-4: Results of MICHBACK program for moduli of pavement layers in the C-LTPP sections 50

Table 3-5: Service lives of the C-LTPP sections, based on the AASHTO overlay design method 56

Table 3-6: Expected service lives for the agency-designed sections based on AASHTO serviceability from present study and the EBA report 58

Table 3-7: Calculated coefficients “a” and “b” in roughness models 69

Table 3-8: The prototype smoothness categories based on the MIRI 71

Table 3-9: Estimated service lives of the C-LTPP test sections by using the developed models for roughness 72

Table 3-10: Coefficients of Equation 3-14 and the estimated service lives for two levels of rutting in all the C-LTPP test sections 84

Table 3-11: The coefficients used by various agencies for Equation 3-15 90

Table 3-12: The coefficients used by various agencies for Equation 3-16 91

Table 3-13: Results of EVERSTRESS and ELSYM5 for tensile strain at the bottom of the asphalt layer and the compressive strain at the top of the subgrade 92

Table 3-14: The allowable traffics and service lives of the C-LTPP test sections, based on Asphalt Institute and Shell models for rutting 96

Table 3-15: The allowable traffic and service lives of the C-LTPP test sections based on the Asphalt Institute and Shell models for fatigue cracking 98

Table 3-16: Experimental design of the C-LTPP Project and test sections with service lives less than 10 years because of high fatigue cracking 101

Table 3-17: Estimated service lives of the C-LTPP sections, based on rut and fatigue crack using the REPP2000 program 105

Table 4-1: The IRI rates of the C-LTPP sections 115

Table 4-2: IRI rate values within the experimental design matrix of the C-LTPP project 118

Table 4-3: ANOVA test results for IRI rates related to different climate conditions in the C-LTPP project 120

Table 4-4: Kruskal-Wallis test results for IRI rates related to different climate conditions in the C-LTPP project 122

Table 4-5: ANOVA test results for IRI rates related to different traffic levels in the C-LTPP project 124

Table 4-6: Mann-Whitney test results for IRI rates related to different traffic levels in the C-LTPP project 124

Table 4-7: ANOVA test results for IRI rates related to different overlay thicknesses in the C-LTPP project 126

Table 4-8: Kruskal-Wallis test results for IRI rates related to different overlay thicknesses in the C-LTPP project 127

Table 4-9: ANOVA test results for IRI rates related to different overlay material types in the C-LTPP project 129

Table 4-10: Mann-Whitney test results for IRI rates related to different overlay material types in the C-LTPP project 129

Table 4-11: ANOVA test results for IRI rates related to different subgrade material types in the C-LTPP project 131

Table 4-12: Mann-Whitney test results for IRI rates related to different subgrade material types in the C-LTPP project 131

Table 4-13: ANOVA test results for IRI rates related to different preparation of old pavement in the C-LTPP project 133

Table 4-14: Mann-Whitney test results for IRI rates related to different levels of preparation of old pavement in the C-LTPP project 134

Table 4-15: Comparison between findings from present study and other studies of roughness 136

Table 4-16: The IRI rates for different design practices in the C-LTPP project. 138

Table 4-17: ANOVA test results for IRI rates related to different design practices in the C-LTPP project 140

Table 4-18: The rutting rates in the C-LTPP test sections 141

Table 4-19: The rut rates for the test sections in the experimental design of the C-LTPP project 145

Table 4-20: ANOVA test results for rutting rates related to different climate conditions in the C-LTPP project 146

Table 4-21: Kruskal-Wallis test results for rutting rates related to different climate conditions in the C-LTPP project 147

Table 4-22: ANOVA test results for rutting rates related to different traffic levels in the C-LTPP project 148

Table 4-23: Mann-Whitney test results for rutting rates related to different traffic levels in the C-LTPP project 149

Table 4-24: ANOVA test results for rutting rates related to different overlay thickness levels in the C-LTPP project 151

Table 4-25: Kruskal-wallis test results for rutting rates related to different overlay thickness levels in the C-LTPP project 151

Table 4-26: ANOVA test results for rutting rates related to different overlay material types in the C-LTPP project 153

Table 4-27: Mann-Whitney test results for rutting rates related to different overlay material types in the C-LTPP project 153

Table 4-28: ANOVA test results for rutting rates related to different subgrade material types in the C-LTPP project 155

Table 4-29: Mann-Whitney test results for rutting rates related to different subgrade material types in the C-LTPP project 155

Table 4-30: ANOVA test results for rutting rates related to different levels of pavement preparation in the C-LTPP project 157

Table 4-31: Mann-Whitney test results for rutting rates related to different levels of pavement preparation in the C-LTPP project 157

Table 4-32: Results from present research project and other researches for pavement rutting 159

Table 4-33: The rut rates for different design practices in the C-LTPP project.. 160

Table 4-34: ANOVA test results for rutting rates related to different design practices in the C-LTPP project 162

Table 4-35: Architectures of and the results from roughness ANN models 169

Table 4-36: Architectures of and the results from rutting ANN models............. 171

List of Figures

Figure 3-1: Equipment for FWD test, and the deflection bowl 35

Figure 3-2: Correction factor for FWD deflection at load centerline 39

Figure 3-3: The general module of the EVERCALC program 44

Figure 3-4: The deflection module of the EVERCALC program 46

Figure 3-5: Comparison of SN values from the AASHTO backcalculation method and the EVERCALC program 52

Figure 3-6: Comparison of the backcalculated moduli from two programs, EVERCALC and MICHBACK. 53

Figure 3-7: Comparison between the results from this study and the EBA report 59

Figure 3-8: Service lives of the agency-designed test sections in the C-LTPP project, based on the IRI trend analysis 74

Figure 3-9: 1.8 m and 3.7 m straight edge indices for rut measurement 80

Figure 3-10: Different stages of rut 82

Figure 3-11: Service lives of agency-designed test sections in the C-LTPP project, based on rut trend analysis 87

Figure 3-12: Comparison of results from EVERSTRESS and ELSYM5 94

Figure 3-13: Service lives of the C-LTPP test sections for agency- designed test sections, based on the AI model for fatigue cracking 100

Figure 4-1: Box plot of IRI rates for all the C-LTPP sections 117

Figure 4-2: Box plot of IRI rates for different weather climates in the C-LTPP project 119

Figure 4-3: Box plot of IRI rates for different traffic levels in the C-LTPP project 123

Figure 4-4: Box plot of IRI rates for different overlay thicknesses in the C-LTPP project 126

Figure 4-5: Box plot of IRI rates for different overlay materials in the C-LTPP project 128

Figure 4-6: Box plot of IRI rates for different subgrade materials in the C-LTPP project 130

Figure 4-7: Box plot of IRI rates for different preparation of old pavement in the C-LTPP project 133

Figure 4-8:Box plot of rutting rates for all the C-LTPP sections 143

Figure 4-9: Box plot of rutting rates for different weather climates in the C-LTPP project 146

Figure 4-10: Box plot of rutting rates for different traffic levels in the C-LTPP project 148

Figure 4-11: Box plot of Rut rates for different overlay thicknesses in the C-LTPP project 150

Figure 4-12: Box plot of rutting rates for different overlay materials in the C-LTPP project 152

Figure 4-13: Box plot of rutting rates for different subgrade materials in the C-LTPP project 154

Figure 4-14: Box plot of rutting rates for different preparation of old pavement in the C-LTPP project 156

Figure 4-15: The architecture of a three-layer Neural Network 164

Figure 4-16: Contribution levels from neural network for roughness model 170

Figure 4-17: Contribution levels from neural network for rutting model 172

List of Appendices

Appendix A: The Backcalculation, based on the AASHTO procedure 191

Appendix B: Average of FWD deflections for the C-LTPP test sections after overlay 194

Appendix C: The EVERCALC backcalculation program outputs (Sample) 196

Appendix D: The MICHBACK backcalculation program outputs (Sample) 203

Appendix E: The traffic data for the C-LTPP project at the year of overlay 205

Appendix F: Roughness trends in the C-LTPP project 206

Appendix G: Rutting trends in the C-LTPP project 223

Appendix H: The outputs from EVERSTRESS and ELSYM5 pavement analysis programs (Sample) 240

Appendix I: The REPP2000 program 250

Appendix J: The NEUROSHELL2 program 254

List of Symbols, Abbreviations

AB = Alberta
AC = Asphalt Cement
ANN = Artificial Neural Network
AASHTO = American Association of State Highway and Transportation Officials
AI = Asphalt Institute
ASTM = American Society of Testing Materials
BC = British Columbia
C-LTPP = Canadian Long-Term Pavement Performance
C-SHRP = Canadian Strategic Highway Research Program
D = Pavement total thickness
ESAL = Equivalent Single Axle Load
E_P = Effective elastic modulus of pavement
E_{ac}= Modulus of asphalt layer
E_b= Modulus of base layer
ε_c = Compressive strain at the top of subgrade
ε_t = Tensile strain at the bottom of asphalt layer
FHWA = Federal Highway Administration
FWD test = Falling Weight Deflectometer test
HMAC = Hot Mixed Asphalt Cement
IRI = International Roughness Index
M-E = Mechanistic-Empirical
MB = Manitoba
M_r = Subgrade resilient modulus
NB = New Brunswick
NCHRP = National Co-operative Highway Research Program
NDT = Nondestructive Deflection Tests
N_f= Allowable number of load repetition for a limited level of fatigue cracking

N_d = Allowable number of load repetition for a limited rut

NF = New Foundland

NHS = National Highway System

NS = Nova Scotia

ON = Ontario

PE = Prince Edward Island

PMS = Pavement Management System

PSI = Present Serviceability Index

QC = Quebec

R_0 = Initial roughness

RAP = Reclaimed Asphalt Pavement

RCI = Riding Comfort Index

RMSE = Root Mean Square Error

SN = Structure Number

SK = Saskatchewan

TAC = Transportation Association of Canada

TDOT = Texas Department of Transportation

W_{18} = Number of 18000 Ib (80 kN) single axle load application, Equivalent Single Axle Load (ESAL)

WSDOT = Washington State Department of Transportation

CHAPTER 1: INTRODUCTION

1.1. Background

In North America during the 1950s and 1960s, a rapid expansion of roadway networks occurred because of a high demand, and now, most of these pavements have reached to end of their serviceability and need extensive upgrading to an acceptable service level. For example, according to Federal Highway Administration (FHWA) reports, highway pavements in the National Highway System in the USA require $50 billion dollars of spending annually to maintain the system at its present levels, while the United States currently spends only $25 billion dollars per year (Gary et al., 1999). In Canada, about 80% of highways need some form of rehabilitation or maintenance (NRC, 2002). In Alberta, approximately $160 million dollars are spent annually for maintenance of the roads (AT&U, 2003).

Limitations of highway agencies' budgets and lack of adequate funding have resulted in the preservation of the pavement infrastructures through the implementation of timely maintenance and appropriate rehabilitation methods. These rehabilitation methods vary, depending on the pavement type, traffic, environmental condition, available budget, and numerous other constraints. They are generally classified in two main groups: routine maintenance and major rehabilitation. Routine maintenance methods include activities such as crack sealing, pothole repair, drainage improvement, and shallow patching. When the condition of the pavement is so poor that these maintenance techniques are no longer able to cost-effectively maintain the pavement at an acceptable level, major maintenance and resurfacing, which are considered as rehabilitation, are required.

1.2. Problem definition

Resurfacing or overlaying with asphalt concrete is one of the most common methods of restoring an old pavement. This method usually involves the repair of specific problems such as sealing the cracks or milling the rutted pavement and then paving with a new asphalt layer. Although overlaying is more expensive than other pavement repair methods, it prevents a greater loss of money in the future (TAC Report, 1997). Thus highway agencies must find the most cost-effective overlay designs and construction methods to extend the serviceability of pavements. An effective way to understand the performance of overlaid pavements is to monitor pavements before and after overlay. By analyzing collected data, it is possible to incorporate findings in future projects and, in the long-term, make overlay projects more efficient.

In Canada, one of the important projects with the overall goal of evaluating and improving overlaid pavements under traffic loads and different climate conditions is the Canadian Long-Term Pavement Performance (C-LTPP) project, which was initiated under the supervision of the Canadian Strategic Highway Research Program (C-SHRP) in 1989. This program monitors the performance of 65 in-service overlaid pavement test sites, which are distributed across all provinces of

Canada. In the C-LTPP project, pavement test sections constructed with asphalt concrete overlay on an existing pavement with a granular base course, are monitored.

At the time of this research study, the C-LTPP database comprised information for 12 years of the C-LTPP program. Analyzing the C-LTPP data can help to identify important factors in the performance of overlaid asphalt pavement in Canadian traffic and climate conditions. Findings from such a project could have a significant impact on future considerations for pavement rehabilitation in Canada.

1.3. Objectives and scope of the study

This research is a network level analysis of available data from the C-LTPP program, from 1989 to 2002. The main objectives of this study were (1) to evaluate the performance of the C-LTPP test sections, and (2) to study the effects of different factors on C-LTPP pavement performance. The main performance criteria considered for the C-LTPP sections were roughness and rutting, which are the main reasons for the low serviceability and the need to repair asphalt pavement.

1.4. Methodology and thesis organization

To meet the objectives of this study, various techniques, methodologies, and types of software were employed. For different parts of the research project, the relevant literature was studied. A brief explanation of each chapter of this research study is presented below:

In Chapter 2, the Canadian Long-Term Pavement Performance (C-LTPP) program and its database are introduced, and available literature related to the C-LTPP program is reviewed.

In Chapter 3, several strategies are described for estimating the service lives of the C-LTPP test sections. These strategies are the use of AASHTO method, the use of threshold values for pavement roughness and rut, the Mechanistic-Empirical (M-E) approach, and the use of REPP2000 – a software developed by the Department Of Transportation at Texas University.

By using the AASHTO method, the C-LTPP pavement sections were evaluated based on the AASHTO overlay design guideline. This evaluation provided a uniform basis for comparing the adequacy of the as-built overlaid test sections. This method was used to estimate the service life of the C-LTPP test sections, which were designed and constructed with different Canadian highway agencies' specifications.

By using the threshold level method, the historical data for pavement roughness and rutting that have been collected during the last 12 years of performance in the C-LTPP project were used to correlate pavement distresses with time. Then the service lives of test sections for each distress were estimated by considering threshold values for them. Using trigger values for all the test sections provided a uniform basis for evaluating the functionality of the C-LTPP test sections.

By using the Mechanistic-Empirical approach, the Asphalt Institute (AI) and Shell models were used in order to estimate the service lives of the C-LTPP test sections for a maximum value for pavement rutting and fatigue cracking.

Finally, REPP2000 (Rational Estimation of Pavement Performance), a software developed in a Joint project by the Texas Department Of Transportation (TDOT) and Texas University, was used to estimate service lives of the C-LTPP sections. REPP2000 program uses the Artificial Neural Network (ANN) to estimate the service life of pavement based on the Mechanistic-Empirical approach.

Using the above methodologies to estimate service lives of the C-LTPP sections made it possible to compare the results and obtain more realistic conclusions.

In Chapter 4, three different methods are employed to investigate the effect of different factors on pavement roughness and rutting. These methodologies are the use of parametric and non-parametric statistics, and the ANN. The studied factors, considered from the C-LTPP experimental design, include climate, traffic, subgrade material type, overlay thickness, overlay type, and milling.

By using the statistical method, the average annual increase in roughness and rut for all test sections are determined. Using the ANOVA test, the impact of each factor on pavement performance is investigated. To justify the results from ANOVA test, another approach, the non-parametric technique, was employed.

The SPSS program is used to perform the Mann-Whitney U and Kruskal-Wallis statistical tests. The two statistical methods are compared to confirm the results. For ANN approach, data from the C-LTPP project for roughness and rut are analyzed using the NEUROSHELL2 program. The contribution of considered factors will be studied to recognize the importance of factors in pavement performance.

More information about and discussions of the employed methods are provided in the different sections of this study. Conclusions from this research study and suggestions for future research related to the C-LTPP project are presented in Chapter 5.

CHAPTER 2: THE C-LTPP PROJECT AND A LITERATURE REVIEW

2.1. Introduction

This chapter provides information about the Canadian Long-Term Pavement Performance (C-LTPP) program and its database as a background for the present research study. As well, the available literature related to the C-LTPP project is reviewed and summarized.

The Canadian Long-Term Pavement Performance (C-LTPP) program was started in 1989 under the supervision of the Canadian Strategic Highway Research Program (C-SHRP). The C-LTPP program was designed to complement the US-LTPP experiment, one of the research areas for the SHRP study in the USA. In the C-LTPP program, some particular factors that were of interest for the Canadian highway agencies were considered in the experiment.

The overall goal of the C-LTPP program was "increasing the pavement life through the development of a cost effective pavement rehabilitation procedure, based upon a systematic observation of in service pavement performance" (TAC Report, 1996).

The C-LTPP program monitors the pavement performance of 65 in-service test sections that are geographically distributed across all provinces in Canada. The C-LTPP project compasses pavement sections constructed with asphalt overlay on an existing pavement with a granular base course. During the C-LTPP experiment, it was intended to compare various scenarios for overlay designs and rehabilitation methods in particular traffic, climate, and soil conditions. The pavement sections for the C-LTPP project were chosen, designed, constructed, and are monitored by the local Canadian highway agencies.

The main focus of the C-LTPP program is to evaluate and to improve the performance of asphalt pavement overlay as the most common practiced rehabilitation method. Other objectives that could be achieved by this project are explained in the C-LTPP Database Users' Guide (1996):

1- To evaluate the Canadian provincial design practices for pavement rehabilitation and to develop more sophisticated techniques for the maintenance of the flexible pavements.

2- To calibrate and to apply the pavement performance prediction models, which were developed through the US-LTPP experiment, to the Canadian situation.

3- To develop a national and uniform basis for pavement performance evaluation across Canada.

4- To provide a nation-wide comprehensive database that could be utilized to achieve the objectives of the C-LTPP experiment, or used for other future studies.

Numerous products could be expected from the C-LTPP program that could meet the above objectives:

1- Evaluation and improvement of current pavement rehabilitation procedures.

2- Quantification of the influence of environment, traffic, materials, and original pavement condition on the performance of asphalt concrete overlays.

3- Development of standardized pavement evaluation methods.

4- Independent validation of US-SHRP pavement performance prediction models.

Table 2-1 shows the experimental design of the C-LTPP project, which consists of 24 pavement test sites in different weather and traffic conditions on the major provincial highway systems across Canada. Unlike the US-LTPP project, which covered different types of pavement maintenance and rehabilitation, in the C-LTPP program a single type of pavement rehabilitation method (asphalt overlay on original asphalt pavement) was practiced.

Each test site has two to four adjacent sections, which represent various pavement structures and overlay design criteria. The objective of using different test sections is to evaluate different overlay treatments in specific traffic and weather conditions.

			Moisture, Freezing Index and Subgrade Condition					
			Wet					Dry
			No to Low Freeze			High Freeze		High Freeze
Traffic	Overlay Material	Overlay Thickness(mm)	Fine	Coarse		Fine	Coarse	Fine
Low	Recycled AC(RAP)	30-60						8104044(AB)
		60-100						8104043(AB)
		100-185	8205021(BC)					
			8205022(BC)					
			8705054(ON)					
	HMAC	30-60	8206051(BC)		8202051(BC)	8707011(ON)		
			8701022(ON)		8606033(NS)			
					8802031(PE)			
					8802033(PE)			
		60-100	8206052(BC)	8202052(BC)	8506012(NF)			8104041(AB)
			8701021(ON)	8402042(NB)	8606031(NS)			8304031(MB)
			8705051(ON)	8502012(NF)	8606032(NS)			9004021(SK)
			8705052(ON)	8502062(NF)	8802034(PE)			
		100-185	8705053(ON)		8402041(NB)	8707012(ON)		8104042(AB)
					8502011(NF)			8304032(MB)
					8502061(NF)			8304033(MB)
					8506011(NF)			9004022(SK)
					8802032(PE)			
High	Recycled AC(RAP)	30-60						
		60-100			8401013(NB)			
		100-185			8401012(NB)			8308011(MB)
					8406041(NB)			8308012(MB)
	HMAC	30-60	8605011(NS)		8406043(NB)	8907021(QC)	8905031(QC)	9008021(SK)
			8605013(NS)		8406044(NB)		8905032(QC)	
					8705041(ON)			
		60-100	8605012(NS)		8406042(NB)	8907022(QC)	8905034(QC)	9008022(SK)
					8705042(ON)			
		100-185			8401011(NB)		8905033(QC)	8308013(MB)
								8308014(MB)
								9008023(SK)
								9008031(SK)
								9008032(SK)

Table 2-1: The experimental design of the C-LTPP project

(The C-LTPP Database Users' Guide, 1996)

The alternative rehabilitation scenarios that were incorporated in the C-LTPP program are:

1- Three levels for overlay thickness: 30-60 mm, 60-100 mm, 100-185 mm (one section based on highway agency overlay design, one section over-designed, and one section under-designed),

2- Two levels for asphalt mixture: original, and recycled (hot and cold), 3- Two levels for preparation of old pavement prior to overlay (milled, not milled),

4- A combination of the above scenarios.

Table 2-2 outlines different types of the experiments in the C-LTPP program. It consists of five main experiment types whose combinations result in a total of nine experiment types. Table 2-3 presents the location and the experiment code of the different test sections in the C-LTPP program. All the provincial highway agencies participated in the C-LTPP project to monitor and to collect data. Pre-overlay pavement data was collected during the years 1989 and 1990. Post-overlay pavement performance was monitored on a regular basis by local Canadian highway agencies.

Experiment Type	Experiment Description	No. of Sites
1	Performance comparison of overlay thickness (HMAC) With two adjacent test sections	14
2	Performance comparison of overlay thickness (RAP) With two adjacent test sections	0
3	Performance comparison of overlay material type(HMAC vs. RAP) With two adjacent test sections	0
4	Performance comparison of overlay thickness (HMAC) With three adjacent test sections	2
5	Performance comparison of an overlay additive or mix property variation	1
6	Combination of experiments 1 , 2 and 3	2
7	Combination of experiments 1 and 3	1
8	Combination of experiments 1 , 3 and 5	2
9	Combination of experiments 1 and 5	2
	Total	24

Table 2-2: The outline of the specific experiments under study in the C-LTPP program

(The C-LTPP database users' guide, 1996)

Location	C-SHRP ID.	Test Section	Location	Experiment type
Alberta (AB)	810404	1	Hwy 16, Wolf creek	6
		2	Hwy 16, Wolf creek	6
		3	Hwy 16, Wolf creek	6
		4	Hwy 16, Wolf creek	6
British Columbia (BC)	820205	1	Hwy 19 , Vancouver island	1
		2	Hwy 19 , Vancouver island	1
	820502	1	Hwy 99, north site	5
		2	Hwy 99, north site	5
	820605	1	Hwy 99, south site	1
		2	Hwy 99, south site	1
Manitoba (MB)	830403	1	Hwy 2, near Wawanesa	4
		2	Hwy 2, near Wawanesa	4
		3	Hwy 2, near Wawanesa	4
	830801	1	Hwy 1, near Brokenhead River	6
		2	Hwy 1, near Brokenhead River	6
		3	Hwy 1, near Brokenhead River	6
		4	Hwy 1, near Brokenhead River	6
New Brunswick (NB)	840101	1	Hwy 15, East of Moncton	7
		2	Hwy 15, East of Moncton	7
		3	Hwy 15, East of Moncton	7
	840204	1	Hwy 101, near Oromocto River	1
		2	Hwy 101, near Oromocto River	1
	840604	1	Hwy 2, West of Mactaqueac	8
		2	Hwy 2, West of Mactaqueac	8
		3	Hwy 2, West of Mactaqueac	8
		4	Hwy 2, West of Mactaqueac	8
Newfoundland (NF)	850201	1	Hwy 1, near Bonavista	1
		2	Hwy 1, near Bonavista	1
	850206	1	Hwy 1, near Red Clift	1
		2	Hwy 1, near Red Clift	1
	850601	1	Hwy 1,near Kely,s pond	1
		2	Hwy 1,near Kely,s pond	1
Nova Scotia (NS)	860501	1	Hwy 102, Hilden	9
		2	Hwy 102, Hilden	9
		3	Hwy 102, Hilden	9
	860603	1	Hwy 103, near Hebbs Cross	4
		2	Hwy 103, near Hebbs Cross	4
		3	Hwy 103, near Hebbs Cross	4
Ontario (ON)	870102	1	Hwy 80, near Petrolia	1
		2	Hwy 80, near Petrolia	1
	870504	1	Hwy 11, North Bracebridge	1
		2	Hwy 11, North Bracebridge	1
	870505	1	Hwy 57, near NewCastle	8
		2	Hwy 57, near NewCastle	8
		3	Hwy 57, near NewCastle	8
		4	Hwy 57, near NewCastle	8

Table 2-3: Location and the experiment code of the C-LTPP test sections (Continued)

Location	C-SHRP ID.	Test Section	Location	Experiment type
Ontario (ON)	870701	1	Hwy 31, in Greely souhj	1
		2	Hwy 31, in Greely souhj	1
Prince Edward Island (PE)	880203	1	Hwy 2, east of junc. 2 7 254	1
		2	Hwy 2, east of junc. 2 7 255	1
		3	Hwy 2, east of junc. 2 7 256	1
		4	Hwy 2, east of junc. 2 7 257	1
Quebec (QC)	890503	1	Hwy 40, Pte-aux-Trembles	9
		2	Hwy 40, Pte-aux-Trembles	9
		3	Hwy 40, Pte-aux-Trembles	9
		4	Hwy 40, Pte-aux-Trembles	9
	890702	1	hwy 73, near St.Marie	1
		2	hwy 73, near St.Marie	1
Saskatchewan (SK)	900402	1	Hwy 5-06, East of Humbildt	1
		2	Hwy 5-06, East of Humbildt	1
	900802	1	Hwy 10-03, West of Yorkton	1
		2	Hwy 10-03, West of Yorkton	1
		3	Hwy 10-03, West of Yorkton	1
	900803	1	Hwy 1-06B, W Indian Head	1
		2	Hwy 1-06B, W Indian Head	1

Table 2-3: Location and the experiment code of the C-LTPP test sections

(The C-LTPP database users' guide, 1996)

2.2. The C-LTPP database and the data collection program

The C-LTPP database encompasses an extensive amount of data, which have been collected during several years. This data include information about the site description for each test section, detailed information about both lab and in-situ material and sampling, climatic data, traffic data, pavement surface distresses, non- destructive tests such as the Benkelman Beam test (BB) and the Falling Weight Deflectometer test (FWD), maintenance records, and miscellaneous data. The C-LTPP database was structured by using Microsoft ACCESS and consists of eleven main modules (Table 2-4).

Module	Description
GENERAL	General information on the C-LTPP project as well as a definition of the codes used throughout the database
SITE DESCRIPTION	Summary information (as-built) on the test sites
MATERIAL SAMPLING AND TESTING	Detailed information on the field and laboratory and testing of the separate layers in the pavement structure, as well as the Construction of the overlay
ENVIRONMENT	Historical and annual climatic data
TRAFFIC	Historical and annual site specific traffic data
PAVEMENT SURFACE DISTRESS	A digitized version of the manual pavement surface defects survey
BENKELMAN BEAM	Annual (up to 1995) seasonal and spring Benkelman Beam rebounds
FALLING WEIGHT DEFLECTOMETER	The FWD test results performed every second year
PROFILE AND CROSS SECTIONS	The annual transverse and longitudinal pavement profiles
SKID RESISTANCE	Skid resistance measurements every second year
MAINTENANCE	A record of all maintenance treatments applied since rehabilitation

Table 2-4: The eleven main modules in the C-LTPP database

(The C-LTPP database users' guide, 1996)

For the C-LTPP data collection program, it was planned to prepare data on an annual or biannual basis. Table 2-5 shows the frequency of data collection, and the organizations responsible for it.

There are several concerns and shortcomings when using the C-LTPP data as follows:

1- Missing data (e.g. in some test sections, the roughness data for earlier years is not available);

2- Not a long-term data collection (e.g. in some test sections, the roughness data for last years is not available);

3- The nature of the experiment (e.g. the number of test sections in different climate conditions are not equal);

4- The quality and accuracy of collected data (e.g. the traffic information).

However as the project continues and more information becomes available, the underlying mechanisms correlating pavement characteristics and pavement performance will become better known than they are presently (EBA Engineering Consultants, 2001).

Activity	Frequency	Responsibility
Test site identification	One time	Provincial Highway Agency
Pavement Rehabilitation	One time	Provincial Highway Agency
Material sampling and Testing	Prior, during and after the overlay	Provincial Highway Agency
Surface Distress Survey	Prior to overlay and after (yearly)	Provincial Highway Agency
Longitudinal & Transverse profile	Prior to overlay and after (yearly)	Provincial Highway Agency
Benkelman Beam - Long-Term Changes	Prior to overlay and after (up to 1995)	Provincial Highway Agency
Benkelman Beam - seasonal variations	Monthly in one year	Provincial Highway Agency
Benkelman Beam - Spring Factor	Weekly in three different years	Provincial Highway Agency
Falling weight Deflectometer	Every second year	C-SHRP/Highway Agency
Environmental Data	Historical (yearly)	C-SHRP
Traffic Data	Historical (yearly)	Provincial Highway Agency
Skid Resistance	Every second year	Provincial Highway Agency
Pavement Maintenance	As required	Provincial Highway Agency
Video Logging	One time	Provincial Highway Agency

Table 2-5: The frequency of data collection in the C-LTPP project and the organizations responsible for it (The C-LTPP Database Users' Guide, 1996)

The available data from the C-LTPP experiment has passed a minimum level of Quality Control and Quality Assurance (QC/QA) to enhance the integrity of ongoing project and the accuracy of the results based on this program. This QC/QA procedure, which was performed by the C-LTPP data administrators, includes the following aspects (The C-LTPP Database Users' Guide, 1996):

1- All the procedures for measuring, collecting, and reporting data are clarified through the data collection guidelines to make sure that all of the C-LTPP data are collected consistently across the entire test sections.

2- All the data are manually reviewed before input into the C-LTPP database to catch any obvious errors that might have been made while collecting or reporting data.

3- When entering the data into the C-LTPP database, some input range checks are made and if the reported data do not fall in the expected rang, then they are verified.

4- When a correlation is expected among the information from different fields, an inter-related check is performed to assure the consistency among data.

5- A time-history tracking of certain performance factors such as rut and roughness is carried out to make sure that if the variable changed over time on a reasonable manner.

6- For the reported data that seem to be unrealistic or erroneous, there is a feedback loop with the provincial agency engineer who is in charge of collecting and reporting data. If the information is wrong, it is omitted from the database, and when it is correct in specific situations, the data are noted accordingly.

Not all of these quality data procedures have been implemented on an ongoing basis, and the C-LTPP database still needs more quality control.

As the main reference about the Canadian Long-Term Pavement Performance program, the program's database user's guide provides more information about this project.

2.3. Literature review about the C-LTPP Project

The available literature related to the C-LTPP project and particularly about the performance of the C-LTPP pavement sections was reviewed. More information about products and research studies based on the C-LTPP data is available on the C-SHRP home page (www.cshrp.org).

1- Dore et al. (2002) analyzed pavement longitudinal profiles of the C-LTPP test sections. This study's main objectives were to asses the wavelength content of the longitudinal profiles of the C-LTPP test sections and to establish the major factors affecting pavement roughness, based on surface-distortion characteristics. The wavelength analysis of pavement longitudinal profiles was conducted by filtering raw profiles, which was used in the assessment of the performance of the C-LTPP pavement sections. The proportion of the International Roughness Index (IRI) value that could be attributed to the specific wavelength range was obtained and analyzed. The researchers found that 80-130 mm thick overlays gave the best results in reducing roughness associated with short wavelength deformations. The benefit of 80-130 mm overlays was, however, found to be limited to several years. The researchers observed that the long wavelength distortions tended to dominate the longitudinal profiles of thin pavement structures or pavement laid on fine soils.

2- Dore (1995) developed pavement performance models for frost condition in a joint C-SHRP/Quebec Bayesian application program. The main objectives of his study were to revisit the whole approach to pavement design for frost conditions and to develop a rational method dealing specifically with the freezing and thawing of pavement structures. Several types of design approaches are typically used for the mitigation of frost action on pavements, but few of them allow for the assessment of the expected performance of a pavement structure in given climatic and traffic conditions, nor do they allow for the assessment of the consequence of actions taken to migrate frost-related problems. By using the Bayesian method, a design procedure was proposed in this study as a complement to the existing design methods. This study used 5 years of the C-LTPP data for 38 test sections. Using the XLBayes, the Bayesian method software, the following models were developed for roughness and crack in frost condition:

$$R_t = R_0 + K_r \times A^{0.6} \tag{2-1}$$

where

$$K_r = e^{-2.15-0.0016T+0.0003P+0.0012FI+0.0037FS} \tag{2-2}$$

and in which

R_t = Roughness at time t (IRI)

R_o= Initial roughness (IRI)

A= Age of the pavement (year)

K_r= Aggressiveness factor

T= Total pavement thickness (mm)

P= Yearly precipitation (equivalent rain, mm)

FI= Freezing index (^{o}C. day)

FS= Frost susceptibility (mm/ ^{o}C ×sec × 10^{-5})

For longitudinal cracking,

$C_L = K_c \cdot (A-A_i)^m$

(2-3)

where

$$K_c = e^{-0.6-0.002T+0.000133P+0.0007FI+0.01FS} \tag{2-4}$$

C_L= Crack length (Longitudinal and meandering) per 100 lane meters

K_c= Aggressiveness factor, function of precipitation, frost susceptibility of subgrade soils, freezing index, and total pavement thickness

A= Age of the pavement (year)

A_i= Crack initiation offset factor

m= Regression coefficient

Dore concluded that the developed models could assist pavement designers to assess the consequences of different design scenarios and also be used as pavement management tools.

3- EBA Engineering Consultants, Ltd. (2001) conducted a study about rutting trends after almost 7 to 9 years of collecting rut data for the C-LTPP test sections. They evaluated the early rutting performance of the C-LTPP sections. One of this study's main objectives was to compare and to evaluate pavement rutting across all C-LTPP test sites in Canada. As well, the researchers assessed different rut indices such as the 1.2 m straight edge rut, 1.8 m straight edge rut, 3.7 m straight edge rut, maximum rut depth, 5-point rut depth, 11-point rut depth, fill area, and positive and negative fill area. This assessment indicated that the 1.8 m straight edge rut depth index was an appropriate measure of rut, and so this index was selected as the primary index for evaluating pavement rutting. The researchers observed that the early rut trends were rather linear and concluded that with a normal traffic, the cumulative ESAL was a significant factor in pavement rutting and that test sections with lower traffic had a higher rate of rut. The agencies practices were found to meet the required level for early rutting. However, because of the test sections' short life-times and the expectation that more data would be available in the future, the researchers recommended to study the long-term rut performance in order to see whether the agencies' design practices were adequate. The EBA study reported limitations in the extent of the analysis of rut trends and the correlation between rut and pavement characteristics because of low rut progression. The impact of some of the pavement factors such as binder stiffness, pavement structure, and climatic condition was not apparent because of missing data, invalid data, and the limited number of test sections with significant rutting. No statistical method was used to confirm the results from this study.

4- The EBA Engineering Consultants, Ltd. (1996) conducted a study regarding the overlay design and the pavement's structural issues in the C-LTPP project.

This study's main objective was to examine the adequacy of agency overlay design practices for the C-LTPP sections. This study was conducted by utilizing three major overlay design methods including those of the American Association of State Highway and Transportation Officials (AASHTO) method, Asphalt Institute (AI) method, and the Saskatchewan method (a modified Shell method).

In the EBA report, the effective structural number (SN_{eff}) before overlay was determined by using the backcalculation procedures from the AASHTO design guideline. The lack of FWD test before rehabilitation in the C-LTPP project made them to deploy several assumptions in order to estimate the original SN_{eff} based on the FWD results from after overlay. One of the major assumptions was that the effective modulus of the multilayer system could be determined by assuming the elastic moduli of base and subbase layers equal to 10% of that in asphalt layer. Also, the Poisson ratio of subgrade for all the test sections was set to 0.5.

The EBA study concluded that the application of different design methodologies did not show any apparent correlation with the agency's design methods. The required overlay calculated from the AASHTO and AI design procedures was generally less than that of the agency's design sections. The Saskatchewan method showed that 11 sites out of 24, has been constructed with an overlay thicker than required by the method.

5- Frechette et al., (1997) conducted a study about reflective cracking trends in the C-LTPP project. The objective of this study was to evaluate the effectiveness of different rehabilitation strategies in retarding the reflective cracking, based on a comparative evaluation within the C-LTPP test sites after five years of operation. The crack reflection in 5 years was calculated by using the following equation:

Crack reflection in 5 years (%) =

$$\frac{Total\ Crack\ Extent\ In\,5\ Years - Total\ Crack\ Extent\ Prior\ To\ Overlay}{Total\ Crack\ Extent\ Prior\ To\ Overlay} \times 100$$

(2-5)

where all terms for crack extent are in m/km.

This study observed the strong influence of environmental and traffic conditions on the cracking patterns. Overlay thickness was not a controlling attribute in the pavement cracking, while asphalt mix design, milling, and recycled material were more significant. Crack reflection was higher in overlaid pavements with a coarse subgrade. Crack reflection was higher in a wet environment than a dry environment. Overlays having binders with low penetration or high viscosity showed significantly higher cracking. Similarly, overlays with higher stiffness showed more cracking.

Within the C-LTPP project cracks are classified as transverse, wheel path, and edge or centerline, cracks based on the crack orientation. It was observed that

- Among different types of cracks, edge and transverse cracks showed the most noticeable reflection.
- Edge cracks in some of the C-LTPP sections could have been a result of increasing the lane width when the overlay was constructed.

- A difference in structural support and frost conditions between the original road and its shoulder could have caused the overlay to crack closer to the edges.
- Traffic affected crack reflection to some extent, particularly the wheel path cracking.

6- Frechette et al., (1995) conducted a study about the seasonal behavior of the C-LTPP pavement sections. The objective of this study was to calculate a pavement response index representing the seasonal response of each C-LTPP pavement section and to quantify the effect of different variables on the seasonal variations in pavement strength.

The Benkelman Beam data from the C-LTPP project, for different times of the year after overlay were used to monitor the seasonal response. Different types of deflection profiles were recognized in the C-LTPP Program, which generally showed a spring peak followed by a recovery period. Four pavement response indices were developed to represent the annual seasonal variations in the pavement deflections. It was found that main factors contributing to the seasonal variations were pavement temperature, total pavement thickness, annual precipitation, freezing index, traffic load, age of overlay, and frost susceptibility of subgrade soil. No distinct relationship was found between the seasonal-variation indicators and the influential factors. It was recommended that a deflection correction table should be made and used as a tool to improve the pavement design procedure. To provide this table, the future pavement performance experiments should be carried out on pavement factor combinations not covered by the C-LTPP.

7- Goodman (2001) conducted a study of assessing the variability of surface distress surveys in the C-LTPP Program for cracking. His study's objectives were

1- To determine the variability in the severity ratings and extent ratings for different crack types;

2- To rank the distresses in order of their reliability;

3- To suggest ways that the inherent error can be accommodated in performance modeling or other analysis using cracking data;

4- To identify major sources of error and suggest potential improvements to the C-LTPP's surface distress-mapping process and data-entry process.

As only two distress surveys for each test section were available for comparison, traditional variance analysis was not possible, and instead, Cohen's Weighted Kappa Statistic was utilized to compare the level of agreement between the surveys. The Kappa statistic considered the likelihood of chance agreement and also allowed the introduction of penalty values for individual cases of disagreement. The analysis results indicated that agreement based on the crack type was very high while less agreement was observed for the severity level of cracks. Agreement significantly increased with increased data aggregation, indicating that less variability was present for network level analysis than for project level analysis. The effect of rater experience was also investigated, although no firm conclusions were made with the available data. Recommended methods to reduce the variability of future distress surveys included the reduction of the number of severity levels from five to three, reduction of the number of individual agency raters, more frequent training of raters, and the use of rating teams. In general, the results of the C-LTPP distress variability analysis agreed with the results of previous studies in the US-LTPP program.

8- Haas et al. (2002) developed C-LTPP pavement performance models for asphalt overlay. A series of models was developed for predicting the rate of pavement deterioration occurring for the first 8 years of service in the C-LTPP asphalt overlay test sections. By using the SPSS statistical analysis program, these models were developed with data analysis from 59 pavement sections. Since the performance indicators incorporated into the C-LTPP test sections are spread out over a number of different sites, complete pavement performance models were developed through two separate components including within-site models and between-site models. The within-site performance factors were overlay thickness, degree of surface preparation, type of overlay material, pavement roughness and cracking prior to rehabilitation, and various performance indicators determined from mechanistic-empirical analysis. The between-site factors included various climatic measurements, subgrade type, accumulated traffic, and the prior roughness for each site. Developed models have different forms and various factors are involved in each of them that takes longer to introduce each model here. Site location was found to be the primary influence on the rate of pavement deterioration. Overlay thickness and prior cracking were also determined to impact the pavement deterioration at a strong statistical level. The models were provided for benchmarking the performance of pavements across Canada; for comparison with individual, more detailed project designs; and for estimating the performance of designs with different overlay thicknesses.

9- Kandil (2001) studied the effect of overlay thickness and mix type (virgin versus recycled) on the C-LTPP pavement's long-term performance. He used the PSI (Present Serviceability Index) as an indicator of pavement performance in the C-LTPP project. The C-LTPP pavement sections were classified into seven different groups according to their environmental conditions, subgrade types, and traffic levels. For each studied group, a mathematical model was developed that determined the serviceability (PSI) as a function of age, overlay thickness, original pavement thickness, age of original pavement, and overlay material. The general form of these models was as following:

$$PSI = C_o + C_1.t^3 + C_2.\ TH + C_3.\ EQTH + C_4.\ SLIFE + C_5.\ M \qquad (2\text{-}6)$$

where

PSI= Present Serviceability Index

t= Expected service life for the overlay to reach a certain PSI

TH= Overlay thickness

EQTH= Equivalent thickness of the original pavement

SLIFE= Service life of original pavement before overlay

M= Overlay material

The coefficients of above equation (C_i) were calculated for each class of study. These models were used to predict when a pavement section would reach a final serviceability level of $PSI=2.5$. It was concluded that the effect of increasing overlay thickness on the expected service life was negligible in the conditions of low traffic, coarse subgrade, and wet low-freeze environmental conditions. Using recycled asphalt pavement in low-traffic level and dry condition yielded the same service life that was achieved with virgin asphalt pavement.

10- Kavanagh (1995) attempted to model and to predict the immediate and long term maximum Benkelman Beam Rebound (BBR) or deflection of a flexible pavement after overlay. The study's purpose was to verify the current rehabilitation design procedure for use in Manitoba and to quantify the significant contributing variables and their impacts on the design. Field data from the C-LTPP and SHRP Specific Pavement Studies (SPS5) sites of asphalt concrete overlay of asphalt concrete pavement in Manitoba were used in this analysis. A two-stage model to predict the BBR was developed and analyzed by using the Bayesian approach. Model 1 was developed to predict the reduction in the maximum BBR of a flexible pavement immediately after overlay. Based on expert judgment, it was concluded that the BBR_{max} after overlay was a function of the overlay thickness, the rebound before the overlay, and the design traffic. Model 2 was the propagation model developed to predict the rebound of an overlay over time. The experts concluded that the maximum BBR over time was a function of the overlay thickness, the rebound immediately after the overlay, the age of the overlay, the cumulative traffic, and an environmental factor expressed in annual precipitation. This method produced relatively good BBR prediction equations and indicated the magnitude of the impacts of each variable on the BBR prediction.

11- The New Brunswick Department Of Transportation (NBDOT, 1995) in a joint Bayesian program with the C-SHRP, developed models to predict rut in asphalt overlay pavements. In this study, it was not intended to produce definitive predictive performance models ready for deign application, but to evaluate the Bayesian modeling as a tool that could be used to predict pavement performance. By using the C-LTPP Bayesian guideline, models were developed to predict rut. The model developed for thin overlay was as follows:

$$Rut = 0.12652 - 1.79063\, V - 0.11282\, R + 0.88664\, A - 0.16013\, C + 4.91527\, T_1$$

(2-7)

and for thick overlay

$$Rut = 3.3169 - 1.3381\, V - 0.10573\, R + 0.4542\, A - 0.1199C + 3.3029\, T_2$$

(2-8)

where

V = % air voids, R = % retained on the 4.75mm sieve, A = age of the overlay in years, C = % crushed particles, T_1 = annual log traffic measured in KESAL/year, and T_2 = cumulative log traffic measured in KESAL/year.

It was concluded that Bayesian methodology is a viable tool and has application for NBDOT. This methodology demonstrated that it had the potential to assist in optimizing the rehabilitation design of overlays. The researchers made several recommendations for future modeling, both in reference to further development of the rutting model and in other areas where expert judgment could be combined with data to obtain earlier results.

12- Tighe et al. (1999) conducted a study of pavement roughness in the C-LTPP project. The researchers studied the roughness trends and observed a steady progression of roughness for approximately seven years after overlay for the C-LTPP project. During the studied period, the roughness of the C-LTPP test sections changed from a mean as-built IRI of about 1.1 m/km to a mean IRI of about 1.37 in 1997, yet presented very smooth pavements. The researchers used a linear extrapolation of the data and estimated that the mean IRI would reach about 2 m/km after 22 years of overlay service. They also reported some inconsistency in IRI measurements and explained that it could be associated with the changes of data measurement staff or equipment. The researchers concluded that

1- Climate was a major factor that substantially affected roughness progression. It was seen that a higher rate of roughness progression took place in wet low-freeze zone and that a lower rate occurred in the wet-high freeze or dry -high freeze zone.

2- Thinner overlays (30-60 mm) deteriorated at a significantly higher rate than the medium and thick overlays, while little comparative difference was observed between the medium and thick class of overlays.

3- In wet-high freeze zones, thinner overlays showed a higher rate of roughness progression than thicker overlays, regardless of subgrade type. In dry-high-freeze zones, the roughness progression rate for medium and thick overlays was relatively low. In wet-low freezing condition, thinner overlays over a fine subgrade showed the highest rate of roughness progression.

4- Traffic had no significant effect on roughness. The researchers emphasized that the apparent lack of a traffic effect might be largely due to the boundary that had been chosen to distinguish high and low traffic levels. (200,000 ESALs per year). It was suggested that in order to obtain further insight into the effect of traffic, at least three traffic levels such as low, medium, and high should be defined.

5- Pavements on fine-grained subgrade soil deteriorated faster than the pavements on coarse-grained soils in the same period of time.

6- Because of very limited test sections and observations, it was not apparent whether overlay materials and overlay construction (milling and the milling depth) had any impact on roughness progression.

The researchers final conclusion was that overlay thickness, climatic condition, and subgrade material type were major factors significantly influencing roughness progression, and that the combination of these three factors governed the overall pavement performance in term of roughness progression. For example, the combination of thin overlay thickness, wet-low freezing condition, and fine-grained subgrade in high traffic resulted in the worst pavement roughness.

This report covered numerous features of pavement roughness for the C-LTPP project and suggested that the same methodology could be applied to performance trend analysis for other C-LTPP data, however, this study lacked the kind of statistical analysis that could have provided a confirmed approach with a specific level of reliability for studying the impact of different factors on pavement roughness.

CHAPTER 3: EVALUATION OF PAVEMENT PERFORMANCE IN THE C-LTPP PROJECT

3.1. Introduction

As was mentioned in Chapter 1, with a large network of old pavements the highway agencies' activities have shifted from construction to maintenance. To facilitate the management of existing networks, Pavement Management System (PMS) has evolved over the last three decades. A PMS is a set of tools or methods that assist decision makers in finding optimum strategies for providing and maintaining pavements in a serviceable condition over a given period of time (Haas et al., 1994). Prediction of the future condition of pavement is an essential element of a successful PMS. The information contained in a PMS is used to assess the serviceability of pavements and to determine their remaining (future useful) lives. This type of assessment is conducted at both the network and project levels. Accurately predicting the serviceability of pavements' remaining life is of utmost importance in planning short-term and long-term maintenance, rehabilitation, and reconstruction strategies (Nazarian et al., 1998). For future planning and budgeting purposes, the remaining life of pavements must be estimated. Doing so is not only useful for timing a major rehabilitation but also assists managers in forecasting the long-term needs of the network (Vepa et al., 1996).

Knowledge of the service life facilitates decision-making in regard to strategies for the reconstruction–rehabilitation of roads, thereby leading to the efficient use of exiting resources.

Ullidtz (1987) differentiated pavements from other civil engineering icons, such as structures and foundations, in that a pavement design system or rehabilitation design system should not only indicate the needed structure but also permit the prediction of both functional and structural deterioration over time. The functional condition involves the ride quality, and the structure condition involves the bearing capacity. Therefore to evaluate pavement performance, it must be evaluated for both its serviceability (functional), and its load bearing capacity (structural). If a pavement fails in earlier of these requirements, it needs maintenance or rehabilitation (M/R).

In this chapter, the service lives of the C-LTPP test sections are predicted by using different methodologies. Both functional and structural aspects for all the C-LTPP test sections are evaluated to compare pavement sections with a uniform basis.

3.2. Evaluation of the C-LTPP sections, based on the AASHTO design method

Canadian highway agencies use different procedures for the design of their asphalt overlay pavements. However, using one overlay evaluation procedure could provide a uniform basis for comparing the C-LTPP sections in a network level. The American Association of State Highway and Transportation Officials (AASHTO) overlay design procedure was used to estimate the service lives of the C-LTPP test sections.

The Structure Number (SN) is the main input for the AASHTO overlay design procedure. Different methods can be used to determine the structure number of the existing pavement structure (SN_{eff}); however, the most accurate and effective one is based on the results of the Falling Weight Deflectometer (FWD) test.

3.2.1. FWD data and backcalculation

Nondestructive Deflection Tests (NDT) have been extensively used to evaluate the structural capacity of in-situ pavements. There are different types of NDT instruments but the most common one is the Falling Weight Deflectometer (FWD) test. Using FWD test, a load is dropped on the pavement, and the surface deflections are measured at different distances from load impact centerline. Figure 3-1 shows the FWD test's equipment and resulted deflection bowl.

By knowing the amount of applied load and deflections at different distances, FWD test results can be used to backcalculate the moduli of pavement layers. Several pavement backcalculation methods and computer programs are available for determining the moduli of pavement layers. These methods and programs could give different results based on the assumptions used in them. Generally backcalculating computer programs use an initial set for moduli of pavement layers and calculate the deflection of pavement surface at different geophones under testing load.

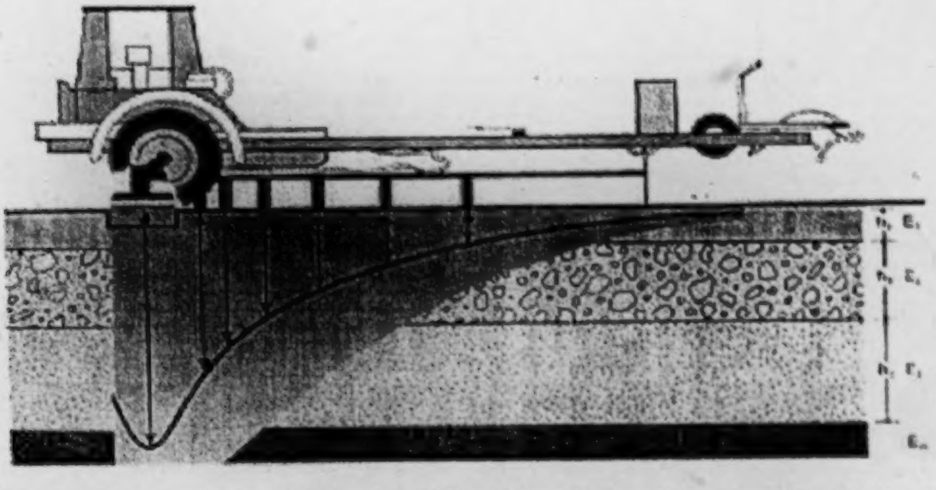

Figure 3-1: Equipment for FWD test, and the deflection bowl (Nazarian et al., 1998)

The initial values for moduli are called the seed moduli, which could be defined by the user. Then the calculated deflections are compared with the measured deflections, and through a specific algorithm, program tries a new set of data for the modulus of paving materials. This process is carried on until that the difference between calculated deflections and the measured ones become negligible.

FWD test has been used in the C-LTPP project after pavement overlaying. All the C-LTPP sections were tested by FWD test in each 10-meter interval, in every second year after overlay. In order to backcalculate the moduli of pavement layers of the C-LTPP sections in this study, several methods or computer programs were deployed to compare the results of backcalculation. The AASHTO backcalculation method was used as the base and two other computer programs, EVERCALC and MICHBACK, were used to validate the AASHTO results.

3.2.1.1. AASHTO backcalculation method

In the AASHTO backcalculation procedure, pavement is viewed as a multi-layered elastic system, and the underlying assumption is that a unique set of layer moduli exists such that the theoretically predicted deflection basin is equivalent to the measured deflection basin. However a limitation of this approach is that the developed mathematical complexities require a computerized solution. AASHTO suggest that the results must be compared with the agencies' prior experiences with similar materials to ensure that the results are reasonable (AASHTO, 1993).

The first step in AASHTO backcalculation procedure is to determine the modulus of subgrade based on the following equation (AASHTO, 1993):

$$M_r = \frac{0.24(p)}{(r)(D_r)} \tag{3-1}$$

where

P = FWD load (lbs)

r = Radial distance of measured deflection from load centerline (inch)

D_r = Pavement deflection in distance r (inch)

A very important constraint to Equation 3-1 is that D_r must be taken at an optimum distance from the load centerline. Doing so ensures that the right geophone will be chosen at an appropriate distance from the load centerline, so that the deflection of the other layers will be zero, and the result will be based only on the subgrade deflection. In the Washington State Department of Transportation pavement guide (1999), the following equation is suggested to estimate the minimum required distance

$$r \geq 0.7 \times a_e \qquad (3\text{-}2)$$

in which r is the minimum distance from the load centerline for deflections (inches), and a_e is determined from the following formula:

$$a_e = \sqrt{\left(a^2 + \left(D \times \left(\frac{E_p}{M_r} \right)^{1/3} \right)^2 \right)} \qquad (3\text{-}3)$$

in which

a_e = Effective radius of the stress bulb at the subgrade-pavement interface (in.)

D = Pavement total thickness (in.)

E_P = Effective elastic modulus of pavement (psi)

M_r = Subgrade resilient modulus (psi)

a = FWD load plate radius (inches)

After determining the modulus of subgrade (M_r), the equivalent modulus of the pavement layers (E_P) will be calculated by using the following equation (AASHTO, 1993)

$$D_0=1.5(p)(a)\left[\frac{1}{M_r\sqrt{1+\left(\frac{D}{a}\sqrt[3]{\frac{E_p}{M_r}}\right)^2}}+\frac{\left(1-\frac{1}{\sqrt{1+\left(\frac{D}{a}\right)^2}}\right)}{E_p}\right] \quad (3\text{-}4)$$

where

D_0= adjusted d0 (inches); (d0 is the deflection measured at the center of the load plate and adjusted to a standard temperature of 20°C)

P = FWD load plate pressure (psi)

a = FWD load plate radius (inches)

D = Total thickness of pavement (inches)

M_r = Subgrade resilient modulus (psi)

E_p = Effective elastic modulus of pavement (psi)

Asphalt is a viscous material; therefore, its properties are highly dependent on the temperature, which has a significant impact on the results from the FWD test and the backcalculated resilient modulus. AASHTO has provided procedures to modify the backcalculation results by using the temperature adjustment that can be applied to correct either the measured deflections or, directly, the results from the backcalculation (resilient modulus). In either alternative, the information about the pavement temperature at the time of FWD test is required.

In this study, for the AASHTO backcalculation procedure, the highest deflection from FWD test (d0) was adjusted by using the temperature-deflection correction factor in Equation 3-5:

$$d_{adjusted} = d_{tp} \times F_d \qquad (3\text{-}5)$$

where

$d_{adjusted}$ = Corrected (normalized) deflection measurement at load centerline

d_{tp} = Uncorrected or measured deflection at centerline from FWD test

F_d = temperature-deflection correction factor

Figure 3-2 presents AASHTO graph to determine F_d related to different pavement temperatures at the time of conducting the FWD test.

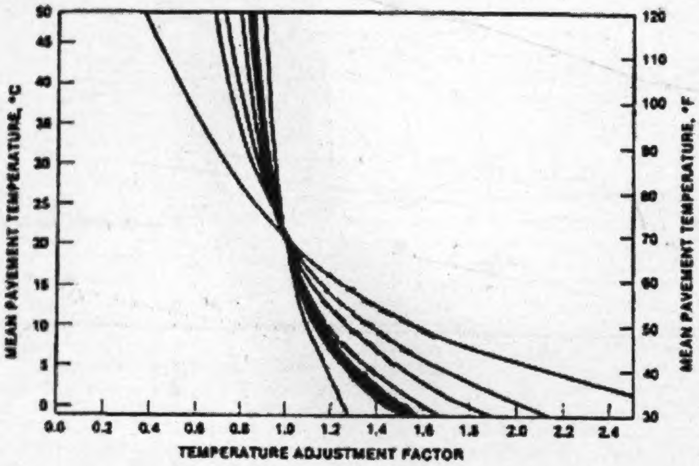

Figure 3-2: Correction factor for FWD deflection at load centerline (AASHTO, 1993)

The AASHTO backcalculation procedure and the FWD testing results after overlay for all the C-LTPP sections were used to backcalculate Equivalent modulus (E_P), modulus of subgrade (M_r), and finally structure number (*SN*) of pavement. Given the extensive amount of FWD data in the C-LTPP project, a computer program was developed to perform the AASHTO backcalculations. Detailed information regarding developed program is available in Appendix A.

		AASHTO backcalculation results (Mpa)		
CSHRP ID	SECTION ID	Equivalent modulus (Ep)	Modulus of subgrade(Mr)	SN (in)
810404	1	727	45	4.29
810404	2	875	49	4.97
810404	3	976	55	5.15
810404	4	662	48	4.33
820502	1	782	141	15.04
820502	2	783	86	15.22
820605	1	950	72	9.75
820605	2	1133	97	10.66
830403	1	925	31	3.07
830403	2	1255	29	3.53
830403	3	1424	30	4.06
830801	1	1175	93	6.85
830801	2	759	88	5.29
830801	3	773	78	5.44
830801	4	1426	91	7.23
840101	1	2152	96	4.37
840101	2	1766	85	4.26
840101	3	996	56	3.52
840204	1	879	35	4.31
840204	2	601	30	3.63
840604	1	657	76	5.09
840604	2	705	111	5.34
840604	3	683	108	5.35
840604	4	783	104	5.74
850201	1	613	78	6.74
850201	2	527	87	5.99
850206	1	645	80	5.96
850206	2	721	89	6.91
850601	1	820	108	8.17
850601	2	752	132	7.57
860501	1	814	68	5.32
860501	2	930	63	5.99
860501	3	673	64	4.80
860603	1	685	81	5.99
860603	2	739	99	7.15
860603	3	656	92	6.70
870102	1	468	40	5.89
870102	2	356	40	5.06
870504	1	725	66	10.12
870504	2	847	82	10.80
870505	1	601	81	5.99
870505	2	761	102	6.46
870505	3	1048	94	7.50
870505	4	405	74	5.20

Table 3-1: Results of AASHTO backcalculation procedure for moduli of pavement layers and SN for the C-LTPP sections (Continued)

		AASHTO backcalculation results (Mpa)		
CSHRP ID	SECTION ID	Equivalent modulus (Ep)	Modulus of subgrade(Mr)	SN (in)
870701	1	774	84	10.00
870701	2	1744	177	13.78
880203	1	443	78	1.84
880203	2	585	48	2.40
880203	3	559	60	2.33
880203	4	968	69	3.31
890503	1	503	68	13.51
890503	2	584	90	14.39
890503	3	675	59	15.42
890503	4	711	74	15.49
890702	1	436	118	9.16
890702	2	527	110	10.07
900402	1	508	62	3.13
900402	2	725	54	4.24
900802	1	373	52	2.90
900802	2	471	56	3.17
900802	3	777	55	4.04
900803	1	1217	43	4.66
900803	2	735	35	3.51

Table 3-1: Results of AASHTO backcalculation procedure for moduli of pavement layers and SN for the C-LTPP sections

Results of AASHTO backcalculation method and the calculated moduli of pavement layers for the C-LTPP sections are presented in Table 3-1.

After determining the moduli of the pavement layers, the SN relevant to each layer can be calculated by using Equation 3-6 from the AASHTO guideline:

$$SN=0.0045\times D_i\times\sqrt[3]{E_i} \qquad (3\text{-}6)$$

where

E_i = Modulus of pavement layer i (psi)

D_i = Thickness of pavement layer i (in)

The structure number of the total pavement system could be determined by adding up the structural numbers of all the pavement layers. By using Equation 3-6, the

SN of the C-LTPP pavement sections was calculated based on the equivalent modulus of pavement layers (E_p), which was obtained from the AASHTO backcalculation procedure. The values of the SN for all the C-LTPP sections are also presented in Table 3-1.

3.2.1.2. EVERCALC backcalculation computer program

The EVERCALC program, developed by the Washington State Department Of Transportation (WSDOT), was employed in the present study to determine the moduli of pavement layers in the C-LTPP test sections. This program has a user-friendly interface and provides an appropriate environment for manipulating input data.

The EVERCALC program uses WESLEA (provided by the Waterways Experiment Station and U.S. Army Corps of Engineers) as the layered elastic solution to compute the theoretical deflections. The basic assumptions of the layered elastic theory include

1- Layers are infinitely long in the horizontal directions,

2- Layers have uniform thickness,

3- Subgrade is semi-infinite in vertical direction, and

4- Layers are composed of homogenous, isotropic, linearly elastic materials, characterized by elastic modulus and Poisson's ratio.

As the discussion in Section 3.2.1 explains, the EVERCALC program calculates the moduli of pavement layers from an initial rough estimate of the layer moduli (seed values) and program iteratively searches for the final modulus for each pavement layer. When more than one deflection data set at a given location is analyzed, the final moduli from the previous deflection data set are used as seed moduli for the next one in order to improve the program's performance. The calculated deflections are compared with the measured ones.

Temperature normalization of asphalt concrete is accomplished by using the relationship between the modulus and temperature. This relationship was obtained for the WSDOT asphalt concrete as below,

$$Log\ Eac = 6.4721 - 1.47362 \times 10^{-4}(T_p)^2 \qquad (3\text{-}7)$$

Eac= Modulus of asphalt concrete (psi)

T_p= Pavement Temperature (°F)

In addition, EVERCALC is capable of calculating the depth to stiff layer. The basic assumption is that no surface deflection will occur beyond the intercept of the applied stress zone and the stiff layer.

The two main interfaces for introducing FWD data in to the program are the general and deflection interfaces. The general interface asks for information such as number of layers, number of sensors and their distances from load centerline, depth of stiff layer, temperature adjustment, Poisson ratio of different layers and their thicknesses, as well as the seed values for calculating the moduli of pavement layers. Figure 3-3 shows the general interface of the EVERCALC program:

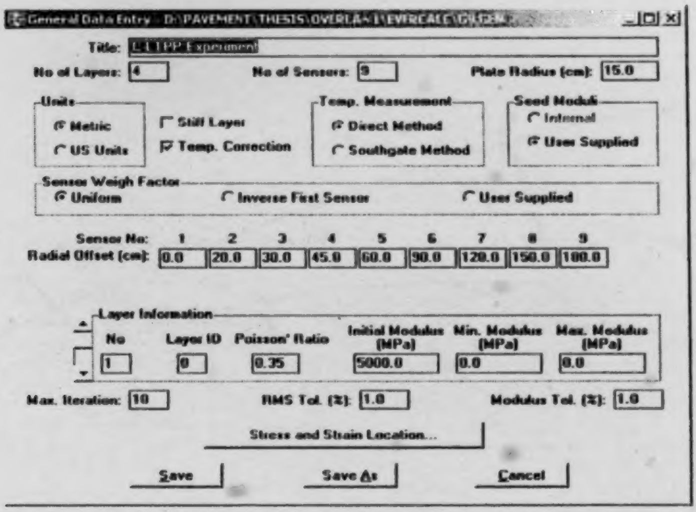
General Data Entry - D:\PAVEMENT\THESIS\OVERLA~1\EVERCALC\
Stress and Strain Location...
Save
Save As
Cancel

Title: LTPP Experiment

No of Layers: 4
No of Sensors: 9
Plate Radius (cm): 15.0

Units: ● Metric ○ US Units

☐ Stiff Layer
☑ Temp. Correction

Temp. Measurement: ● Direct Method ○ Southgate Method

Seed Moduli: ○ Internal ● User Supplied

Sensor Weigh Factor: ● Uniform ○ Inverse First Sensor ○ User Supplied

Sensor No:	1	2	3	4	5	6	7	8	9
Radial Offset (cm):	0.0	20.0	30.0	45.0	60.0	90.0	120.0	150.0	180.0

Layer Information

No	Layer ID	Poisson' Ratio	Initial Modulus (MPa)	Min. Modulus (MPa)	Max. Modulus (MPa)
1	0	0.35	5000.0	0.0	0.0

Max. Iteration: 10
RMS Tol. (%): 1.0
Modulus Tol. (%): 1.0

Figure 3-3: The general module of the EVERCALC program

To simplify the backcalculation procedures, the base and subbase layers can be considered as one layer with similar properties. Therefore a multilayer pavement system was introduced into the program, encompassing the total asphalt layer (including overlay), base+subbase, and subgrade. For all the test sections, the depth of the subgrade was chosen equal to 100 m so that the effect of the stiff layer could be omitted, and an unbounded subgrade could be simulated. For the Poisson ratio values of the different pavement layers, the suggested typical values from the AASHTO guide were chosen. Table 3-2 shows the general range and the typical values for the Poisson ratio (AASHTO, 1993). The typical values of the Poisson ratio used in this study were set to 0.35 for asphalt layer, 0.35 for base+subbase layer, and 0.40 for subgrade based on averages of AASHTO suggested values.

Material	General range	Typical value
Asphalt concrete	0.15 ~ 0.45	0.35
Granular Base/Subbase	0.30 ~ 0.40	0.35
Subgrade	0.30 ~ 0.50	0.4

Table 3-2: The general ranges and the typical values for Poisson ratio (AASHTO, 1993)

The applied load (close to 40 kN) and the measured deflections were put into the program through the deflection interface, which is shown in Figure 3-4. For each FWD test, the applied load and the deflection measurements must be plugged into the program through the specified input boxes.

As was mentioned before, a huge amount of FWD data for the C-LTPP sections were collected in each 10-meter interval in each test section. Using all available data makes the backcalculation process a time-consuming task. To simplify the backcalculation process, it was assumed that each C-LTPP pavement section has uniform and similar properties along the section. Therefore, the averages of FWD testing results were used in the backcalculating programs. These mean values were obtained by calculating the average of measured deflections in the same sensor for each test station. The average FWD deflections are presented in Appendix B.

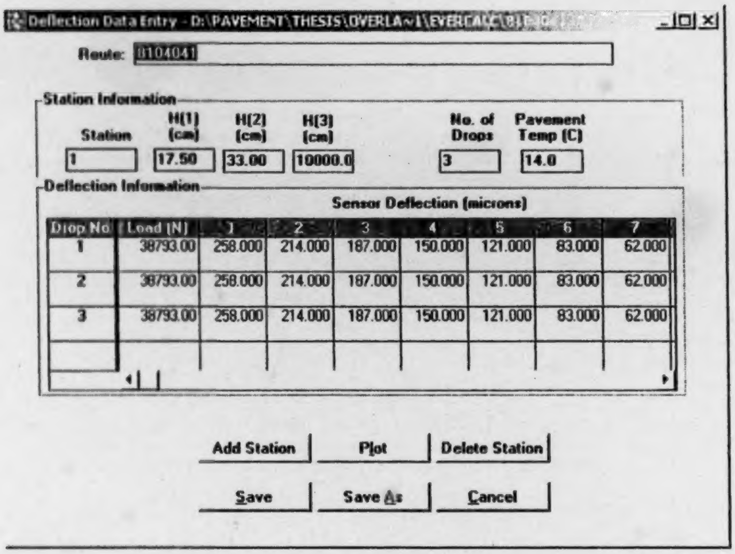
Deflection Data Entry - D:\PAVEMENT\THESIS\OVERLA~1\EVERCALC\

Route: 0104041

Station Information

Station: 1
H(1) (cm): 17.50
H(2) (cm): 33.00
H(3) (cm): 10000.0
No. of Drops: 3
Pavement Temp (C): 14.0

Deflection Information

Sensor Deflection (microns)

Drop No	Load (N)	1	2	3	4	5	6	7
1	38793.00	258.000	214.000	187.000	150.000	121.000	83.000	62.000
2	38793.00	258.000	214.000	187.000	150.000	121.000	83.000	62.000
3	38793.00	258.000	214.000	187.000	150.000	121.000	83.000	62.000

Add Station
Plot
Delete Station
Save
Save As
Cancel

Figure 3-4: The deflection module of the EVERCALC program

The backcalculated modulus of subgrade (M_r) based on the FWD test results needs to be corrected due to the loading conditions in the FWD test. AASHTO provides a correction factor to decrease M_r to the actual design range, no more than 0.33 (AASHTO, 1993). The same reduction factor is used in the present study in order to provide a uniform basis for investigating the consistency between the results of the EBA study and those of the current report. EVERCALC's calculations of the moduli of pavement layers for the C-LTPP sections are summarized in Table 3-3. Appendix C provides a sample of the EVERCALC outputs for some C-LTPP sections.

		EVERCALC backcalculation results (Mpa)				
C-SHRP ID	Section	Eac	Eb+sb	Mr	Corrected Mr	SN (in)
810404	1	3498	276	141	47	4.63
810404	2	3640	271	160	53	5.32
810404	3	4269	257	184	61	5.47
810404	4	3030	199	159	52	4.61
820502	1	22304	207	518	171	12.60
820502	2	20381	168	287	95	12.41
820605	1	29948	233	233	77	9.11
820605	2	22430	230	350	116	9.63
830403	1	2146	122	103	34	3.10
830403	2	3514	115	100	33	3.67
830403	3	2727	140	101	33	3.94
830801	1	7254	199	372	123	7.12
830801	2	6300	172	350	116	5.52
830801	3	5248	198	287	95	5.66
830801	4	8381	221	360	119	7.29
840101	1	2286	*	357	118	4.55
840101	2	2285	*	320	106	4.74
840101	3	1316	*	213	70	3.95
840204	1	4200	67	136	45	4.28
840204	2	4554	43	122	40	3.89
840604	1	4930	162	330	109	5.45
840604	2	7150	200	383	126	5.19
840604	3	4262	198	367	121	4.97
840604	4	3583	211	353	116	5.15
850201	1	5263	128	367	121	6.23
850201	2	8582	141	367	121	5.78
850206	1	5004	175	336	111	6.83
850206	2	9094	156	363	120	6.57
850601	1	4610	132	390	129	7.59
850601	2	5379	122	530	175	7.01
860501	1	6365	75	360	119	5.39
860501	2	4454	81	300	99	5.74
860501	3	5439	83	301	99	4.88
860603	1	2725	122	581	192	6.56
860603	2	4043	142	476	157	6.45
860603	3	3521	156	390	129	6.10
870102	1	2705	88	158	52	5.53
870102	2	2131	103	147	49	4.83
870504	1	9448	152	234	77	8.96
870504	2	10721	145	333	110	9.36
870505	1	5319	134	355	117	5.66
870505	2	6581	190	412	136	6.18
870505	3	8213	188	406	134	7.02
870505	4	2633	135	266	88	4.98

Table 3-3: Results of EVERCALC program for moduli of pavement layers in the C-LTPP sections (= No base and subbase);(Continued)*

		EVERCALC backcalculation results (Mpa)				
C-SHRP ID	Section	Eac	Eb+sb	Mr	Corrected Mr	SN (in)
870701	1	6708	118	384	127	8.47
870701	2	5458	130	779	257	9.42
880203	1	3677	18	350	116	2.59
880203	2	2783	11	279	92	3.01
880203	3	2979	14	321	106	3.01
880203	4	3012	22	336	111	3.81
890503	1	2430	158	468	154	10.82
890503	2	1342	162	313	103	10.70
890503	3	1473	170	1675	553	11.34
890503	4	1864	157	256	84	11.09
890702	1	2779	122	337	111	7.52
890702	2	2277	122	317	105	7.90
900402	1	2814	190	190	63	3.49
900402	2	2715	143	185	61	4.45
900802	1	5239	96	172	57	3.32
900802	2	6564	100	192	63	3.60
900802	3	6697	134	197	65	4.37
900803	1	10605	93	166	55	4.92
900803	2	14681	60	140	46	3.99

Table 3-3: Results of EVERCALC program for moduli of pavement layers in the C-LTPP sections (= No base and subbase)*

3.2.1.3. MICHBACK backcalculation computer program

MICHBACK, developed at the Michigan State Department of Transportation (MSDOT), is another backcalculation program that was used in this study. MICHBACK uses a modified Newton method for the backcalculation of the pavement layers' moduli from measured surface deflections. The backcalculation procedure is iterative and requires several forward calculations. Each layer in a pavement cross-section is assumed to extend infinitely in the horizontal directions, and the last layer is assumed to be infinitely deep. All the pavement layers are assumed to be fully bonded so that no slip occurs due to the applied load. The load applied by the FWD is assumed to exert a uniform pressure over a circular area. The pavement layers are assumed to be composed of linear elastic material.

The Asphalt Concrete (AC) modulus is corrected to the reference temperature by predicting the temperature at the mid-depth of the AC layer from the temperature measured at the pavement surface, and then multiplying the backcalculated modulus by a corrections factor. This correction factor is based on the observations and experiments of MSDOT:

$$CF = 10^{0.0224(T-T_r)} \qquad (3\text{-}8)$$

where

CF = Temperature correction factor

T = Mid-depth temperature (^{o}C)

T_r= Reference temperature of 20^{o}C

As they were with the EVERCALC program, the average deflections were used with the MICHBACK program. The results for the modulus of subgrade were modified by a corrections factor 0.33, as was explained before. The results for moduli of pavement layers in the C-LTPP sections from MICHBACK program are summarized in Table 3-4. Appendix D provides a sample of the MICHBACK outputs for some C-LTPP sections.

		MICHBACK backcalculation results				
C-SHRP ID	Section	Eac	Eb+sb	Mr	Corrected Mr	SN (in)
810404	1	3332	291	141	47	4.63
810404	2	3788	249	162	53	5.31
810404	3	4574	231	186	61	5.48
810404	4	3226	181	161	53	4.61
820502	1	22150	190	485	160	12.34
820502	2	19780	145	260	86	11.97
820605	1	29500	220	212	70	8.99
820605	2	22200	205	335	111	9.41
830403	1	2685	97	106	35	3.20
830403	2	3848	75	103	34	3.67
830403	3	3033	93	103	34	3.96
830801	1	5970	270	344	114	7.09
830801	2	6799	158	350	116	5.54
830801	3	5497	188	285	94	5.67
830801	4	8633	211	358	118	7.29
840101	1	*	*	*	-	-
840101	2	*	*	*	-	-
840101	3	*	*	*	-	-
840204	1	4437	62	139	46	4.32
840204	2	4727	40	125	41	3.91
840604	1	4953	166	327	108	5.48
840604	2	7756	188	398	131	5.20
840604	3	4503	191	377	124	4.97
840604	4	3978	196	371	122	5.15
850201	1	5502	124	374	123	6.24
850201	2	9063	136	375	124	5.79
850206	1	5287	171	348	115	6.86
850206	2	9484	149	371	122	6.56
850601	1	4732	127	398	131	7.59
850601	2	5335	121	551	182	6.99
860501	1	6570	71	368	121	5.41
860501	2	4672	77	302	100	5.78
860501	3	5651	78	309	102	4.89
860603	1	2723	134	469	155	6.65
860603	2	4193	137	491	162	6.46
860603	3	3706	149	406	134	6.10
870102	1	2854	84	162	53	5.55
870102	2	2314	95	152	50	4.82
870504	1	9492	153	235	78	8.97
870504	2	10568	146	332	110	9.35
870505	1	5398	132	350	116	5.66
870505	2	6506	188	404	133	6.15
870505	3	8185	187	396	131	7.01
870505	4	2714	131	265	87	4.97

Table 3-4: Results of MICHBACK program for moduli of pavement layers in the C-LTPP sections (= Not applicable for two-layer pavement system); (Continued)*

		MICHBACK backcalculation results				
C-SHRP ID	Section	Eac	Eb+sb	Mr	Corrected Mr	SN (in)
870701	1	6678	117	378	125	8.45
870701	2	5850	115	689	227	9.35
880203	1	3830	17	358	118	2.62
880203	2	2911	16	281	93	3.08
880203	3	3089	16	329	109	3.05
880203	4	3119	21	350	116	3.85
890503	1	2414	163	233	77	10.90
890503	2	1394	158	336	111	10.66
890503	3	1453	181	193	64	11.51
890503	4	1881	156	265	87	11.08
890702	1	2899	120	347	115	7.52
890702	2	2408	122	334	110	7.95
900402	1	2977	176	192	63	3.49
900402	2	2822	128	188	62	4.44
900802	1	5735	85	179	59	3.33
900802	2	6765	94	194	64	3.60
900802	3	6822	127	199	66	4.36
900803	1	10574	88	169	56	4.90
900803	2	13861	65	138	46	3.97

Table 3-4: Results of MICHBACK program for moduli of pavement layers in the C-LTPP sections (= Not applicable for two-layer pavement system)*

3.2.1.4. Comparison between backcalculation results

Unlike the AASHTO backcalculation method, which determines the equivalent modulus for all pavement system, the EVERCALC program calculates the modulus of each pavement layer. In Figure 3-5, the SN values for the C-LTPP pavement sections resulting from the AASHTO backcalculation method and the EVERCALC backcalculation program are compared by using the line of equality. For most C-LTPP sections, a high correlation occurred between the results from the AASHTO method and the EVERCALC program, close to line of equality. However, for some test sections with higher SN values the results from the AASHTO method were higher than the SN values from the EVERCALC program. This could be associated with different assumptions that are involved in the AASHTO method and the EVERCALC program regarding the stiff layer, temperature normalization, and so on.

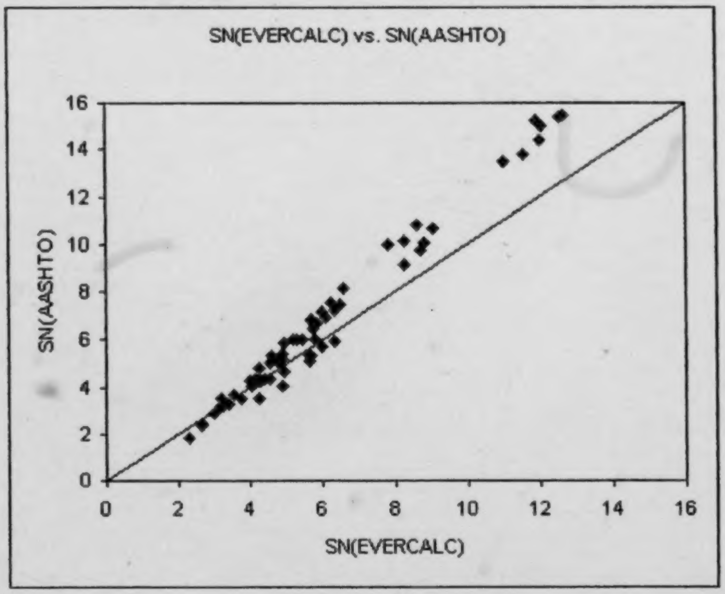

Figure 3-5: Comparison of SN values from the AASHTO backcalculation method and the EVERCALC program

Figure 3-6 compares the moduli of pavement layers from two programs, EVERCALC and MICHBAC, using the line of equality. As it can be seen there was a high correlation between the outputs of two programs.

There was a high correlation between the results from EVERCALC program and other twofold: the AASHTO method, the MICHBACK backcalculation program. In addition, the EVERCALC program provided the modulus of each pavement layer, while AASHTO backcalculation method estimated the Equivalent modulus

(E_P) for pavement. Therefore the backcalculated moduli of pavement layers from the EVERCALC program and the resulted SN values were used for the rest of this study.

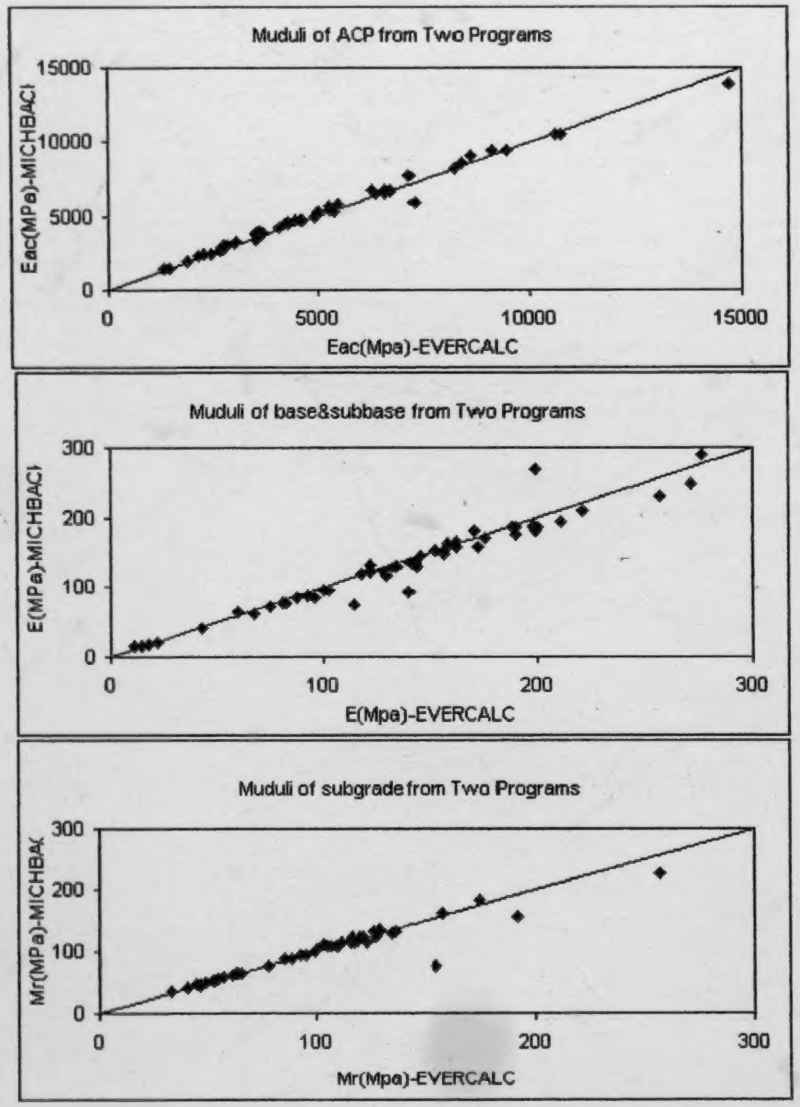

Figure 3-6: Comparison of the backcalculated moduli from two programs, EVERCAL and MICHBACK.

3.2.2. Service lives of the C-LTPP sections, based on the AASHTO method

With the AASHTO pavement design method, it is possible to predict the total traffic that pavement will tolerate until reaching an acceptable service level by using Equation 3-9 (AASHTO, 1993):

$$Log\ W_{18} = Z_R \times S_o + 9.36 \times [log\,(SN+1)] - 0.20 + \frac{log \dfrac{\Delta PSI}{4.2 - 1.5}}{0.4 + \dfrac{1094}{(SN+1)^{5.19}}} + 2.32 \times log\, M_r - 8.07 \qquad (3\text{-}9)$$

where

W_{18} = Number of 18000 Ib (80 kN) single axle load application, Equivalent Single Axle Load (ESAL)

Z_R = Standard normal deviate corresponding to the reliability R

S_o = Overall standard deviation

SN = Structural number indicative of the total pavement thickness

M_r = Modulus of the subgrade

$\Delta PSI = PSI_i - PSI_t$

PSI_i = Initial serviceability index

PSI_t = Terminal serviceability index

To calculate the cumulative traffic, W_{18}, it is necessary to know all the factors on the right side of Equation 3-9. To use Equation 3-9, the following assumptions were applied to all the C-LTPP sections

1- A reliability of 95% was chosen in order to represent the major highways and the value of Z_R was set to –1.645.

2- According to the AASHTO recommendations the value of standard deviation for overlay design was set to 0.49.

3- AASHTO recommends a terminal serviceability of 2.5 for primary highways. With an initial serviceability of 4.2, the value of ΔPSI is equal to 1.7.

The structure number (*SN*) and modulus of subgrade (M_r) for the C-LTPP sections were calculated in 3.2.1. By using the values of SN and M_r in the AASHTO design equation, Equation 3-9, the cumulative traffic (W_{18}) was determined for all the C-LTPP test sections. Then by using Equation 3-10, the service life of pavement sections corresponding to the calculated traffic was determined:

$$ESAL\ in\ service\ life = original\ ESAL \times \frac{(1+g)^y - 1}{g} \tag{3-10}$$

where

g = Traffic growth factor in percent

y = Service life (years)

The original traffic (ESALs) at the time of overlay for all the C-LTPP sections, were extracted from the C-LTPP database, presented in Appendix E. A traffic growth factor of 3% was used in order to determine the service lives. The calculated service lives of the C-LTPP test sections, based on AASHTO procedure are presented in Table 3-5. In cases where the estimated service life was more than 50 years, 50+ was replaced. The highlighted sections are the agency-designed test sections.

C-SHRP ID	Section	Overlay (mm)	Service life (years)
810404	1	61	9.67
810404	2	103	22.69
810404	3	94	30.78
810404	4	55	9.85
820502	1	104	50+
820502	2	118	50+
820605	1	50	50+
820605	2	73.2	50+
830403	2	113.3	23.48
830403	3	148	44.25
830801	1	185	50+
830801	2	103.3	50+
830801	3	126	50+
830801	4	170	50+
840101	1	174	49.98
840101	2	179	33.20
840101	3	87	3.65
840204	1	114	50+
840204	2	88	18.09
840604	1	107.3	50+
840604	2	89.9	50+
840604	3	29.5	50+
840604	4	35	50+
850201	1	117	50+
850201	2	73	50+
850206	1	106	50+
850206	2	63	50+
850601	1	122	50+
850601	2	74	50+
860501	1	55	38.75
860501	2	85	48.48
860501	3	41	20.33
860603	1	85.6	50+
860603	2	80	50+
860603	3	34	50+
870102	1	94.5	50+
870102	2	46.2	36.51
870504	1	31	50+
870504	2	61.3	50+

Table 3-5: Service lives of the C-LTPP sections, based on the AASHTO overlay design method (Continued)

C-SHRP ID	Section	Overlay (mm)	Service life (years)
870505	1	75	50+
870505	2	72.5	50+
870505	3	105	50+
870505	4	106.3	50+
870701	1	42.5	50+
870701	2	106	50+
880203	1	51	3.92
880203	2	109	5.45
880203	3	51	7.35
880203	4	99	26.31
890503	1	39.7	50+
890503	2	50.7	50+
890503	3	105.7	50+
890503	4	82.7	50+
890702	1	44	50+
890702	2	85	50+
900402	1	86.3	7.17
900402	2	125.6	21.75
900802	1	54.5	2.76
900802	2	66.7	5.46
900802	3	104.3	17.78
900803	1	157.5	43.56
900803	2	107.6	8.53

Table 3-5: Service lives of the C-LTPP sections, based on the AASHTO overlay design method

Except for the two test sections, 880203-1(PE) and 900802-2(SK), which this methodology showed had short service lives, the rest of the sections had service lives of more than 20 years. Given that, generally, an overlay does not last more than 20 years, the results from the AASHTO overlay design method seemed to be unrealistic for most of the C-LTPP test sections. This method have resulted to very high service lives for several reasons, such as

1- The quality of the FWD test results and traffic information in the C-LTPP database,

2- The choice of a very high reliability of 95 %; with a lower reliability level such as 50%, the estimated service lives will decrease.

3.2.3. Comparison of results from this study with those from EBA study

As was mentioned in 2.3, a similar study about estimating the service lives of the C-LTPP sections was performed by the EBA Engineering Consultants, Ltd. Table 3-6 presents the expected service life for the agency-designed test sections according to the present study and the EBA report.

		Expected Service Life for agency-designed Overlay (years)	
C-SHRP ID	Section	This study	EBA
810404	3	30.8	4.6
820502	1	50+	50+
820605	1	50+	50+
830403	2	23.5	22.9
830801	1	50+	50+
840101	1	50.0	14.3
840204	1	50+	37.8
840604	1	50+	23.9
850201	1	50+	50+
850206	1	50+	50+
850601	1	50+	50+
860501	2	48.5	50+
860603	1	50+	50+
870102	2	36.5	50+
870504	1	50+	50+
870505	2	50+	50+
870701	1	50+	50+
880203	1	3.9	0.6
890503	1	50+	50+
890702	1	50+	50+
900402	2	21.7	32.3
900802	2	5.5	2.5
900803	1	43.6	42.8

Table 3-6: Expected service lives for the agency-designed sections based on AASHTO serviceability from present study and the EBA report

From Table 3-6, in 6 test sections (25%), there is more than 10 years difference between predicted service lives from this study with predicted ones from the EBA study. However, there is a consistency in prediction of service life for the rest of the C-LTPP sections (≈75%). For most of them, the service lives found in this study were higher than those found in the EBA study. This difference could have resulted from the different backcalculation methods used to determine the moduli of pavement layers. Overall, the results from both studies were consistent for the expected service lives.

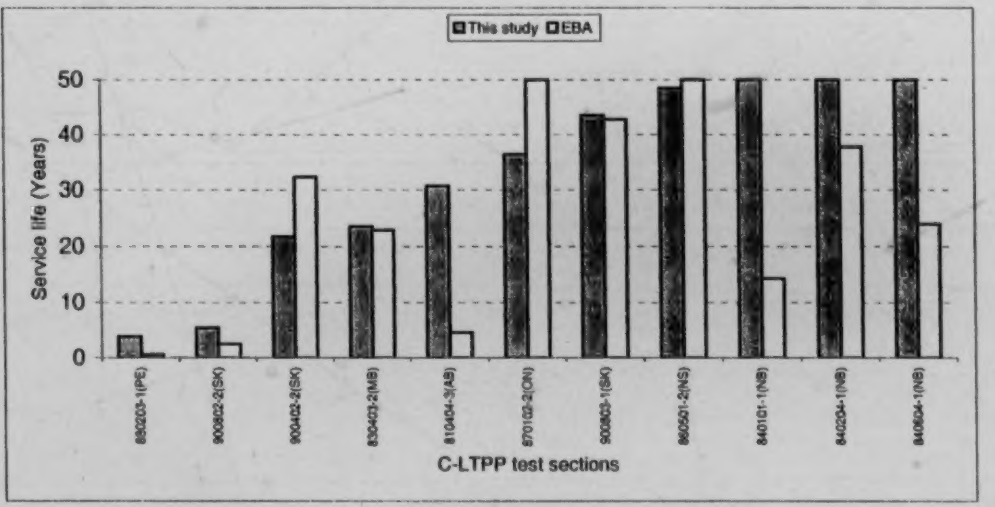

Figure 3-7: Comparison between the results from this study and the EBA report (Excluding test sections with service lives more than 50 years from both studies)

As it can be seen from Figure 3-7, results from this study and EBA research shows that test sections 880203-1(PE) and 900802-2(SK) have reached their terminal serviceability (*PSI=2.5*) in less than 10 years after overlay. EBA study suggested that section 810404-3 in Alberta, has reached its terminal serviceability, while the methodology utilized in this study suggested a longer service life for it.

In other cases, all sections will have a reasonable serviceability for al least 20 years after overlay.

3.3. Roughness and its importance in pavement evaluation

"Pavement roughness" is defined by the American Society of Testing Materials as the deviation of surface from a true planar surface with characteristic dimensions that affect vehicle dynamics, ride quality, dynamic loads and drainage (ASTM, 1996). Pavement roughness is an indicator of pavement performance and is associated with driving comfort, vehicle operating costs, and safety. Even though the concept of the functional performance of pavements was not developed until the AASHTO Road test in the late 1950s, the need to evaluate roughness had been recognized in 1920s (Haas et al., 1994).

Roughness is commonly viewed in terms of the distortion of the pavement surface, which contributes to an undesirable or uncomfortable ride. Such distortions can generate both vertical and lateral accelerations in a vehicle. Vertical acceleration is the major contributing factor to occupant comfort and derives from longitudinal distortion of the pavement profile. Roughness can create driver fatigue and therefore affects safety.

In the economic prospective, roughness is a very important issue. First, maintenance activities and treating roughness cost road agencies large amounts of money. Second, roughness has a significant impact on user costs for vehicle maintenance and repair (Papagiannakis et al., 1999).

As was mentioned in 3.2.2, AASHTO uses "serviceability" as the main performance criterion in pavement design. Studies in the AASHTO road test indicated that about 95% of pavement serviceability was attributed to the surface roughness (Haas et al., 1994). Serviceability can be conveniently estimated from a correlation with roughness measurements; however, serviceability is rather subjective and such correlation varies with time and region.

3.3.1. Roughness measurement

The definition of pavement roughness as distortion in the pavement surface generates the conclusion that road-roughness evaluation requires measurement of the longitudinal profile of the pavement in the vehicle wheel path. For engineering interpretation, roughness measurements are done by using a mathematical model that generates a summary statistic for the length of the pavement being evaluated. A variety of such summary statistics has been used, including various types of roughness index.

Roughness measurements of roadways were conducted and documented at the beginning of the 20th century (TAC Report, 2001). During the industrial era, automobile manufacturers studied the roughness of the roadways, with particular interest in the performance of vehicle suspension systems. Different devices were developed to measure the dynamic component of vehicle suspension. These measurements varied due to the devices being used; therefore, in 1960, the General Motors (GM) developed a vehicle-based profiler to quickly and accurately measure the roadway profile. This profiler was the forerunner of modern profilers. Following GM's profiler development, the National Cooperative Highway Research Program sponsored a project about different profiling systems, which included vehicle dynamic simulations. From these simulations, the researchers developed a set of parameters related to roughness that, best correlated with the field tests, which was a standard quarter car simulation model identified as golden car (NCHRP Report No. 228, 1978).

In 1982, the World Bank funded an experiment in Brazil. The focus of this study was to correlate and provide calibration standards for roadway-based roughness measurements. After this experiment, the golden car simulation was accepted as the basis for calculating a new roughness index with the additional constraint that the simulated vehicle survey speed was fixed at 80 km/h. This index was called "the International Roughness Index"(IRI). In 1990, the Federal Highway Administration (FHWA) in the United States was instrumental in the adoption and acceptance of the IRI by requiring state transportation agencies to report roughness for the Highway Performance Monitoring System (HPMS) by using the IRI. Over the years, the IRI became a widely used and internationally recognized index for roadway-surface roughness and is commonly used by transportation agencies for roughness measurement. Many agencies have adopted or are moving forward to adopt the IRI for a multitude of applications including the Pavement Management System (PMS).

IRI is calculated from the measured single longitudinal road profile by accumulating the outputs from a quarter-car model and dividing by the profile length to yield a summary roughness index with units of slope such as meter per kilometer or millimeter per meter. An IRI of 0 m/km means that the road is very smooth. The upper limits of IRI have no practical value; however, when IRI exceeds 8 m/km, it is almost impossible to drive on a normal speed.

In Canada, the Riding Comfort Index (RCI) is a subjective index to show the roughness of pavement that has been used for a long time; however, many of Canadian agencies are switching or have switched to the IRI for use in their PMS programs (TAC Report, 2001).

3.3.2. Roughness evaluation of the C-LTPP sections

There are several methods that can be used to predict service lives of the C-LTPP sections. One of them was the AASHTO design method, discussed in 3.2. Another approach is to consider specific pavement functionality or distresses such as roughness and rut to estimate the service life of overlay. In Section 3.3, it was attempted to evaluate pavement roughness in the C-LTPP sections.

The surface roughness of the C-LTPP sections is measured, and the measurements are collected every year. The basic measurements are made at 300 mm intervals for each wheel path by using the Dipstick profiler. RoadRuf software, which was developed at the University of Michigan Research Institute, is used to verify the roughness calculations (Tighe et al., 1999). The measurements are conducted during the fall season in order to reduce the variations caused by the season variability and weather condition. The roughness values for each wheel path are determined from these measurements and are collected in the C-LTPP database (*iri.sum*).

3.3.3. Analysis of the roughness trends for the C-LTPP sections

Transportation Association of Canada (TAC) recommended that IRI be calculated for each wheel path separately and then that the average value, termed as "Mean IRI" (MIRI), should be reported and used (TAC Report, 2001). Hence, the IRI data in the C-LTPP database for both wheel paths were used to calculate the average IRI in each year after overlay. In Appendix F, average IRI data versus time are presented for all the C-LTPP pavement sections. These graphs were prepared from the available data by year 2002. For most pavement sections, IRI data for almost one decade of pavement performance was available. However in some years, the reported roughness had no consistency with the pavement roughness, in the previous and following years. Such measurements were ignored in this study.

Even though the roughness progression in the studied period of time was rather low, pavement practitioners believe that a higher progression will occur in the future. For instance, in the LTPP project, it was reported that the flexible pavement roughness remained constant over the initial years of pavement performance and, at a certain point, showed a rapid increase (FHWA, 1998).

3.3.4. Prediction of future roughness in the C-LTPP project

Predictive equations are important tools that highway professionals use to design, maintain, and manage highway infrastructures. The purpose of a predictive equation, which also can be referred to as "a deterioration model", is to estimate the future rate of deterioration (TAC Report, 1997). Such models can be used to determine the remaining service life or the roughness in the future.

Many predicative models can be used to estimate the future roughness. Most have two common factors significantly influencing roughness: the initial roughness just after the overlay construction, and the age of the overlay. Any predictive model for roughness must meet the following considerations:

1- The roughness value must converge to the initial value at the time of construction or immediately after overlay ($t = 0$).

2- The slope of model cannot be negative since the roughness increases over time.

3- A nonlinear correlation must exist between pavement roughness and time.

In this study, it was attempted to predict roughness as a function of time. Three different mathematical functions were employed and calibrated for the C-LTPP data. The calibration procedure was performed by using the regression method to fit each model to the available C-LTPP data.

By using the roughness trends in Appendix F, the test sections that showed a decrease or a very slow increase in roughness over the time, such as test sections 820502-1, 820605-2, 830403-1, 840101-1, 850201-1, 850201-2, 850206-1, 900402-1, 900402-2, and 900802-3, were omitted from this part of study.

In some cases in the estimation of the service lives, no recorded value for the IRI_0 (pavement roughness immediately after resurfacing) was available. Generally, the IRI_0 is in the range of 0.8 to 1.2; therefore, for cases in which the IRI_0 was not available, the IRI_0 was assumed to be equal to 1 (mm/m) or equal to the first measured IRI after overlay if the first measurement was less than 1 (mm/m).

Three predictive models were considered in this study and are explained below:

3.3.4.1. Roughness-prediction model 1

Tighe et al. (1999) considered the following functional format that correlates roughness with time:

$$IRI = a \times e^{b.t} \qquad (3\text{-}11)$$

Their study was based on the information from 1990 until 1997; however, with more data available in the present study, the results could be different, and the coefficients of "a" and "b" may differ.

Equation 3-11 is one of the defaulted functions available in Microsoft Excel. This software was used to identify coefficients "a" and "b", which are presented with the roughness trends in Appendix D. The results for coefficients "a" and "b" are tabulated in Table 3-7.

3.3.4.2. Roughness-prediction model 2

In a joint C-SHRP/Quebec Bayesian application study, mentioned in 2.3, the general form proposed and practiced for roughness was the following (TAC Report, 1995):

$$R_t = R_0 + K_r \times A^n \quad (3\text{-}12)$$

where

R_t = Roughness at time t

R_0 = Initial roughness

K_r = Aggressiveness factor, which is a function of other pavement conditions such as pavement thickness, precipitation, freezing index, and frost susceptibility of subgrade soil

A = Age of the pavement

n = Coefficient of model

Hence, the following function form was considered for use as the second roughness model for this study:

$$IRI_t = IRI_0 + a \times t^b \quad (3\text{-}13)$$

in which IRI_t, IRI_0 and t have the same definition as they do in Equation 3-12. To determine coefficients "a" and "b" in this Equation, it was required to transform

Equation 3-13 to a linear model. The following transformation was used for this purpose:

$IRI_t - IRI_0 = a \times t^b$

$Ln(IRI_t - IRI_0) = Ln(a) + b\ Ln(t)$

$$Ln(IRI_t - IRI_0) = a' + b \times Ln(t) \qquad (3\text{-}14)$$

Consequently, the regression analysis was performed by using the transformed Ln(ΔIRI) as a function of Ln(t). Table 3-7 shows the results for coefficients "a" and "b" of roughness model 2 in all C-LTPP sections.

3.3.4.3. Roughness-prediction model 3

Another mathematical form that meets the conditions for roughness model, mentioned in 3.3.4, could be considered as the following:

$$IRI_t = IRI_0 + a \times t^2 \qquad (3\text{-}15)$$

Regression analysis was used to find the coefficients of following equation:

$\Delta IRI = a \times t^2 + b$

Table 3-7 summarizes the results of regression analysis for the roughness model 3 for each test section.

Table 3-7 shows that the coefficients for model 2 could not be obtained for some test sections because the initial IRI (IRI_0) was higher than the reported IRI during the following years, and the mathematical calculation for the transformed function of Ln(ΔIRI) was impossible [Ln (a)=N/A when a < 0].

		$IRI = a \times e^{b.t}$			$IRI_t = IRI_0 + a \times t^b$			$IRI = IRI_0 + a \times t^2 + b$		
C-SHRP ID	Section	a	b	R-square(%)	a	b	R-square(%)	a	b	R-square(%)
810404	1	1.343	0.024	90	0.770	-2.880	69	0.003	0.102	87
810404	2	1.096	0.035	59	1.215	-3.820	36	0.005	0.041	56
810404	3	1.176	0.021	64	2.130	-6.460	56	0.004	-0.038	81
810404	4	1.085	0.034	53	1.700	-5.700	17	0.007	-0.087	72
820205	1	0.751	0.085	80	0.870	-2.500	67	0.015	0.068	87
820205	2	0.959	0.026	35	-0.310	-1.880	81	0.003	0.042	20
820502	2	0.806	0.010	10	N/A	N/A	N/A	0.001	0.017	4
820605	1	1.193	0.011	36	0.370	-3.330	11	0.001	0.032	19
830403	2	1.151	0.020	41	0.920	-3.930	19	0.002	0.009	25
830403	3	1.329	0.011	13	N/A	N/A	N/A	0.002	-0.240	27
830801	1	0.877	0.028	3	N/A	N/A	N/A	0.001	-0.006	58
830801	2	0.958	0.029	57	0.724	-2.780	57	0.003	0.065	90
830801	3	1.409	0.015	22	0.550	-2.920	11	0.003	-0.023	78
830801	4	0.816	0.017	24	2.270	-6.430	76	0.001	0.057	56
840101	2	1.020	0.007	5	N/A	N/A	N/A	0.002	-0.025	47
840101	3	1.308	0.020	36	N/A	N/A	N/A	0.004	-0.114	37
840204	1	1.189	0.032	55	1.440	-4.330	17	0.006	-0.080	60
840204	2	1.158	0.037	45	1.180	-3.840	21	0.006	0.046	61
840604	1	1.145	0.039	75	2.850	-7.150	79	0.007	-0.131	28
840604	2	1.230	0.027	45	N/A	N/A	N/A	0.006	-0.310	96
840604	3	1.160	0.011	11	N/A	N/A	N/A	0.004	-0.311	65
840604	4	1.353	0.051	69	N/A	N/A	N/A	0.012	-0.300	91
850206	2	0.956	0.038	85	N/A	N/A	N/A	0.003	0.118	84
850601	1	0.810	0.027	81	0.800	-3.100	97	0.002	0.106	94
850601	2	0.832	0.021	75	0.700	-3.020	62	0.001	0.132	48
860501	1	1.440	0.066	90	1.180	-2.600	95	0.010	0.023	92
860501	2	1.241	0.020	56	0.280	-2.000	28	0.003	0.097	56
860501	3	1.098	0.025	75	0.410	-2.220	41	0.003	0.107	79
860603	1	1.555	0.042	85	0.550	-1.640	48	0.007	0.049	92
860603	2	1.346	0.038	75	0.360	-1.380	32	0.005	0.236	81
860603	3	1.270	0.041	70	0.470	-1.800	25	0.007	0.114	80
870102	1	0.752	0.090	95	1.100	-2.600	93	0.011	0.128	98
870102	2	1.053	0.104	83	2.620	-4.810	70	0.016	0.325	78
870504	1	0.971	0.031	71	0.750	-3.100	65	0.005	0.040	81
870504	2	0.868	0.027	60	0.540	-3.150	23	0.004	0.023	78
870505	1	0.858	0.034	85	0.980	-3.400	84	0.005	0.044	96
870505	2	0.876	0.028	67	0.840	-3.500	66	0.003	0.031	74
870505	3	0.778	0.014	11	0.910	-4.100	20	0.002	0.011	21
870701	1	1.187	0.035	88	0.950	-3.060	91	0.005	0.065	88
870701	2	0.755	0.035	76	0.910	-3.420	68	0.003	0.052	75
880203	1	1.080	0.041	55	0.790	-2.650	66	0.007	0.053	64
880203	2	0.918	0.072	59	0.740	-2.060	53	0.014	0.031	74
880203	3	0.897	0.060	76	0.790	-2.410	70	0.008	0.066	76
880203	4	1.032	0.019	42	0.600	-3.400	16	0.003	0.027	64

Table 3-7: Calculated coefficients "a" and "b" in roughness models (Continued)

		$IRI = a \times e^{b.t}$			$IRI_t = IRI_0 + a \times t^b$			$IRI = IRI_0 + a \times t^2 + b$		
C-SHRP ID	Section	a	b	R-square(%)	a	b	R-square(%)	a	b	R-square(%)
890503	1	0.927	0.065	76	3.700	-8.900	89	0.009	-0.274	92
890503	2	0.658	0.089	92	1.300	-3.100	85	0.008	0.167	90
890503	3	0.852	0.041	61	3.680	-10.000	43	0.005	-0.216	89
890503	4	0.739	0.053	81	2.230	-5.800	91	0.005	-0.009	75
890702	1	1.394	0.015	42	0.290	-2.780	18	0.001	0.057	28
890702	2	1.339	0.018	71	1.000	-3.620	80	0.003	0.047	84
900802	1	0.724	0.043	73	0.760	-3.270	60	0.004	0.016	77
900802	2	0.916	0.020	64	3.530	-10.000	94	0.002	-0.070	83
900803	1	0.900	0.032	77	1.420	-5.000	78	0.004	-0.024	90
900803	2	1.043	0.066	98	1.600	-3.700	92	0.009	0.076	96

Table 3-7: Calculated coefficients "a" and "b" in roughness models

A comparison between the R-square values in Table 3-7, showed that a higher correlation occurred between the measured IRI and the predicted IRI in model 3.

3.3.5. Service lives of the C-LTPP sections based on roughness

The "roughness trigger level" is defined as an IRI value at which a pavement section can be considered as a candidate for rehabilitation. In a survey performed by the Transportation Association of Canada (TAC), five Canadian agencies use roughness as a criterion for their rehabilitation, and seven of them combine roughness with other parameters.

In the literature, some attempts have been made to develop trigger values that could help to provide a uniform basis for the pavement performance evaluation and roadway classifications applicable to all across Canada, however it could be a challenge to obtain a nation wide consensus on the triggers values and they vary from jurisdiction to jurisdiction. TAC suggests a standard IRI scale for a hypothetical National Highway System (NHS) classification posted at 100 km/h, which is presented in Table 3-8 (TAC Report, 2001).

In establishing trigger values for maintenance and rehabilitation (M/R) based on roughness indices or IRI, it must be mentioned that the use of a value as a trigger criterion for identifying rehabilitation needs will have a significant effect on the feasible treatment methods.

Smoothness Categories	MIRI (mm/m)
Very Good	< 1.10
Good	1.10 ~ 1.60
Fair	1.61 ~ 2.50
Poor	2.51 ~ 3.50
Very Poor	> 3.50

Table 3-8: The prototype smoothness categories based on the MIRI (TAC report, 2001)

For example, a higher level of the maximum acceptable IRI trigger may preclude a thin overlay and require extensive treatments. Therefore, establishing IRI trigger values for all the Canadian highway agencies, with their unique infrastructure needs, characteristics, and available resources, may not be either feasible or practical (TAC Report, 2001).

From Table 3-8, two roughness trigger values, 3 and 3.5 mm/m, were employed in order to determine the service lives of the C-LTPP test sections by using the developed models. The results are presented in Table 3-9.

From Table 3-9, It can be seen that a lower trigger of IRI=3 mm/m for pavement roughness (comparing to IRI= 3.5 mm/m) resulted in higher service lives for all models, which was expected.

		Estimated service life (years)					
		Model 1		Model 2		Model 3	
		$IRI = a \times e^{b.t}$		$IRI_t = IRI_0 + a \times t^b$		$IRI = IRI_0 + a \times t^2 + b$	
C-SHRP ID	Section	IRI=3.5(mm/m)	IRI=3 (mm/m)	IRI=3.5(mm/m)	IRI=3 (mm/m)	IRI=3.5(mm/m)	IRI=3 (mm/m)
810404	1	39.3	32.9	50+	50+	25.8	22.5
810404	2	33.1	28.7	47.4	39.0	21.6	19.2
810404	3	50+	44.0	30.5	27.2	25.0	22.2
810404	4	34.2	29.7	47.1	40.9	19.2	17.1
820205	1	18.1	16.3	50+	42.7	13.1	11.8
820205	2	50+	44.7	0.0	0.0	29.1	26.1
820502	2	50+	50+	N/A	N/A	50+	50+
820605	1	50+	50+	50+	50+	45.4	40.5
830403	2	50+	48.9	50+	50+	34.7	30.7
830403	3	50+	50+	N/A	N/A	32.3	28.3
830801	1	49.1	43.6	N/A	N/A	50+	46.7
830801	2	45.3	39.9	50+	50+	28.1	25.2
830801	3	50+	50+	50+	50+	26.2	23.0
830801	4	50+	50+	26.5	24.2	45.4	40.9
840101	2	50+	50+	N/A	N/A	32.4	29.0
840101	3	49.5	41.7	N/A	N/A	24.9	21.9
840204	1	33.6	28.8	35.1	29.4	19.9	17.6
840204	2	30.1	25.9	50+	46.6	19.9	17.8
840604	1	28.6	24.7	16.2	14.8	18.4	16.3
840604	2	39.2	33.4	N/A	N/A	19.3	17.1
840604	3	50+	50+	N/A	N/A	26.2	23.3
840604	4	18.8	15.8	N/A	N/A	13.4	11.7
850206	2	33.8	29.8	N/A	N/A	27.2	24.2
850601	1	50+	48.0	50+	50+	39.4	35.5
850601	2	50+	50+	50+	50+	50+	45.6
860501	1	13.5	11.2	16.7	13.1	14.2	12.4
860501	2	50+	43.5	50+	50+	29.7	26.1
860501	3	45.8	39.7	50+	50+	29.4	26.1
870102	2	11.6	10.1	8.9	8.2	11.7	10.2
870504	1	41.1	36.2	50+	50+	23.1	20.6
870504	2	50+	45.4	50+	50+	25.9	23.2
870505	1	40.9	36.4	50+	50+	23.8	21.4
870505	2	49.5	44.0	50+	50+	27.8	25.0
870505	3	50+	50+	50+	50+	37.8	34.2
870701	1	31.3	26.8	50+	50+	21.2	18.9
870701	2	43.3	39.0	50+	50+	27.9	25.1
880203	1	28.4	24.7	50+	50+	19.1	17.0
880203	2	18.6	16.5	50+	41.3	13.3	11.9
880203	3	22.6	20.0	50+	50+	17.0	15.2
880203	4	50+	50+	50+	50+	30.8	27.5

Table 3-9: Estimated service lives of the C-LTPP test sections by using the developed models for roughness (Continued)

		Estimated service life (years)					
		Model 1		Model 2		Model 3	
		$IRI = a \times e^{b.t}$		$IRI_t = IRI_0 + a \times t^b$		$IRI = IRI_0 + a \times t^2 + b$	
C-SHRP ID	Section	IRI=3.5(mm/m)	IRI=3 (mm/m)	IRI=3.5(mm/m)	IRI=3 (mm/m)	IRI=3.5(mm/m)	IRI=3 (mm/m)
890503	1	20.5	18.1	13.9	13.0	16.6	14.9
890503	2	18.8	17.1	23.0	19.6	18.1	16.2
890503	3	34.5	30.7	19.3	18.1	23.0	20.7
890503	4	29.2	26.3	20.9	19.1	24.2	21.8
890702	1	50+	50+	50+	50+	49.4	44.1
890702	2	50+	44.3	50+	50+	29.1	26.0
900802	1	37.1	33.5	50+	50+	26.2	23.7
900802	2	50+	50+	22.0	20.7	32.8	29.4
900803	1	42.3	37.5	50+	50+	26.4	23.7
900803	2	18.3	15.9	17.5	15.1	15.9	14.1

Table 3-9: Estimated service lives of the C-LTPP test sections by using the developed models for roughness

Comparing the three roughness models for estimating service lives of the C-LTPP sections, it was observed that the results from model 3 were closest to the expectations for an overlay's service life, which is in the range of 15-25 years. Generally, pavements deteriorate faster during the second decade of performance than during the first decade because of the increase in traffic, the developing cracks, and the other damages to the pavement.

The estimated service lives obtained by using model 3 showed that most of the C-LTPP test sections had an acceptable roughness performance and that only six test sections needed roughness rehabilitation in less than 15 years after the overlay: 820205-1(BC), 840604-4(NB), 860501-1(NS), 870102-1(ON), 880203-2(PE), and 900803-2(SK). Based on the experimental design of the C-LTPP project (Table 2-1), it was observed that these test sections were located in various climate, traffic, and pavement material conditions. The only similar attribute for three of them (test sections 820205-1, 840604-4, and 860501-1) was that they had a thin overlay in the range of 30-60 mm.

Figure 3-8 represents the service-lives results for the agency-designed test sections by using an ascending graphical format based on model 3. In Figure 3-8, for test sections located in low traffic zone (traffic <200,000 ESAL per year), the service lives are estimated related to an IRI trigger value equal to 3.5 mm/m, and for sections located in high traffic zone (traffic >200,000 ESAL per year), service lives are estimated related to an IRI trigger value equal to 3.0 mm/m. Using two different roughness threshold values to estimate the service lives could help to reach a more realistic approach that can reflect the importance of high class roads with extensive traffic streams, which are usually in highway agencies' priorities for M/R.

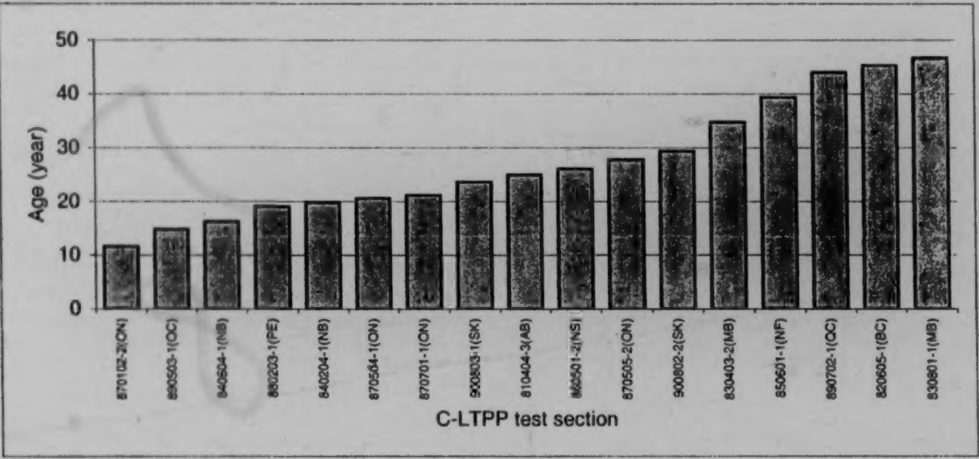

Figure 3-8: Service lives of the agency-designed test sections in the C-LTPP project, based on the IRI trend analysis (excluding test sections with service lives >50 years)

From Figure 3-8, only two agency-designed sections, sections 870102-2 (ON) and 890503-1 (QC), showed a service life of less than 15 years. The experimental design of the C-LTPP program (Table 2-1), reveals that test section 870102-2 is classified as a section with low traffic, 30-60 mm overlay thickness with HMAC, wet-no freeze weather climates, and fine subgrade aggregate. Test section 890503-1 is classified as a section with high traffic, 30-60 mm overlay thickness with HMAC, wet-high freeze weather condition, and coarse subgrade. The only attribute that both test sections 870102-2 and 890503-1 had in common is the overlay thickness of 30-60 mm and wet weather condition. The test sections with thin overlays in wet climate appeared to have deteriorated faster than other sections.

Based on the available data from the C-LTPP program until the year 2002, and considering the different prediction models used for roughness progression, roughness, based on the IRI, did not appear to be the main factor for pavement failure in the C-LTPP project.

These findings must be reviewed and then confirmed by using additional data in the future. Normally, pavements show a higher rate of deterioration after the first ten years of service than they show during their first ten years. Therefore, it is recommended that with more available data the in future, the presented models must be re-calibrated.

3.4. Rutting evaluation of the C-LTPP sections

In Section 3.3, the functionality of the C-LTPP sections based on the pavement roughness was studied. Another criterion for the functional behavior of pavement is rut, which could be used to estimate the service lives of the C-LTPP sections.

3.4.1. Rut definition, its importance, and measurement

Rut is the permanent deformation of flexible pavement, which is recognized as the most common problem in flexible pavements (Hesham et al., 1998). Since the early 1980s, rut has been considered a main distress and deterioration mechanism in North America. A main part of Transportation Association of Canada's annual conference in 1988, was devoted to the "Rutting and frost problems"(RTAC, 1998). One year later, TAC conducted pavement-rutting seminars in various locations across Canada in order to provide some information about this performance criterion for the Canadian highway agencies. For most of the Canadian provincial agencies, developing solutions to decrease pavement rut was a high priority (TAC Report, 2001). Rut is a major problem for municipalities' roads and especially at intersections.

Safety is a main concern that justifies the importance of rut study, since rut is one of the main components of pavement safety and can be of concern for at least two reasons (Sousa et al., 1991):

1) The ruts trap water and, at depths of about 5 mm, hydroplaning (particularly for passenger cars) is a definite threat.

2) As the rut progresses in depth, steering becomes increasingly difficult, leading to added safety concerns.

During the last two decades, there have been significant researches regarding pavement rut. A comprehensive review of mechanism, models, and performance tests for asphalt pavement rut, was reported by Sousa et al. (1991) during SHRP study. Some of the literatures about mechanism of rut and the factors that are significantly involved in pavement rutting are presented here.

Rutting in pavement materials develops gradually with an increasing number of load applications and is caused by a combination of densification and shear deformation that may occur in one or any paving layer or subgrade. The studies based on the AASHTO road test revealed that the shear deformation rather than the densification is the primary rutting mechanism (Sousa et al., 1991).

Emery et al., (1990) recognized different types of rutting that might happen in pavement, either separately or in combination:

1- Instability rutting: This kind of rut usually happens in the wheel path and mainly because of the lateral displacement of material in the paving layer. Frequent heavy loading on an asphalt concrete layer that does not meet a certain level of adequacy in material properties is the main reason for this type of rutting.

2- Wear rutting: It occurs when there is a loss of coated aggregate particles from the pavement surface and could be caused by a combination of construction deficiencies, and environmental, and traffic influences.

3- Structural rutting: This kind of rut is caused by the permanent deformation of the paving layers.

Overall, it is accepted that most of the pavement rutting is confined to the non-subgrade layers (Hesham et al., 1998).

Asphalt mixture properties have a significant role in pavement rutting. Sousa et al. (1991) classified the main asphalt mixture factors that contribute in rutting as follows:

1- Aggregate characteristics such as surface texture, gradation, shape, and size of particles;

2- Binder characteristics such as stiffness;

3- Mixture characteristics such as binder content, air void;

4- Field conditions such as temperature, traffic, and moisture.

There are different indices for rut depth measurement. These indices are 1.2 m straight edge, 1.8 m straight edge, 3.7 m straight edge, 5-points, 11-points, fill area, and the maximum rut depth. A brief explanation for each index is presented below (EBA Engineering Consultants, 2001):

In the maximum rut depth, the centerline is identified as the point of highest elevation in an area ±0.6 m from the physical centre point of the profile. A straight line is then placed between the located centre of the lane and each roadway edge such that the chord touches the roadway profile at a maximum of two locations. The rut depth is calculated as the maximum difference between the chords and the roadway.

In the 1.2 m straight edge rut, the centre of the lane is identified as the point of highest elevation in an area of ±0.6 m from the physical centre point of the cross section profile. A straight line of 1.2 m length is placed in contact with the roadway profile at a maximum of two points from the roadway edge to the centre of lane. At each location, the rut depth is calculated as the maximum difference between the chord and the measured profile. A similar definition applies to the 1.8 m straight edge and 3.7 m straight edge indices, except that the rut measurements are limited to 1.8 m and 3.7 m straight edges, respectively. Figure 3-9 shows the 1.8 m and 3.7 m straight edge indices in an illustration.

In the five-point rut depth, a discrete five-point profile sampling method for rut depth measurements is simulated. The centre of the lane is identified as the point of highest elevation in an area of ±0.6 m from the physical center point of the profile. The sample offsets based on typical inertial profiler configurations used are ±1420, ±840 and 0 mm relative to the centre lane. The rut measurement chord is established from the centre of lane to a point 1240 mm towards each roadway edge and profile

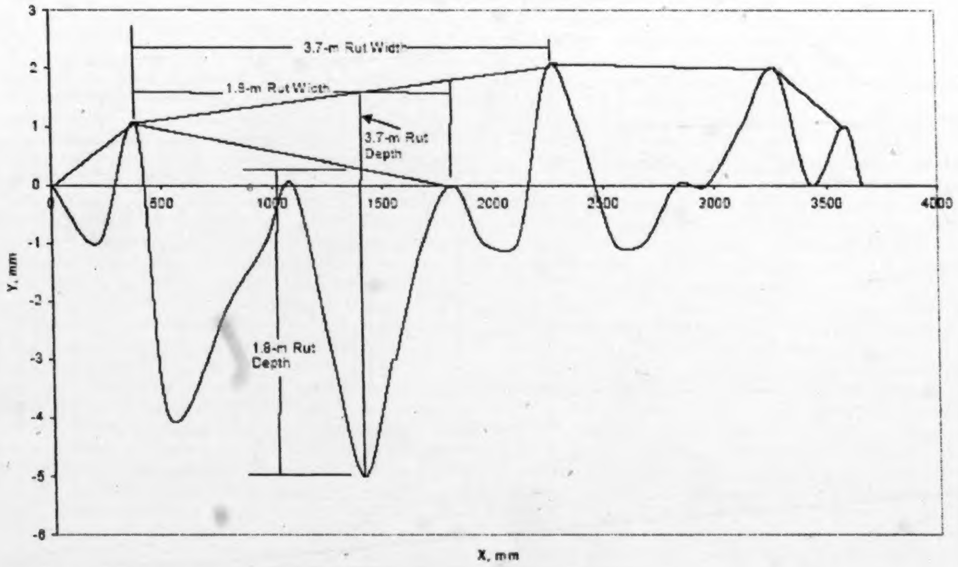

Figure 3-9: 1.8 m and 3.7 m straight edge indices for rut measurement

(EBA Engineering Consultants Ltd., 2001)

depth is determined at an offset of 840 mm. The rut depth is calculated as the maximum difference between the chord and the measured profile. A similar definition applies to 11-point rut depth except that the sample offsets are ±1600, ±1200, ± 900, ±600, ±300, and 0 mm relative to the centre lane.

The fill area approach is similar to that of the maximum rut depth except that the fill area is calculated as the area above the roadway profile and below the chord.

It must be mentioned that different indices give different rut results. Simpson (1995) studied the correlation between different rut indices and found that 1.8 m straight edge has the best correlation with other indices. Similar conclusion was found in the EBA study (2001).

In the C-LTPP project, the Dipstick profiler is used to collect the transverse profile data at 50-mm intervals at six equally spaced stations along each 150 m of test section. The stations were permanently marked to ensure the same station is profiled each year (EBA Engineering Consultants, 2001). In the C-LTPP program, different rut measurements are available, however the rut summary data is based on 1.2 m straight edge rut.

3.4.2. Rut progression in asphalt pavement

The prediction of the future condition of pavement and the progression of distresses such as rut is an essential element of a PMS. Such prediction can help highway agencies to use preventive maintenance activities to prevent large expenditures of money and to provide higher serviceability to the road users in the future.

The development of rut-prediction models is crucial for rut evaluation in the C-LTPP project. Generally, the progression of pavement deformation versus traffic or time has three stages (Carpenter, 1993), and (Ullidtz, 1987): densification, rut, and tertiary (see Figure 3-10).

Many researchers have considered a linear relationship over time for rut progression. Monismith (1976), Kenis (1976), Krutz (1990), and Witczak (1998) used laboratory data and observed that rut increases rapidly during the initial phase of loading but then develops slowly with time. Archilla et al. (2001), Kim et al. (2000), and Carpenter (1993) also reported a linear rut progression by using field data in their studies.

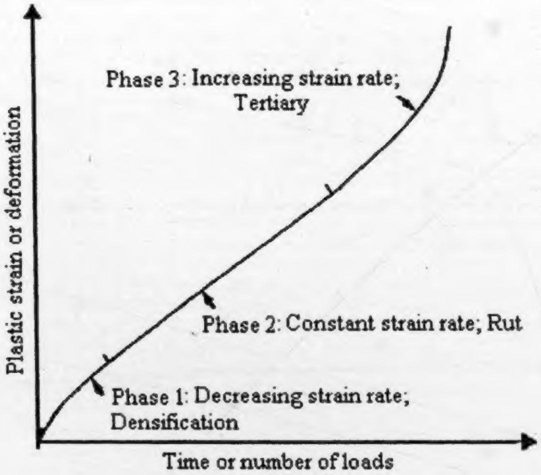
Plastic strain or deformation
Phase 3: Increasing strain rate; Tertiary
Phase 2: Constant strain rate; Rut
Phase 1: Decreasing strain rate; Densification
Time or number of loads

Figure 3-10: Different stages of rut

In addition, the EBA study (2001), considered a linear relationship for rut progression by time for the C-LTPP sections. Generally, pavement rutting develops most quickly after the opening of the road, but after leveling the roughness and rutting, only small plastic deformations will develop by time (Ullidtz, 1987).

3.4.3. Analysis of rutting for the C-LTPP sections

For the C-LTPP project, plots of rut progress versus time were provided for all test sections (see Appendix G). While analyzing the rut data for the C-LTPP project, some inconsistencies were observed. For some C-LTPP sections, the measured rut versus time showed zero or negative slopes. Additionally, some collected rut data were not consistent with the expected trend before or after that year's data. Overall, for most of the C-LTPP test sections, rut data from 9-11 years of pavement performance were available.

As it can be seen from the plots of rut versus time in Appendix G, the rut progression has been rather linear over time after almost one decade of pavement service and a linear relationship between rut and age of overlay could be developed. Considering the explanations for rut progression in 3.4.2, the rut in the C-LTPP program could conveniently be presented by a linear mathematical function such as

$$Rut_t = a \times t + b \tag{3-16}$$

where t is the age after overlay, and "a" and "b" are the coefficients of the model. Using Microsoft Excel, coefficients "a" and "b" were identified for each test section. The results are provided in Table 3-10.

3.4.4. Service lives of the C-LTPP sections, based on rut

Similar to the description of "roughness trigger" in Section 3.3.5, the definition of "rut trigger value" is a rut-measurement level, which a pavement section can be considered as a candidate for rehabilitation. Using such a value for the rut study could provide a uniform basis for evaluating rut; however, obtaining a nation-wide consensus for the rut triggers values could be difficult.

		Regression constants		Expected service life (years)	
C-SHRP ID	Section	a	b	Rut =15mm	Rut =25mm
810404	1	0.0466	1.910	50+	50+
810404	2	0.0078	2.705	50+	50+
810404	3	0.0345	2.460	50+	50+
810404	4	0.0331	1.910	50+	50+
820205	1	0.155	0.365	50+	50+
820205	2	0.165	0.355	50+	50+
820502	1	0.661	2.211	19.3	34.5
820502	2	0.391	0.606	36.8	50+
820605	1	0.546	1.696	24.3	42.7
820605	2	0.510	1.480	26.5	46.1
830403	1	0.0391	1.070	50+	50+
830403	2	0.0328	1.110	50+	50+
830403	3	0.0189	0.910	50+	50+
830801	1	0.411	2.967	29.3	50+
830801	2	0.326	1.090	42.7	50+
830801	3	0.427	0.671	33.6	50+
830801	4	0.445	1.385	30.6	50+
840101	1	0.0466	1.907	50+	50+
840101	2	1.146	-0.067	13.1	21.9
840101	3	0.999	-0.310	15.3	25.3
840204	1	0.445	1.931	29.4	50+
840204	2	0.338	0.977	41.5	50+
840604	1	0.930	1.142	14.9	25.7
840604	2	0.770	1.088	18.1	31.1
840604	3	0.587	2.047	22.1	39.1
840604	4	0.703	2.385	17.9	32.2
850201	1	0.704	-0.785	22.4	36.6
850201	2	0.669	-0.010	22.4	37.4
850206	1	0.055	2.336	50+	50+
850206	2	0.145	0.748	50+	50+
850601	1	0.831	4.791	12.3	24.3
850601	2	0.705	2.132	18.3	32.4
860501	1	1.855	3.756	6.1	11.5
860501	2	0.602	2.408	20.9	37.5
860501	3	0.435	2.844	28.0	50+
860603	1	0.430	6.519	19.7	43.0
860603	2	0.707	4.608	14.7	28.9
860603	3	0.662	5.017	15.1	30.2
870102	1	0.316	0.852	44.8	50+
870102	2	0.627	0.312	23.4	39.3
870504	1	0.222	2.446	50+	50+
870504	2	0.344	3.166	34.4	50+
870505	1	0.346	0.688	41.4	50+
870505	2	0.311	0.919	45.3	50+
870505	3	0.215	0.764	50+	50+
870505	4	0.384	0.983	36.5	50+

Table 3-10: Coefficients of Equation 3-14 and the estimated service lives for two levels of rutting in all the C-LTPP test sections (Continued)

		Regression constants		Expected service life (years)	
C-SHRP ID	Section	a	b	Rut =15mm	Rut =25mm
870701	1	0.0339	0.704	50+	50+
870701	2	0.124	0.355	50+	50+
880203	1	0.297	0.905	47.5	50+
880203	2	0.422	0.527	34.3	50+
880203	3	0.166	1.904	50+	50+
880203	4	0.175	0.944	50+	50+
890503	1	1.470	-1.650	11.3	18.1
890503	2	1.360	-1.379	12.0	19.4
890503	3	1.380	-0.533	11.3	18.5
890503	4	1.073	-0.792	14.7	24.0
890702	1	0.556	2.157	23.1	41.1
890702	2	0.442	1.043	31.6	50+
900402	1	0.123	2.321	50+	50+
900402	2	0.25	2.240	50+	50+
900802	1	-.0609	5.810	50+	50+
900802	2	-0.0532	5.390	50+	50+
900802	3	0.120	3.322	50+	50+
900803	1	0.153	1.238	50+	50+
900803	2	0.186	1.061	50+	50+

Table 3-10: Coefficients of Equation 3-14 and the estimated service lives for two levels of rutting in all the C-LTPP test sections

Highway agencies use a maximum rut depth or a combination of rut depth and other distresses as a trigger value for M/R. However no widely accepted definition of "final acceptable rutting value" exists, for its meaning varies in different jurisdictions. For instance, the Asphalt Institute model considers 12.7 mm as a failure level (AI, 1982), while the Alberta Transportation and Utilities (AT&U) uses the trigger value of 15 mm as the extreme rut (AT&U, 1997). Other highway agencies use other trigger values in accordance to their unique conditions and available budgets. As well, the trigger value can be also a function of the type of the road.

For the purpose of this study, two maximum acceptable rut triggers were considered in order to estimate the service lives of the C-LTPP sections. These two levels cover different agencies' policies and road types in Canada. For high-class roads, the trigger value of 15 mm was employed, and for the low-class roads, the final acceptable rut was set to 25 mm. The last column of Table 3-10 presented the results for the estimated service lives based on each trigger value for rut, respectively.

Some test sections showed a lower service life compared to those of other test sections. These test sections were: 840101-2(NB), 840101-3(NB), 840604-1(NB), 850601-1(NF), 860501-1(NS), and particularly the test sections located in site 890503 (QC). The C-LTPP experimental design in Table 2-1, reveals that all the above test sections are located in areas with wet-weather condition. Except for one test section (850601-1), all the test sections are in high-traffic area. Also, except for test section (860501-1), all the sections have a coarse subgrade aggregate.

Figure 3-11 represents, in an ascending sorted graphical format, the service lives for the agency-designed test sections. The test sections with service lives of more than 50 years are not shown in Figure 3-11. For test sections that are located in low-traffic zone the service lives based on rutting trigger equal to 25 mm and for those located in high-traffic zone service lives based on rutting trigger equal to 15 mm are presented. (The traffic level for each test section was taken from Table 2-1.)

Figure 3-8 shows that the agency-designed test sections 890503-1(QC) and 840604-1(NB) had service lives of less than 15 years.

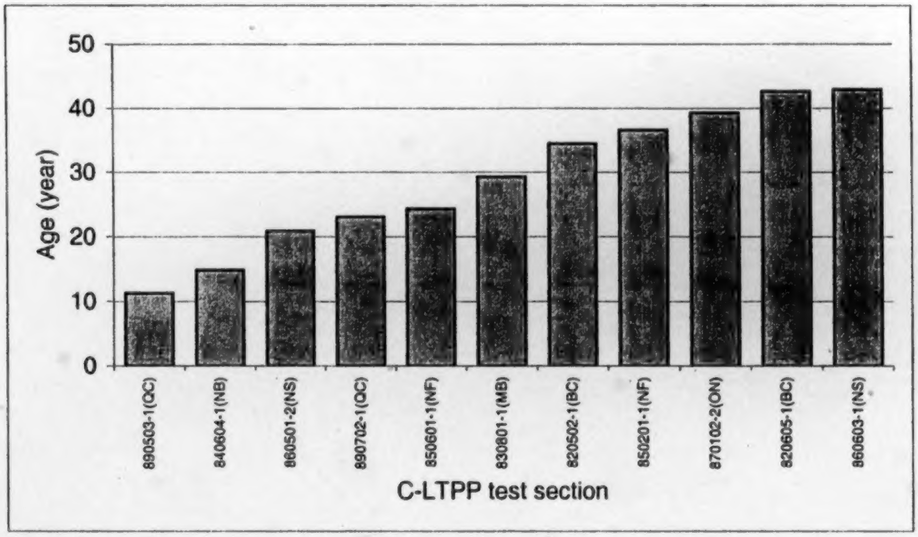

Figure 3-11: Service lives of agency-designed test sections in the C-LTPP project, based on rut trend analysis (excluding test sections with service lives >50 years)

By considering the C-LTPP experimental design, Table 2-1, it may reveal that traffic, weather condition (moisture), and subgrade material are the main factors affecting rut progression. Hence, the test sections located in site 890503(QC) with high traffic, wet-weather condition, and coarse subgrade material had the worst rut performance. There is possibility that other mixture and pavement factors that are not shown in Table 2-1 be responsible for the low service life in these test sections.

Generally, it was observed that for most of the C-LTPP test sections, rut was not a critical criterion in pavement failure. This finding is comparable with the results of the rut study in the LTPP program in the USA. FHWA (2000) reported that although rut is a problem nationwide, it was not a significant problem in the LTPP test sections. For the majority of asphalt overlays in the LTPP program, rutting became serious enough to require rehabilitation only after 15 years or more (FHWA-RD-00-165, 2000).

Another reason is that all the C-LTPP sections are located in rural areas and they do not experience low speed traffic like the urban roads.

3.5. Evaluation of the C-LTPP sections, based on a Mechanistic-Empirical (M-E) approach

Since 1950s, when the techniques for analyzing pavement response to loading became available, many attempts have been made to develop rational design procedures to define and describe the development of distresses in pavements (Hesham et al., 1998). The result of such procedures led to the models referred to as "Mechanistic-Empirical (M-E) models". Pavement engineers have been advocating a movement toward M-E design models, and even the proposed revision of the AASHTO guide for the deign of pavement structures will be based on M-E models.

Generally, M-E models correlate traffic load to the stress or strain in the pavement layers and confine the total traffic with a threshold value for pavement distress. Therefore, M-E models can be used to estimate the service life of pavement for the total traffic from M-E models.

Among several M-E procedures, the Asphalt Institute and Shell models are two well-known and practical M-E models that can be used to predict pavement rutting and fatigue cracking. These models were developed based on the mechanistic multilayer theory in conjunction with empirical failure criteria (Huang, 1993).

In these models, the development of pavement rutting is attributed to the repeated load application and the compressive strain at the top of the subgrade. The general form of these models for rutting is as below (Huang, 1993):

$N_d = a\,(\varepsilon_c)^{-b}$ (3-17)

where

N_d= Allowable number of load repetition for a limited rut of 12.7 mm.

ε_c= Compressive strain at the top of subgrade

a, b = Coefficients of the model

Table 3-11 summarizes the coefficients in Equation 3-17 used by different agencies:

Agency	a	b	Rut depth (mm)
Asphalt Institute	1.365×10^{-9}	4.477	12.7
Shell 50% reliability	6.15×10^{-7}	4	12.7
Shell 85% reliability	1.94×10^{-7}	4	12.7
Shell 95% reliability	1.05×10^{-7}	4	12.7
Transport and road research laboratory, 85% reliability	6.18×10^{-8}	3.95	10.2
Belgian road research centre	3.05×10^{-9}	4.35	10.2

Table 3-11: The coefficients used by various agencies for Equation 3-15 (Huang, 1993)

For fatigue cracking, the allowable number of the load repetition is related to the tensile strain at the bottom of the asphalt layer and can be presented by the following Equation (Huang, 1993):

$N_f = a\,(\varepsilon_t)^{-b}\,(E_{ac})^{-c}$ (3-18)

where

N_f= Allowable number of load repetition for a limited level of fatigue cracking (20% of area cracked)

ε_t= Tensile strain at the bottom of asphalt layer

E_{ac}= Modulus of asphalt layer (psi)

a, b, c = Coefficients of the model

Coefficients “a” and “b” and “c” are presented in Table 3-12. This table also summarizes the coefficients in Equation 3-18 used by different agencies:

Agency	a	b	c
Asphalt Institute	0.0796	3.291	0.854
Shell	0.0685	5.671	2.363
Illinois DOT	5×10^{-6}	3	0
Transport and road research laboratory	1.66×10^{-10}	4.32	0
Belgian road research centre	4.92×10^{-14}	4.76	0

Table 3-12: The coefficients used by various agencies for Equation 3-16 (Huang, 1993)

Equations 3-17 and 3-18 show, the compressive strain at the top of the subgrade and the tensile strain at the bottom of the asphalt layer are the main pavement responses for a M-E evaluation of pavement based on distresses such as rut and fatigue cracking. Therefore, to evaluate pavement service life, one must calculate the compressive strain at the top of the subgrade and the tensile strain at the bottom of the asphalt layer.

3.5.1. Pavement analysis of the C-LTPP sections

In Section 3.2.1, the backcalculation software was used in order to determine the pavement layer properties from FWD data. By using the thicknesses and moduli of pavement layers, the compressive strain at the top of the subgrade and the tensile strain at the bottom of the asphalt layer can be calculated by using EVERSTRESS software. This pavement-analysis program uses the same assumptions of EVERCALC, discussed in 3.2.1.2.

To confirm the outputs from EVERSTRESS, another pavement analysis program, ELSYM5, was employed. The compressive strain at the top of subgrade and the tensile strain at the bottom of asphalt layer from EVERSTRESS and ELSYM5 are tabulated in Table 3-13. (See Appendix H for a sample of the outputs from the two programs)

		Compressive Strain at top of subgrade, E-6		Tensile Strain at bottom of asphalt, E-6	
C-SHRP ID	Section	EVERSTRESS	ELSYM5	EVERSTRESS	ELSYM5
810404	1	475	224	223	184
810404	2	205	204	183	184
810404	3	195	193	175	175
810404	4	476	284	268	268
820205	1	NO FWD	NO FWD	NO FWD	NO FWD
820205	2	NO FWD	NO FWD	NO FWD	NO FWD
820502	1	27	26	120	120
820502	2	42	32	110	110
820605	1	63	62	89	89
820605	2	54	53	91	90
830403	1	423	362	235	171
830403	2	322	321	168	142
830403	3	246	242	137	136
830801	1	136	136	167	167
830801	2	243	206	269	269
830801	3	259	188	244	244
830801	4	147	112	122	122
840101	1	134	135	112	112
840101	2	83	82	72	72
840101	3	163	163	139	139
840204	1	337	336	194	195
840204	2	590	591	334	334
840604	1	178	151	166	166
840604	2	142	142	137	137
840604	3	137	136	132	132
840604	4	121	120	116	116
850201	1	146	146	261	261
850201	2	156	156	248	248
850206	1	112	111	201	202
850206	2	126	126	193	192
850601	1	110	109	181	181
850601	2	92	125	208	208
860501	1	284	286	237	238
860501	2	221	221	185	185
860501	3	320	320	290	289

Table 3-13: Results of EVERSTRESS and ELSYM5 for tensile strain at the bottom of the asphalt layer and the compressive strain at the top of the subgrade (Continued)

		Compressive Strain at top of subgrade, E-6		Tensile Strain at bottom of asphalt, E-6	
C-SHRP ID	Section	EVERSTRESS	ELSYM5	EVERSTRESS	ELSYM5
860603	1	94	136	258	258
860603	2	112	126	215	215
860603	3	130	130	227	227
870102	1	237	235	359	357
870102	2	265	262	439	438
870504	1	97	384	164	164
870504	2	65	64	138	138
870505	1	172	168	254	254
870505	2	129	171	206	203
870505	3	106	105	144	144
870505	4	247	207	389	389
870701	1	81	80	164	165
870701	2	33	29	26	26
880203	1	2418	2418	475	475
880203	2	2577	2603	447	447
880203	3	2275	2260	422	420
880203	4	1176	1183	273	273
890503	1	33	33	298	298
890503	2	37	30	121	121
890503	3	24	22	103	103
890503	4	29	29	80	80
890702	1	70	68	154	154
890702	2	63	61	133	133
900402	1	702	450	364	364
900402	2	339	339	283	284
900802	1	751	600	441	441
900802	2	516	517	366	366
900802	3	439	321	234	234
900803	1	246	245	128	129
900803	2	477	479	210	210

Table 3-13: Results of EVERSTRESS and ELSYM5 for tensile strain at the bottom of the asphalt layer and the compressive strain at the top of the subgrade

Figure 3-12 provides a comparison of the results from EVERSTRESS and ELSYM5, based on the line of equity. As Figure 3-12 shows, the results from two programs for tensile strain at the bottom of the asphalt layer and compressive strain at the top of the subgrade were highly consistent.

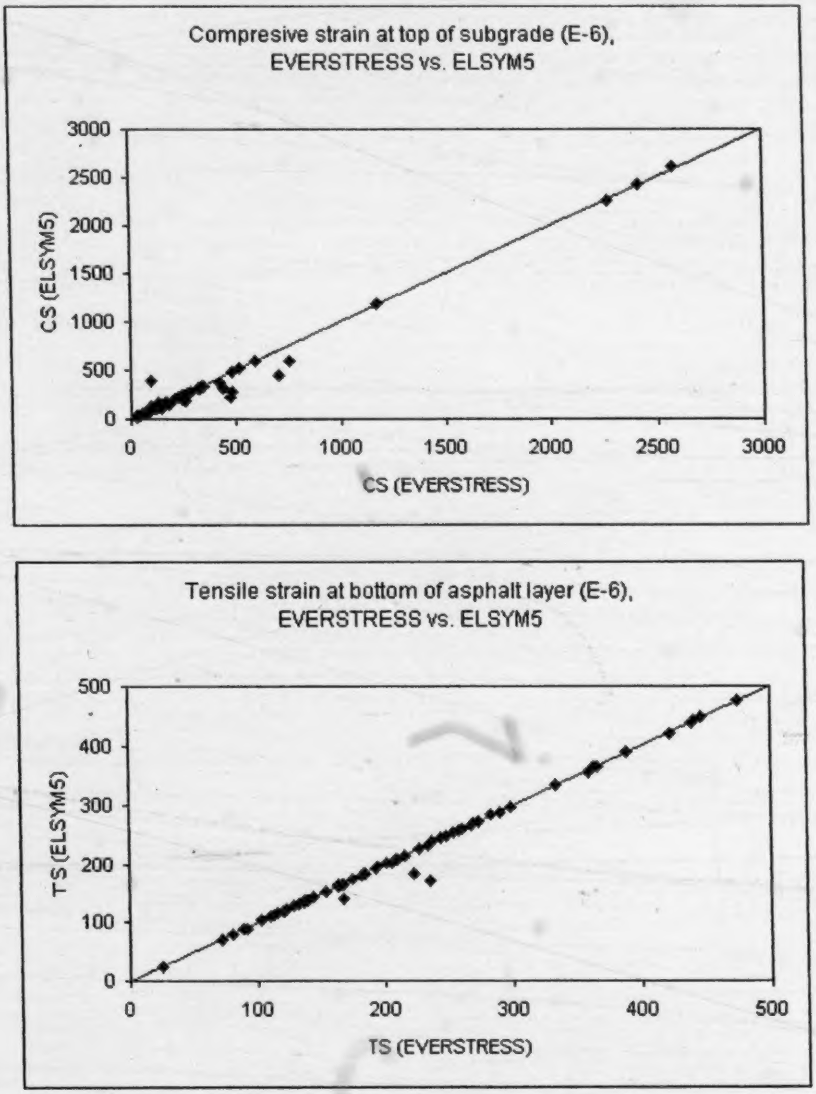

Figure 3-12: Comparison of results from EVERSTRESS and ELSYM5

3.5.2. Service lives of the C-LTPP sections, based on M-E models for rut

Calculated compressive strain at the top of subgrade from EVERSTRESS, were used to predict the allowable traffics based on Equation 3-17 for a maximum rut.

Resulted traffics in all the C-LTPP sections are presented in Table 3-14 for both AI and Shell models. Using Equation 3-10, service lives for all the C-LTPP sections were calculated. In calculating service life the traffic growth factor of 3% was considered. Estimated service lives are shown in Table 3-14 for both AI and Shell models.

For most of the test sections, both Asphalt Institute and Shell models predicted a high service life of more than 50 years (50+), however, it was observed that these models did not provide a realistic estimation of the service lives in the C-LTPP program for pavement rutting.

ERES Consultants, Ltd. reported that the AI and Shell models were not able to estimate the rutting of the LTPP sections accurately and that these models could be applied only to pavement sections not exhibiting permanent deformation in any of the layers above the subgrade (ERES Engineering Consultants Ltd., 1999).

In another study using the LTPP data, Hesham et al. (1998) used the AI and Shell models to predict the development of rutting for 61 LTPP test sections. The rutting damages calculated by using these models did not appear to be good predictors of the observed rutting depth. The researchers concluded that the AI model assumes that all the layers above the subgrade do not contribute much to rutting; however, a significant contribution to rutting by other non-subgrade layers was found. Data from the AASHTO road-test experiment showed that the subgrade contributes only about 9% of the total measured rut.

			Compressive Strain	AI model		Shell model	
C-SHRP ID	Section	ESAL(first year)	on top of SG E-6	Nd	year	Nd	year
810404	1	183714	475	1.03E+06	5.3	2.06E+06	9.8
810404	2	183714	205	4.44E+07	50+	5.95E+07	50+
810404	3	183714	195	5.55E+07	50+	7.26E+07	50+
810404	4	183714	476	1.02E+06	5.2	2.05E+06	9.7
820205	1	-	NO FWD	-	-	-	-
820205	2	-	NO FWD	-	-	-	-
820502	1	239963	27	3.88E+11	50+	1.98E+11	50+
820502	2	239963	42	5.37E+10	50+	3.37E+10	50+
820605	1	239963	63	8.74E+09	50+	6.67E+09	50+
820605	2	239963	54	1.74E+10	50+	1.23E+10	50+
830403	1	25502	423	1.73E+06	37.6	3.28E+06	50+
830403	2	25502	322	5.88E+06	50+	9.77E+06	50+
830403	3	25502	246	1.96E+07	50+	2.87E+07	50+
830801	1	117761	136	2.79E+08	50+	3.07E+08	50+
830801	2	117761	243	2.07E+07	50+	3.01E+07	50+
830801	3	117761	259	1.56E+07	50+	2.33E+07	50+
830801	4	117761	147	1.97E+08	50+	2.25E+08	50+
840101	1	229500	134	2.98E+08	50+	3.26E+08	50+
840101	2	229500	83	2.54E+09	50+	2.21E+09	50+
840101	3	229500	163	1.24E+08	50+	1.49E+08	50+
840204	1	18000	337	4.80E+06	50+	8.14E+06	50+
840204	2	18000	590	3.91E+05	17.0	8.67E+05	30.2
840604	1	364800	178	8.36E+07	50+	1.05E+08	50+
840604	2	364800	142	2.30E+08	50+	2.58E+08	50+
840604	3	364800	137	2.70E+08	50+	2.98E+08	50+
840604	4	364800	121	4.70E+08	50+	4.90E+08	50+
850201	1	70822	146	2.03E+08	50+	2.31E+08	50+
850201	2	70822	156	1.51E+08	50+	1.77E+08	50+
850206	1	68695	112	6.65E+08	50+	6.67E+08	50+
850206	2	68695	126	3.92E+08	50+	4.17E+08	50+
850601	1	172156	110	7.21E+08	50+	7.17E+08	50+
850601	2	172156	92	1.60E+09	50+	1.47E+09	50+
860501	1	399840	284	1.03E+07	19.4	1.61E+07	26.8
860501	2	399840	221	3.17E+07	41.2	4.40E+07	49.4
860501	3	399840	320	6.05E+06	12.7	1.00E+07	19.0
860603	1	132720	94	1.46E+09	50+	1.34E+09	50+
860603	2	132720	112	6.65E+08	50+	6.67E+08	50+
860603	3	132720	130	3.41E+08	50+	3.68E+08	50+
870102	1	49500	237	2.32E+07	50+	3.33E+07	50+
870102	2	49500	265	1.41E+07	50+	2.13E+07	50+
870504	1	324480	97	1.27E+09	50+	1.19E+09	50+
870504	2	324480	65	7.60E+09	50+	5.88E+09	50+
870505	1	108000	172	9.74E+07	50+	1.20E+08	50+
870505	2	108000	129	3.53E+08	50+	3.79E+08	50+
870505	3	108000	106	8.51E+08	50+	8.32E+08	50+
870505	4	108000	247	1.93E+07	50+	2.82E+07	50+
870701	1	368147	81	2.84E+09	50+	2.44E+09	50+
870701	2	368147	33	1.58E+11	50+	8.85E+10	50+
880203	1	87053	2418	7.07E+02	0.0	3.07E+03	0.0
880203	2	87053	2577	5.32E+02	0.0	2.38E+03	0.0
880203	3	87053	2275	9.29E+02	0.0	3.92E+03	0.0
880203	4	87053	1176	1.78E+04	0.2	5.49E+04	0.6

Table 3-14:The allowable traffics and service lives of the C-LTPP test sections, based on Asphalt Institute and Shell models for rutting (continued)

			Compressive Strain	AI model		Shell model	
C-SHRP ID	Section	ESAL(first year)	on top of SG E-6	Nd	year	Nd	year
890503	1	386590	33	1.58E+11	50+	8.85E+10	50+
890503	2	386590	37	9.47E+10	50+	5.60E+10	50+
890503	3	386590	24	6.58E+11	50+	3.16E+11	50+
890503	4	386590	29	2.82E+11	50+	1.48E+11	50+
890702	1	399012	70	5.45E+09	50+	4.37E+09	50+
890702	2	399012	63	8.74E+09	50+	6.67E+09	50+
900402	1	76440	702	1.80E+05	2.3	4.32E+05	5.3
900402	2	76440	339	4.67E+06	35.2	7.95E+06	47.9
900802	1	127125	751	1.33E+05	1.0	3.30E+05	2.5
900802	2	127125	516	7.12E+05	5.3	1.48E+06	10.1
900802	3	127125	439	1.47E+06	10.1	2.83E+06	17.3
900803	1	85185	246	1.96E+07	50+	2.87E+07	50+
900803	2	85185	477	1.01E+06	10.3	2.03E+06	18.2

Table 3-14: The allowable traffics and service lives of the C-LTPP test sections based on Asphalt Institute and Shell models for rutting

The Asphalt, base and sub base layers contribute about 34%, 14% and 45% to rutting, respectively. Therefore, the contribution of all layers in pavement rutting must be considered (Hesham et al., 1998). Future studies could develop some other M-E models that take account of the plastic deformation of all the layers. As well, another possible reason for the unrealistic results from AI model could be the low quality of the collected data from the C-LTPP project, especially for the traffic.

Based on the AI model for pavement rutting, some test sections showed a lower service life compared with that of other sections. These tests sections are 810404-1(AB), 810404-4(AB), 840204-2(NB), 860501-3(NS), all test sections in site 880203 (PE), and all test sections in site 900802(SK). However, the limitations of AI and Shell models in predicting the permanent deformation in the non-subgrade layers do not allow us to make realistic conclusions based on the unrealistic results for such test sections.

3.5.3. Service lives of the C-LTPP sections, based on M-E models for fatigue cracking

Calculating the tensile strain at the bottom of asphalt layer, Equation 3-18 was used to predict the total traffic to reach the threshold value for fatigue, with 20% of the area cracked. Also from Equation 3-10, the service lives of the C-LTPP sections based on 3% traffic growth factor, were found. The total traffic and service lives of the C-LTPP sections based on the AI and Shell models, are shown in Table 3-15. As it can be seen in Table 3-15, the results obtained from AI and Shell models were reasonably consistent. More than half of the pavement sections

				Tensile Strain	AI model		Shell model	
C-SHRP ID	Section	ESAL(first year)	Eac(psi)	at bottom of asphalt layer,E-6	Nf	year	Nf	year
810404	1	183714	205797	223	2.40E+06	11.2	9.75E+06	32.2
810404	2	183714	199855	183	4.72E+06	19.3	3.20E+07	50+
810404	3	183714	234493	175	4.78E+06	19.5	2.83E+07	50+
810404	4	183714	155652	268	1.67E+06	8.1	6.65E+06	24.9
820205	1	-	NO FWD	NO FWD	-	-	-	-
820205	2	-	NO FWD	NO FWD	-	-	-	-
820502	1	239963	1224783	120	4.03E+06	13.8	4.84E+06	16.0
820502	2	239963	1198986	110	5.46E+06	17.6	8.33E+06	24.1
820605	1	239963	2034928	89	6.98E+06	21.2	7.94E+06	23.3
820605	2	239963	1319565	91	9.39E+06	26.3	1.95E+07	41.7
830403	1	25502	342029	235	1.31E+06	31.6	2.18E+06	43.0
830403	2	25502	560000	168	2.60E+06	47.4	4.56E+06	50+
830403	3	25502	529275	137	5.33E+06	50+	1.66E+07	50+
830801	1	117761	211594	167	6.08E+06	31.7	4.70E+07	50+
830801	2	117761	205797	269	1.30E+06	9.7	3.36E+06	20.9
830801	3	117761	192319	244	1.89E+06	13.3	6.87E+06	34.2
830801	4	117761	368116	122	1.07E+07	44.4	7.54E+07	50+
840101	1	229500	231449	112	2.10E+07	44.6	3.67E+08	50+
840101	2	229500	401449	72	5.61E+07	50+	1.22E+09	50+
840101	3	229500	190725	139	1.22E+07	32.2	1.70E+08	50+
840204	1	18000	443913	194	1.97E+06	49.2	3.49E+06	50+
840204	2	18000	287681	334	4.78E+05	19.8	4.47E+05	18.8
840604	1	364800	544203	166	2.77E+06	6.9	5.22E+06	12.1
840604	2	364800	1086377	137	2.89E+06	7.2	3.03E+06	7.5
840604	3	364800	1016232	132	3.45E+06	8.5	4.38E+06	10.4
840604	4	364800	1002609	116	5.34E+06	12.3	9.41E+06	19.4

Table 3-15: The allowable traffic and service lives of the C-LTPP test sections based on the Asphalt Institute and Shell models for fatigue cracking (Continued)

				Tensile Strain	AI model		Shell model	
C-SHRP ID	Section	ESAL(first year)	Eac(psi)	at bottom of asphalt layer,E-6	Nf	year	Nf	year
850201	1	70822	261739	261	1.17E+06	13.6	2.26E+06	22.7
850201	2	70822	504928	248	7.87E+05	9.7	6.40E+05	8.1
850206	1	68695	274783	201	2.64E+06	26.0	8.87E+06	50+
850206	2	68695	499420	193	1.81E+06	19.7	2.72E+06	26.5
850601	1	172156	190870	181	5.09E+06	21.5	3.80E+07	50+
850601	2	172156	236232	208	2.69E+06	13.0	1.04E+07	35.1
860501	1	399840	279565	237	1.51E+06	3.6	3.35E+06	7.6
860501	2	399840	262029	185	3.62E+06	8.1	1.59E+07	26.5
860501	3	399840	246377	290	8.68E+05	2.1	1.44E+06	3.5
860603	1	132720	116232	258	2.42E+06	14.8	1.64E+07	50+
860603	2	132720	229710	215	2.47E+06	15.0	9.25E+06	38.2
860603	3	132720	248406	227	1.93E+06	12.3	5.65E+06	27.8
870102	1	49500	126232	359	7.62E+05	12.8	2.08E+06	27.6
870102	2	49500	125362	439	3.95E+05	7.3	6.75E+05	11.6
870504	1	324480	470000	164	3.27E+06	8.9	7.91E+06	18.6
870504	2	324480	533188	138	5.17E+06	13.2	1.56E+07	30.2
870505	1	108000	313043	254	1.09E+06	9.0	1.73E+06	13.3
870505	2	108000	361304	206	1.93E+06	14.5	4.04E+06	25.5
870505	3	108000	466667	144	5.04E+06	29.6	1.68E+07	50+
870505	4	108000	160435	389	4.77E+05	4.2	7.48E+05	6.4
870701	1	368147	368261	164	4.02E+06	9.6	1.41E+07	25.9
870701	2	368147	2262029	26	3.66E+08	50+	6.63E+09	50+
880203	1	87053	232174	475	1.80E+05	2.0	1.01E+05	1.2
880203	2	87053	175652	447	2.79E+05	3.1	2.75E+05	3.1
880203	3	87053	188116	422	3.18E+05	3.5	3.24E+05	3.6
880203	4	87053	190145	273	1.32E+06	12.7	3.73E+06	28.0
890503	1	386590	165072	298	1.12E+06	2.8	3.17E+06	7.4
890503	2	386590	555942	121	7.70E+06	15.8	2.98E+07	40.5
890503	3	386590	485942	103	1.47E+07	25.7	1.02E+08	50+
890503	4	386590	868551	80	2.05E+07	32.2	1.09E+08	50+
890702	1	399012	736667	154	2.74E+06	6.3	3.91E+06	8.7
890702	2	399012	603768	133	5.25E+06	11.3	1.44E+07	24.8
900402	1	76440	144928	364	6.47E+05	7.7	1.39E+06	14.7
900402	2	76440	139565	283	1.53E+06	15.9	6.32E+06	42.2
900802	1	127125	287681	441	1.91E+05	1.5	9.24E+04	0.7
900802	2	127125	360435	366	2.92E+05	2.3	1.56E+05	1.2
900802	3	127125	422899	234	1.11E+06	7.9	1.35E+06	9.4
900803	1	85185	987101	128	3.92E+06	29.3	5.59E+06	36.8
900803	2	85185	1036812	210	7.36E+05	7.8	3.00E+05	3.4

Table 3-15: The allowable traffic and service lives of the C-LTPP test sections based on the Asphalt Institute and Shell models for fatigue cracking

deteriorated from fatigue cracking in less than 15 years, so in terms of this deterioration mode, the pavement performance in the C-LTPP program was not satisfactory.

In Figure 3-13, the estimated service lives of the agency-designed test sections are represented in an ascending graphical format, based on the AI model for fatigue cracking.

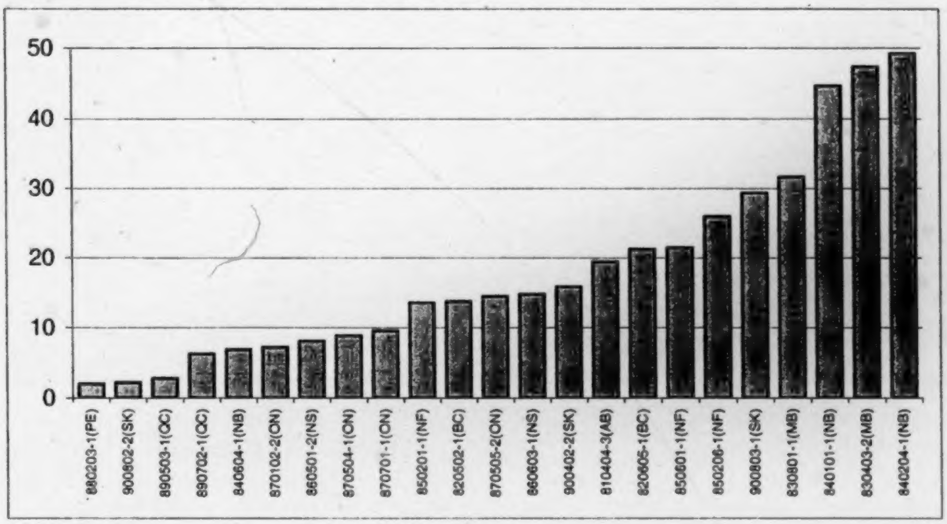

Figure 3-13: Service lives of the C-LTPP test sections for agency- designed test sections, based on the AI model for fatigue cracking

Figure 3-13 shows, 9 test sections (almost one third of the C-LTPP agency-designed tests sections) had service lives of less than 10 years because of fatigue cracking. These test sections were 840604-1(NB), 860501-2(NS), 870102-2(ON), 870504-1(ON), 870701-1(ON), 880203-1(PE), 890503-1(QC), 890702-1(QC), and 900802-2(SK). Table 3-16 presents these test sections in accordance with the experimental design of the C-LTPP project. The test sections with high fatigue cracks were located in areas with different classifications of traffic, weather conditions, and subgrade material, but most of them have 30-60 mm overlay thickness (thin overlay). As well, test section 860501-2(NS) with a 85 mm overlay and test section 900802-2(SK) with a 67 mm overlay were quite close to thin overlay class.

			Moisture, Freezing Index and Subgrade Condition					
			Wet					Dry
			No to Low Freeze			High Freeze		High Freeze
Traffic	Overlay Type	Overlay Thickness(mm)	Fine	Coarse		Fine	Coarse	Fine
Low	RAP	30-60						8104044(AB)
		60-100						8104043(AB)
		100-185	8205021(BC)					
			8205022(BC)					
			8705054(ON)					
	HMAC	30-60	8206051(BC)		8202051(BC)	8707011(ON)		
			8701022(ON)		8606033(NS)			
					8802031(PE)			
					8802033(PE)			
		60-100	8206052(BC)	8202052(BC)	8506012(NF)			8104041(AB)
			8701021(ON)	8402042(NB)	8606031(NS)			8304031(MB)
			8705051(ON)	8502012(NF)	8606032(NS)			9004021(SK)
			8705052(ON)	8502062(NF)	8802034(PE)			
		100-185	8705053(ON)		8402041(NB)	8707012(ON)		8104042(AB)
					8502011(NF)			8304032(MB)
					8502061(NF)			8304033(MB)
					8506011(NF)			9004022(SK)
					8802032(PE)			
High	RAP	30-60						
		60-100			8401013(NB)			
		100-185			8401012(NB)			8308011(MB)
					8406041(NB)			8308012(MB)
	HMAC	30-60	8605011(NS)		8406043(NB)	8907021(QC)	8905031(QC)	9008021(SK)
			8605013(NS)		8406044(NB)		8905032(QC)	
					8705041(ON)			
		60-100	8605012(NS)		8406042(NB)	8907022(QC)	8905034(QC)	9008022(SK)
					8705042(ON)			
		100-185			8401011(NB)		8905033(QC)	8308013(MB)
								8308014(MB)
								9008023(SK)
								9008031(SK)
								9008032(SK)

Table 3-16: Experimental design of the C-LTPP Project and test sections with service lives less than 10 years because of high fatigue cracking (highlighted test sections)

Therefore, it could be concluded that thin overlay thickness was a major attribute in development of fatigue cracks and low service life (less than 15 years) for the C-LTPP pavement sections regardless of the traffic level and weather climate.

3.6. Evaluation of the C-LTPP sections, based on the REPP2000 program

In Section 3.5, M-E models were used to predict the service lives of the C-LTPP sections related to rut and fatigue. It required using the information about moduli of pavement layers in order to perform pavement analysis and to calculate the compressive strain at the top of the subgrade and tensile strain at the bottom of the asphalt layer.

In a joint project, the Texas Department Of Transportation (TDOT) and the University of Texas conducted a study to estimate the remaining service life of asphalt pavements. This project's main objectives were

1- To develop Artificial Neural Network models to compute the remaining lives of flexible pavements associated with the rutting and fatigue cracking failure modes,

2- To account for the uncertainties in the variables used for predicting remaining life,

3- To develop pavement performance curves and their confidence bounds, and

4- To create a software tool to integrate the models developed.

This project resulted in the development of a software tool called REPP2000 (Rational Estimate of Pavement Performance). REPP2000 program does not require the information based on backcalculation and pavement analysis.

The Artificial Neural Network (ANN) was the main tool used in this program. To develop the neural network models for this software, examples of pavement performance for training and testing the neural networks were required. Because of limited information about pavement performance, a synthetic and comprehensive database was generated to simulate and cover a wide range of possible pavement sections. FWD tests and traffic loading on the pavement were simulated to obtain the deflection basin and the critical strains in a number of pavement sections. Furthermore the Asphalt Institute's models for predicting the remaining life based on rutting and fatigue cracking were used. In this study, a total of 360,000 data patterns of different pavement scenarios were created for training and testing neural network models. Four ANN models were developed for a three-layer flexible pavement. Two of the models predict rut and fatigue according to the Asphalt Institute model, and the other two models predict the maximum tensile and compressive strain at the layer interfaces. As well, to describe the continuous performance of a pavement over time or, alternatively, with passing traffic, the Pavement Performance Curve (PPC) was proposed. The proposed approach also allows for the definition of confidence bounds for the PPC by using the Monte Carlo simulation algorithm. The employed methodology was initially validated with data obtained from one of the Texas Mobile Load Simulator (TxMLS) test sites. Figures in Appendix I, present the different stages of the use of the REPP2000.

3.6.1. Service lives of the C-LTPP sections, based on the REPP2000 Program

The REPP2000 was provided by University of Texas at El Paso for the purpose of this study and it was utilized to estimate the service lives of the C-LTPP test sections. The required information about FWD test and traffic information was introduced into the REPP2000 for all the 65 C-LTPP test sections. The estimated service lives for both pavement rutting and fatigue cracking are presented in Table 3-17.

It was observed that the estimated service lives for most of the test sections, based on pavement rutting were more than 50 years. However, fatigue cracking was a more critical mode in pavement deterioration. The estimated service lives for different test sections within each test site were similar, and it seemed that this program was not capable to differentiate various pavement design practices or construction alternatives within each test site. After all there can be seen a reasonable consistency between results from REPP2000 program and estimated service lives based on M-E method. Using REPP200 program, the shortest service lives were predicted in test sites 830403(MB), 840604(NB), 870504(ON), 890503(QC), and 890702(QC).

		Predicted service life from REPP2000	
C-SHRP ID	Section	Rut	Fatigue
810404	1	50+	22.4
810404	2	50+	22.4
810404	3	50+	22.4
810404	4	50+	22.4
820205	1	N/A	N/A
820205	2	N/A	N/A
820502	1	50+	19.4
820502	2	50+	19.4
820605	1	50+	19.4
820605	2	50+	19.4
830403	1	50+	50+
830403	2	21.5	50+
830403	3	13.6	50+
830801	1	50+	28.5
830801	2	50+	28.5
830801	3	50+	28.5
830801	4	50+	28.5
840101	1	N/A	N/A
840101	2	N/A	N/A
840101	3	N/A	N/A
840204	1	50+	50+
840204	2	37.7	50+
840604	1	45.0	15.4
840604	2	45.0	15.4
840604	3	45.0	15.4
840604	4	45.0	15.4
850201	1	50+	37.2
850201	2	50+	37.2
850206	1	50+	37.8
850206	2	50+	37.8
850601	1	50+	50+
850601	2	50+	23.2
860501	1	43.0	14.7
860501	2	43.0	14.7
860501	3	43.0	14.7
860603	1	50+	26.7
860603	2	50+	26.7
860603	3	50+	26.7
870102	1	50+	44.8
870102	2	50+	44.8
870504	1	48.0	16.5
870504	2	48.0	16.5
870505	1	50+	29.8
870505	2	50+	29.8
870505	3	50+	29.8
870505	4	50+	29.8

Table 3-17: Estimated service lives of the C-LTPP sections, based on rut and fatigue crack using the REPP2000 program (Continued)

		Predicted service life from REPP2000	
C-SHRP ID	Section	Rut	Fatigue
870701	1	50+	18.7
870701	2	50+	18.7
880203	1	50+	33.4
880203	2	50+	33.4
880203	3	50+	33.4
880203	4	50+	34.4
890503	1	43.8	15.0
890503	2	43.8	15.0
890503	3	43.8	15.0
890503	4	43.8	15.0
890702	1	43.1	14.7
890702	2	43.1	14.7
900402	1	50+	35.7
900402	2	50+	35.7
900802	1	50+	27.3
900802	2	50+	27.3
900802	3	50+	27.3
900803	1	50+	33.8
900803	2	50+	34.8

Table 3-17: Estimated service lives of the C-LTPP sections, based on rut and fatigue crack using the REPP2000 program

3.7. Comparison of the service lives of the C-LTPP sections, from different methods

In this chapter, several methods have been employed in order to predict the service lives of the C-LTPP sections. These methods have included the use of AASHTO overlay design method, threshold values for roughness and rutting, M-E models, and the use of the REPP2000 program. For these methods, the predicted service lives of the C-LTPP sections were tabulated and shown in numerous tables.

Table 3-18 summarizes the predicted service lives from different above methods for all the C-LTPP sections. In this table, only the service lives less than 20 years are shown. Generally, it is expected that an overlay will exist for 20 years. When performance failure occurs in less than 20 years, it can show a poor performance. As well, Table 3-18 presents the design type of each test section: under agency-design, agency-design, and over agency-design. There are some test sections that do not have either under agency-design sections or over agency-design adjacent section. Table 3-18 reveals that most of test sections that had a short service life, based on the AASHTO, were under agency-design test sections. Fatigue cracking predicted, based on AI model, was the most popular failure mode for the C-LTPP sections. However, the estimated service lives related to fatigue from REPP2000 program were generally higher than those from AI model.

Site	Section	Design type	Expected service lives of C-LTPP test sections (year)									
			AASHTO	IRI=3.5(mm/m)	IRI=3 (mm/m)	Rut =15mm	Rut =25mm	Rut(AI)	Fatigue(AI)	Rut(REPP)	Fatigue(REPP)	Minimum (year)
810404(AB)	1	Under agency-design	9.7					5.3	11.2			5.3
	2	Over agency-design			19.2				19.3			19.2
	3	Agency-design							19.5			19.5
	4	Under agency-design	9.9	19.2	17.1			5.2	8.1			5.2
820205(BC)	1	Under agency-design		13.1	11.8							11.8
	2	Agency-design										
820502(BC)	1	Agency-design				19.3			13.8		19.4	13.8
	2	Over agency-design							17.6		19.4	17.6
820605(BC)	1	Agency-design									19.4	19.4
	2	Over agency-design									19.4	19.4
830403(MB)	1	Under agency-design										
	2	Agency-design										
	3	Over agency-design								13.6		13.6
830801(MB)	1	Agency-design										
	2	under agency-design							9.7			9.7
	3	under agency-design							13.3			13.3
	4	under agency-design										
840101(NB)	1	Agency-design										
	2	Over agency-design				13.1						13.1
	3	Under agency-design	3.6			15.3						3.6
840204(NB)	1	Agency-design			17.6							17.6
	2	Under agency-design	18.1		17.8			17.0	19.8			17
840604(NB)	1	Agency-design		18.4	16.3	14.9			6.9		15.4	6.9
	2	Under agency-design		19.3	17.1	18.1			7.2		15.4	7.2
	3	Under agency-design							8.5		15.4	8.5
	4	Under agency-design		13.4	11.7	17.9			12.3		15.4	12.3
850201(NF)	1	Agency-design							13.6			13.6
	2	Under agency-design							9.7			9.7
850206(NF)	1	Agency-design										
	2	Under agency-design							19.7			19.7
850601(NF)	1	Agency-design				12.3						12.3
	2	Under agency-design				18.3			13.0			13

Table 3-18: The predicted service lives for all the C-LTPP sections from different methods (Excluding service lives >20 years);(Continued)

Site	Section	Design type	Expected service lives of C-LTPP test sections (year)									
			AASHTO	IRI=3.5(mm/m)	IRI=3 (mm/m)	Rut =15mm	Rut =25mm	Rut(AI)	Fatigue(AI)	Rut(REPP)	Fatigue(REPP)	Minimum (year)
860501(NS)	1	Under agency-design		14.2	12.4	6.1	11.5	19.4	3.6		14.7	3.6
	2	Agency-design							8.1		14.7	8.1
	3	Over agency-design						12.7	2.1			2.1
860603(NS)	1	Agency-design				19.7			14.8			14.8
	2	Under agency-design				14.7			15.0			14.7
	3	Under agency-design				15.1			12.3			12.3
870102(ON)	1	Over agency-design							12.8			12.8
	2	Agency-design		11.7	10.2				7.3			7.3
870504(ON)	1	Agency-design							8.9		16.5	8.9
	2	Over agency-design							13.2		16.5	13.2
870505(ON)	1	Over agency-design							9.0			9
	2	Agency-design							14.5			14.5
	3	Over agency-design										
	4	Over agency-design							4.2			4.2
870701(ON)	1	Agency-design			18.9				9.6		18.7	9.6
	2	Over agency-design									18.7	18.7
880203(PEI)	1	Agency-design	3.9	19.1	17.0			0.0	2.0			0
	2	Over agency-design	5.4	13.3	11.9			0.0	3.1			0
	3	Under agency-design	7.3	17.0	15.2			0.0	3.5			0
	4	Over agency-design						0.2	12.7			0.2
890503(QC)	1	Agency-design		16.6	14.9	11.3	18.1		2.8		15.0	2.8
	2	Over agency-design		18.1	16.2	12.0	19.4		15.8		15.0	12
	3	Over agency-design				11.3	18.5				15.0	11.3
	4	Over agency-design				14.7	24.0				15.0	14.7
890702(QC)	1	Agency-design							6.3		14.7	6.3
	2	Over agency-design							11.3		14.7	11.3
900402(SK)	1	Under agency-design	7.2					2.3	7.7			2.3
	2	Agency-design							15.9			15.9
900802(SK)	1	Under agency-design	2.8					1.0	1.5			1
	2	Agency-design	5.5					5.3	2.3			2.3
	3	Over agency-design	17.8					10.1	7.9			7.9
900803(SK)	1	Agency-design										
	2	Under agency-design	8.5	15.9	14.1			10.3	7.8			7.8

Table 3-18: The predicted service lives for all the C-LTPP sections from different methods
(Excluding service lives >20 years)

With a rut threshold value of 15mm more test sections reached the final serviceability in less than 20 years, than did so with a threshold level of rut=25mm. For roughness two different trigger values of 3 and 3.5 mm/m were used; however, there was not a noticeable difference between the predicted service lives.

Figure 3-14 shows the estimated service lives for agency-designed test sections in the C-LTPP program

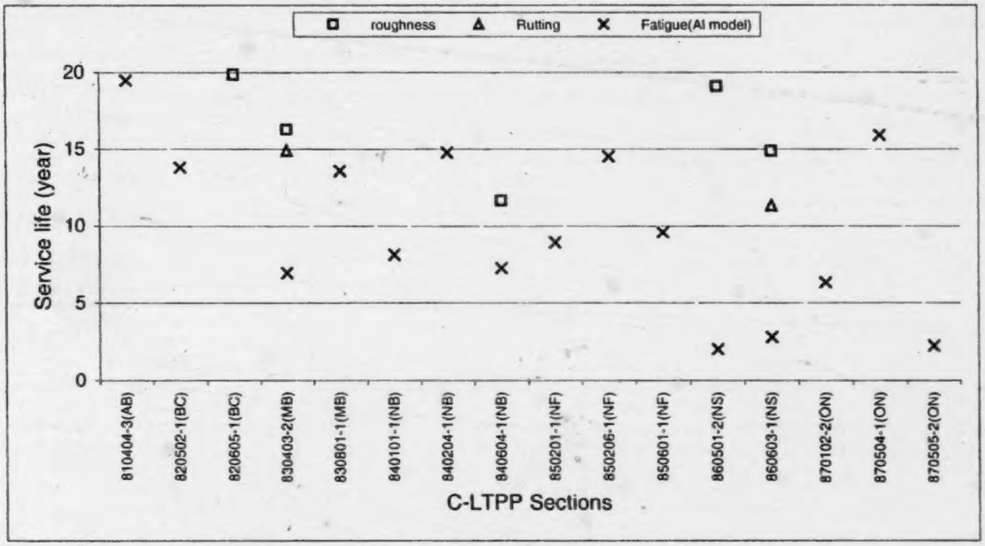

Figure 3-14: Comparison of service lives of the C-LTPP sections from different methodologies

A comparison of the AASHTO overlay design method with other methods revealed that this method resulted in higher service lives in most of test sections than that from other methods.

The ERES Engineering Consultants, Ltd. (1999) evaluated the LTPP sections by using the AASHTO flexible pavement design equitation and reported that it did not accurately predict the pavement performance of the SHRP LTPP test sections. The AASHTO design method predicted that many more ESALs would be needed to cause a measured loss in the present serviceability index (*PSI*) than the pavements had actually experienced. As well, the researchers mentioned that *PSI=2.5*, generally considered to represent final serviceability and failure at a road, does not really present highway practices because decision makers do not allow the pavement to deteriorate to this level.

Figure 3-14 shows that fatigue cracking is a critical criterion for the C-LTPP sections and that gave most of them a shorter service life than they would have had other case.

Compared with fatigue cracking and roughness, rut was a less important mode in the pavement deterioration of the C-LTPP sections. Some of the test sections showed a low service life for both fatigue and roughness. They were test sections 840604-1(ON), 870102-2(ON), 870504-1(ON), 870701-1(ON), 880203-1(PE), 890503-1(QC), and 900802-2(SK). All of them except for one, 840604-1(ON), have thin overlay with less than 70 mm thickness, which appeared to be the most important attribute for a poor pavement performance in the C-LTPP sections. All these test sections, except for 900802-2(SK), are located in East of Canada.

CHAPTER 4: FACTORS AFFECTING THE PERFORMANCE OF THE C-LTPP TEST SECTIONS

4.1. Introduction

In Chapter 3, different methods were used to evaluate and to compare the pavement performance of the C-LTPP sections. Pavements' service lives were predicted, based on roughness and rut, and accordingly, test sections that showed a shorter service life or a poor performance were indicated.

In Chapter 4, it is attempted to investigate the effect of different factors on pavement roughness and rutting in order to recognize the factors that significantly affect the pavement performance of the C-LTPP sections.

The C-LTPP project provides information regarding different pavements' characteristics, traffic levels, weather conditions, and material properties, which all govern pavement performance.

Several factors were considered in the C-LTPP experimental design, presented in Table 2-1, which can be classified as follows

1) Two levels of traffic (low and high),

2) Three climatic zones (wet no-low freeze; wet high freeze; dry high freeze),

3) Two subgrade types (fine and coarse),

4) Three levels of overlay thickness (30-60 mm; 60-100 mm; 100-185 mm),

5) Two types of asphalt materials (conventional and recycled),

6) Two levels for pavement preparation prior to overlay (milled, not milled).

Complete information for above factors is available in the C-LTPP database, which makes it possible to perform a reliable analysis for above factors. The impact of weather climate, traffic, overlay thickness, overlay material type, subgrade material type, and milling before overlay, on pavement performance in the C-LTPP project is studied in this chapter. It must be mentioned that there are also other factors that affect pavement performance including asphalt viscosity, asphalt air void, pavement temperature, etc.; however, there was a lack of information for these factors in the C-LTPP database. Thus they were not involved in this part of study. As well, the impact of different design practices such as agency-design, under agency-design, and over agency-design on roughness and rut is studied in this chapter.

4.2. Factors affecting roughness in the C-LTPP sections

As was mentioned in Chapter 3, data on pavement roughness is collected in the C-LTPP program every year after overlaying. By using the roughness data collected for the years up to 2002, the rates of the roughness progression in all the C-LTPP sections were calculated by deploying Equation 4-1:

$$IRI\ Rate = \frac{(IRI_j - IRI_i)}{j - i} \qquad (4\text{-}1)$$

where

j = The latest year that the IRI measurement was recorded

i = The first year after overlaying that the IRI measurement was recorded

IRI_j = IRI in year j

IRI_i = IRI in year i

This rate identifies the average annual increase of roughness in each test section. Equation 4-1 represents a linear function of roughness versus time, whereas, as discussed in Chapter 3, roughness models are rather nonlinear. Although the relationship between roughness (IRI) and time in the whole life of a pavement is non-linear, most of C-LTPP sections still are in the first stage of their lives, so that the relationship of the IRI versus time can be considered linear.

By using Equation 4-1, the IRI rates were calculated for all the C-LTPP sections and results are presented in Table 4-1. For most of test sections, the latest measurement was made after or close to 10 years of pavement service. Five test sections showed a negative value for the IRI rate, which is unrealistic. These test sections were 820502-1(BC), 820502-2(BC), 830403-3(MB), 840101-1(NB), and 840604-3(NB). These test sections with negative IRI rates, which might be due to various issues associated with data collecting, were omitted from the study.

Figure 4-1 shows the box plot of the IRI rates in Table 4-1. In this graph, Max, Min, Q3, and Q1 correspond to maximum value, minimum value, third quartile (75%) and first quartile (25%) respectively. From Figure 4-1, the following conclusions could be drawn:

C-SHRP ID	Section	Year after overlaid (i)	IRI(i)	Year after overlaid(j)	IRI(j)	IRI rate (mm/m per year)
810404	1	0	1.33	9	1.70	0.041
810404	2	0	1.12	9	1.66	0.060
810404	3	0	1.22	9	1.53	0.034
810404	4	0	1.16	9	1.71	0.061
820205	1	1	0.85	5	1.18	0.083
820205	2	1	0.92	5	1.06	0.035
820502	1	1	0.96	7	0.93	-0.005
820502	2	1	0.82	7	0.81	-0.002
820605	1	1	1.17	7	1.24	0.012
820605	2	1	1.22	7	1.25	0.005
830403	1	0	1.07	11	1.13	0.005
830403	2	0	1.20	11	1.29	0.008
830403	3	0	1.55	11	1.42	-0.012
830801	1	0	0.82	12	0.96	0.012
830801	2	0	0.90	12	1.40	0.042
830801	3	0	1.39	12	1.89	0.042
830801	4	0	0.76	12	0.98	0.018
840101	1	0	1.20	9	1.12	-0.009
840101	2	1	1.00	9	1.03	0.004
840101	3	0	1.44	9	1.48	0.004
840204	1	0	1.29	9	1.50	0.023
840204	2	1	1.44	9	1.71	0.034
840604	1	0	1.30	9	1.75	0.050
840604	2	0	1.50	9	1.68	0.020
840604	3	0	1.41	9	1.32	-0.010
840604	4	0	1.65	9	2.21	0.062
850201	1	0	1.53	12	1.59	0.005
850201	2	0	1.38	12	1.51	0.011
850206	1	0	1.13	11	1.24	0.010
850206	2	0	0.94	11	1.46	0.047
850601	1	0	0.75	12	1.10	0.029
850601	2	0	0.79	12	1.02	0.019
860501	1	0	1.45	11	2.79	0.122
860501	2	0	1.20	11	1.78	0.053
860501	3	0	1.06	11	1.59	0.048
860603	1	0	1.50	11	2.66	0.105
860603	2	0	1.24	11	2.27	0.094
860603	3	0	1.24	11	2.33	0.099
870102	1	2	0.93	9	1.79	0.123
870102	2	2	1.06	9	2.33	0.181
870504	1	1	1.02	7	1.25	0.038
870504	2	1	0.93	7	1.11	0.030
870505	1	1	0.90	8	1.18	0.040
870505	2	1	0.91	8	1.19	0.040
870505	3	1	0.77	8	1.04	0.039
870505	4	1	1.24	8	1.62	0.054

Table 4-1:The IRI rates of the C-LTPP sections (continued)

C-SHRP ID	Section	Year after overlaid (i)	IRI(i)	Year after overlaid(j)	IRI(j)	IRI rate (mm/m per year)
870701	1	1	1.24	8	1.54	0.043
870701	2	1	0.79	8	0.96	0.024
880203	1	1	1.15	10	2.13	0.109
880203	2	1	1.09	10	2.82	0.192
880203	3	1	1.01	10	2.05	0.116
880203	4	1	1.07	10	1.43	0.040
890503	1	0	1.21	11	1.88	0.061
890503	2	2	0.85	11	1.65	0.089
890503	3	0	1.06	11	1.40	0.031
890503	4	0	0.82	11	1.23	0.037
890702	1	1	1.39	9	1.52	0.016
890702	2	1	1.38	9	1.59	0.026
900402	1	0	1.12	10	1.26	0.014
900402	2	0	1.11	10	1.16	0.005
900802	1	0	0.75	10	1.27	0.052
900802	2	0	0.99	10	1.19	0.020
900802	3	0	0.91	10	0.99	0.008
900803	1	0	0.95	10	1.35	0.040
900803	2	0	1.09	10	2.06	0.097

Table 4-1:The IRI rates of the C-LTPP sections

1- The average annual IRI rate is 0.042 mm/m/year. In Section 3.3.4, it was mentioned that, generally, for the roughness of a new overlaid pavement, it can be assumed that IRI_0=1 mm/m. Hence the average roughness after 20 years of pavement performance in the C-LTPP project will be 1.84 mm/m. This low value for roughness after 20 years of service life agrees with the results from Section 3.3.5 where it was concluded that roughness based on the IRI is not the main factor in pavement failure for the C-LTPP sections.

2- The maximum and minimum IRI rates for the C-LTPP sections were: 0.192 (mm/m/year), and 0.005 (mm/m/year), respectively. The difference between maximum and minimum IRI rates, for 10-20 years of pavement performance, seems to be quite a wide range for pavement roughness in the C-LTPP project.

3- The distribution of the IRI rates is not symmetric and cannot be considered as a normal distribution. Hence, any statistical analysis related to IRI rates that requires the assumption of normality must be confirmed by using other methods.

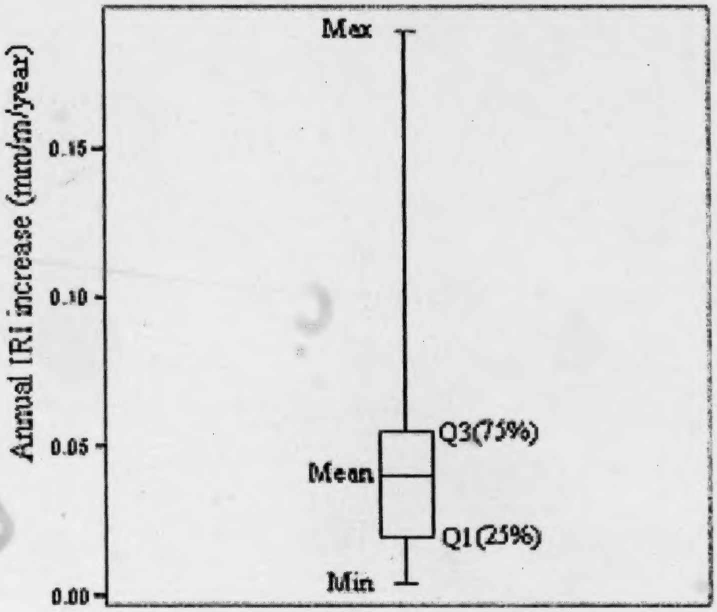

Figure 4-1: Box plot of IRI rates for all the C-LTPP sections

Table 4-2 presents the IRI rates from Table 4-1 within the C-LTPP experimental design. It was decided to use statistical analysis to study the impact of important factors such as weather climate, traffic, overlay thickness, overlay material type, subgrade material type, and milling before overlaying on IRI rates.

			Moisture, Freezing Index and Subgrade Condition					
			Wet					Dry
	Overlay Type	Overlay Thick.(mm)	No to Low Freeze			High Freeze		High Freeze
Traffic			Fine	Coarse		Fine	Coarse	Fine
Low	RAP	30-60						0.061
		60-100						0.034
		100-185	-0.005					
			-0.002					
			0.050					
	HMAC	30-60	0.013		0.083	0.040		
			0.180		0.100			
					0.110			
					0.120			
		60-100	0.004	0.035	0.020			0.041
			0.120	0.034	0.010			0.005
			0.040	0.010	0.090			0.014
			0.040	0.047	0.040			
		100-185	0.040		0.024	0.024		0.060
								0.008
					0.010			-0.012
					0.030			0.005
					0.190			
High	RAP	30-60						
		60-100			0.004			
		100-185			0.005			0.011
					0.050			0.042
	HMAC	30-60	0.120		-0.010	0.020	0.060	0.050
			0.050		0.060		0.090	
					0.038			
		60-100	0.050		0.020	0.030	0.040	0.020
					0.030			
		100-185			-0.009		0.030	0.042
								0.018
								0.008
								0.040
								0.097

Table 4-2: IRI rate values within the experimental design matrix of the C-LTPP project

4.2.1. Effect of climate on pavement roughness

As it can be seen in Table 4-2, three weather climates including wet-low freeze, wet-high freeze, and dry-high freeze were distinguished in the C-LTPP project. Figure 4-2 summarizes the IRI rate for each climate condition. When comparing the means of IRI rate, it was observed that the test sections in the wet-low freeze condition had a higher IRI rate than the other test sections. IRI rates in the wet-high freeze condition and the dry-high freeze condition are very similar. Box plot in Figure 4-2 shows that the distribution of IRI rates are rather right skewed, which means IRI rates have not a normal distribution.

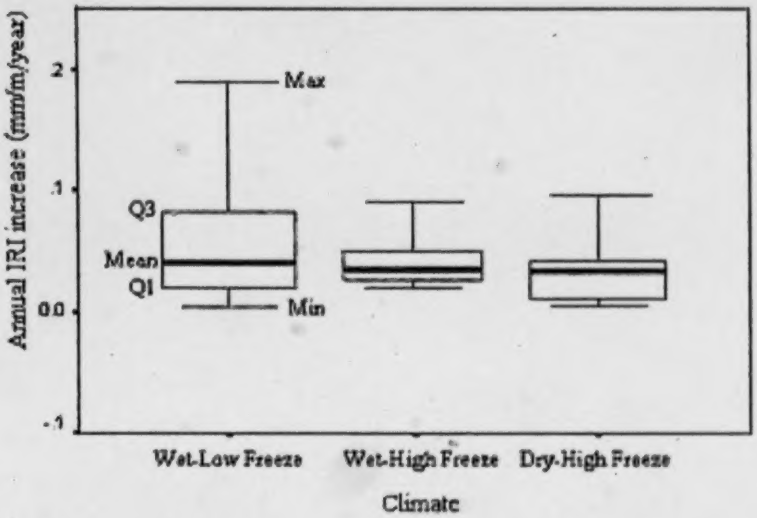

Figure 4-2: Box plot of IRI rates for different weather climates in the C-LTPP project

Figure 4-2 does not show an apparent difference among the averages of the IRI rates and the mean values are fairly close; however, to confirm this observation, a statistical test was conducted to investigate whether the IRI rates related to climate zones are different or in other words whether the climate is a significant factor in pavement roughness. An ANOVA test was conducted on the roughness rates related to the three climate conditions.

ANOVA could test the null hypothesis that no difference exists between the climate levels and that climate is not a significant factor in pavement roughness (H_0). Table 4-3 shows the ANOVA test results.

Groups	Count	Sum	Average	Variance
Wet Low Freeze	34	1.867	0.055	0.002
Wet High Freeze	8	0.334	0.042	0.001
Dry High Freeze	17	0.553	0.033	0.001

ANOVA

Source of Variation	SS	df	MS	F	P-value	F crit
Between Groups	0.006	2.000	0.003	1.832	0.170	3.162
Within Groups	0.090	56.000	0.002			
Total	0.096	58.000				

Table 4-3: ANOVA test results for IRI rates related to different climate conditions in the C-LTPP project

To reject the null hypothesis, the obtained P-value from ANOVA test must be less than the significance level, which is 0.05 for this study, with 95% reliability. For the impact of climate on roughness, the P-value was more than α=0.05, so the null hypothesis cannot be rejected. As well, the calculated F can be compared with $F_{critical}$, and the test fails to reject the null hypothesis because $F<F_{critical}$. Therefore, it can be concluded with 95% of reliability that climate is not a significant factor in the pavement roughness.

In application of ANOVA, as a statistical tool, for the C-LTPP sections several points must be considered:

1- The main assumption of the ANOVA test is the normal distribution of the data; however, the boxplot reveals that this assumption was not correct for the distribution of IRI rates in the three different weather climates.

2- According to the central limit theorem, when the number of samples increases, the resulting distribution of their means rapidly approaches the normal distribution. Sample sizes of less than 30 probably affect the advantages of central limit theorem (Bethea et al., 1991).

3- The distribution of the test sections and the nature of the C-LTPP experiment are *unbalanced*. In other words, the sample sizes in different levels of each factor vary.

These issues might influence the accuracy of the results from ANOVA test; therefore, it was attempted to use another approach in order to validate the results.

Non-parametric statistic could be incorporated to answer these challenges while it does not require the assumption of normality. As well, the non-parametric technique is based on rank order statistics and can be used to analyze different sample sizes in the various groups being studied (SPSS 11.0, 2001).

Several non-parametric methods use the ranking approach. Two that can be used in order to compare the locations of samples (average, median) are the Mann-Whitney and Kruskal-Wallis tests. The Mann-Whitney method is used for two independent samples, and when the number of studied groups is more than two, the Kruskal-Wallis test is employed. These tests can provide the critical value and the probability for accepting the null hypothesis (Gibbous, 1985), and (Mosteller and Rourke, 1973).

The Mann-Whitney and Kruskal-Wallis tests were performed for the studied factors by using the SPSS program, and the results were compared with those from the ANOVA test.

For the three weather climates, the Kruskal-Wallis test was performed. The results are presented in Table 4-4:

Climate Levels	Observation No.	Mean Rank
0 (Wet-low freeze)	34	32.26
1 (Wet-high freeze)	8	30.19
2 (Dry-high freeze)	17	25.38
Total	59	
Test Results		
Test Statistics	IRI	
Asymptotic Sig. (P-Value)	0.401	

Table 4-4: Kruskal-Wallis test results for IRI rates related to different climate conditions in the C-LTPP project

The P-value (Asymptotic significance) is more than the significance level of 0.05; therefore, the H_o was not rejected and there was no difference in the rate of the IRI among the climate zones. In other words, with 95% reliability, climate was not a significant factor in pavement roughness.

Tighe et al. (1999) conducted a study about pavement roughness in the C-LTPP project. They observed that a higher rate of roughness progression took place in wet low-freeze zone, and a lower rate occurred in the wet- high freeze and the dry -high freeze zones. Although in Table 4-4, higher mean rank in the wet-low freeze shows that average IRI rate in this climate is more than the others, with 95%

reliability both parametric and non-parametric analysis showed that climate zone is not a significant factor in pavement roughness rates.

4.2.2. Effect of traffic on pavement roughness

By using traffic data from Table 4-2, the effect of two traffic levels on the IRI rates was studied. In the C-LTPP experimental design, the low traffic is defined as less than 200,000 ESAL/year. Figure 4-3 summarizes the IRI rates for each traffic level. This box plot shows that roughness progressions in two groups are fairly close and their distribution are not symmetric, especially for the low traffic zone, which rejects the assumption of normal distribution.

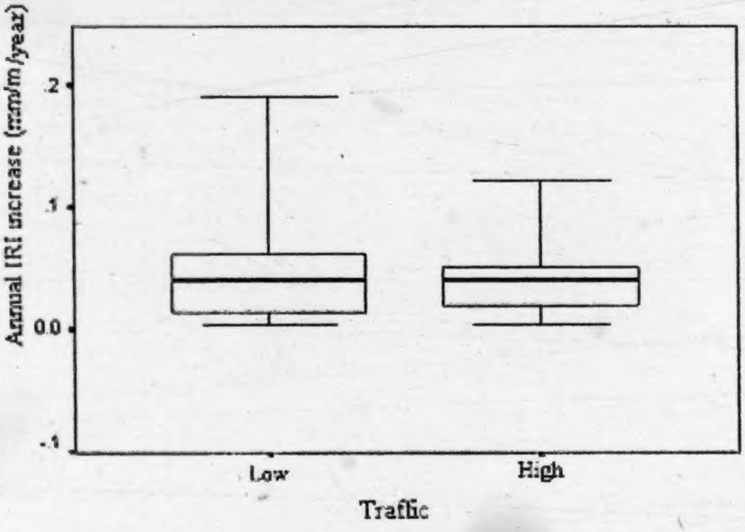

Figure 4-3: Box plot of IRI rates for different traffic levels in the C-LTPP project

The ANOVA test results for the IRI rates related to different traffic levels are shown in Table 4-5:

Groups	Count	Sum	Average	Variance
Low traffic	34	1.732	0.051	0.002
High traffic	25	1.025	0.041	0.001

ANOVA

Source of Variation	SS	df	MS	F	P-value	F crit
Between Groups	0.001	1.000	0.001	0.858	0.358	4.010
Within Groups	0.094	57.000	0.002			
Total	0.096	58.000				

Table 4-5: ANOVA test results for IRI rates related to different traffic levels in the C-LTPP project

Table 4-5 shows that the P-value was more than 0.05 and therefore, the test failed to reject the H_o and traffic was not a significant factor in pavement roughness. For the non-parametric analysis, since there were two groups of samples, the SPSS program was utilized to perform the Mann-Whitney test. The results are presented in Table 4-6:

Traffic Levels	Observation No.	Mean Rank
0 (Low)	34	30.31
1(High)	25	29.58
Total	59	
Test Results		
Test Statistics	IRI	
Asymptotic Sig. (P-Value)	0.401	

Table 4-6: Mann-Whitney test results for IRI rates related to different traffic levels in the C-LTPP project

The P-value was more than the significance level of $\alpha=0.05$; therefore, there was no difference between the traffic groups. In other words traffic was not a significant factor in pavement roughness progression.

With 95% reliability, both parametric and non-parametric analysis showed that traffic was not a significant factor in the roughness rate. Tighe et al. (1999)

reported the same conclusion and explained that such a result could be due to the inappropriate classification of traffic in the C-LTPP project and two levels of low and high traffic could not show the impact of traffic on pavement roughness.

As well, another issue that may result to such finding could be the low amount of traffic in the C-LTPP sections. In the C-LTPP program, the Annual Average Daily Traffic (AADT) ranges from 1100 to 14500 (see Appendix E), which is a low traffic and it is possible that higher traffics may show a higher impact on pavement roughness.

4.2.3. Effect of overlay thickness on pavement roughness

Three classes of overlay thickness are distinguished in the C-LTPP project (see Table 4-2). These thickness classes are 30-60mm (thin), 60-100mm (medium), and 100-185mm (thick). Figure 4-4 shows the box plot of the IRI rates for these three overlay thicknesses. Thin overlay, 30-60mm, has higher IRI rates compared with medium and thick overlays, while in two other groups the roughness progression shows similar average IRI rates. No apparent distinction could be seen between thickness categories 60-100 mm and 100-185 mm in their impact on the roughness rates. In addition, Figure 4-4 shows that the distribution of IRI rates in three categories is close to symmetric, which justifies the robustness of results from ANOVA test.

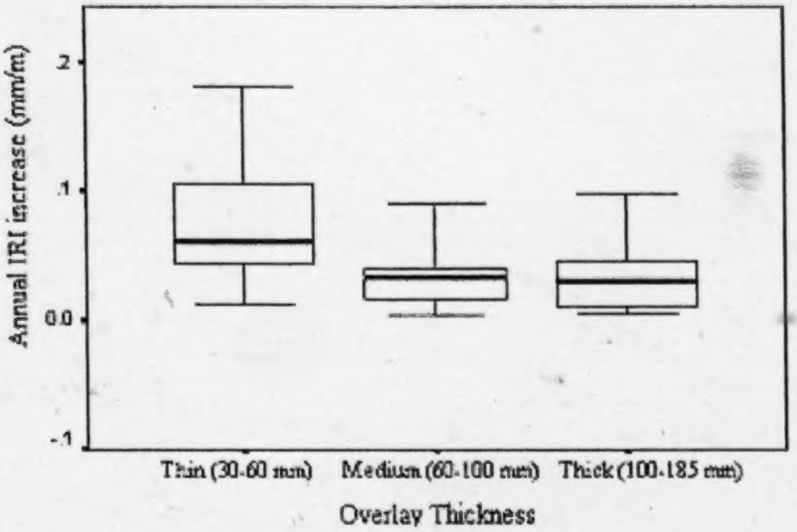

Figure 4-4: Box plot of IRI rates for different overlay thicknesses in the C-LTPP project

ANOVA test results for IRI rates related to different overlay thicknesses in the C-LTPP project are presented in Table 4-7. P-value was less than α=0.05 and therefore, overlay thickness was a significant factor in the pavement roughness rates.

Groups	Count	Sum	Average	Variance
30-60	16	1.195	0.075	0.002
60-100	23	0.778	0.034	0.001
100-185	20	0.784	0.039	0.002

ANOVA

Source of Variation	SS	df	MS	F	P-value	F crit
Between Groups	0.017	2.000	0.009	6.237	0.004	3.162
Within Groups	0.078	56.000	0.001			
Total	0.096	58.000				

Table 4-7: ANOVA test results for IRI rates related to different overlay thicknesses in the C-LTPP project

To confirm the ANOVA test results, the Kruskal-Wallis test was conducted. The results are presented in Table 4-8:

Overlay Thickness Levels	Observation No.	Mean Rank
0 (Thin)	16	43.06
1 (Medium)	23	24.43
2 (Thick)	20	25.95
Total	59	
Test Results		
Test Statistics	IRI	
Asymptotic Sig. (P-Value)	0.002	

Table 4-8: Kruskal-Wallis test results for IRI rates related to different overlay thicknesses in the C-LTPP project

P-value was less than the significance level of $\alpha=0.05$; therefore, with 95% reliability, overlay thickness was a significant factor on pavement roughness. Although ANOVA test examines the H_0, it cannot identify which level has the most impact on roughness. In rank order statistics, comparison between mean ranks of different studied levels shows which level has the most impact on the variable (SPSS 11.0, 2001). In other words, Table 4-8 reveals that thin overlay with a mean rank equal to 43.06 had the highest IRI rate. Medium and thick overlays had similar mean rank values less than that for thin overlay, which reveals that average IRI rate related to test sections with medium and thick overlays was almost the same and less than average IRI rate related to sections with thin overlay.

With 95% reliability, both parametric and non-parametric analysis showed that overlay thickness was a significant factor in pavement roughness. Tighe et al. (1999) reported a similar finding of that in present study and that thinner overlay deteriorated at a significantly higher rate than the medium and thick overlays, while there was little comparative difference between the medium and thick class of overlays.

4.2.4. Effect of overlay material on pavement roughness

Two different types of overlay material were practiced in the C-LTPP project: recycled material (RAP), and conventional material (HMAC). Figure 4-5 shows the box plot for the IRI rates for two overlay types. This graph compares the impact of overlay material type on the roughness rates in combination with other factors. The average IRI rates related to the overlay material types were fairly close and IRI rates' distribution can approximately be assumed a normal distribution.

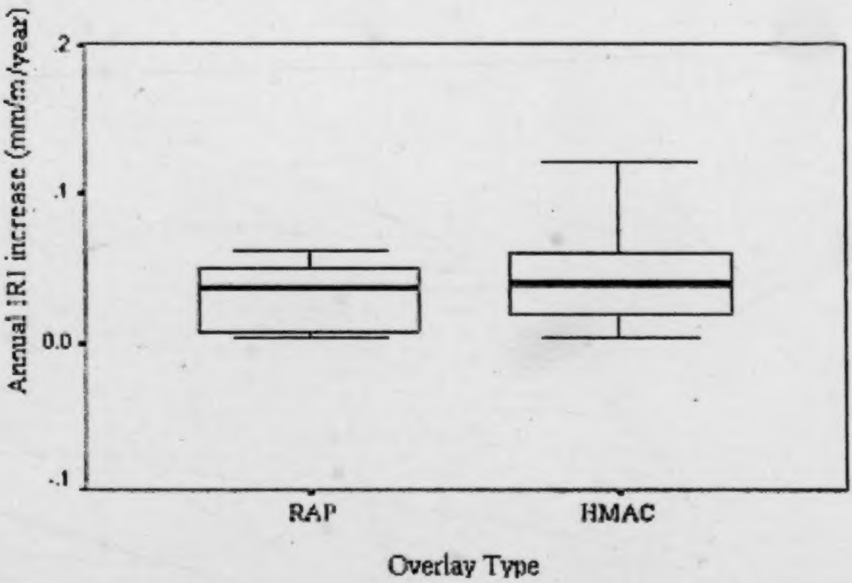

Figure 4-5: Box plot of IRI rates for different overlay materials in the C-LTPP project

The ANOVA test was conducted for IRI rates related to overlay types, and the results are shown in Table 4-9:

Groups	Count	Sum	Average	Variance
RAP	8	0.257	0.032	0.001
HMAC	51	2.505	0.049	0.002

ANOVA

Source of Variation	SS	df	MS	F	P-value	F crit
Between Groups	0.002	1.000	0.002	1.218	0.274	4.010
Within Groups	0.093	57.000	0.002			
Total	0.095	58.000				

Table 4-9: ANOVA test results for IRI rates related to different overlay material types in the C-LTPP project

ANOVA test did not reject the null hypothesis; hence, overlay type was not a significant factor in the roughness progression. As there are two groups of samples, the Mann-Whitney test was performed. The results are presented in Table 4-10:

Overlay Type Levels	Observation No.	Mean Rank
0 (RAP)	8	26.38
1 (HAMC)	51	30.57
Total	59	
Test Results		
Test Statistics	IRI	
Asymptotic Sig. (P-Value)	0.52	

Table 4-10: Mann-Whitney test results for IRI rates related to different overlay material types in the C-LTPP project

P-value was more than the significance level of α=0.05; therefore, the type of overlay material had no impact on pavement roughness. With 95% of reliability, Both parametric and non-parametric analysis showed that overlay material type was not a significant factor in pavement roughness. Tighe et al. (1999) did not report any finding about the impact of overlay type in pavement roughness, because of very limited observations at the time that their study was conducted.

4.2.5. Effect of subgrade material on pavement roughness

As it can be seen in Table 4-2, there are two classes of subgrade material in the C-LTPP project: fine and coarse aggregates. In Figure 4-6, the box plot for the IRI rates within each subgrade class is presented. This graph compares the impact of subgrade materials on roughness progression, in combination with other factors. In terms of the subgrade material, no explicit difference between IRI rates was observed.

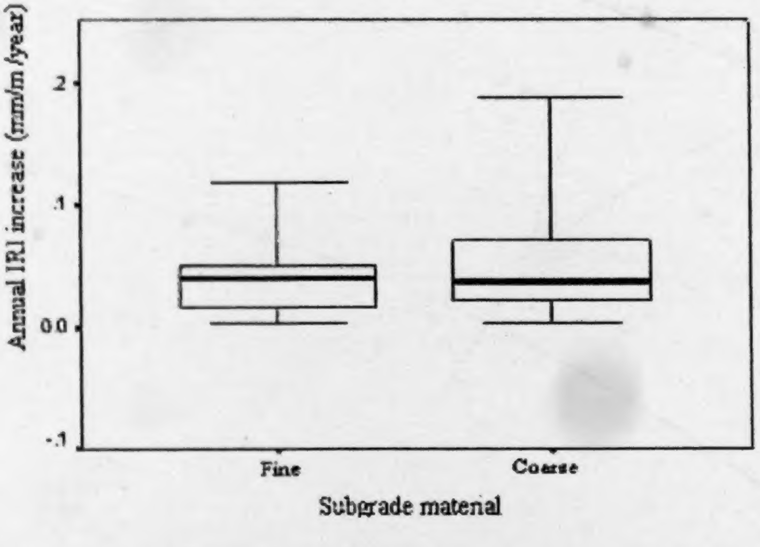

Figure 4-6: Box plot of IRI rates for different subgrade materials in the C-LTPP project

Despite of a non-symmetric distribution for coarse material, the ANOVA test was performed and the obtained P-value was more than 0.05; therefore, with 95% of reliability, subgrade material was not significant in roughness. The results of ANOVA test are shown in Table 4-11.

Groups	Count	Sum	Average	Variance
Fine	32	1.377	0.043	0.001
Coarse	27	1.380	0.051	0.002

ANOVA

Source of Variation	SS	df	MS	F	P-value	F crit
Between Groups	0.001	1.000	0.001	0.572	0.452	4.010
Within Groups	0.095	57.000	0.002			
Total	0.096	58.000				

Table 4-11: ANOVA test results for IRI rates related to different subgrade material types in the C-LTPP project

For observations within two classes of subgrade, the Mann-Whitney test was performed. The results are presented in Table 4-12. P-value was more than the significance level of $\alpha = 0.05$; therefore, the type of subgrade material had no impact on pavement roughness.

Subgrade material Levels	Observation No.	Mean Rank
0 (Fine)	32	29.00
1 (Coarse)	27	31.19
Total	59	
Test Results		
Test Statistics	IRI	
Asymptotic Sig. (P-Value)	0.626	

Table 4-12: Mann-Whitney test results for IRI rates related to different subgrade material types in the C-LTPP project

With 95% of reliability, both parametric and non-parametric analysis showed that subgrade material type was not a significant factor in pavement roughness; however, Tighe et al. (1999) observed that, in the same period of time, the C-LTPP sections which were built on fine-grained subgrade soil, deteriorated faster than the pavements on coarse-grained soils. Such discrepancy between the findings from this study and those from theirs, could be because of

1- More IRI data was studied in present study. Tighe et al. used the IRI data from approximately 7 years of service life, while in present study the IRI data for almost one decade of service life was used (see Table 4-1).

2- Tighe et al. conclusion was based on observation to find the impact of different factors on pavement roughness and they did not use kind of statistical analysis with a certain level of reliability, while different findings could be expected based on different levels of reliability.

4.2.6. Effect of milling on pavement roughness

Regarding the pavement preparation before overlay, two types of test sections were available in the C-LTPP program: test sections with milling and those without milling. Figure 4-7 shows the box plot for roughness progression in test sections within each group. The data distribution for test sections with milling was rather right skewed and was not symmetric enough to be assumed a normal distribution. The average values of IRI rates in two levels were fairly close.

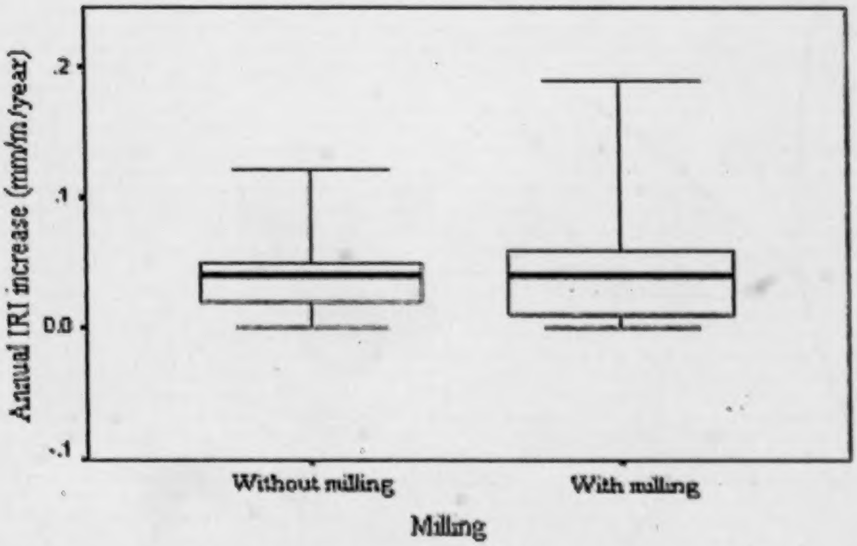

Figure 4-7: Box plot of IRI rates for different preparation of old pavement in the C-LTPP project

The results of ANOVA test for the IRI rates related to different pavement preparation is tabulated in Table 4-13. The P-value form ANOVA test was more than 0.05; hence, milling did not affect pavement roughness.

Groups	Count	Sum	Average	Variance
No milling	37	1.584	0.043	0.001
With milling	25	1.273	0.051	0.003

ANOVA

Source of Variation	SS	df	MS	F	P-value	F crit
Between Groups	0.001	1.000	0.001	0.558	0.458	4.001
Within Groups	0.105	60.000	0.002			
Total	0.106	61.000				

Table 4-13: ANOVA test results for IRI rates related to different preparation of old pavement in the C-LTPP project

The Mann-Whitney test was applied for two levels of milling and result is presented in Table 4-14:

Pavement preparation levels	Observation No.	Mean Rank
0 (No milling)	37	31.58
1 (With milling)	25	31.38
Total	62	
Test Results		
Test Statistics	IRI	
Asymptotic Sig. (P-Value)	0.965	

Table 4-14: Mann-Whitney test results for IRI rates related to different levels of preparation of old pavement in the C-LTPP project

Based on the Mann-Whitney test, P-value was more than the significance level of $\alpha = 0.05$; therefore, the pavement preparation before overlay had no impact on pavement roughness.

With 95% of reliability, both parametric and non-parametric analysis showed that milling was not a significant factor in pavement roughness, while as was mentioned in 2.3, Tighe et al. (1999) did not report any apparent observation regarding the overlay type because of very limited observations at the time that their study was conducted.

4.3. Summary of the factors affecting roughness in the C-LTPP project

A statistical approach including both parametric and non-parametric techniques was employed in order to investigate the effect of climate, traffic, overlay thickness, overlay material type, subgrade material types, and milling in the roughness progression in the C-LTPP Program. With 95% of reliability, both methods showed that the only attribute that affected roughness, IRI rates, was overlay thickness. Thinner overlays deteriorated at a significantly higher rate than the medium and thick overlays, while little comparative difference was found between the medium and thick class overlays. In 3.3.5, in discussion of the roughness evaluation of the C-LTPP sections, it was observed that test sections with thinner overlays have shorter service lives than other sections, which agrees with the findings from the statistical analysis of the IRI rates.

The lack of distinction between IRI rates related to medium and thick overlays may reveal that it could be reasonable to consider two levels of thin (less than 60 mm) and thick (more than 60 mm) overlays for study in the C-LTPP program.

It is useful to validate findings from this section of study with those from other studies. Some of the findings from other researches are summarized below:

1- Using the LTPP data, the FHWA reported that overlay thickness was a significant factor in pavement roughness (FHWA-RD-98-149, 1998). The FHWA also found that that pavements constructed on fine-grained soils with higher plasticity had a higher roughness index (FHWA-RD-97-147).

2- McGhee (2000) used the field data from 4270 lane-kilometer pavement at Virginia Department Of Transportation (VDOT), and reported that thicker overlays were usually smoother. He also reported that the milling of the original surface rarely affected pavement roughness.

3- The National Co-operative Highway Research Program (NCHRP2002) reported that for the LTPP program in the USA, initial IRI did not depend on overlay thickness, milling or asphalt type.

4- Perera and Kohn (1999) conducted a study about roughness by using LTPP data from the SPS-5 experiment. The SPS-5 experiment investigates the performance of selected asphalt concrete rehabilitation treatment factors, including overlay mix type (virgin, recycled), overlay thickness, and the surface preparation of the original asphalt layer (milled, non-milled) on roughness of test sections in the LTPP program. Researchers reported overlay thickness did not affect the IRI, but made no specific conclusion about the overlay materials on roughness.

Table 4-15 summarizes and compares the findings from present research project and other researches.

Study Attribute	FHWA (1998)	Tighe et al. (1999)	Perera et al. (1999)	McGhee (2000)	NCHRP (2002)	Present (2003)
Weather climate	*	Yes	*	*	*	No
Traffic	*	No	*	*	*	No
Overlay thickness	Yes	Yes	No	Yes	No	Yes
Overlay material	*	*	*	*	No	No
Subgrade material	Yes	No	*	*	*	No
Milling	*	*	*	No	No	No

Table 4-15: Comparison between findings from present study and other studies of roughness (=Not investigated / No result)*

Table 4-15 shows reasonable consistency between the results from the present research project and other studies; however, the results from various studies regarding pavement roughness progression had some differences that could be caused by the following issues

1- Differences in data collecting in various projects,

2- Differences in quality control of data in different projects,

3- Differences in methodologies for data analyzing,

4- Differences in the reliability level of similar methodologies,

5- Differences between the age of the overlaid sections in various projects and subsequently the stage that roughness had reached (the initial stage with linear roughness progression vs. the older stage with non-linear roughness progression).

It must be mentioned that in this study, the interactions of the factors and their effects on pavement roughness were not considered.

4.4. Evaluation of design practices for roughness of the C-LTPP sections

Table 4-16 represents the roughness progression based on the IRI rates in the C-LTPP project for different agency-designed practices including; under agency design, agency design, and over agency design. In each test site are different adjacent sections that correspond to different agency design practices for the C-LTPP project; however, there are some test sites that do not have either the under

		Under agency designed			Agency designed			Over agency designed		
Location	C-SHRP ID	Section	Overlay (mm)	IRI rate (mm/m/year)	Section	Overlay (mm)	IRI rate (mm/m/year)	Section	Overlay (mm)	IRI rate (mm/m/year)
Alberta	810404	1	61	0.041	3	94	0.034	2	103	0.06
		4	55	0.061						
British Columbia	820205	1	60	0.083	2	83	0.035			
	820502				1	104	*	2	118	*
	820605				1	50	0.012	2	73.2	0.005
Manitoba	830403	1	100.3	0.005	2	113.3	0.008	3	148	*
	830801	2	103.3	0.042	1	185	0.012			
		3	126	0.042						
		4	170	0.018						
New Brunswick	840101	3	87	0.004	1	174	*	2	179	0.004
	840204	2	88	0.034	1	114	0.023			
	840604	2	89.9	0.02	1	107.3	0.05			
		3	29.5	*						
		4	35	0.062						
New Foundland	850201	2	73	0.011	1	117	0.005			
	850206	2	63	0.047	1	106	0.01			
	850601	2	74	0.019	1	122	0.029			
Nova Scotia	860501	1	55	0.122	2	85	0.053	3	41	0.048
	860603	2	80	0.094	1	85.6	0.105			
		3	34	0.099						
Ontario	870102				2	46.2	0.181	1	94.5	0.123
	870504				1	31	0.038	2	61.3	0.03
	870505				2	72.5	0.04	1	75	0.04
								3	105	0.039
								4	106.3	0.054
	870701				1	42.5	0.043	2	106	0.024
Prince Edward Island	880203	3	51	0.116	1	51	0.109	2	109	0.192
								4	99	0.04
Quebec	890803				1	39.7	0.061	2	50.7	0.089
								3	105.7	0.031
								4	82.7	0.037
	890702				1	44	0.016	2	85	0.026
Saskatchewan	900402	1	86.3	0.014	2	125.6	0.005			
	900802	1	54.5	0.052	2	66.7	0.02	3	104.3	0.008
	900803	2	107.6	0.097	1	157.5	0.04			

Table 4-16: The IRI rates for different design practices in the C-LTPP project

agency design or over agency design section. The IRI rates, extracted form Table 4-1, are shown in Table 4-16. Asterisks show test sections with negative IRI rates, omitted from this study. As well, the overlay thicknesses are shown to provide a better comparison between the design scenarios.

The different sections within each site have similar climate, traffic, and subgrade material, but differ in overlay thickness, overlay material type, and pavement preparation prior to overlay.

Based on the discussion in Section 4.3, it was expected that overlay thicknesses must affect the IRI rates of different design practices. In other words, the IRI rate of under agency design sections was expected to be higher than that of the agency design sections and the IRI rates of over agency design sections was expected to be less than that of agency-designed sections.

The highlighted sections in Table 4-16, are those test sections that had IRI rates higher than the average IRI rate from all the C-LTPP sections, 0.042 mm/m/year, discussed in Section 4.2. This table reveals that 10 of the under agency-designed test sections showed a higher IRI rate than 0.042 mm/m/year, which was 48% of all the under agency-designed test sections; 7 of the agency-designed test sections showed a higher IRI rate than 0.042 mm/m/year, which was 29% of all the agency-designed test sections; and 6 of the over agency-designed test sections showed a higher IRI rate than 0.042 mm/m/year, which was 32% of all the over agency-designed test sections. It was thus observed that agency-designed and over agency-designed test sections have lower roughness rates than that of the under agency-designed test sections.

To compare the design scenarios, ANOVA test was conducted for IRI rates related to different design practices. The results of ANOVA test are shown in Table 4-17. The high P-value did not reject the null hypothesis and the ANOVA test showed that different design practices did not significantly affect the roughness rates in the C-LTPP sections.

Groups	*Count*	*Sum*	*Average*	*Variance*
Under agency-designed	21	1.08	0.05	0.0014
Agency-designed	22	0.93	0.04	0.0018
Over agency-designed	17	0.85	0.05	0.0022

ANOVA

Source of Variation	*SS*	*df*	*MS*	*F*	*P-value*	*F crit*
Between Groups	0.001	2	0.001	0.30	0.74	3.16
Within Groups	0.100	57	0.002			
Total	0.101	59				

Table 4-17: ANOVA test results for IRI rates related to different design practices in the C-LTPP project

4.5. Factors affecting pavement rutting

To investigate the influence of different factors on pavement rutting in the C-LTPP project, procedures similar to those used for pavement roughness study, in 4.4, were employed. The annual rut increase for all the test sections was calculated using Equation 4-2:

$$Rut\ Rate = \frac{\left(Rut_j - Rut_i\right)}{j-i}, \qquad (4\text{-}2)$$

where

j = The year that rut measurement was recorded

i = The first year after overlaying that rut measurement was recorded

Rut_j = Rut in year j

Rut_i = Rut in year i.

Table 4-18 shows the rut rates for all the C-LTPP test sections.

C-SHRP ID	Section	Year after overlaid (i)	Rut-i(mm)	Year after overlaid (j)	Rut-j(mm)	Rut rate (mm/year)
810404	1	0	1.70	9	2.15	0.050
810404	2	0	2.50	9	2.55	0.006
810404	3	0	2.50	9	2.75	0.028
810404	4	0	1.90	9	2.15	0.028
820205	1	1	0.50	5	1.10	0.150
820205	2	1	0.45	5	1.20	0.188
820502	1	1	2.70	7	6.55	0.642
820502	2	1	0.90	7	3.25	0.392
820605	1	1	2.00	7	5.20	0.533
820605	2	1	1.85	7	4.85	0.500
830403	1	0	1.35	11	1.65	0.027
830403	2	0	1.55	11	1.55	0.000
830403	3	0	1.45	11	1.25	-0.018
830801	1	0	1.40	12	7.45	0.504
830801	2	0	1.10	12	5.50	0.367
830801	3	0	1.20	12	6.50	0.442
830801	4	0	1.45	12	7.50	0.504

Table 4-18: The rutting rates in the C-LTPP test sections (continued)

C-SHRP ID	Section	Year after overlaid (i)	Rut-i(mm)	Year after overlaid (j)	Rut-j(mm)	Rut rate (mm/year)
840101	1	0	0.95	11	14.70	1.250
840101	2	0	1.05	11	15.80	1.341
840101	3	0	1.00	11	13.65	1.150
840204	1	0	2.20	11	8.65	0.586
840204	2	0	1.05	11	5.85	0.436
840604	1	0	1.10	10	10.15	0.905
840604	2	0	0.95	10	8.25	0.730
840604	3	0	2.00	10	7.40	0.540
840604	4	0	3.15	10	9.30	0.615
850201	1	2	1.00	12	7.90	0.690
850201	2	2	1.60	12	8.15	0.655
850206	1	1	2.20	11	3.10	0.090
850206	2	1	1.05	11	2.75	0.170
850601	1	2	5.35	12	15.30	0.995
850601	2	2	3.30	12	11.35	0.805
860501	1	1	6.15	11	25.90	1.975
860501	2	1	2.90	11	10.20	0.730
860501	3	1	3.10	11	9.00	0.590
860603	1	1	6.90	11	11.95	0.505
860603	2	1	5.80	11	13.05	0.725
860603	3	1	6.30	11	13.25	0.695
870102	1	2	1.80	9	4.45	0.379
870102	2	2	1.85	9	6.45	0.657
870504	1	1	2.45	7	4.00	0.258
870504	2	1	3.30	7	5.45	0.358
870505	1	1	0.85	8	3.65	0.400
870505	2	1	1.05	8	3.45	0.343
870505	3	1	0.85	8	2.35	0.214
870505	4	1	1.50	8	4.20	0.386
870701	1	1	0.70	8	0.85	0.021
870701	2	1	0.45	8	1.30	0.121
880203	1	1	1.95	10	4.45	0.278
880203	2	1	1.65	10	5.20	0.394
880203	3	1	2.50	10	4.45	0.217
880203	4	1	1.15	10	3.05	0.211
890503	1	2	1.90	11	15.05	1.461
890503	2	2	1.80	11	13.75	1.328
890503	3	2	2.55	11	14.90	1.372
890503	4	2	1.70	11	11.05	1.039
890702	1	1	2.40	9	6.55	0.519
890702	2	1	1.35	9	4.75	0.425
900402	1	0	1.20	10	3.15	0.195
900402	2	0	0.60	10	4.05	0.345
900802	1	0	5.95	10	5.50	-0.045
900802	2	0	5.35	10	4.90	-0.045
900802	3	0	3.40	10	4.55	0.115
900803	1	0	0.95	10	2.80	0.185
900803	2	0	0.90	10	3.00	0.210

Table 4-18: The rutting rates in the C-LTPP test sections

Table 4-18 shows a negative value for some test sections that represents a consistent decrease in rut during the service time. These test sections are 830403-3(MB), 900802-1(SK), 900802-2(SK). Such test sections were omitted from the study. Figure 4-8 shows the box plot of rutting rates in all the C-LTPP sections.

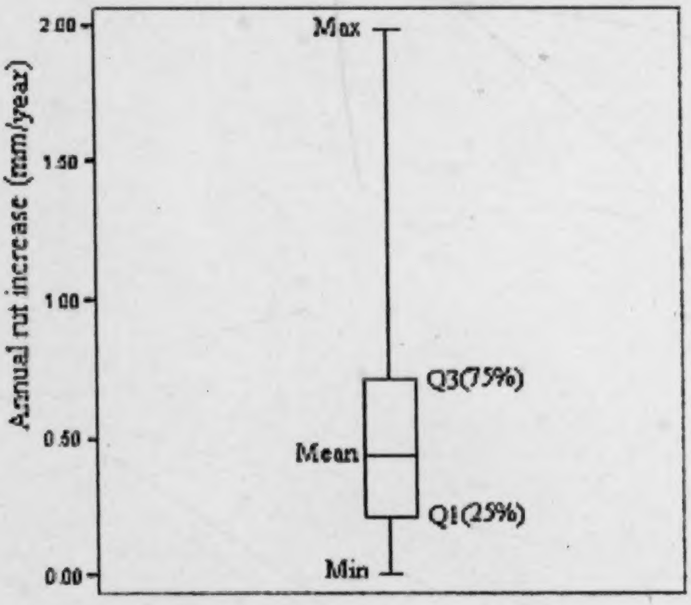

Figure 4-8:Box plot of rutting rates for all the C-LTPP sections

Based on Figure 4-8, the following points can be made:

1- The average annual rut rate for all the C-LTPP sections is 0.45 mm. Hence, the average rut after 20 years of pavement performance in the C-LTPP project will be 9 mm. This low value for rutting after 20 years of service life agrees with the results in Chapter 3, where it was concluded that rutting is not the main factor in pavement failure.

2- The maximum and minimum rut rates for the C-LTPP sections were: 1.98 (mm/year), and 0.02 (mm/year) respectively.

3- The distribution of rutting rates is not symmetric and cannot be considered as a normal distribution. Hence, any statistical analysis related to rut rates that requires the assumption of normality must be confirmed by using other methods.

To investigate the effect of different factors from the C-LTPP experimental design, the rut rates are shown in Table 4-19. Test sections with negative rut rates are highlighted and were not considered in the statistical analysis. Using the statistical analysis a null hypothesis, H_o, was tested. The null hypothesis was that any of factors in the C-LTPP experiment has not significant effect on rut rates.

4.5.1. Effect of climate on pavement rutting

Figure 4-9 presents the box plot of the rutting rates for different weather climates. This graph shows that in wet-high freeze conditions the rut progression was higher than that in the other climates. While in dry-high freeze condition the best rutting performance was obtained. Figure 4-9 shows that the rut rates' distribution is symmetric and that it can be assumed to be a normal distribution.

Traffic	Overlay Type	Overlay Thick.(mm)	Moisture, Freezing Index and Subgrade Condition					
			Wet					Dry
			No to Low Freeze			High Freeze		High Freeze
			Fine	Coarse		Fine	Coarse	Fine
Low	RAP	30-60						0.028
		60-100						0.028
		100-185	0.640					
			0.390					
			0.390					
	HMAC	30-60	0.550		0.150	0.020		
			0.660		0.700			
					0.280			
					0.220			
		60-100	0.500	0.190	0.810			0.050
			0.380	0.440	0.510			0.028
			0.400	0.660	0.730			0.195
			0.340	0.170	0.210			
		100-185	0.210		0.590	0.120		0.006
					0.770			0.000
					0.090			-0.020
					1.000			0.345
					0.390			
High	RAP	30-60						
		60-100			1.150			
		100-185			1.340			0.500
					0.910			0.370
	HMAC	30-60	1.980		0.540	0.520	1.460	-0.050
			0.590		0.620		1.330	
					0.260			
		60-100	0.730		0.730	0.430	1.040	-0.040
					0.360			
		100-185			1.250		1.370	0.440
								0.500
								0.115
								0.185
								0.210

Table 4-19: The rut rates for the test sections in the experimental design of the C-LTPP project

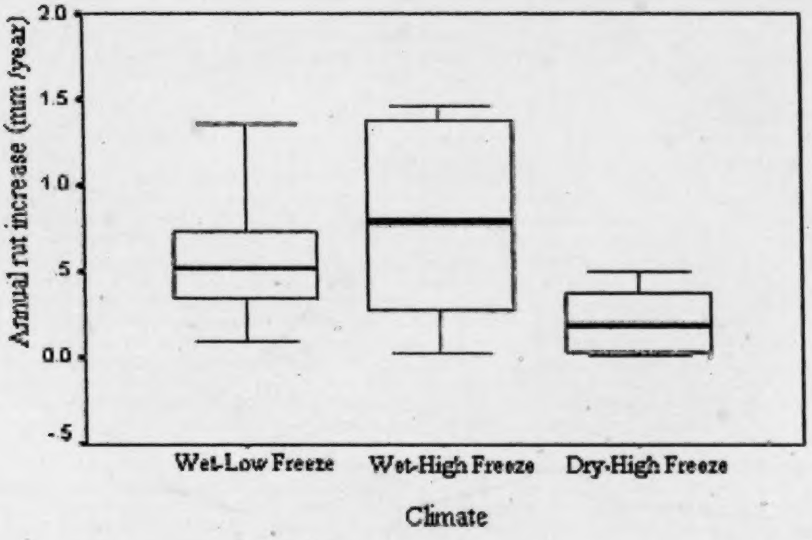

Figure 4-9: Box plot of rutting rates for different weather climates in the C-LTPP project

The ANOVA test was conducted for the rutting rates related to different weather conditions. The results are tabulated in Table 4-20:

Groups	Count	Sum	Average	Variance
Wet-Low	38	22.230	0.585	0.151
Wet-High	8	6.290	0.786	0.341
Dry-High	14	3.000	0.214	0.034

ANOVA

Source of Variation	SS	df	MS	F	P-value	F crit
Between Groups	2.035	2.000	1.017	6.905	0.002	3.159
Within Groups	8.398	57.000	0.147			
Total	10.432	59.000				

Table 4-20: ANOVA test results for rutting rates related to different climate conditions in the C-LTPP project

ANOVA test showed that with a P-value of less than 0.05, the null hypothesis was rejected and that climate was significant factor in pavement rutting. Although the distribution of rutting rates was symmetric for considering a normal distribution, the sample sizes in different levels of climate are quite different. Therefore, to confirm the results from ANOVA test, Kruskal-Wallis test was performed using the SPSS program. The results are presented in Table 4-21:

Climate Levels	Observation No.	Mean Rank
0 (Wet-low freeze)	38	34.49
1 (Wet-high freeze)	8	38.00
2 (Dry-high freeze)	14	15.39
Total	60	
Test Results		
Test Statistics	Rut	
Asymptotic Sig. (P-Value)	0.001	

Table 4-21: Kruskal-Wallis test results for rutting rates related to different climate conditions in the C-LTPP project

P-Value from Kruskal-Wallis test was less than 0.05; hence, this test showed that climate was a significant factor in pavement rut progression. With 95% of reliability, the Kruskal-Wallis test confirmed the result from ANOVA. In addition, comparison of mean rank values in Table 4-21, showed that average rut rate in wet-high freeze zone was the highest and average rut rate in dry-high freeze zone was the lowest for the studied weather climates. It is possible to rank rut rates in wet condition in the same group, which showed a higher rut rate than that in dry condition.

4.5.2. Effect of traffic on pavement rutting

Figure 4-10 represents the box plot for the rutting rates of the C-LTPP sections for two levels of traffic, shown in Table 4-19. This graph showed that in high traffic condition, with more than 200,000 ESAL/year, rut developed faster than that in low traffic zones with less than 200,000 ESAL/year. In addition, the distribution of rut rates due to the traffic levels is almost symmetric and it can be assumed a normal distribution.

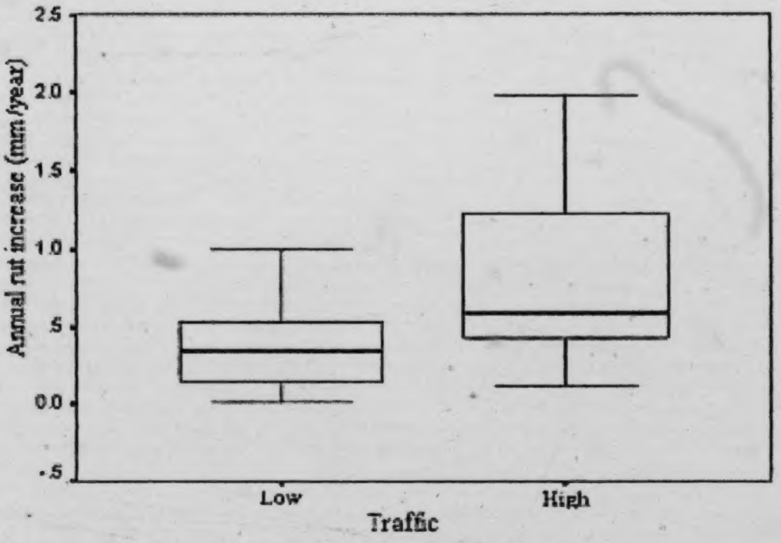

Figure 4-10: Box plot of rutting rates for different traffic levels in the C-LTPP project

The ANOVA test for rutting rates related to different traffic levels in the C-LTPP project was conducted and the results are summarized in Table 4-22:

Groups	Count	Sum	Average	Variance
Low Trafic	35	12.510	0.357	0.070
High Trafic	25	19.010	0.760	0.237

ANOVA

Source of Variation	SS	df	MS	F	P-value	F crit
Between Groups	2.368	1.000	2.368	17.034	0.001	4.007
Within Groups	8.064	58.000	0.139			
Total	10.432	59.000				

Table 4-22: ANOVA test results for rutting rates related to different traffic levels in the C-LTPP project

P-value was less than 0.05; therefore, traffic was significant factor in pavement roughness progression. To confirm the results, the Mann-Whitney analysis was performed for two levels of traffic. The results are presented in Table 4-23:

Traffic Levels	Observation No.	Mean Rank
0 (Low)	35	24.09
1(High)	25	39.48
Total	60	
Test Results		
Test Statistics	Rut	
Asymptotic Sig. (P-Value)	0.001	

Table 4-23: Mann-Whitney test results for rutting rates related to different traffic levels in the C-LTPP project

The P-Value from Mann-Whitney test was less than 0.05; hence, this test showed that traffic was a significant factor in rut progression. With 95% of reliability, the Mann-Whitney test confirms the result from ANOVA. Higher mean rank value for rut rates in high traffic zone, revealed that average rutting rate in this traffic level was more than that in low traffic level.

The EBA Consultant Engineers, Ltd. (2001) conducted a study about rutting trends after almost 7 to 9 years of collecting rut data for the C-LTPP test sections. They did not use the rutting rates over time, but calculated the rutting rates per 100,000 ESAL, and found that rutting rates in low traffic zone were higher than those in high traffic zone.

4.5.3. Effect of overlay thickness on pavement rutting

Figure 4-11 shows the box plot for rutting rates in the C-LTPP sections related to different overlay thickness classification. Thin overlays showed the worst rut performance and had a higher rutting rate than those with medium or thick overlays rut rates.

The rut rates for medium and thick overlays were almost the same. As well, the box plot shows that rutting rates' distribution for thin overlay class was not symmetric.

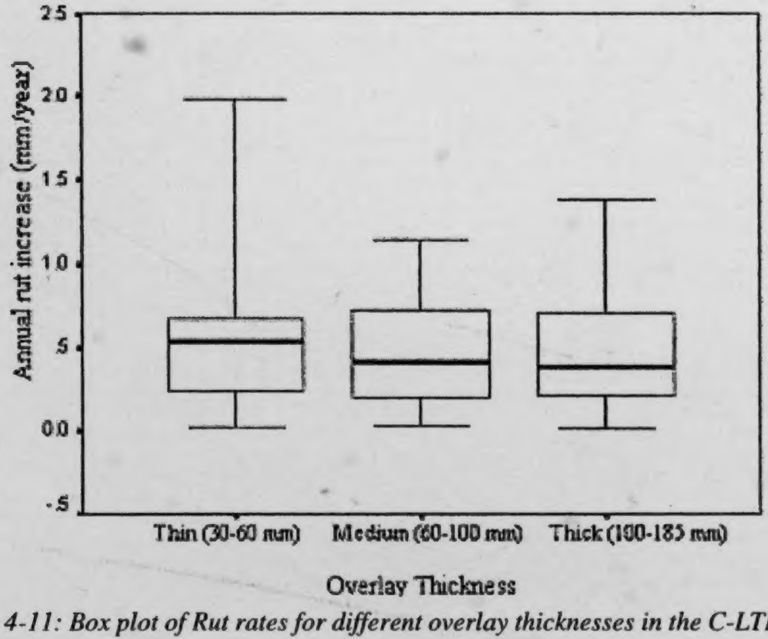

Figure 4-11: Box plot of Rut rates for different overlay thicknesses in the C-LTPP project

Table 4-24 summarizes the results from ANOVA test related to the overlay thickness classification in the C-LTPP program. P-value higher than 0.05 showed that overlay thickness was not significant in rut progression.

To confirm the results from ANOVA test, Kruskal-Wallis test was performed. The outputs of SPSS program are presented in Table 4-25.

Groups	Count	Sum	Average	Variance
30-60	16	9.908	0.619	0.295
60-100	22	10.081	0.458	0.098
100-185	23	12.131	0.527	0.163

ANOVA

Source of Variation	SS	df	MS	F	P-value	F crit
Between Groups	0.240	2.000	0.120	0.692	0.505	3.156
Within Groups	10.070	58.000	0.174			
Total	10.311	60.000				

Table 4-24: ANOVA test results for rutting rates related to different overlay thickness levels in the C-LTPP project

Overlay Thickness Levels	Observation No.	Mean Rank
0 (Thin)	16	33.63
1 (Medium)	22	29.36
2 (Thick)	23	30.74
Total	61	
Test Results		
Test Statistics	Rut	
Asymptotic Sig. (P-Value)	0.763	

Table 4-25: Kruskal-wallis test results for rutting rates related to different overlay thickness levels in the C-LTPP project

With 95% of reliability, the same as ANOVA test; the Kruskal-Wallis test did not show any significance effect by different overlay thickness on the rutting rates.

4.5.4. Effect of overlay material on pavement rutting

Figure 4-12 presents the box plot for the rutting rates of the C-LTPP sections related to two types of overlay material: conventional and recycles asphalt mixtures. It was observed that rutting rate distribution in HMAC sections was rather right skewed and did not meet the assumption for normal distribution. Also, the averages of rut rates in two levels were fairly similar. The ANOVA test was conducted and Table 4-26 summarizes the outputs. P-value was larger than 0.05, therefore, with 95% reliability it was found that overlay material types did not affect rut rates in the C-LTPP program.

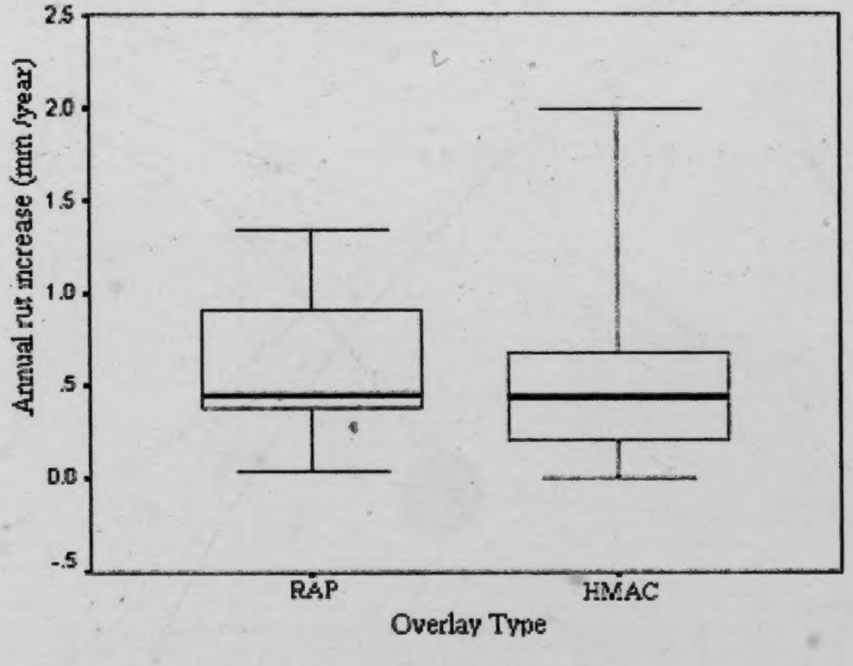

Figure 4-12: Box plot of rutting rates for different overlay materials in the C-LTPP project

Groups	Count	Sum	Average	Variance
RAP	10	5.746	0.575	0.194
HMAC	52	26.374	0.507	0.173

ANOVA

Source of Variation	SS	df	MS	F	P-value	F crit
Between Groups	0.038	1.000	0.038	0.217	0.643	4.001
Within Groups	10.545	60.000	0.176			
Total	10.583	61.000				

Table 4-26: ANOVA test results for rutting rates related to different overlay material types in the C-LTPP project

To confirm the results from ANOVA test, the Mann-Whitney test was conducted. Outputs of the SPSS program for Mann-Whitney test are presented in Table 4-27. The Mann-Whitney test showed that overlay material had no impact on pavement rutting progression, which conformed the result from ANOVA test. However Dawley et al. (1993) based on a study in Lethbridge, Alberta, concluded that RAP material mitigates pavement rutting.

Overlay material Levels	Observation No.	Mean Rank
0 (RAP)	10	33.80
1 (HMAC)	52	31.06
Total	62	
Test Results		
Test Statistics	Rut	
Asymptotic Sig. (P-Value)	0.66	

Table 4-27: Mann-Whitney test results for rutting rates related to different overlay material types in the C-LTPP project

4.5.5. Effect of subgrade material on pavement rutting

Two types of subgrade material, fine and coarse aggregate, are considered in the C-LTPP project. In Figure 4-13, the box plot for rutting rates related to subgrade material classification is presented. It was observed that the average rut rates for the two types of subgrade were different and the rutting rates in the C-LTPP sections built on coarse aggregate were higher then those with fine aggregate subgrade.

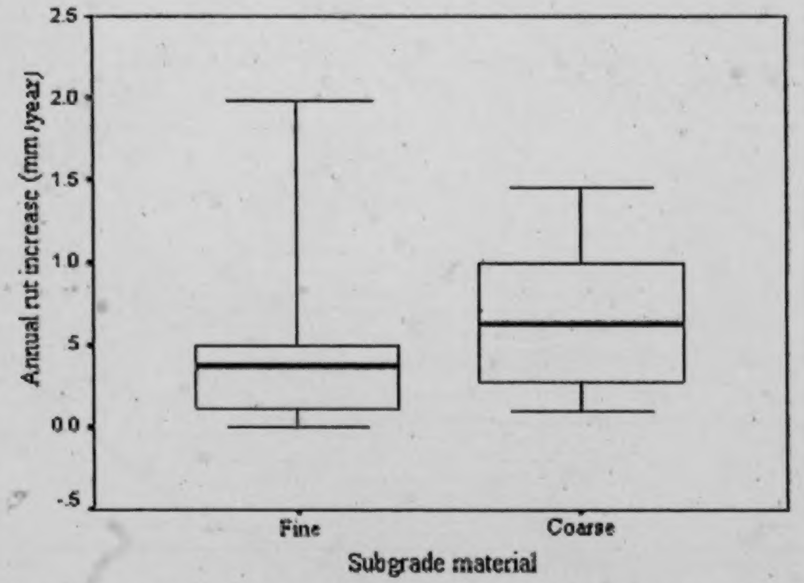

Figure 4-13: Box plot of rutting rates for different subgrade materials in the C-LTPP project

The distribution of rutting rates in sections with fine aggregate was not symmetric, which reject the assumption of normality and questions the accuracy of ANOVA test. The results of ANOVA test are tabulated in Table 4-28. A P-value less than 0.05 demonstrated that subgrade types statistically affected the rut progression in the C-LTPP sections different.

Groups	Count	Sum	Average	Variance
Fine	32	11.870	0.371	0.133
Coarse	30	20.270	0.676	0.173

ANOVA

Source of Variation	SS	df	MS	F	P-value	F crit
Between Groups	1.438	1.000	1.438	9.437	0.003	4.001
Within Groups	9.142	60.000	0.152			
Total	10.580	61.000				

Table 4-28: ANOVA test results for rutting rates related to different subgrade material types in the C-LTPP project

To confirm the above results, the non-parametric method, Mann-Whitney test, was conducted. Outputs of the SPSS program for the Mann-Whitney test are summarized in Table 4-29:

Subgrade material Levels	Observation No.	Mean Rank
0 (Fine)	32	24.39
1 (Coarse)	30	39.08
Total	62	
Test Results		
Test Statistics	Rut	
Asymptotic Sig. (P-Value)	0.001	

Table 4-29: Mann-Whitney test results for rutting rates related to different subgrade material types in the C-LTPP project

The P-value less than 0.05 rejected the H_o and showed the significant impact of subgrade material type in rut rates. A comparison between the mean rank values showed that sections with fine subgrade had lower rut progression than the other test sections.

4.5.6. Effect of milling on pavement rutting

Box plot of rutting rates for two levels of pavement preparation before overlay, milling and not milling, is presented in Figure 4-14. Rutting rates' distribution for test sections without milling was not symmetric that shows it could not be considered as a normal distribution. From Figure 4-14, it was observed that the C-LTPP sections without milling have a higher rut rate than milled sections.

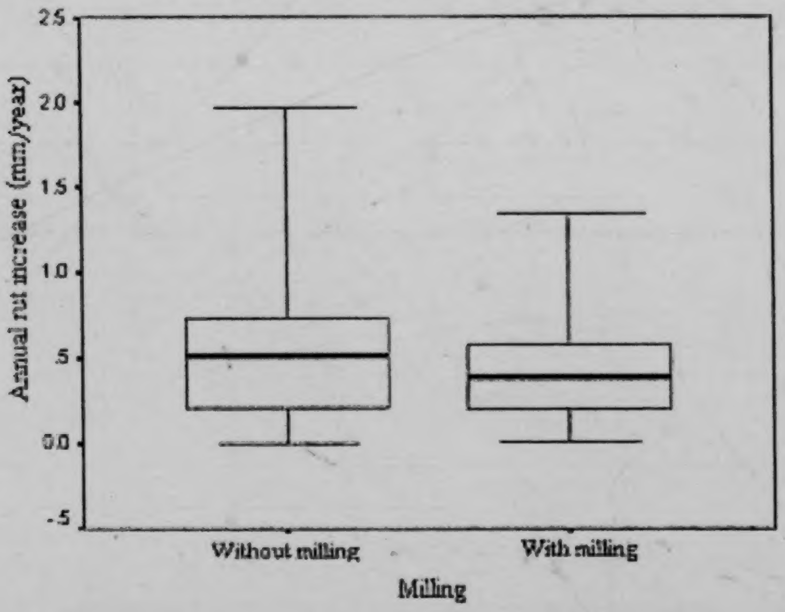

Figure 4-14: Box plot of rutting rates for different preparation of old pavement in the C-LTPP project

ANOVA test was conducted for rutting rates related to different pavement preparation in the C-LTPP project. The results are tabulate in Table 4-30.

The P-value was not less than 0.05; hence, milling did not reduce the rutting rate, with 95% reliability. To confirm the results from ANOVA, the Mann-Whitney test was conducted. The resulted are summarized in Table 4-31.

Groups	Count	Sum	Average	Variance
No milling	38	21	0.569	0.199
With milling	24	10	0.430	0.125

ANOVA

Source of Variation	SS	df	MS	F	P-value	F crit
Between Groups	0.284	1.000	0.284	1.666	0.202	4.001
Within Groups	10.236	60.000	0.171			
Total	10.520	61.000				

Table 4-30: ANOVA test results for rutting rates related to different levels of pavement preparation in the C-LTPP project

Pavement preparation levels	Observation No.	Mean Rank
0 (No milling)	38	33.92
1 (With milling)	24	27.67
Total	62	
Test Results		
Test Statistics	Rut	
Asymptotic Sig. (P-Value)	0.184	

Table 4-31: Mann-Whitney test results for rutting rates related to different levels of pavement preparation in the C-LTPP project

With a confidence level of 95%, there was no difference between the studied groups; however, comparison between mean rank values shows that milled sections showed lower rut progression than other sections. Changing the confidence level from 95% to 80%, shows that milling had a significant impact in rutting rates for the C-LTPP sections.

4.6. Summary for factors affecting pavement rutting in the C-LTPP project

Two statistical approaches including parametric and non-parametric techniques were employed to investigate the affecting factors in rutting rates for the C-LTPP sections. Both methods confirmed findings from this study, summarized as bellow:

1- Weather climate was a significant factor in the rutting rates for the C-LTPP sections and generally, pavement sections in the wet climates with high and low freeze, showed a higher rut progression than the sections in the dry climate zone.

2- Traffic was another factor that significantly affected the rut progression rate, and an increased traffic load resulted to higher rut rates. This was not in agreement with findings from the EBA study, which concluded that rutting rates in low traffic zone were higher than those in high traffic zone.

3- Overlay thickness had no significant impact on the rutting rates.

4- Overlay types (conventional vs. reclaimed) had no significant impact on the rutting rates. Dawley et al. (1993) based on a study in Lethbridge, Alberta, concluded that RAP material mitigates pavement rutting.

5- Subgrade material types showed significant impact on the rut progression, and test sections with fine subgrade showed lower rutting rate than the other test sections.

6- With 95% of reliability, milling of old pavement before overlaying, did not reduced the rutting rates in the C-LTPP sections. By reducing the confidence level to 80%, it was found that milling had significant impact in decreasing the rut rates for the C-LTPP sections.

Table 4-32 summarizes the results from present research project and those from other researches. The difference between the results from this study and that from Dawley research for the effect of overlay material could be due to the different data sources used in these studies. The data that he used was in a project level, but the data used for present study, covered a network level for all provinces in Canada.

It must be mentioned that the effect of the interaction of different factors on rutting rates, were not studied in this research project.

Study Attribute	This study (2003)	EBA (2001)	Dawley (1993)
Weather climate	Yes	Yes	*
Traffic	Yes	Yes	*
Overlay thickness	No	*	*
Overlay material	No	*	Yes
Subgrade material	Yes	*	*
Milling	No(95%),yes(85%)	*	*

Table 4-32: Results from present research project and other researches for pavement rutting (=Not investigated / No result)*

4.7. Evaluation of design practices for rutting of the C-LTPP sections

Table 4-33 presents the rut progression rates in the C-LTPP project for different design practices. These design practices are agency design, under agency design, and over agency design. The first two columns of Table 4-33 show the C-LTPP sites and their locations. In most of C-LTPP test sites, there are several adjacent

7

		Under agency designed			Agency designed			Over agency designed		
Location	C-SHRP ID	Section	Overlay (mm)	Rut rate (mm/ year)	Section	Overlay (mm)	Rut rate (mm/ year)	Section	Overlay (mm)	Rut rate (mm/ year)
Alberta	810404	1	61	0.05	3	94	0.028	2	103	0.006
		4	55	0.028						
British Columbia	820205	1	60	0.15	2	83	0.188			
	820502				1	104	0.642	2	118	0.392
	820605				1	50	0.533	2	73.2	0.5
Manitoba	830403	1	100.3	0.027	2	113.3	0	3	148	*
	830801	2	103.3	0.367	1	185	0.504			
		3	126	0.442						
		4	170	0.504						
New Brunswick	840101	3	87	1.15	1	174	1.25	2	179	1.341
	840204	2	88	0.436	1	114	0.586			
	840604	2	69.9	0.73	1	107.3	0.905			
		3	29.5	0.54						
		4	35	0.615						
New Foundland	850201	2	73	0.655	1	117	0.69			
	850206	2	63	0.17	1	106	0.09			
	850601	2	74	0.805	1	122	0.995			
Nova Scotia	860501	1	55	1.975	2	85	0.73	3	41	0.59
	860603	2	80	0.725	1	85.6	0.505			
		3	34	0.695						
Ontario	870102				2	46.2	0.657	1	94.5	0.379
	870504				1	31	0.258	2	61.3	0.358
	870505				2	72.5	0.343	1	75	0.4
								3	105	0.214
								4	106.3	0.386
	870701				1	42.5	0.021	2	106	0.121
Prince Edward Island	880203	3	51	0.217	1	51	0.278	2	109	0.394
								4	99	0.211
Quebec	890803				1	39.7	1.481	2	50.7	1.328
								3	105.7	1.372
								4	82.7	1.039
	890702				1	44	0.519	2	85	0.425
Saskatchewan	900402	1	86.3	0.195	2	125.6	0.345			
	900802	1	54.5	*	2	66.7	*	3	104.3	0.115
	900803	2	107.6	0.21	1	157.5	0.185			

Table 4-33: The rut rates for different design practices in the C-LTPP project

sections that correspond to different agency design practices for the C-LTPP project. As it can be seen, in some of the test sites either the under agency design or over agency design was not considered. The rutting rates, extracted form Table 4-18, are presented in this table. Asterisks represent sections with negative rutting rates, which were omitted in this study. In addition, the overlay thicknesses are shown to provide a better comparison among design scenarios.

As was summarized in 4.6, three main factors govern the rut progression in the C-LTPP project: climate, traffic, and subgrade material; however, different sections within each site have similar climate, traffic, subgrade material. Other factors such as overlay thickness, overlay material type, and pavement preparation prior to overlay vary among the adjacent sections, but they did not show significant impact on rut.

The highlighted sections in Table 4-33, present those test sections that had rut rates higher than the average rut rate from all the C-LTPP sections, 0.45 mm/year, discussed in Section 4.5. This table revealed that, 10 of the under agency-designed test sections showed a higher rut rate than 0.45 mm/year, which was 48% of all the under agency-designed test sections; 13 of the agency-designed test sections showed a higher rut rate than 0.45 mm/year, which was 56% of all the agency-designed test sections; and 6 of the over agency-designed test sections showed a higher rut rate than 0.45 mm/year, which was 32% of all the over agency-designed test sections. It was thus observed that over agency-designed test sections have lower rutting rates than both the under agency-designed and agency-designed test sections; however, the agency-design practices did not mitigate rut progression compared with under agency-design practices.

To compare the design scenarios for rutting, ANOVA test was conducted for the rut rates related to different design practices. The results of ANOVA test are shown in Table 4-34. The high P-value did not reject the null hypothesis and ANOVA test showed that different design practices did not significantly affect the rut progression of the C-LTPP sections.

SUMMARY

Groups	Count	Sum	Average	Variance
Under agency-designed	21	10.69	0.51	0.20
Agency-designed	23	11.71	0.51	0.15
Over agency-designed	18	9.57	0.53	0.19

ANOVA

Source of Variation	SS	df	MS	F	P-value	F crit
Between Groups	0.007	2	0.003	0.02	0.98	3.15
Within Groups	10.513	59	0.178			
Total	10.520	61				

Table 4-34: ANOVA test results for rutting rates related to different design practices in the C-LTPP project

4.8. Artificial Neural Network (ANN) approach

The Artificial Neural Network (ANN) is attracting an enormous amount of attention in many civil engineering disciplines because it is capable of using data to learn existing relationships among them. The ANN approach was employed as part of this study for the C-LTPP project to investigate the effect of different factors on pavement performance and to examine the ANN's potential for future studies using more data than were available for this present study.

The use of ANN is not new in pavement engineering area, and several studies have applied the ANN in this area. Nazarian et al. (1998) used the ANN to estimate the remaining service life of pavements. The researchers provided a list of several applications of the ANN in pavement engineering and classified them as (1) parameter determination, (2) assessment of pavement condition, and (3) selection of maintenance strategies.

The Neural Networks (NN) are a branch of Artificial Intelligence, which simulate the organization of the human brain in processing data and learning from past experiments. The most important characteristic of the NN is that they can learn from examples, and then as the result of what they have learnt, they can produce correct or nearly correct responses when presented with other similar situations. The NN are capable of generalizing the rules and then applying them to new inputs. The structure of a neural network consists of processing elements (nodes) and the interconnections between them. In fact, a neural network models the biological neuron, while the nodes and connections in the network function as the cells and axons in biological neuron, respectively. Nodes and their connections represent the architecture of the neural network. The architecture of the ANN requires identifying the number of the layers, number of nodes in each layer, and the interconnection scheme among the nodes (Rich et al., 1991).

Figure 4-15 shows a neural network architecture consisting of three layers (input, hidden, and output), nodes, and their connections.

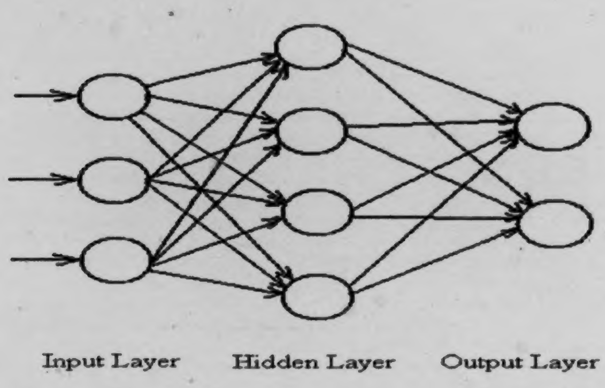

Figure 4-15: The architecture of a three-layer Neural Network

The processing elements pass information in the form of a signal pattern from the input layer to the output layer through the hidden layer(s). The signals travel along the interconnections, whose strength or weight can be adjusted. The excitation level for a node is modeled mathematically as a weighted sum of all the signals that are coming to the node (Meier et al., 1994):

$$N_j = \Sigma W_{ji} \times X_i \qquad (4\text{-}3)$$

where X_i is the signal coming from the i_{th} node in the preceding layer, and W_{ji} is the weight assigned to the connection. The response of the processing node to the entry excitation could be modeled as follows (Meier et al., 1994):

$$A_j = f(N_j) = \frac{1}{\left(1+e^{-N_j}\right)} \tag{4-4}$$

A learning algorithm helps to train the network to obtain the specific weights that could result in a lower difference between the calculated value and the target output. Multilayer feed-forward networks are commonly trained by a technique known as "backpropagation".

The backpropagation learning algorithm is based on the error reduction between the actual output of a processing element and its desired output, by modifying the incoming connections' weights. The weights are modified through an iterative process during which the network modifies the initial random values of W_{ji} to converge the results to the desired/known output. The commonly used backpropagation networks usually have three layers: the input layer, the output layer, and the hidden layer. No well-established procedures have been developed for choosing the number of hidden layers or the number of the nodes in them, and usually, a trial approach is employed. As a rule of thumb, the number of hidden nodes are equal to or more than half of the total number of the input and output nodes (Rich et al., 1991).

Training proceeds by iteratively presenting training examples to the network. Each pass through the set of data is called an "epoch". An ANN commonly needs thousand of epochs to be trained. In each epoch, the program trains the neural network through the training dataset and then applies the resulting network to the test set and calculates the error. More information about artificial neural networks can be obtained from (Rich et al., 1991) and (Wasserman, 1989).

4.8.1. Using the ANN

As was mentioned previously, no rule or practical method exists for choosing the architecture of a network; therefore, different neural network architectures were developed for this study. In the development of ANN architecture, one should keep the number of processing elements to a minimum. The smaller the architecture is, the more robust the ANN model will be (Neural Ware Inc., 1993). In developed ANN models for this present study, the number of nodes or processing elements in the input layer was equal to the number of the input factors, and the only node in the output layer represented the pavement performance criterion.

In order to compare the developed models based on the ANN, two criteria were considered: The coefficient of correlation between the actual measured values and network outputs (R^2), and the Root Mean Square Error (RMSE). To calculate the RMSE the following equation was used:

$$RMSE=\sqrt{\frac{\sum\left(\frac{Actual\ Value-Network\ Value}{Actual\ Value}\right)^2}{n}} \qquad (4\text{-}5)$$

A high correlation between the actual values and resulted values (R^2) or a low RMSE value shows a high reliability in the developed model.

Exclusively, the following stages were followed while developing the neural networks used in this study:

1- Preparing the training data and untouched data for verifying the network,

2- Selecting the network architecture,

3- Training the network until the error reached a constant level,

4- Repeating the training to ensure about the accuracy of the network,

5- Determining the statistics R square and RMSE for both training set and untouched data,

6- Choosing another architecture or excitation function,

7- Repeating steps 3 to 6, and

8- Comparing the results obtained from different architectures in order to choose the most accurate network.

There are various artificial neural network softwares. For this study, the NEUROSHELL 2 was used. This program has a user-friendly format and supports the final output with appropriate graphs and statistical indices.

Figures in Appendix J present the different stages of developing an ANN with NEUROSHELL 2 computer program.

4.8.2. The ANN for roughness in the C-LTPP sections

In section 4.1, statistical methods were deployed to investigate the effect of different factors on pavement performance. To compare the results from those parts of this study the same factors, based on the C-LTPP experimental design, were used in development of ANN models. These factors include climate, traffic, overlay thickness, overlay material type, and subgrade material type.

The first stage in developing NN model for roughness of the C-LTPP sections was to arrange data in order to train and test the network. Therefore the information about roughness and studied factors were extracted from the C-LTPP database for each year after overlay in all the test sections. Roughness and traffic changes annually however the other factors do not change after overlay for each test section. i.e. the overlay type for a specific test section will be the same in different years after overlay while traffic and roughness have increased. Some test sections that showed a negative IRI by time were omitted. Totally 523 data patterns were provided to develop a model for roughness of the c-LTPP sections.

In the development of the NN, it is required to test the network with some data that was not experienced by ANN before. This could demonstrate the accuracy of network in dealing with similar scenarios. Hence all data was divided into two separate groups. A set of data patterns that was called the *untouched data* was extracted from the data set by selecting 50 data patterns from different test sites in different years after overlay. In selection of this group of data, it was attempted to choose the data belonging to starting years of service life as well as those belonging to the latest years, so that it may cover a whole range of roughness in C-LTPP sections. The remaining data patterns were used to train the network, which totally comprised 473 of data patterns.

To develop the network, two different architectures were used. In both, the five nodes in the input layer corresponded to the studied factors, and the only node in the output layer represented the IRI value. The number of hidden layers and hidden nodes vary in different architectures.

Table 4-35 presents the architectures and the results for the roughness models. For each network, training was repeated several times to ensure that the network had reached a stable condition and could not be expected to improve.

Roughness Model	Number of nodes				Training time (min)	For untouched data	
	Input layer	Hidden layer 1	Hidden layer 2	Output layer		R square	RMSE
NO.1	5	4	-	1	4:00	0.19	0.22
NO.2	5	5	3	1	4:00	0.14	0.24

Table 4-35: Architectures of and the results from roughness ANN models

Network architecture No.1 had the highest R^2 and lowest RMSE; therefore, it was more accurate than model No.2. Network No.1 was selected for the rest of study.

NEUROSHELL2 can show in a graphical format the level of contribution for each factor in the network. The contribution level is an index that shows the overall W_{ji} in Equation 4-3 for each factor. Figure 4-16 shows the contribution graph for network No.1. It could be concluded that overlay thickness had the most impact on pavement roughness, compared with the other factors.

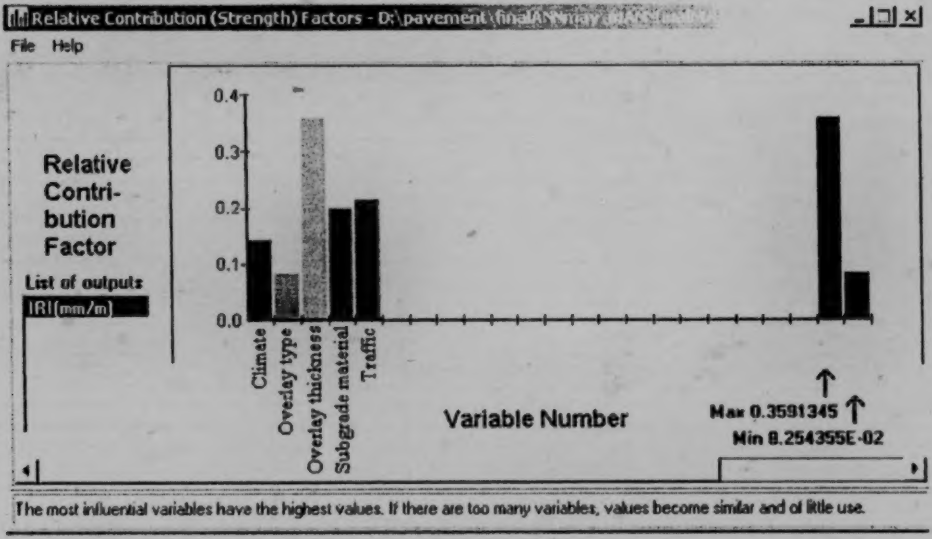
Relative Contribution (Strength) Factors - D:\pavement\finalANN
File
Help
Relative Contribution Factor
List of outputs
IRI(mm/m)
0.4
0.3
0.2
0.1
0.0
Climate
Overlay type
Overlay thickness
Subgrade material
Traffic
Variable Number
Max 0.3591345
Min 8.254355E-02

The most influential variables have the highest values. If there are too many variables, values become similar and of little use.

Figure 4-16: Contribution levels from neural network for roughness model

4.8.3. The ANN for rutting in the C-LTPP sections

In order to develop ANN for pavement rutting in the C-LTPP program, the procedures similar to those used to develop the ANN for pavement roughness was used.

The rut information was extracted from the C-LTPP database, and after omitting test sections with negative rut rates, totally 498 data patterns were available for training and testing the networks. The training data contained 448 data patterns and for the untouched data, 50 data patterns were chosen randomly.

After several trials, two different models were developed for pavement rutting. Table 4-36 presents architecture and results for these models. For each network, training was repeated several times to assure that the network had reached a stable condition and no more improvement was expected for it.

Rutting Model	Number of nodes				Training time (min)	For untouched data	
	Input layer	Hidden layer 1	Hidden layer 2	Output layer		R square	RMSE
NO.1	5	4	-	1	3:45	0.21	0.86
NO.2	5	4	2	1	3:45	0.31	0.97

Table 4-36: Architectures of and the results from rutting ANN models

Network architecture No.1 had a lower R^2 but with a lower RMSE showed better outputs than network architecture No.2. Therefore NN models No.1 was selected for the rest of the study.

By comparing the outputs from these NN models and in-situ rut measurements, it was observed that the obtained results from NN models were different from real observations. Probably, the five factors that this study used for pavement rutting are not significant factors for high-rut situation, and some other factors govern the pavement rutting in such test sections. Network No.1 was chosen to show the studied factors' contribution level. The NEUROSHELL2 program provided the contribution levels of the factors in the network, which are presented in Figure 4-17.

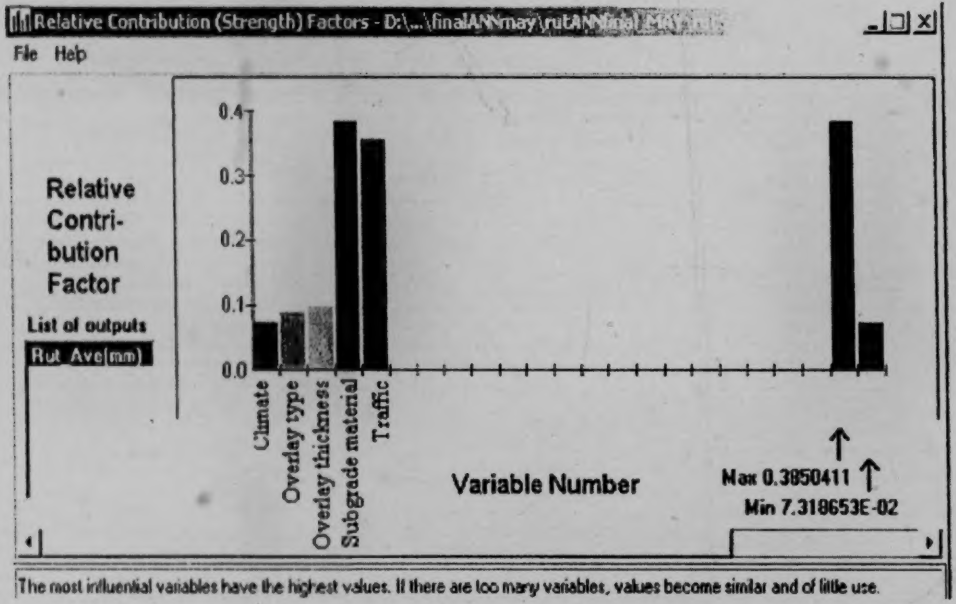
Relative Contribution (Strength) Factors - D:\...\finalANNmay\rutANNfinal
File Help
Relative Contribution Factor
List of outputs
Rut Ave(mm)
0.4
0.3
0.2
0.1
0.0
Climate
Overlay type
Overlay thickness
Subgrade material
Traffic
Variable Number
Max 0.3850411
Min 7.318653E-02

The most influential variables have the highest values. If there are too many variables, values become similar and of little use.

Figure 4-17: Contribution levels from neural network for rutting model

This graph shows that among the studied factors that contributed in the rutting network, traffic and subgrade material type had the more effect on the network output, pavement rutting. Three other factors, overlay thickness, overlay type, and climate, had a lower impact on rut than the others.

4.9. Summary of the ANN application to the C-LTPP project

The ANN method showed that overlay thickness was the most important factor in pavement roughness. As well, the statistical analysis showed that overlay thickness significantly affected the pavement roughness. The ANN technique showed that subgrade material types and traffic were the most important factors in pavement rutting. This finding agreed with the findings from the statistical analysis.

The results from the ANN models were consistent with the findings from other methodologies; however, the ANN method had the following limitations:

1- Although based on the overall weights of the processed elements, the ANN can show which factors contributed most to the output; it cannot provide the reliability (confidence level) of the results.

2- For the untouched data, predicted values for pavement roughness and rutting showed that the amount and range of data was not sufficient to develop an accurate neural network. In this present study, after extracting and organizing data from almost all the C-LTPP sections for different years after overlaying, about 500 data patterns were available for training the networks, while, in studies such as one performed by Nazarian et al. (1999) about 360,000 data patterns were used. Nazarian et al. considered the lack of data from the real world and used a synthetic procedure to provide data for their study.

CHAPTER 5: CONCLUSION

The available data from 65 test sections located in different Canadian climate and traffic conditions were analyzed after 10-12 years of overlay construction. The remaining service lives of all the C-LTPP sections were estimated by using different methodologies. The statistical analysis and Artificial Neural Network (ANN) were used to identify the impact of different factors such as weather climate, traffic, overlay thickness, overlay material type, subgrade material type, and milling on the performance of the C-LTPP sections.

The findings from this study were compared with those from previous studies in this area. Some of this study's most important findings were as follows

1- The service lives of the C-LTPP sections were estimated based on the AASHTO overlay design method. Given that generally, an overlay does not last more than 20 years, the use of the AASHTO overlay design resulted in high and unrealistic service lives for the C-LTPP sections. The reasons for these unrealistic results may include the assumption of a very high reliability of 95 % for the design, the assumptions involved in the backcalculation of pavement's moduli, and the quality of the data from the C-LTPP program. As well, it appears that a Present Serviceability Index (PSI) equal to 2.5, generally considered to represent the final serviceability and the failure level, does not really correspond to highway practices, for decision makers do not allow pavement to deteriorate to this level.

2- All the C-LTPP sections were evaluated for their roughness based on the IRI. The roughness progression in the C-LTPPP sections was rather linear after almost 10 years of the pavements being in service with very low rate values. Several roughness models were evaluated to estimate the service lives of the C-LTPP sections. It was observed that most of the C-LTPP sections showed high service lives; however, some of the agency-designed test sections with thin overlay deteriorated faster than other sections. These test sections were 870102-2 (ON) and 890503-1 (QC). Generally, it could be concluded that after 10 years of service life, roughness was not a very critical criterion for pavement performance in the C-LTPP program.

3- All the C-LTPP sections were evaluated for their rutting. The rut progression in these sections was rather linear after almost one decade of being in service. A linear relationship between rut and time seemed reasonable for all the C-LTPP sections, and by using this relationship, the service lives of the C-LTPP sections were estimated based on rut trigger values.

It was found that the agency-designed test sections 840604-1(NB), and 890503-1(QC), with high traffic, wet weather condition, and coarse subgrade soil, had shorter service lives.

4- By using the FWD testing results to backcalculate the stress and strain in the

C-LTPP pavement sections, the Mechanistic-Empirical (M-E) models including the Asphalt Institute and Shell models were employed to estimate the service lives of the C-LTPP sections for a maximum level of rutting and fatigue cracking.

For most pavement sections, both the AI and Shell models predicted an unrealistically high service life of more than 50 years for rut performance. The main explanation for these unreasonable results could be associated with the main assumption in these models, which ignores the permanent deformation of non-subgrade pavement layers and accounts only for permanent deformation in the subgrade. Rutting in the asphalt layer, rather than rutting in other layers, appear to be the main reasons for pavement failure.

In terms of fatigue cracking, more than half of the pavement sections have deteriorated or will deteriorate in less than 15 years. Therefore, fatigue failure could be the main reason for the failure of the C-LTPP sections, compared to rut and roughness failures. It was observed that the test sections with high fatigue cracks were located in different classifications of traffic, weather condition, and subgrade material, but most were sections with a 30-60 mm overlay thickness, which is a thin overlay in the C-LTPP experimental design. These test sections are 840604-1(NB), 860501-2(NS), 870102-2(ON), 870504-1(ON), 870701-1(ON), 880203-1(PE), 890503-1(QC), 890702-1(QC), and 900802-2(SK). It was concluded that overlay thickness is a major attribute in the fatigue resistance of the C-LTPP pavement sections, regardless of the traffic level and number of vehicle load applications.

5- The REPP2000 program, developed by the University of Texas, was used for estimating the service lives of the C-LTPP sections, based on the M-E method and using the ANN. It was observed that the estimated service lives for most test sections, based on pavement rutting, were more than 50 years. This finding agrees with the findings from the M-E approach used in this study.

The service lives of the C-LTPP sections, based on fatigue cracking from the REPP 2000 program were consistent with the results from the M-E approach used in this study. This program did not appear to be able to differentiate among the adjacent test sections within each site, and so the program assigned similar service lives to different thickness design practices in each site. The REPP2000 program could be a useful tool for estimating future distresses such as rut and fatigue crack without requiring the backcalculation procedures.

6- The comparison of the estimated service lives of the C-LTPP sections, obtained by using different methodologies including the AASHTO overlay design method, the threshold value for roughness and rut, and the M-E models, showed that the predicted service lives for the C-LTPP sections were shorter, based on their fatigue resistance, than predicted service lives related to roughness and rut. It could be concluded that fatigue cracking is more critical criterion than roughness and rut in the C-LTPP project. Rut was a less important failure mode than roughness in deterioration of the C-LTPP pavement sections. It was observed that some of the test sections showed a low service life for both fatigue and roughness. These test sections were 840604-1(ON), 870102-2(ON), 870504-1(ON), 870701-1(ON), 880203-1(PE), 890503-1(QC), and 900802-2(SK). These test sections, with the exception of 8406041(ON), had an overlay thickness less than 70 mm, which seemed to be the most important attribute in the pavement performance of the C-LTPP sections.

7- Statistical approach including both parametric and non-parametric techniques was employed in order to investigate the effect of climate, traffic, overlay thickness, overlay material type, subgrade material types, and milling on roughness progression in the C-LTPP program. With 95% reliability, both methods showed that the only attribute among the studied ones that affected roughness, IRI rates, is overlay thickness. Thinner overlay deteriorated at a significantly higher rate than the medium and thick overlays, while little comparative difference was observed between medium and thick class overlays.

8- With 95% reliability, the statistical analysis showed that climate, traffic, and subgrade material type were the main factors that affected the rut progression in the C-LTPP sections. Generally, in wet climates, a higher rut progression was observed. Increased application of traffic load and the use of coarse aggregate in the subgrade resulted in more severe rutting. It was found that overlay thickness, overlay material types, and milling were not significant factors in rut progression for the C-LTPP sections.

9- The impact of different design practices such as agency-design, under agency-design, and over agency-design on the progression of roughness and rut in the C-LTPP sections was studied. It was observed that agency-designed and over agency-designed test sections had better roughness performance than the under agency-designed test sections; however, the ANOVA test showed that different design practices did not significantly affect the roughness progression in the C-LTPP sections. For pavement rutting, it was observed that over agency-designed test sections had better rut performance than the under agency-designed and agency-designed test sections; however, the agency-design practices did not mitigate rut progression in comparison with the under agency-design practices. The ANOVA test showed that different design practices did not significantly affect the rut rates of the C-LTPP sections.

10- Artificial Neural Network (ANN) models were developed to study the important factors in roughness and rutting, by using the NUEROSHELL2 program. The ANN method showed that overlay thickness was the most important factor in pavement roughness performance. The ANN technique also showed that subgrade material types and traffic were the most important factors in pavement-rutting resistance.

5.1. Recommendations for future studies

Some recommendations for future studies of the C-LTPP project are listed bellow

1- In this research study, attempts were made to analyze the C-LTPP pavement sections to determine the moduli of pavement layers, the compressive strain at the top of the subgrade, and the tensile strain at the bottom of the asphalt layer. These values were used with M-E models such as the AI and Shell models to predict rutting. It appeared that such models, which account only for the permanent deformation in the subgrade, failed to give a realistic estimation of pavement rutting. A number of other models such as direct method and VESYS consider the permanent deformation in all layers. It is recommended that future studies develop or calibrate other M-E models for the C-LTPP project in order to account for plastic deformation in all pavement layers.

2- The new version of the AASHTO 2002 guide for pavement design is forthcoming, and will initiate a new era in pavement design based on the M-E models. It is recommended that this new version be used to evaluate pavement performance in the C-LTPP program and to investigate whether the highway agencies' practices are adequate in terms of this new approach. The findings for the C-LTPP sections could be used to calibrate the AASHTO 2002 guide for the Canadian climate and traffic conditions.

3- This study focused mainly on pavement roughness, rutting, and, to some extent, fatigue cracking, but other types of cracks should also be studied. Methodologies similar to those used in this study might be utilized in order to investigate the affecting factors in crack development.

4- This research did not investigate the interactions of different factors in pavement performance and, in all cases, the combination of factors was studied. Future studies could look at the interactions of different factors and their impacts on pavement performance.

5- The findings from this study must be validated and verified by using more available data in future. As well, the quality of the data in the C-LTPP project must be reviewed for future studies.

REFERENCES

Alberta Transportation, (2003), Future Highway Needs, In the Alberta Transportation website: www.trans.gov.ab.ca.

Alberta Transportation , (1997), Pavement Design Manual, Alberta, Canada.

American Association of State Highway and Transportation Officials, (1993), AASHTO Guide For Design of Pavement, Washington, D.C., USA.

Archilla, A.R., and Madanat, S., (2001), Statistical Model of Pavement Rutting in Asphalt Concrete Mixes, In Transportation Research Record 1764, TRB, National Research Council, Washington, D.C., USA.

Asphalt Institute (1982), Research and Development of the Asphalt Institutes Thickness Design Manual, 9th Edition, Research Report, USA.

ASTM Standard E1274 (1996), Standard Test Method for Measuring Pavement Roughness Using a Profilograph, Annual Book of ASTM Standards 14.02, USA.

Bethea, R.M. and Rhinehart, R.R., (1991), Applied Engineering Statistics, Marcel Dekker Inc., New York, USA.

Carey, W.N. and Irick, P.E., (1960), The Pavement Serviceability – Performance Concept, Highway Research Bulletin 250.

Carpenter, S.H., (1993), Permanent Deformation: Field Evaluation, In Transportation Research Record 1417, TRB, National Research Council, Washington, D.C., USA.

Chan, P.K. and Oppermann, M.C., (1997), North Carolinas' Experience in Development of Pavement Performance Prediction and Modeling, In Transportation Research Record 1592, TRB, National Research Council, Washington, D.C., USA.

Collucci, B., Ramirez-Beltran, N., and Rodrigez, F., (1997), Methodology For Developing Performance Curves For Flexible Pavements In Puerto Rico Using Clustering Techniques, In Transportation Research Record 1592, TRB, National Research Council, Washington, D.C., USA.

Dawley, C.B., Hogeweide, B.L., and Johnston, A.G., (1993), Five Years Performance Assessment of Lethbridge Test Pavements Designed for Instability Rutting Mitigation, Proceedings of CTAA, Ottawa, Canada.

Dore, G., Flamand, M.,and Pascale, P., (2002), Analysis of the Wavelength Content of The Longitudinal Profiles for C-LTPP Test Sections, Canadian Journal of Civil Engineering, Vol. 29, Ottawa, Canada.

Dore, G., (1995), The Development of Models to Predict Pavement Performance in Frost Conditions, A Joint C-SHRP/QUEBEC Bayesian Application, Canadian Strategic Highway Research Program, Ottawa, Canada.

EBA Engineering Consultants Ltd., (2001), Rutting Trends at C-SHRP LTPP Test Sites, EBA Consultant Engineering, Ltd., Transportation Association of Canada, TAC, Ottawa, Canada.

EBA Engineering Consultants Ltd., (1996), Normalization of Asphalt Concrete Overlay Designs for the CLTPP Sections, Transportation Association of Canada, TAC, Ottawa, Canada.

Emery, J. and MacDonald, A.B., (1990), Asphalt Pavement Rutting Experience in Canada, TAC Seminar Series, Transportation Association of Canada, Ottawa, Canada.

ERES Consultants, Inc., (1999), Findings From LTPP Data Analysis Studies Summary List 1990-1999, Federal Highway Administration, FHWA, USA.

FHWA Report, (2000), Performance Trends of Rehabilitated AC Pavements, FHWA-RD-00-165, Federal Highway Administration, U.S. Department Of Transportation, USA.

FHWA Report, (1998), Roughness Trends of Flexible Pavements, FHWA-RD-97-147, Federal Highway Administration, US Department Of Transportation, USA.

FWHA Report, (1998), Mechanistic Evaluation of Test Data from LTPP Flexible Pavement Test Sections, Volume 1, Final Report, FHWA-RD-98-012, Federal Highway Administration, U.S. Department Of Transportation, USA.

FHWA Report, (1998), Reducing Roughness In Rehabilitated Asphalt Concrete Pavements, FHWA-RD-98-149, Federal Highway Administration, U.S. Department Of Transportation, USA.

Frechette, L. and Shalabi, A., (1997), Reflective Cracking Trends in C-SHRP LTPP Sites, The Canadian Strategic Highway Research Program, Ottawa, Canada.

Frechette, L. and Samson, M., (1995), Seasonal Variation of Pavement Strength Based on Benkelman Beam Rebounds, The Canadian Strategic Highway Research Program, Ottawa, ON, Canada.

Gary, H.R., Moulthrop, S., and Daleiden, J., (1999), selecting A Preventive Maintenance Treatment for Flexible Pavements, In Transportation Research Record 1680, TRB, National Research Council, Washington, D.C., USA.

Gibbous, J.D., (1985), Non-parametric Statistical Inference, Marcel Dekker, Inc., New York, USA.

Goodman, S.N., (2001), Assessing the Variability of Surface Distress Surveys in the Canadian Long-Term Pavement Performance Program, In Transportation Research Record 1764, TRB, National Research Council, Washington, D.C., USA.

Haas, R., Raymond, C.M., and Rothenburg, L., (2002), Development of a C-LTPP Pavement Performance Model for Asphalt Overlay, 4th Transportation Specialty Conference of the Canadian Society for Civil Engineers, Montreal, Canada.

Haas, R., Hudson, W.R., and Zaneiwski, J., (1994), Modern Pavement Management, Krieger Publishing Co., FL, USA.

Haas, R. and Meyer, F., (1976), Procedure for Predicting Rut Depth In Flexible Pavements, In Transportation Research Record 616, TRB, National Research Council, Washington, D.C., USA.

Hesham, A.A. and Tayabji, S.D., (1998), Evaluation of Mechanistic-Empirical Performance Prediction Models For Flexible Pavements, In Transportation Research Record 1629, TRB, National Research Council, Washington, D.C., USA.

Hesham, A.A., Tayabji, S.D., and La-Torre, F., (1998), Calibration of Mechanistic-Empirical Rutting Model for In Service Pavements, In Transportation Research Record 1629, TRB, National Research Council, Washington, D.C., USA.

Huang, Y.H., (1993), Pavement Analysis and Design, Prentice-Hall, Inc., NJ, USA.

Kandil, K., (2001), Effect of Overlay Characteristics on Pavements Long-term Performance, the Transportation Association of Canada, Ottawa, Canada.

Kavanagh, L., (1995), Benkelman Beam Rebound Asphalt Overlay Model, A Joint CSHRP/MDHT Bayesian Application, The Manitoba Department of Highways & Transportation (MDHT), The Canadian Strategic Highway Research Program (CSHRP), Ottawa, Canada.

Kenis, W.J. and Sharma, M.G., (1976), Rut Depth Prediction and Test Procedures for Permanent Deformation in Asphalt Pavements, In Transportation Research Record 616, TRB, National Research Council, Washington, D.C., USA.

Kim, H.B., Buch, N., and Park, D.Y., (2000), Mechanistic-Empirical Rut Prediction Model for In-service Pavements, In Transportation Research Record 1730, TRB, National Research Council, Washington, D.C., USA.

Krutz, N.C. and Gardiner, M.S., (1990), Relationship Between Permanent Deformation of Asphalt Concrete and Moisture Sensitivity, In Transportation Research Record 1259, TRB, National Research Council, Washington, D.C., USA.

McGhee, K.K., (2000), Measuring Smoothness of Virginia Asphalt Overlays, In Transportation Research Record 1712, TRB, National Research Council, Washington, D.C., USA.

Meier, R.W. and Rix, G.J., (1994), Backcalculation of Flexible Pavement Moduli Using Artificial Neural Networks, In Transportation Research Record 1448, TRB, National Research Council, Washington, D.C., USA.

Monismith, C.L., (1976), Rutting Prediction In Asphalt Concrete Pavements, In Transportation Research Record 616, TRB, National Research Council, Washington, D.C., USA.

Mosteller, F. and Rourke, R.E., (1973), Sturdy Statistics, Addison-Wesley Publishing Co., MA, USA.

New Brunswick Department Of Transportation (1995), Prediction of Rutting in Alternative Asphalt Concrete Overlay Methods, Canadian Strategic Highway Research Program, Joint CSHRP/NBDOT Bayesian Application, Ottawa, Canada.

Nazarian, S., Ferregut, C., and Abdallah, I., (1998), Artificial Neural Network–Based Methodologies for Rational Assessment of Remaining Life of Existing Pavements, Research Report 1711-11, Centre for Highway Research, University of Texas at El Paso, USA.

Neural Ware Inc., (1993), Neural Computing, Technical Publication Group, Pittsburgh, PA.

NCHRP Report, (2002), LTPP Data Analysis: Factors Affecting Pavement Smoothness, Report No. 264, Transportation Research Board, National Research Council, Washington, D.C., USA.

NCHRP Report, (1978), Calibration of Response-Type Road Roughness Measuring Systems, Report No. 228, Transportation Research Board, National Research Council, Washington, D.C., USA.

NRC, (2002), National Guide to Sustainable Municipal Infrastructure Program, Presentation made by N. Schepers, National Research Council, Ottawa, Canada.

Papagiannakis, T., Carson, J., and Mahoney, J., Delwar, M., (1999), A Review of Pavement Roughness Effects on the Road User, TRB 78th annual meeting, Transportation Research Board, National Research Council, Washington, D.C., USA.

Perera, R.W. and Kohn, S.D., (1999), IRI of Asphalt Concrete Overlays: Analysis of Data from LTPP SPS-5 Projects In Transportation Research Record 1655, TRB, National Research Council, Washington, D.C., USA.

Pierce, L.M. and Mahoney, J.P., (1996), Examination of Washington State Department Of Transportation Transfer Functions for Mechanistic–Empirical Asphalt Concrete Overlay Design, In Transportation Research Record 1539, TRB, National Research Council, Washington, D.C., USA.

Pierce, L.M. and Mahoney, J.P., (1996), Asphalt Concrete Overlay Design Case Studies, In Transportation Research Record 1543, TRB, National Research Council, Washington, D.C., USA.

Rich, E. and Knight, K., (1991), Artificial Intelligence, McGraw-Hill, Inc., New York, USA.

Roads and Transportation Association of Canada, (1998), Proceedings of The 1988 Annual Conference of the Roads and Transportation Association of Canada, RTAC, Ottawa, Canada.

Simpson, A.L., (1995), Characterization of Transverse Profile, Brent Rauhut Consultants Engineer, Ltd., Austin, Texas, USA.

Sousa, J.B., Cruas, J., and Monismith, L., (1991), Summary Report on Permanent Deformation in Asphalt Concrete, Strategic Highway Research Program, National Research Council, Washington D.C., USA.

SPSS 11.0 Online Help, (2001), Non-parametric Tests, Lead Technologies, USA.

TAC Report, (2001), Standardization of IRI Data Collection and Reporting in Canada, Transportation Association of Canada, Ottawa, Canada.

TAC Report, (1997), Pavement Design and Management Guide, Transportation Association of Canada, Ottawa, Ontario.

TAC Report, (1996), Guide to Characteristics, Performance and Selection of Paving Asphalts, Transportation Association of Canada, Ottawa, Canada.

TAC Report, (1996), Canadian Long-Term Pavement Performance: Database Users' Guide, Transportation Association of Canada, Ottawa, Canada.

Tighe, S., Haas, R., and Li, N., (1999), Roughness Trends at C-SHRP LTPP Sites, Transportation Association of Canada (TAC), Ottawa, ON, Canada.

Ullidtz, P., (1987), Pavement Analysis, Elsevier Science Publishers B.V., New York, USA.

Vepa, T.S., Ceorge, K.P., and Shekharan, A.R., (1996), Prediction of Pavement Remaining Life, In Transportation Research Record 1524, TRB, National Research Council, Washington, D.C., USA.

Washington State Department Of Transportation (1999), Pavement Guide, Seattle, WA, USA.

Wasserman, P.D., (1989), Neural Computing: Theory and Practice, Van Nostrand Reinhold, New York, USA.

Witczak, W. and Qi, X., (1998), Time Dependent Permanent Deformation Models of Asphalt Mixtures, In Transportation Research Record 1639, TRB, National Research Council, Washington, D.C., USA.

Appendix A: The Backcalculation, based on the AASHTO procedure

In Chapter 3, the AASHTO backcalculation procedure was used in order to calculate the structure number. The required calculations can be performed in an EXCEL spreadsheet by using Macro programming. The following program was prepared to perform the AASHTO backcalculation:

```
Sub Macro3()
' Macro recorded 5/20/2002 by ASadri
Dim mes, title, default
mes = "enter row number for the beginning"
title = "input"
default = "2"
k = InputBox(mes, title, default)
MsgBox (k)
 100 a = b = c = d = e = f = 0: i = 100000
    Cells(k, 26).Select
    ActiveCell.FormulaR1C1 = i
 10  a = Abs(Cells(k, 30).Value)
    i = i + 50000
    ActiveCell.FormulaR1C1 = i
    If Abs(Cells(k, 30).Value) < a Then
    GoTo 10
    Else
    GoTo 20
    End If
 20      b = Abs(Cells(k, 30).Value)
```

```
        i = i - 5000
        ActiveCell.FormulaR1C1 = i
        If Abs(Cells(k, 30).Value) < b Then
        GoTo 20
        Else
        GoTo 30
        End If
30              c = Abs(Cells(k, 30).Value)
            i = i + 500
            ActiveCell.FormulaR1C1 = i
            If Abs(Cells(k, 30).Value) < c Then
            GoTo 30
            Else
            GoTo 40
            End If
40                  d = Abs(Cells(k, 30).Value)
                i = i - 50
                ActiveCell.FormulaR1C1 = i
                If Abs(Cells(k, 30).Value) < d Then
                GoTo 40
                Else
                GoTo 50
                End If
50                      e = Abs(Cells(k, 30).Value)
                    i = i + 10
                    ActiveCell.FormulaR1C1 = i
                    If Abs(Cells(k, 30).Value) < e Then
                    GoTo 50
                    Else
                GoTo 60
                End If
60                    f = Abs(Cells(k, 30).Value)
                    i = i - 1
                    ActiveCell.FormulaR1C1 = i
                    If Abs(Cells(k, 30).Value) < f Then
                    GoTo 60
                    Else
  k = k + 1: GoTo 100
  End If
  End Sub
```

Appendix B: Average of FWD deflections for the C-LTPP test sections after overlay

C-SHRP ID	Section	Load(N)	D1(um)	D2(um)	D3(um)	D4(um)	D5(um)	D6(um)	D7(um)	D8(um)	D9(um)
810404	1	38792	258.2	213.8	186.9	150.2	120.7	82.7	61.5	50.4	43.0
810404	2	39013	208.3	175.7	156.4	128.9	106.8	75.7	56.5	45.5	37.8
810404	3	39572	189.4	160.0	142.9	118.0	97.5	68.4	50.8	40.3	33.4
810404	4	40612	266.7	218.0	190.1	151.4	120.6	80.5	58.1	46.2	38.7
820502	1	39919	157.4	135.5	118.8	96.9	75.8	46.8	29.2	19.0	13.5
820502	2	40153	170.5	151.8	137.2	116.3	96.3	65.5	45.6	32.2	23.9
820605	1	40095	161.1	141.1	126.4	105.7	86.1	59.2	42.8	32.3	25.7
820605	2	40246	129.6	112.7	100.8	84.6	68.6	46.6	32.5	23.4	17.7
830403	1	41454	408.8	340.2	299.3	239.7	192.3	128.3	92.5	72.6	58.2
830403	2	40084	347.8	299.3	270.1	225.9	187.8	131.5	96.4	74.5	58.6
830403	3	39223	315.8	269.2	244.5	207.5	174.0	124.6	92.9	73.1	58.5
830801	1	44566	127.3	107.8	97.6	81.7	67.8	45.7	31.8	23.8	18.8
830801	2	43599	192.1	154.5	134.3	104.8	80.6	47.3	30.0	22.1	18.2
830801	3	43729	195.3	160.1	140.0	110.5	86.1	53.4	35.9	27.6	22.5
830801	4	43605	121.7	100.9	91.7	77.4	65.2	45.6	32.1	24.1	18.6
840101	1	41646	141.1	113.0	98.1	80.9	65.4	43.2	18.8	N/A	N/A
840101	2	42136	146.1	117.8	103.4	86.1	70.6	47.7	22.2	N/A	N/A
840101	3	42521	222.3	185.9	163.6	135.4	111.1	72.9	29.8	N/A	N/A
840204	1	42008	316.3	268.9	238.6	200.1	166.4	114.4	56.6	N/A	N/A
840204	2	42176	392.6	340.0	301.6	250.3	205.2	135.2	63.9	N/A	N/A
840604	1	43067	236.5	179.4	148.0	111.6	83.7	48.6	21.1	N/A	N/A
840604	2	41973	237.9	173.3	137.4	96.8	68.4	36.5	16.7	N/A	N/A
840604	3	41836	267.6	183.9	142.6	98.5	69.2	37.4	17.8	N/A	N/A
840604	4	40966	246.3	172.6	135.7	94.9	67.4	37.6	17.8	N/A	N/A
850201	1	42905	235.7	191.4	162.9	125.7	95.8	53.2	19.9	N/A	N/A
850201	2	42017	266.9	211.0	174.6	127.2	91.0	46.2	18.3	N/A	N/A
850206	1	42579	195.3	156.3	134.0	105.9	82.5	49.7	22.2	N/A	N/A
850206	2	42269	204.5	165.8	141.7	110.5	85.5	49.7	19.7	N/A	N/A
850601	1	42375	162.7	129.0	114.0	95.9	79.7	53.3	23.0	N/A	N/A
850601	2	41779	171.4	136.0	118.5	96.4	76.9	46.2	16.3	N/A	N/A
860501	1	42538	199.7	163.9	143.7	118.1	94.7	60.1	22.8	N/A	N/A
860501	2	41657	188.7	156.1	139.0	116.3	94.8	62.9	27.7	N/A	N/A
860501	3	41564	236.5	191.6	166.4	132.3	103.1	61.4	24.0	N/A	N/A
860603	1	42345	193.7	154.1	130.0	99.5	76.5	43.8	16.5	N/A	N/A
860603	2	41529	192.4	151.6	128.2	98.2	74.6	41.8	15.4	N/A	N/A
860603	3	40818	220.5	168.7	139.8	104.1	77.5	42.7	17.4	N/A	N/A
870102	1	40838	315.2	266.3	236.3	191.5	154.4	100.5	68.3	49.3	38.2
870102	2	39718	398.8	320.7	273.2	204.3	155.1	93.4	62.5	47.0	38.0
870504	1	42256	196.6	171.6	156.3	130.2	107.9	73.2	51.0	36.6	27.7
870504	2	41555	163.5	141.1	128.5	108.6	91.4	61.9	42.4	29.2	21.3
870505	1	40866	237.0	191.0	162.3	120.8	88.8	48.4	29.3	20.4	15.8
870505	2	39671	180.7	145.8	123.8	92.1	66.9	37.5	23.8	17.0	13.6
870505	3	38774	138.5	116.3	102.5	82.1	64.2	40.0	26.3	18.6	14.1
870505	4	38671	318.0	242.8	196.9	136.5	94.5	49.8	32.7	25.0	21.0

Table B-1: The average of deflections extracted from the FWD data (Continued)

C-SHRP ID	Section	Load(N)	D1(um)	D2(um)	D3(um)	D4(um)	D5(um)	D6(um)	D7(um)	D8(um)	D9(um)
870701	1	40471	175.7	151.5	138.9	115.3	95.2	61.0	39.5	26.7	17.7
870701	2	39395	126.5	105.3	95.7	80.6	66.1	43.3	27.6	17.1	10.1
880203	1	42591	382.9	289.9	233.5	164.4	112.6	52.4	18.0	N/A	N/A
880203	2	41414	376.7	304.4	259.6	200.6	152.1	83.3	26.1	N/A	N/A
880203	3	41129	341.3	267.2	223.8	169.9	125.9	66.6	21.3	N/A	N/A
880203	4	40606	223.3	175.7	150.9	120.1	94.1	56.4	21.7	N/A	N/A
890503	1	42532	313.4	245.1	203.6	153.4	115.6	68.8	36.3	N/A	N/A
890503	2	40614	332.4	237.5	190.1	136.6	100.0	57.8	26.3	N/A	N/A
890503	3	41772	292.3	220.7	183.9	139.8	108.4	70.3	41.1	N/A	N/A
890503	4	40785	291.3	218.0	183.3	140.6	109.3	68.2	31.7	N/A	N/A
890702	1	41308	377.0	274.0	220.2	160.8	117.7	63.2	21.8	N/A	N/A
890702	2	40815	321.5	239.7	197.5	150.3	114.2	65.8	24.2	N/A	N/A
900402	1	40875	317.5	246.8	203.2	145.4	105.4	63.3	47.3	39.2	33.0
900402	2	40420	244.3	202.1	177.9	141.0	111.4	71.9	50.7	39.9	32.6
900802	1	40782	412.2	325.2	268.6	189.4	134.5	74.4	50.5	39.7	32.4
900802	2	39879	339.3	272.8	228.8	167.2	121.7	68.8	46.3	35.9	29.4
900802	3	39545	244.0	204.0	178.8	141.3	110.3	68.3	46.5	35.6	28.5
900803	1	42324	237.4	206.8	189.2	160.7	134.3	93.4	66.1	49.1	37.6
900803	2	41421	345.8	298.1	268.2	221.3	175.2	113.8	76.0	55.1	42.9

Table B-1: The average of deflections extracted from the FWD data

In Table B-1, D_i corresponds to the average of pavement surface deflections measured at 0, 20, 30, 45, 60, 90, 120/150, 150, 180 cm from FWD loading centerline. In some of the C-LTPP sections, the FWD test was conducted with 7 geophones. In such cases, *D7=150 cm* and there was no deflection at *D8* and *D9*.

Appendix C: The EVERCALC backcalculation program outputs (Sample)

```
Backcalculation by Evercalc 5.0 - Detail Output
Route: 8705051
Plate Radius (cm): 15.0     No of Layers: 4
No of Sensors:  9 Stiff Layer: No
Offsets (cm):    .0  20.0  30.0  45.0  60.0  90.0  120.0  150.0  180.0  P-Ratio:  .350  .350  .400
.400
Station: average            No of Drops:  2   Average RMS Error(%):    .70
Thickness (cm):  16.40  59.00 *******        Pavement Temperature (C):  14.0
Drop No:  1       Load (N):  40866.0         No of Iterations: 3
Convergence: RMS Error Tolerance Satisfied             RMS Error (%):  .70
Sensor No:          1          2          3          4          5          6          7          8          9
Measured Deflections (microns):     237.000 191.000 162.000 121.000  89.000   48.000   29.000
20.000     16.000
Calculated Deflection (microns):    237.614 191.396 160.992 120.928  89.151   48.523   28.905
20.164     16.218
Difference (%):       -.26       -.21       .62        .06       -.17      -1.09      .33       -.82      -1.36
Layer No:           1          2          3          4          1-(adj)
Seed Moduli (MPa):            5000.00  500.00   250.00   250.00 N/A
Calculated Moduli (MPa):  5319.27  134.30   355.40   250.00 2159.172
Layer No:           1          2          3
Radial Distance (cm):          .00         .00         .00
Position:Bottom   Middle   Top
Vertical Stress (kPa):          -77.70   -36.84   -23.20
Radial Stress (kPa):            1171.62  -4.00     -2.80
Bulk Stress (kPa):              2265.55  -44.83   -28.80
Deviator Stress (kPa):         -1249.32  -32.84   -20.39
Vertical Strain (10^-6):       -168.79  -253.43   -58.96
Radial Strain (10^-6):          148.28    76.64    21.38
Drop No:  2       Load (N):  40866.0         No of Iterations: 0
Convergence: RMS Error Tolerance Satisfied             RMS Error (%):  .70
Sensor No:          1          2          3          4          5          6          7          8          9
```

```
Measured Deflections (microns):    237.000 191.000 162.000 121.000 89.000  48.000  29.000
20.000    16.000
Calculated Deflection (microns):   237.614 191.396 160.992 120.928 89.151  48.523  28.905
20.164    16.218
Difference (%):    -.26    -.21    .62    .06    -.17    -1.09    .33    -.82    -1.36
Layer No:        1        2        3        4        1-(adj)
Seed Moduli (MPa):          5319.27  134.30  355.40  250.00 N/A
Calculated Moduli (MPa): 5319.27  134.30  355.40  250.00 2159.172
Layer No:        1        2        3
Radial Distance (cm):        .00        .00        .00
Position:Bottom  Middle  Top
Vertical Stress (kPa):       -77.70   -36.84   -23.20
Radial Stress (kPa):         1171.62  -4.00     -2.80
Bulk Stress (kPa):           2265.55  -44.83   -28.80
Deviator Stress (kPa):       -1249.32 -32.84   -20.39
Vertical Strain (10^-6):     -168.79  -253.43  -58.96
Radial Strain (10^-6):        148.28   76.64    21.38
Layer No:        1        2        3        4        1-(adj)
Mean Moduli (MPa):           5319.27  134.30  355.40  250.00  2159.17
Normalized Moduli (MPa):              .00       .00       .00       .00       .000
K1 (MPa):        N/A        143.54   24.04  N/A
K2:      N/A        .16        .86   N/A
R-Squared:       N/A        12790.50            790.16 N/A
Soil Type:       N/A        Coarse   Coarse   N/A
```

Backcalculation by Evercalc 5.0 - Detail Output

Route: 8705052

```
Plate Radius (cm): 15.0    No of Layers: 4
No of Sensors:  9 Stiff Layer: No
Offsets (cm):    .0  20.0  30.0  45.0  60.0  90.0  120.0  150.0  180.0  P-Ratio:  .350  .350  .400
.400
Station: average               No of Drops:  2   Average RMS Error(%):    .89
Thickness (cm):  16.10   59.00 *******       Pavement Temperature (C):  13.0
Drop No:  1        Load (N):  39671.0        No of Iterations: 3
Convergence: RMS Error Tolerance Satisfied            RMS Error (%):   .89
```

```
Sensor No:      1       2       3       4       5       6       7       8       9
Measured Deflections (microns):     181.000 146.000 124.000 92.000  67.000  38.000  24.000
17.000   14.000
Calculated Deflection (microns):    182.435 146.091 122.428 91.749  67.867  37.969  23.712
17.210   14.053
Difference (%):     -.79    -.06    1.27    .27     -1.29   .08     1.20    -1.24   -.38
Layer No:       1       2       3       4       1-(adj)
Seed Moduli (MPa):          5000.00 500.00  250.00  250.00 N/A
Calculated Moduli (MPa): 6581.22 189.95  412.27  250.00 2493.875
Layer No:       1       2       3
Radial Distance (cm):       .00     .00     .00
Position:Bottom  Middle  Top
Vertical Stress (kPa):      -83.22  -37.52  -22.78
Radial Stress (kPa):        1120.44 -3.35   -2.24
Bulk Stress (kPa):          2157.66 -44.23  -27.27
Deviator Stress (kPa):      -1203.66 -34.17 -20.54
Vertical Strain (10^-6):    -131.82 -185.17 -50.91
Radial Strain (10^-6):      115.09  57.66   18.84
Drop No:  2      Load (N):  39671.0         No of Iterations: 0
Convergence: RMS Error Tolerance Satisfied          RMS Error (%):   .89
Sensor No:      1       2       3       4       5       6       7       8       9
Measured Deflections (microns):     181.000 146.000 124.000 92.000  67.000  38.000  24.000
17.000   14.000
Calculated Deflection (microns):    182.435 146.091 122.428 91.749  67.867  37.969  23.712
17.210   14.053
Difference (%):     -.79    -.06    1.27    .27     -1.29   .08     1.20    -1.24   -.38
Layer No:       1       2       3       4       1-(adj)
Seed Moduli (MPa):          6581.22 189.95  412.27  250.00 N/A
Calculated Moduli (MPa): 6581.22 189.95  412.27  250.00 2493.875
Layer No:       1       2       3
Radial Distance (cm):       .00     .00     .00
Position:Bottom  Middle  Top
Vertical Stress (kPa):      -83.22  -37.52  -22.78
Radial Stress (kPa):        1120.44 -3.35   -2.24
Bulk Stress (kPa):          2157.66 -44.23  -27.27
```

```
Deviator Stress (kPa):      -1203.66  -34.17   -20.54
Vertical Strain (10^-6):    -131.82  -185.17   -50.91
Radial Strain (10^-6):       115.09    57.66    18.84
Layer No:         1        2        3        4       1-(adj)
Mean Moduli (MPa):          6581.22  189.95   412.27   250.00  2493.88
Normalized Moduli (MPa):             .00      .00      .00     .00      .000
K1 (MPa):         N/A      235.15   .00      N/A
K2:       N/A        .49        3.92   N/A
R-Squared:        N/A      4891.16  446.85   N/A
Soil Type:        N/A      Coarse   Coarse   N/A
```

Backcalculation by Evercalc 5.0 - Detail Output

Route: 8705053

```
Plate Radius (cm): 15.0     No of Layers: 4
No of Sensors:  9 Stiff Layer: No
Offsets (cm):    .0  20.0  30.0  45.0  60.0  90.0  120.0  150.0  180.0  P-Ratio:  .350  .350  .400
.400
Station: average              No of Drops:  2    Average RMS Error(%):  1.45
Thickness (cm):   19.40   59.00 *******          Pavement Temperature (C):  13.5
Drop No:  1       Load (N):  38775.0             No of Iterations: 4
Convergence: Modulus Tolerance Satisfied         RMS Error (%):  1.45
Sensor No:          1        2         3         4         5         6         7         8         9
Measured Deflections (microns):      138.000  116.000  103.000  82.000   64.000   40.000   26.000
19.000    14.000
Calculated Deflection (microns):     138.811  115.923  101.459  81.645   64.734   40.337   26.123
18.396    14.273
Difference (%):      -.59      .07      1.50      .43      -1.15     -.84      -.47      3.18     -1.95
Layer No:            1         2         3         4        1-(adj)
Seed Moduli (MPa):             5000.00   500.00   250.00   250.00  N/A
Calculated Moduli (MPa):  8212.99   187.77   406.00   250.00  3220.207
Layer No:          1         2         3
Radial Distance (cm):      .00       .00       .00
Position:Bottom   Middle   Top
Vertical Stress (kPa):     -53.31    -26.90    -17.51
Radial Stress (kPa):       916.56    -3.16     -2.14
```

```
Bulk Stress (kPa):           1779.80  -33.22   -21.80
Deviator Stress (kPa):       -969.87  -23.73   -15.37
Vertical Strain (10^-6):      -84.61 -131.45   -38.91
Radial Strain (10^-6):         74.81   39.19    14.09
Drop No:  2      Load (N):  38775.0         No of Iterations: 1
Convergence: Modulus Tolerance Satisfied  RMS Error (%):  1.45
Sensor No:           1         2        3        4        5        6        7        8        9
Measured Deflections (microns):       138.000  116.000  103.000  82.000  64.000  40.000  26.000
19.000    14.000
Calculated Deflection (microns):      138.811  115.923  101.459  81.645  64.734  40.337  26.123
18.396    14.273
Difference (%):      -.59      .07      1.50      .43      -1.15     -.84      -.47      3.18      -1.95
Layer No:            1         2        3        4        1-(adj)
Seed Moduli (MPa):        8212.99  187.77   406.00   250.00  N/A
Calculated Moduli (MPa):  8212.98  187.77   406.00   250.00  3220.205
Layer No:            1         2        3
Radial Distance (cm):        .00      .00      .00
Position:Bottom   Middle   Top
Vertical Stress (kPa):       -53.31   -26.90   -17.51
Radial Stress (kPa):         916.56    -3.16    -2.14
Bulk Stress (kPa):          1779.80   -33.22   -21.80
Deviator Stress (kPa):      -969.87   -23.73   -15.37
Vertical Strain (10^-6):     -84.61  -131.45   -38.91
Radial Strain (10^-6):        74.81    39.19    14.09
Layer No:            1         2        3        4        1-(adj)
Mean Moduli (MPa):          8212.99  187.77   406.00   250.00  3220.21
Normalized Moduli (MPa):              .00      .00      .00      .00      .000
K1 (MPa):            N/A       ********          .11      N/A
K2:        N/A          16.19      2.61     N/A
R-Squared:           N/A       101.62    82.84    N/A
Soil Type:           N/A       Coarse    Coarse   N/A
```

Backcalculation by Evercalc 5.0 - Detail Output

Route: 8705054

Plate Radius (cm): 15.0   No of Layers: 4

```
No of Sensors:  9 Stiff Layer: No
Offsets (cm):    .0  20.0  30.0  45.0  60.0  90.0  120.0  150.0  180.0  P-Ratio:  .350  .350  .400
.400
Station: average             No of Drops:  2   Average RMS Error(%):  1.19
Thickness (cm):  15.50  59.00 *******      Pavement Temperature (C):  14.5
Drop No:  1      Load (N):  38670.0           No of Iterations: 5
Convergence: Modulus Tolerance Satisfied   RMS Error (%):  1.19
Sensor No:          1          2          3          4          5          6          7          8          9
Measured Deflections (microns):     318.000 243.000 197.000 137.000 95.000  50.000  33.000
25.000    21.000
Calculated Deflection (microns):     323.387 242.218 193.462 135.773 95.350  51.091  32.872
24.965    20.815
Difference (%):     -1.69      .32       1.80       .90       -.37      -2.18       .39       .14       .88
Layer No:           1          2          3          4          1-(adj)
Seed Moduli (MPa):          5000.00 500.00  250.00   250.00 N/A
Calculated Moduli (MPa): 2633.25  134.98   266.59   250.00 1107.184
Layer No:           1          2          3
Radial Distance (cm):        .00        .00        .00
Position:Bottom   Middle   Top
Vertical Stress (kPa):       -116.69  -45.58   -25.56
Radial Stress (kPa):          923.26   -2.44    -1.77
Bulk Stress (kPa):           1729.83  -50.46   -29.09
Deviator Stress (kPa):      -1039.95  -43.14   -23.79
Vertical Strain (10^-6):     -289.75 -325.02   -90.56
Radial Strain (10^-6):        243.41  106.43    34.37
Drop No:  2       Load (N):  38670.0           No of Iterations: 1
Convergence: Modulus Tolerance Satisfied   RMS Error (%):  1.19
Sensor No:          1          2          3          4          5          6          7          8          9
Measured Deflections (microns):     318.000 243.000 197.000 137.000 95.000   50.000  33.000
25.000    21.000
Calculated Deflection (microns):     323.386 242.218 193.462 135.773 95.350   51.091  32.872
24.965    20.815
Difference (%):     -1.69      .32       1.80       .90       -.37      -2.18       .39       .14       .88
Layer No:           1          2          3          4          1-(adj)
Seed Moduli (MPa):          2633.25  134.98   266.59   250.00 N/A
```

```
Calculated Moduli (MPa):  2633.28  134.98   266.59   250.00 1107.197
Layer No:         1        2        3
Radial Distance (cm):      .00      .00      .00
Position:Bottom  Middle   Top
Vertical Stress (kPa):    -116.69  -45.58   -25.56
Radial Stress (kPa):       923.27   -2.44    -1.77
Bulk Stress (kPa):        1729.84  -50.46   -29.09
Deviator Stress (kPa):   -1039.96  -43.14   -23.79
Vertical Strain (10^-6):  -289.74 -325.02   -90.56
Radial Strain (10^-6):     243.41  106.43    34.37
Layer No:         1        2        3        4        1-(adj)
Mean Moduli (MPa):        2633.27  134.98   266.59   250.00  1107.19
Normalized Moduli (MPa):            .00      .00      .00      .00      .000
K1 (MPa):         N/A      208.75 ********          N/A
K2:      N/A       1.26    -12.47 N/A
R-Squared:        N/A      101.44  228.59 N/A
Soil Type:        N/A      Coarse  Fine    N/A
```

Appendix D: The MICHBACK backcalculation program outputs (Sample)

```
Michback Filename:     8705051.bkd
Control Section:
Job Number:
Route:
Lane:
Region:
Trial Number:
Units:   Load: kPa        Deflection: mm   Temperature: C   Modulus: kPa

Sta./Mp Load    D0       D3       D4       D5       D6       D7       D8       D9       D10
        Air Temp.        Layer Moduli(1)   Layer Moduli(2)   Layer Moduli(3)   RMS(%)
        Converge y/n
 1        40866.00        237.00000        191.00000        162.00000        121.00000
89.00000         48.00000         29.00000         20.00000         16.00000         14.00
5397725.         131793.          350173.          0.8251           Y

Michback Filename:     8705052.bkd
Control Section:
Job Number:
Route:
Lane:
Region:
Trial Number:
Units:   Load: kPa        Deflection: mm   Temperature: C   Modulus: kPa

Sta./Mp Load    D0       D3       D4       D5       D6       D7       D8       D9       D10
        Air Temp.        Layer Moduli(1)   Layer Moduli(2)   Layer Moduli(3)   RMS(%)
        Converge y/n
 1        39671.00        180.99998        146.00000        123.99998        92.00000
67.00000         38.00000         23.00000         17.00000         14.00000         13.00
6505908.         188197.          404318.          1.3081           Y
```

```
Michback Filename:      8705053.bkd
Control Section:
Job Number:
Route:
Lane:
Region:
Trial Number:
Units:   Load: kPa        Deflection: mm    Temperature: C    Modulus: kPa

Sta./Mp Load     D0       D3        D4        D5        D6        D7        D8        D9        D10
        Air Temp.         Layer Moduli(1)  Layer Moduli(2)  Layer Moduli(3)  RMS(%)
        Converge y/n
 1        38774.00        138.00000        116.00000        103.00000         82.00000
64.00001          40.00000         26.00000          19.00000          14.00000           14.00
8185223.          187075.          396335.           1.4651            Y
```

```
Michback Filename:      8705054.bkd
Control Section:
Job Number:
Route:
Lane:
Region:
Trial Number:
Units:   Load: kPa        Deflection: mm    Temperature: C    Modulus: kPa

Sta./Mp Load     D0       D3        D4        D5        D6        D7        D8        D9        D10
        Air Temp.         Layer Moduli(1)  Layer Moduli(2)  Layer Moduli(3)  RMS(%)
        Converge y/n
 1        38671.00        318.00000        242.99998        196.99998        137.00000
94.99999          50.00000         33.00000          25.00000          21.00000           15.00
2714534.          131075.          265129.           1.5439            Y
```

Appendix E: The traffic data for the C-LTPP project at the year of overlay

C-SHRP	AADT	DDF	%TRUCK	truck factor	LDF	DAYS	ESAL
810404	4570	0.5	13.4	2	1	300	183714
820205	1775	0.53	5	2	1	300	28222.5
820502	13720	0.53	5.5	2	1	300	239962.8
820605	13720	0.53	5.5	2	1	300	239962.8
830403	1104	0.5	7.7	2	1	300	25502.4
830801	3530	0.5	13.9	2	0.8	300	117760.8
840101	12750	0.5	6	2	1	300	229500
840204	1200	0.5	5	2	1	300	18000
840604	6400	0.5	19	2	1	300	364800
850201	3325	0.5	7.1	2	1	300	70822.5
850206	2632	0.5	8.7	2	1	300	68695.2
850601	4947	0.5	11.6	2	1	300	172155.6
860501	11900	0.5	14	2	0.8	300	399840
860603	3160	0.5	14	2	1	300	132720
870102	1100	0.5	15	2	1	300	49500
870504	10400	0.5	13	2	0.8	300	324480
870505	3600	0.5	10	2	1	300	108000
870701	5700	0.5	15	2	1	300	256500
880203	3087	0.5	9.4	2	1	300	87053.4
890503	14510	0.5	10.7	2	0.83	300	386589.93
890702	10740	0.5	14.4	2	0.86	300	399012.48
900402	1960	0.5	13	2	1	300	76440
900802	2825	0.5	15	2	1	300	127125
900803	1893	0.5	15	2	1	300	85185

Table E-1: The traffic information for the C-LTPP test sections at year of overlay

In above table all the information belong to overlay time, where

$$ESAL = AADT \times DDF \times Truck\ percentage \times Truck\ factor \times LDF \times Days$$

AADT= Annual Average Daily Traffic
DDF= Directional Distribution Factor
% Truck= Percentage of Trucks in the traffic stream
LDF= Lane Distribution Factor
ESAL= Equivalent Single Axle Load (18000 lb)

Appendix F: Roughness trends in the C-LTPP project

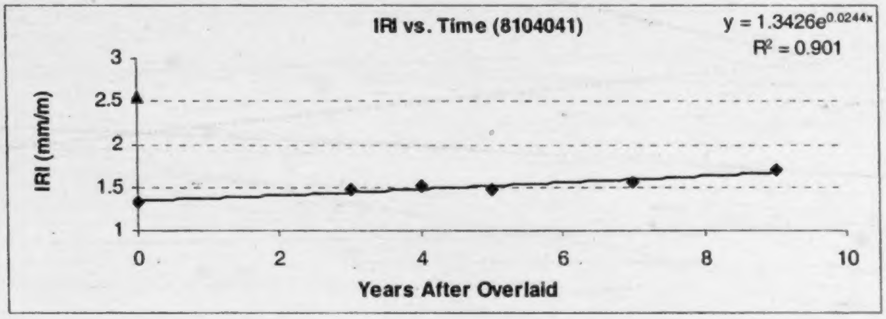

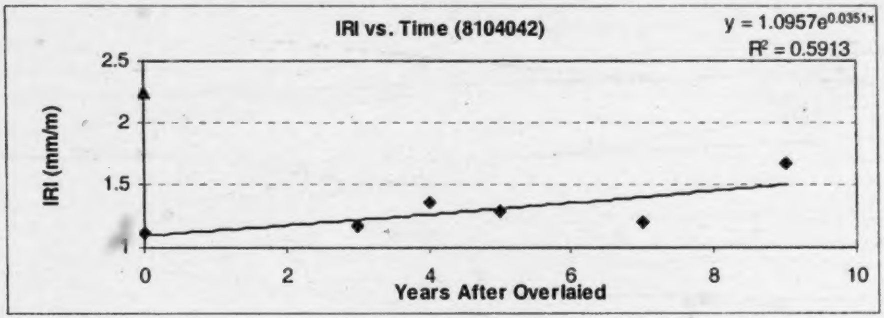

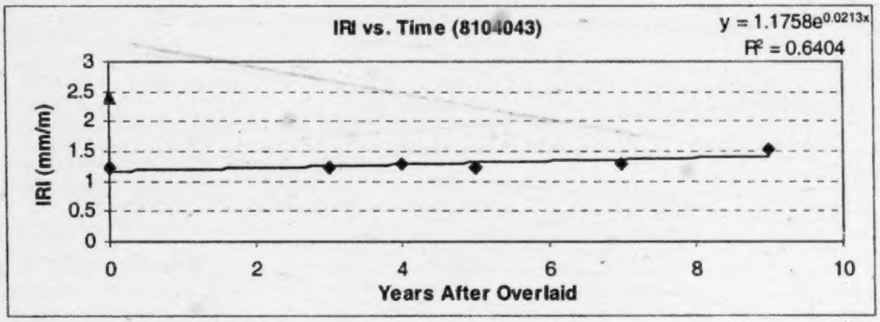

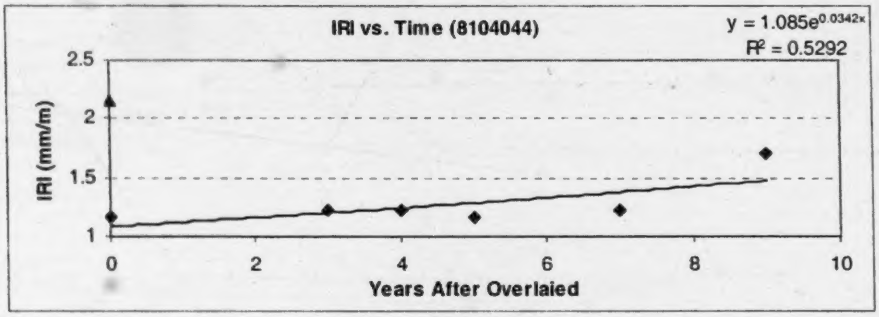
IRI vs. Time (8104044)
y = 1.085e^0.0342x
R² = 0.5292
2.5
2
1.5
1
IRI (mm/m)
0
2
4
6
8
10
Years After Overlaied

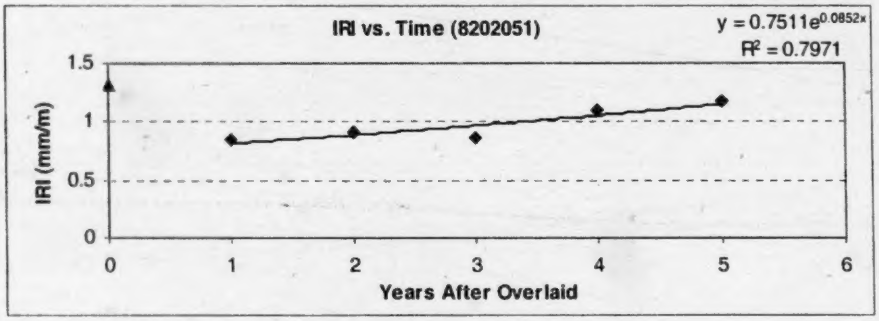
IRI vs. Time (8202051)
y = 0.7511e^0.0852x
R² = 0.7971
1.5
1
0.5
0
IRI (mm/m)
0
1
2
3
4
5
6
Years After Overlaid

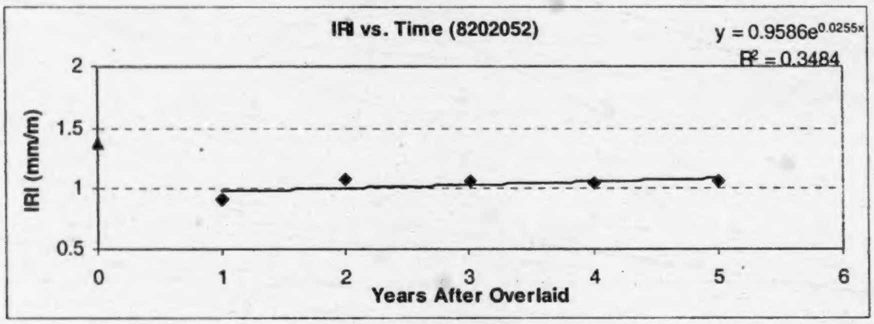
IRI vs. Time (8202052)
y = 0.9586e^0.0255x
R² = 0.3484
2
1.5
1
0.5
IRI (mm/m)
0
1
2
3
4
5
6
Years After Overlaid

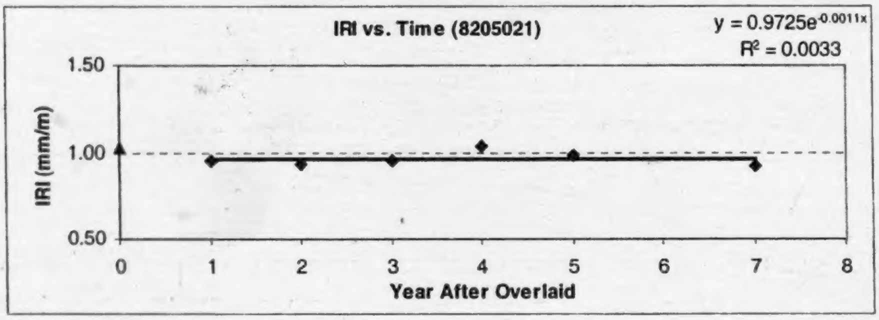
IRI vs. Time (8205021)
y = 0.9725e^-0.0011x
R² = 0.0033
1.50
1.00
0.50
IRI (mm/m)
0
1
2
3
4
5
6
7
8
Year After Overlaid

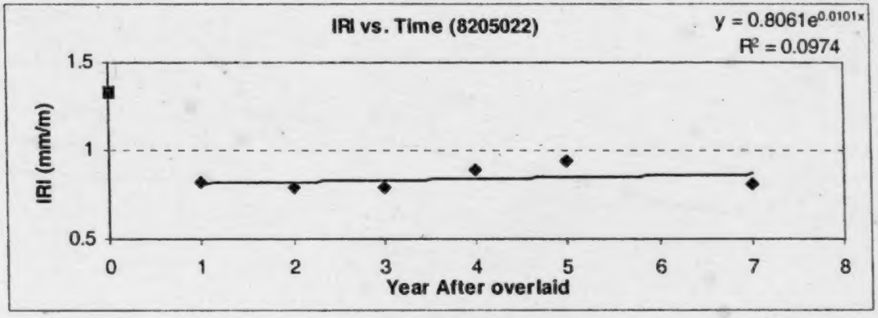
IRI vs. Time (8205022)
$y = 0.8061e^{0.0101x}$
$R^2 = 0.0974$
IRI (mm/m)
1.5
1
0.5
0
1
2
3
4
5
6
7
8
Year After overlaid

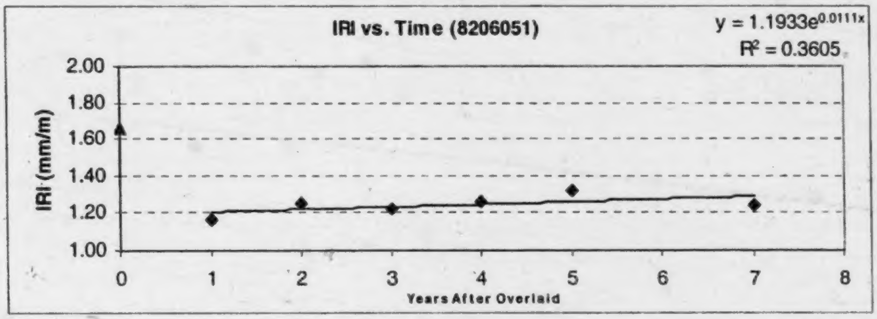
IRI vs. Time (8206051)
$y = 1.1933e^{0.0111x}$
$R^2 = 0.3605$
IRI (mm/m)
2.00
1.80
1.60
1.40
1.20
1.00
0
1
2
3
4
5
6
7
8
Years After Overlaid

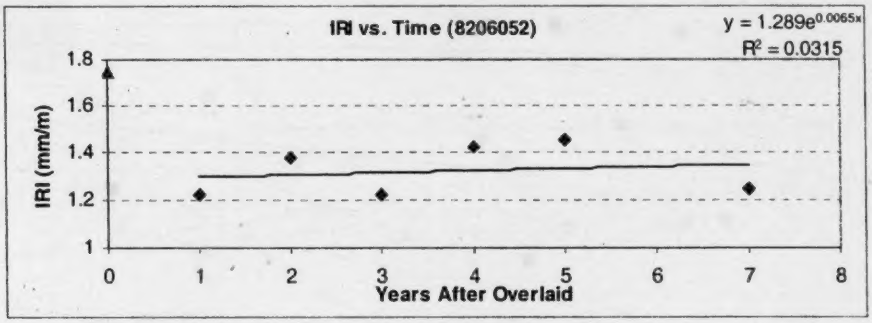
IRI vs. Time (8206052)
$y = 1.289e^{0.0065x}$
$R^2 = 0.0315$
IRI (mm/m)
1.8
1.6
1.4
1.2
1
0
1
2
3
4
5
6
7
8
Years After Overlaid

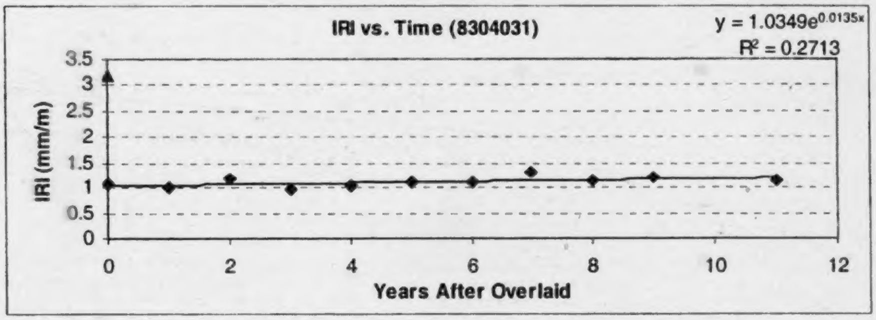
IRI vs. Time (8304031)
$y = 1.0349e^{0.0135x}$
$R^2 = 0.2713$
IRI (mm/m)
3.5
3
2.5
2
1.5
1
0.5
0
0
2
4
6
8
10
12
Years After Overlaid

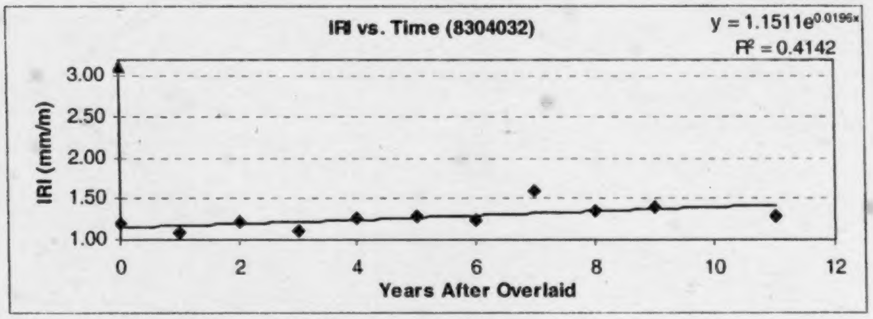
IRI vs. Time (8304032)
y = 1.1511e^0.0196x
R² = 0.4142
IRI (mm/m)
3.00
2.50
2.00
1.50
1.00
0
2
4
6
8
10
12
Years After Overlaid

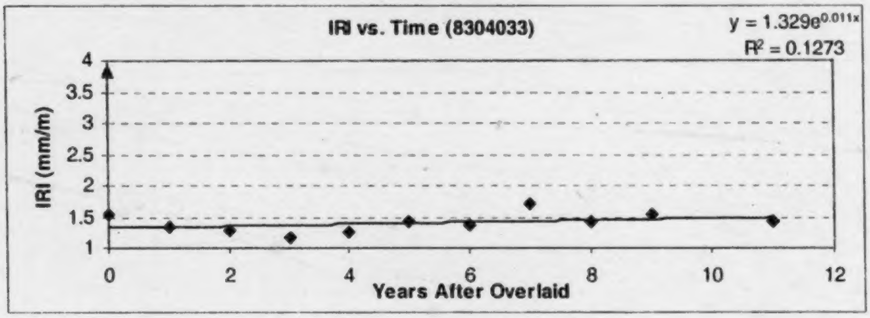
IRI vs. Time (8304033)
y = 1.329e^0.011x
R² = 0.1273
IRI (mm/m)
4
3.5
3
2.5
2
1.5
1
0
2
4
6
8
10
12
Years After Overlaid

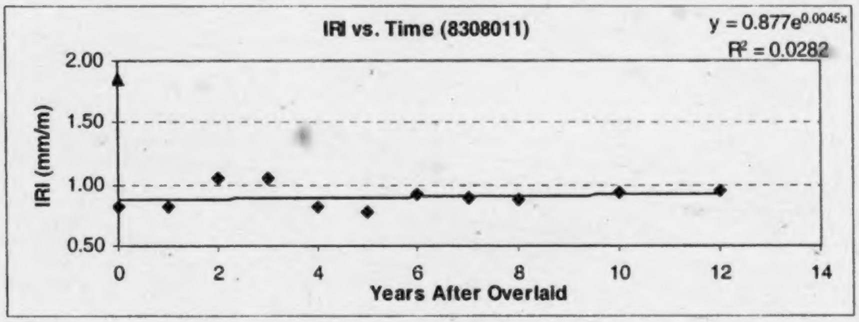
IRI vs. Time (8308011)
y = 0.877e^0.0045x
R² = 0.0282
IRI (mm/m)
2.00
1.50
1.00
0.50
0
2
4
6
8
10
12
14
Years After Overlaid

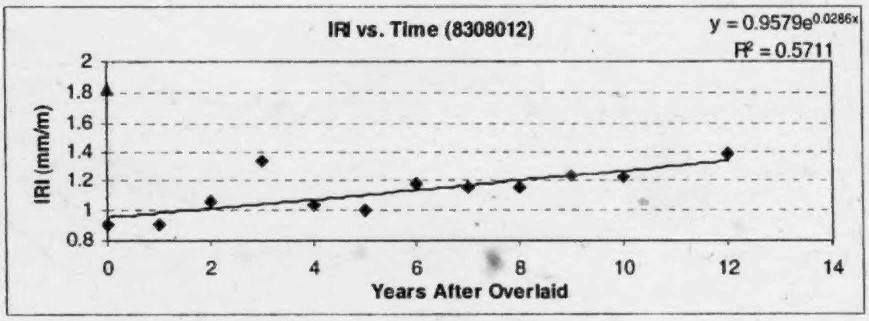
IRI vs. Time (8308012)
y = 0.9579e^0.0286x
R² = 0.5711
IRI (mm/m)
2
1.8
1.6
1.4
1.2
1
0.8
0
2
4
6
8
10
12
14
Years After Overlaid

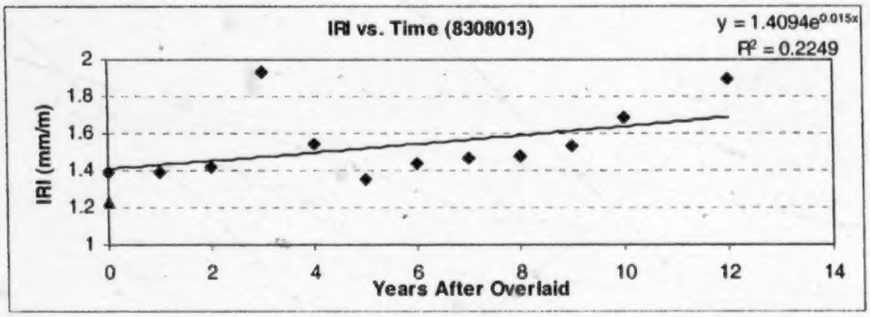
IRI vs. Time (8308013)
y = 1.4094e^0.015x
R² = 0.2249
IRI (mm/m)
2
1.8
1.6
1.4
1.2
1
0
2
4
6
8
10
12
14
Years After Overlaid

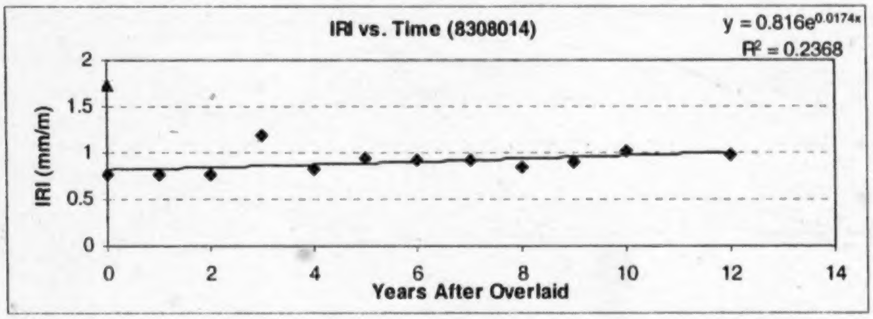
IRI vs. Time (8308014)
y = 0.816e^0.0174x
R² = 0.2368
IRI (mm/m)
2
1.5
1
0.5
0
0
2
4
6
8
10
12
14
Years After Overlaid

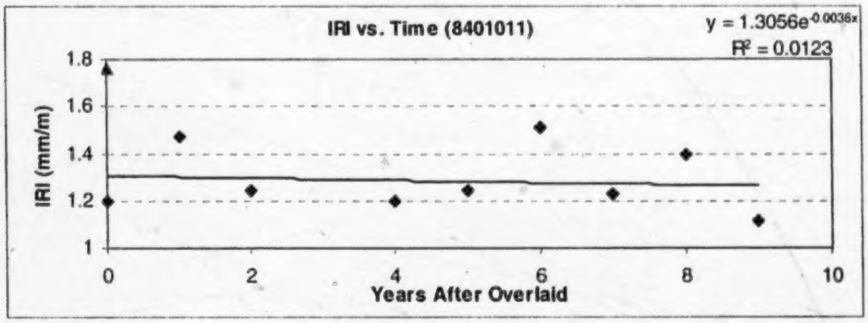
IRI vs. Time (8401011)
y = 1.3056e^-0.0036x
R² = 0.0123
IRI (mm/m)
1.8
1.6
1.4
1.2
1
0
2
4
6
8
10
Years After Overlaid

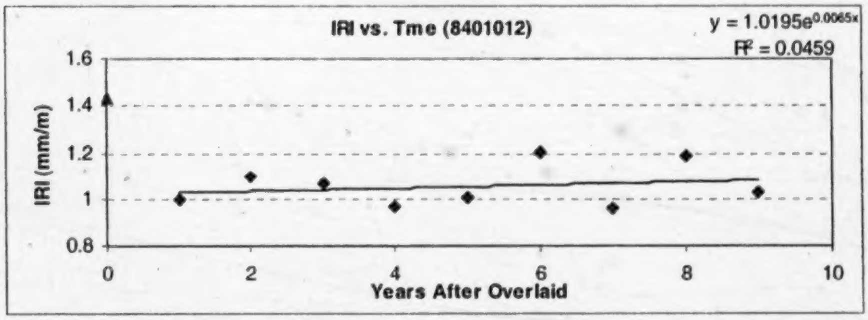
IRI vs. Tme (8401012)
y = 1.0195e^0.0065x
R² = 0.0459
IRI (mm/m)
1.6
1.4
1.2
1
0.8
0
2
4
6
8
10
Years After Overlaid

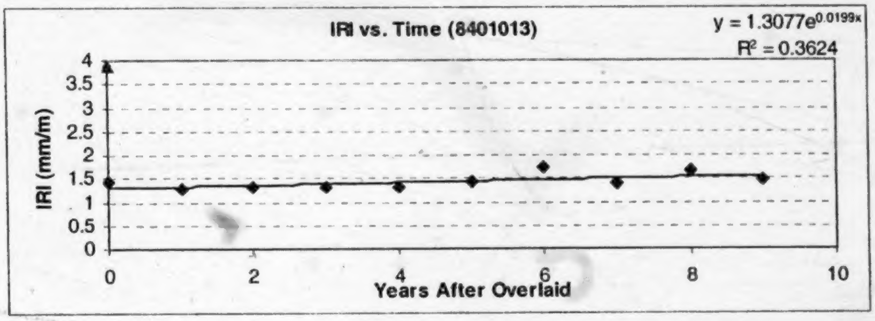
IRI vs. Time (8401013)
y = 1.3077e^0.0199x
R² = 0.3624
IRI (mm/m)
0
0.5
1
1.5
2
2.5
3
3.5
4
0
2
4
6
8
10
Years After Overlaid

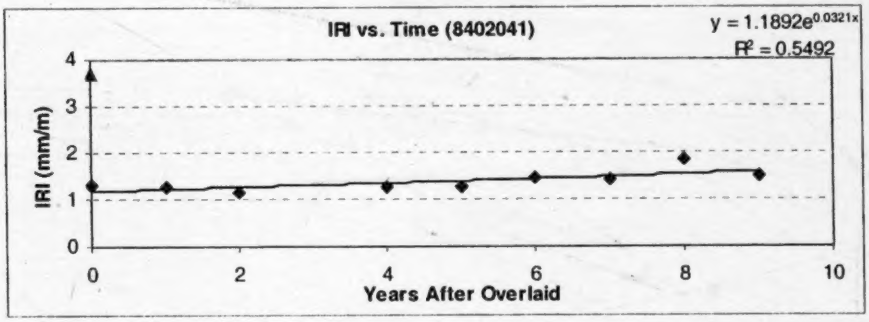
IRI vs. Time (8402041)
y = 1.1892e^0.0321x
R² = 0.5492
IRI (mm/m)
0
1
2
3
4
0
2
4
6
8
10
Years After Overlaid

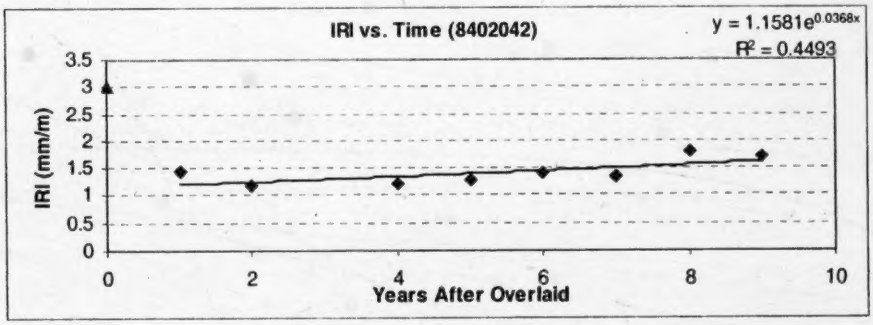
IRI vs. Time (8402042)
y = 1.1581e^0.0368x
R² = 0.4493
IRI (mm/m)
0
0.5
1
1.5
2
2.5
3
3.5
0
2
4
6
8
10
Years After Overlaid

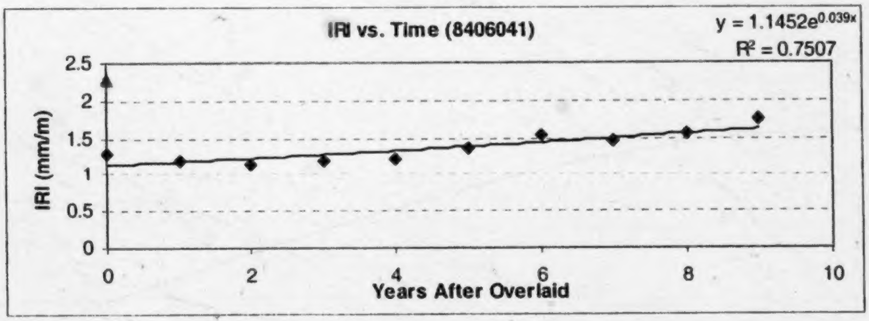
IRI vs. Time (8406041)
y = 1.1452e^0.039x
R² = 0.7507
IRI (mm/m)
0
0.5
1
1.5
2
2.5
0
2
4
6
8
10
Years After Overlaid

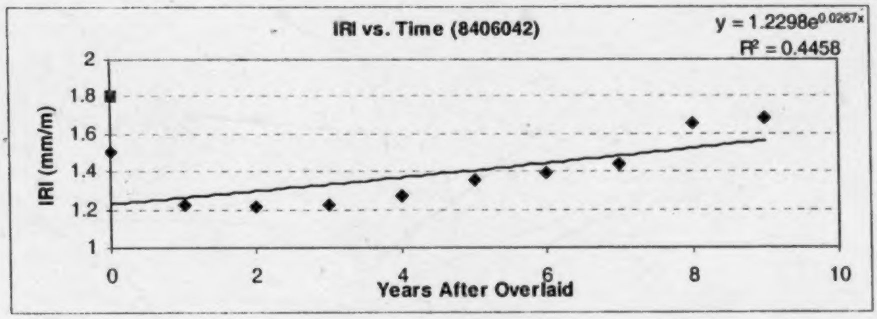
IRI vs. Time (8406042)
y = 1.2298e^0.0267x
R² = 0.4458
IRI (mm/m)
2
1.8
1.6
1.4
1.2
1
0
2
4
6
8
10
Years After Overlaid

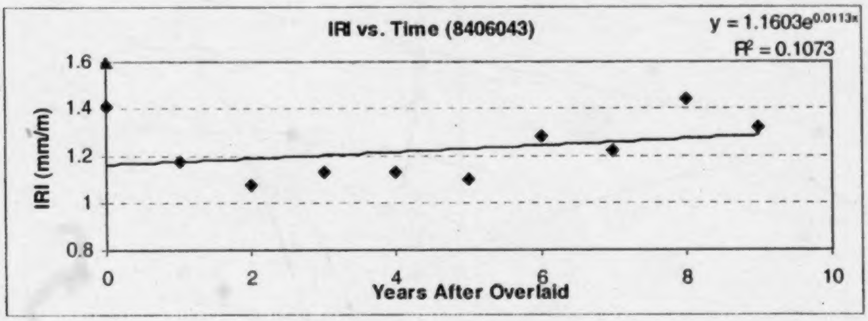
IRI vs. Time (8406043)
y = 1.1603e^0.0113x
R² = 0.1073
IRI (mm/m)
1.6
1.4
1.2
1
0.8
0
2
4
6
8
10
Years After Overlaid

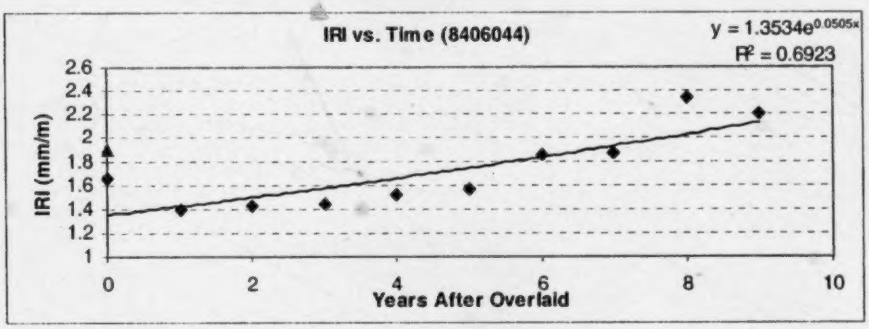
IRI vs. Time (8406044)
y = 1.3534e^0.0505x
R² = 0.6923
IRI (mm/m)
2.6
2.4
2.2
2
1.8
1.6
1.4
1.2
1
0
2
4
6
8
10
Years After Overlaid

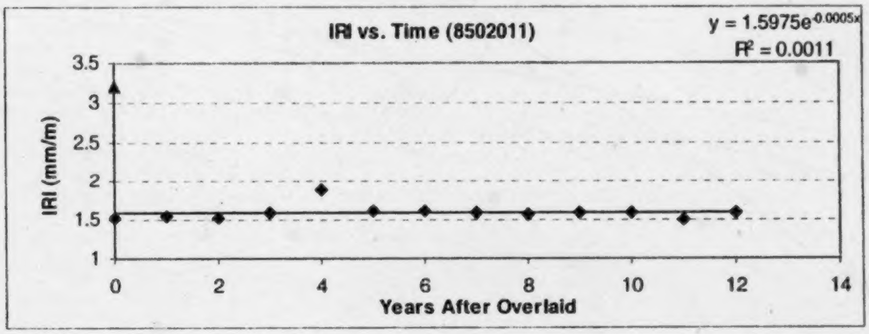
IRI vs. Time (8502011)
y = 1.5975e^-0.0005x
R² = 0.0011
IRI (mm/m)
3.5
3
2.5
2
1.5
1
0
2
4
6
8
10
12
14
Years After Overlaid

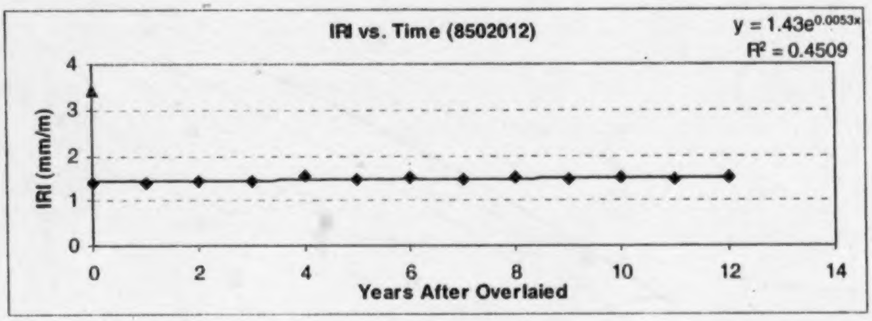
IRI vs. Time (8502012)
y = 1.43e^0.0053x
R² = 0.4509
IRI (mm/m)
0
1
2
3
4
0
2
4
6
8
10
12
14
Years After Overlaied

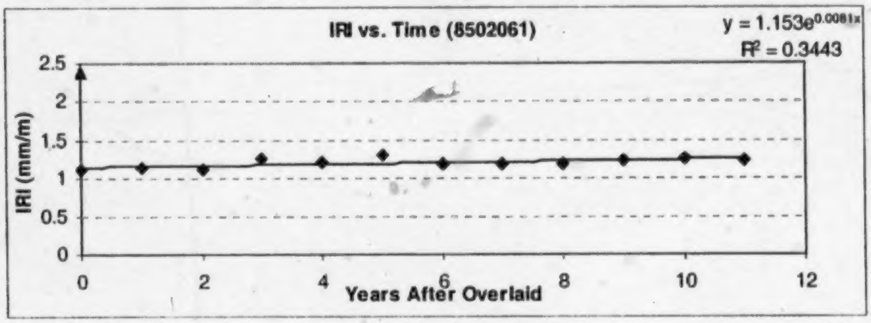
IRI vs. Time (8502061)
y = 1.153e^0.0081x
R² = 0.3443
IRI (mm/m)
0
0.5
1
1.5
2
2.5
0
2
4
6
8
10
12
Years After Overlaid

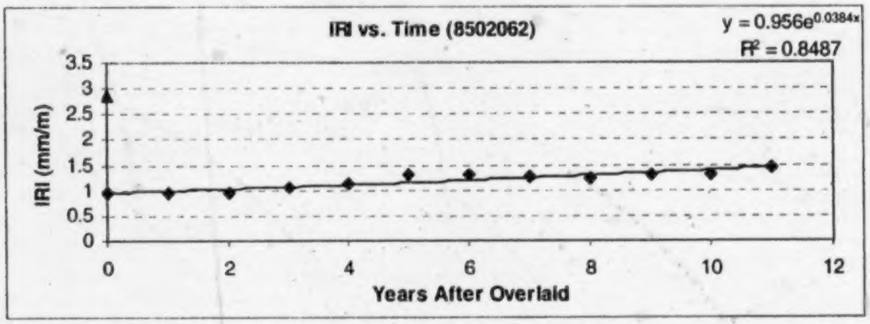
IRI vs. Time (8502062)
y = 0.956e^0.0384x
R² = 0.8487
IRI (mm/m)
0
0.5
1
1.5
2
2.5
3
3.5
0
2
4
6
8
10
12
Years After Overlaid

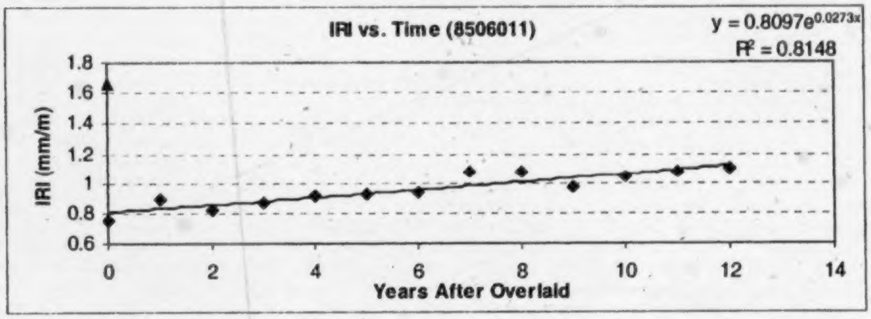
IRI vs. Time (8506011)
y = 0.8097e^0.0273x
R² = 0.8148
IRI (mm/m)
0.6
0.8
1
1.2
1.4
1.6
1.8
0
2
4
6
8
10
12
14
Years After Overlaid

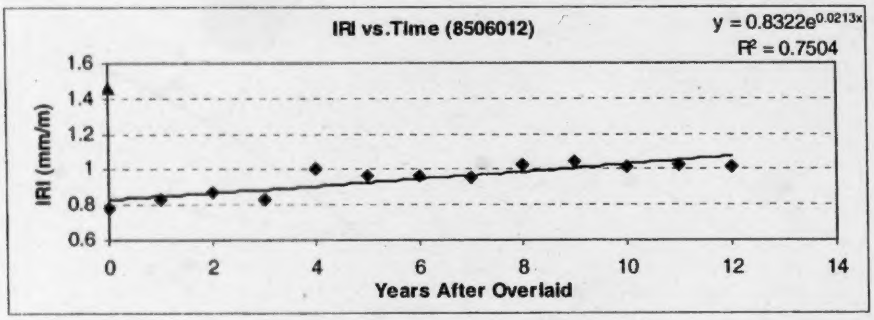
IRI vs.Time (8506012)
y = 0.8322e^0.0213x
R² = 0.7504
IRI (mm/m)
1.6
1.4
1.2
1
0.8
0.6
0
2
4
6
8
10
12
14
Years After Overlaid

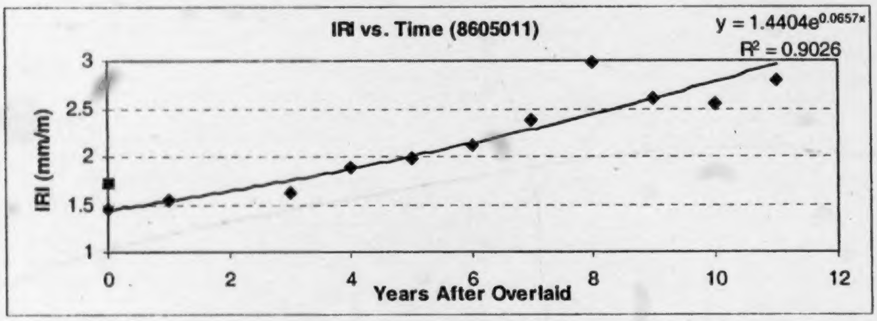
IRI vs. Time (8605011)
y = 1.4404e^0.0657x
R² = 0.9026
IRI (mm/m)
3
2.5
2
1.5
1
0
2
4
6
8
10
12
Years After Overlaid

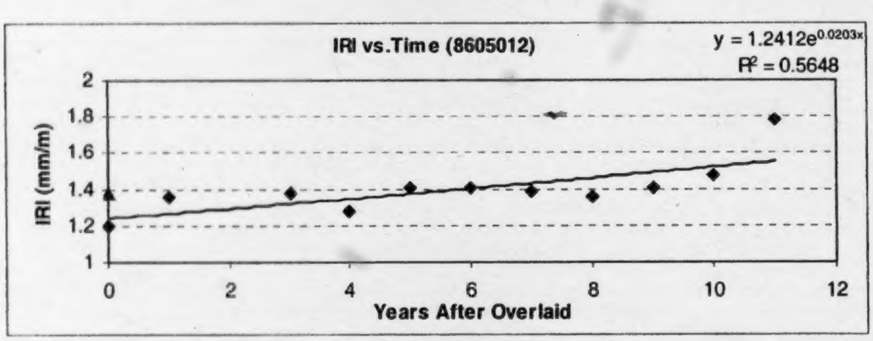
IRI vs.Time (8605012)
y = 1.2412e^0.0203x
R² = 0.5648
IRI (mm/m)
2
1.8
1.6
1.4
1.2
1
0
2
4
6
8
10
12
Years After Overlaid

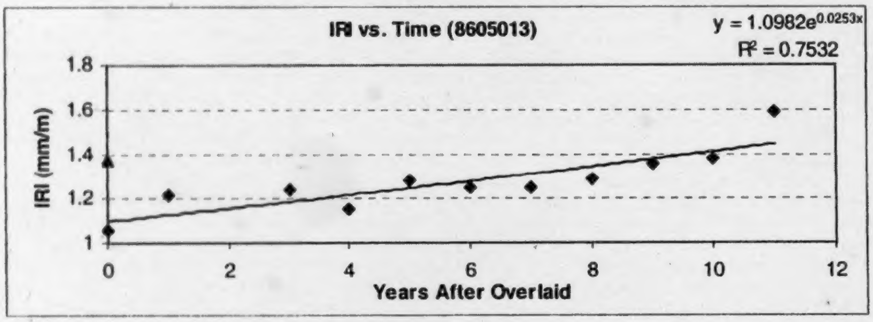
IRI vs. Time (8605013)
y = 1.0982e^0.0253x
R² = 0.7532
IRI (mm/m)
1.8
1.6
1.4
1.2
1
0
2
4
6
8
10
12
Years After Overlaid

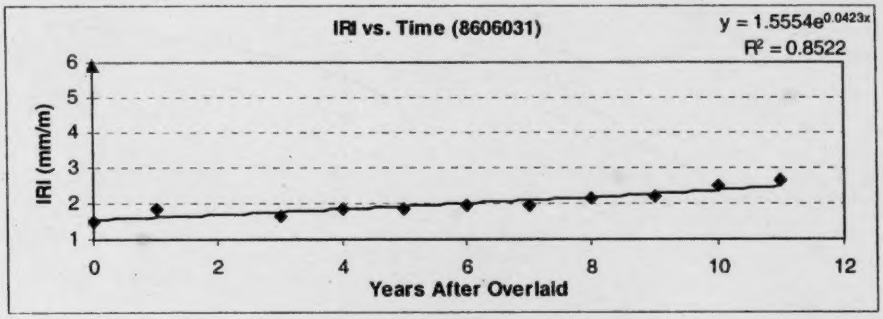
IRI vs. Time (8606031)
y = 1.5554e^0.0423x
R² = 0.8522
IRI (mm/m)
6
5
4
3
2
1
0
2
4
6
8
10
12
Years After Overlaid

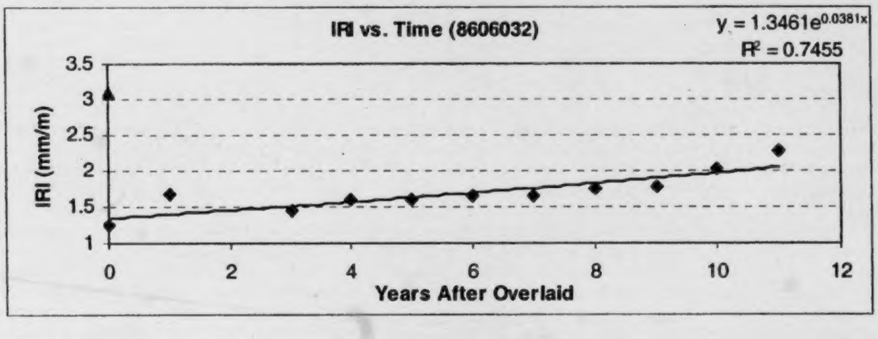
IRI vs. Time (8606032)
y = 1.3461e^0.0381x
R² = 0.7455
IRI (mm/m)
3.5
3
2.5
2
1.5
1
0
2
4
6
8
10
12
Years After Overlaid

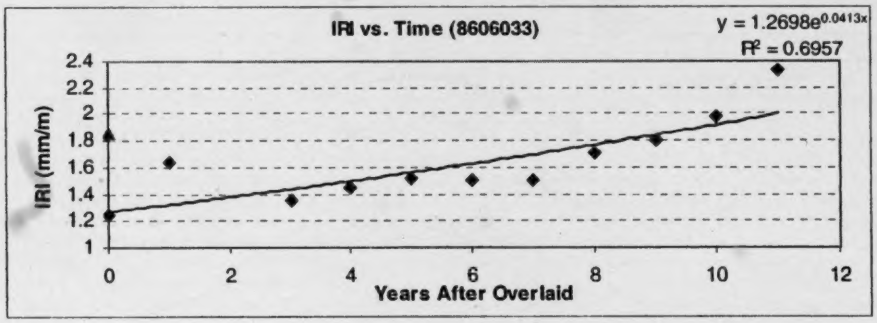
IRI vs. Time (8606033)
y = 1.2698e^0.0413x
R² = 0.6957
IRI (mm/m)
2.4
2.2
2
1.8
1.6
1.4
1.2
1
0
2
4
6
8
10
12
Years After Overlaid

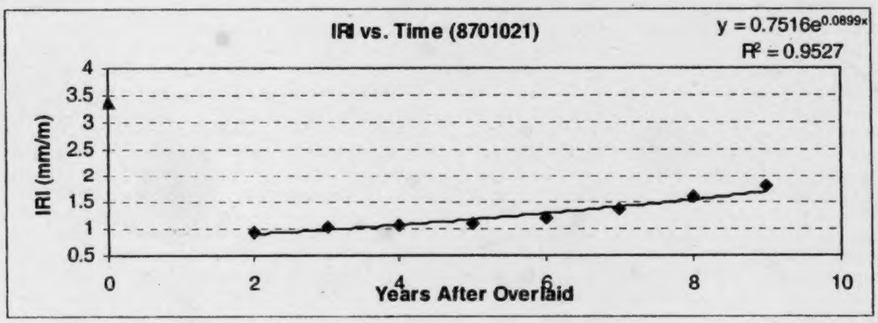
IRI vs. Time (8701021)
y = 0.7516e^0.0899x
R² = 0.9527
IRI (mm/m)
4
3.5
3
2.5
2
1.5
1
0.5
0
2
4
6
8
10
Years After Overlaid

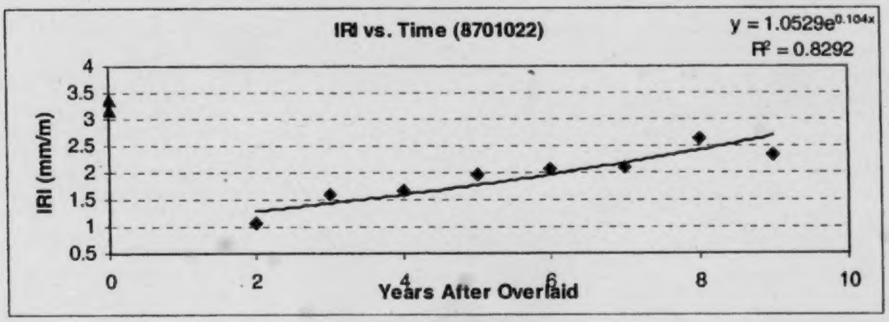
IRI vs. Time (8701022)
y = 1.0529e^0.104x
R² = 0.8292
IRI (mm/m)
4
3.5
3
2.5
2
1.5
1
0.5
0
2
4
6
8
10
Years After Overlaid

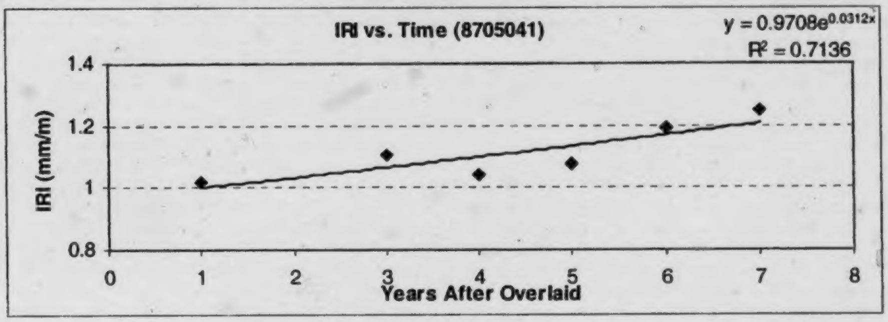
IRI vs. Time (8705041)
y = 0.9708e^0.0312x
R² = 0.7136
IRI (mm/m)
1.4
1.2
1
0.8
0
1
2
3
4
5
6
7
8
Years After Overlaid

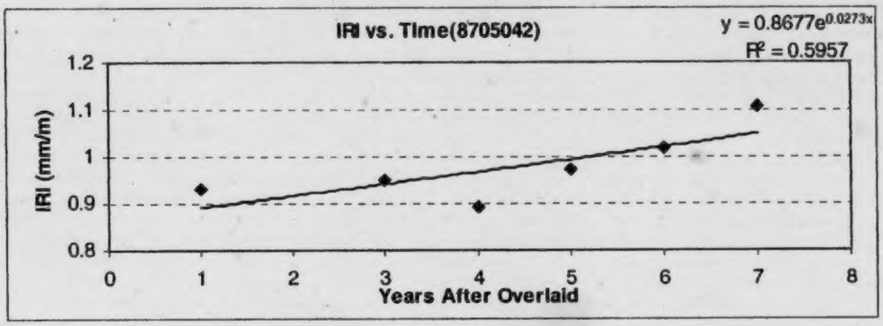
IRI vs. Time(8705042)
y = 0.8677e^0.0273x
R² = 0.5957
IRI (mm/m)
1.2
1.1
1
0.9
0.8
0
1
2
3
4
5
6
7
8
Years After Overlaid

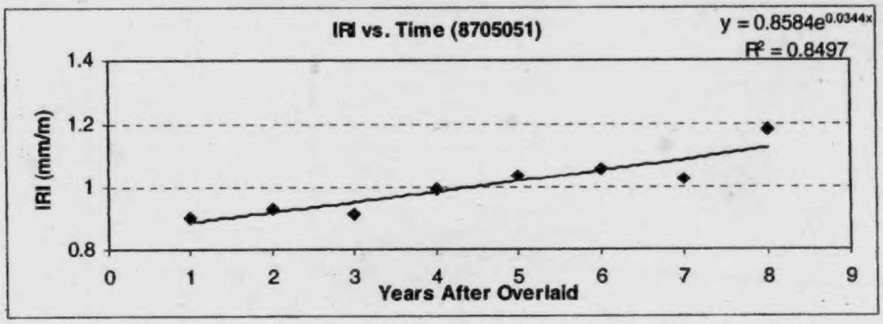
IRI vs. Time (8705051)
y = 0.8584e^0.0344x
R² = 0.8497
IRI (mm/m)
1.4
1.2
1
0.8
0
1
2
3
4
5
6
7
8
9
Years After Overlaid

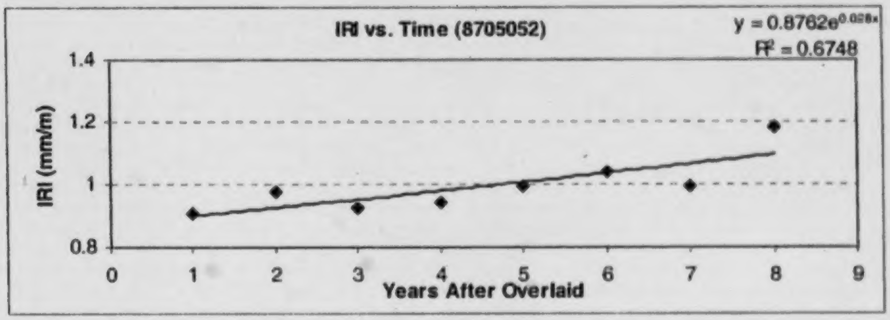
IRI vs. Time (8705052)
$y = 0.8762e^{0.028x}$
$R^2 = 0.6748$
IRI (mm/m)
1.4
1.2
1
0.8
0
1
2
3
4
5
6
7
8
9
Years After Overlaid

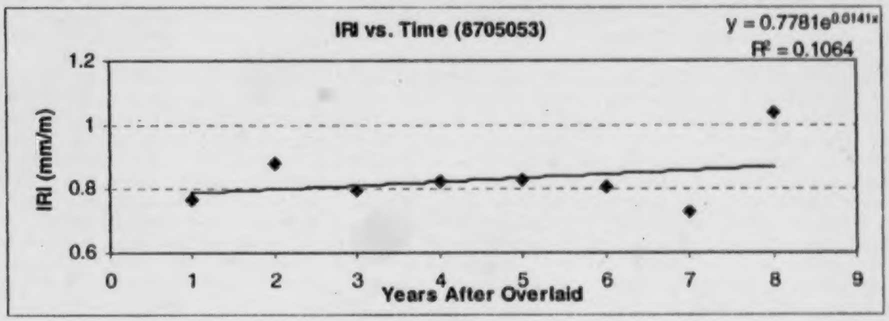
IRI vs. Time (8705053)
$y = 0.7781e^{0.0141x}$
$R^2 = 0.1064$
IRI (mm/m)
1.2
1
0.8
0.6
0
1
2
3
4
5
6
7
8
9
Years After Overlaid

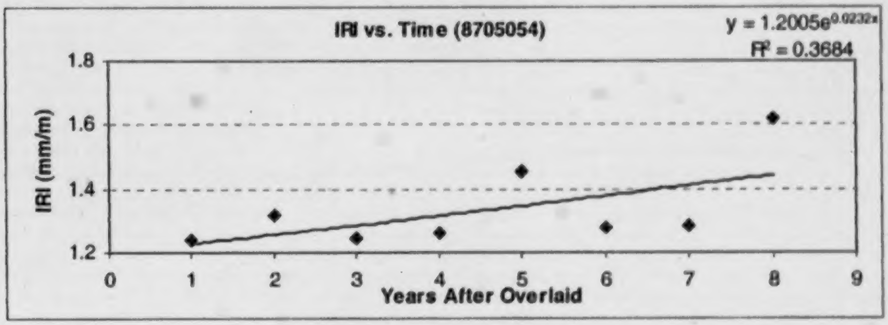
IRI vs. Time (8705054)
$y = 1.2005e^{0.0232x}$
$R^2 = 0.3684$
IRI (mm/m)
1.8
1.6
1.4
1.2
0
1
2
3
4
5
6
7
8
9
Years After Overlaid

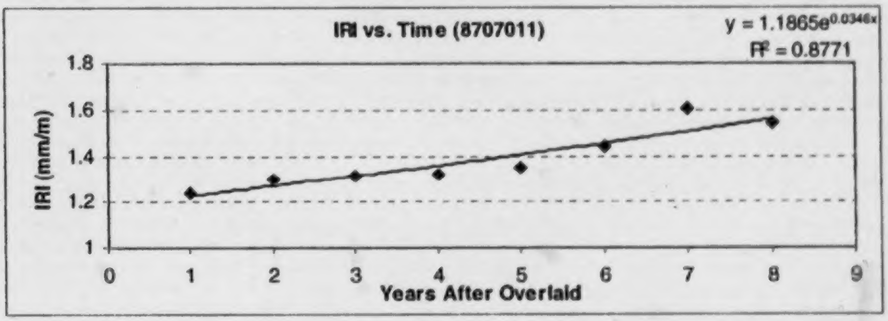
IRI vs. Time (8707011)
$y = 1.1865e^{0.0346x}$
$R^2 = 0.8771$
IRI (mm/m)
1.8
1.6
1.4
1.2
1
0
1
2
3
4
5
6
7
8
9
Years After Overlaid

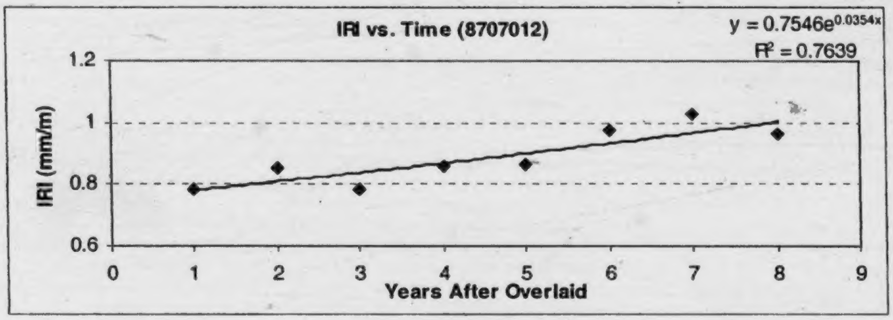
IRI vs. Time (8707012)
y = 0.7546e^0.0354x
R² = 0.7639
IRI (mm/m)
1.2
1
0.8
0.6
0
1
2
3
4
5
6
7
8
9
Years After Overlaid

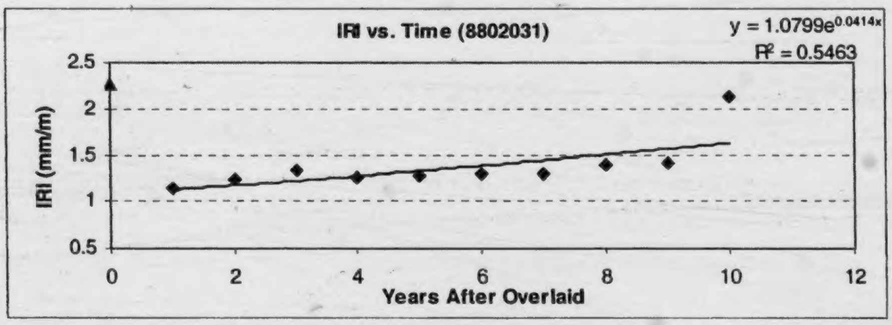
IRI vs. Time (8802031)
y = 1.0799e^0.0414x
R² = 0.5463
IRI (mm/m)
2.5
2
1.5
1
0.5
0
2
4
6
8
10
12
Years After Overlaid

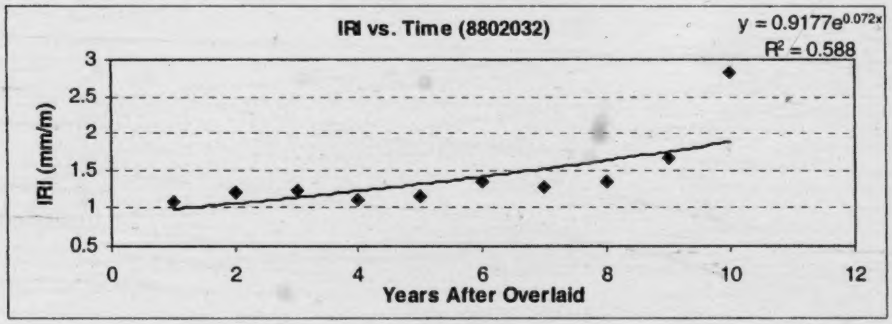
IRI vs. Time (8802032)
y = 0.9177e^0.072x
R² = 0.588
IRI (mm/m)
3
2.5
2
1.5
1
0.5
0
2
4
6
8
10
12
Years After Overlaid

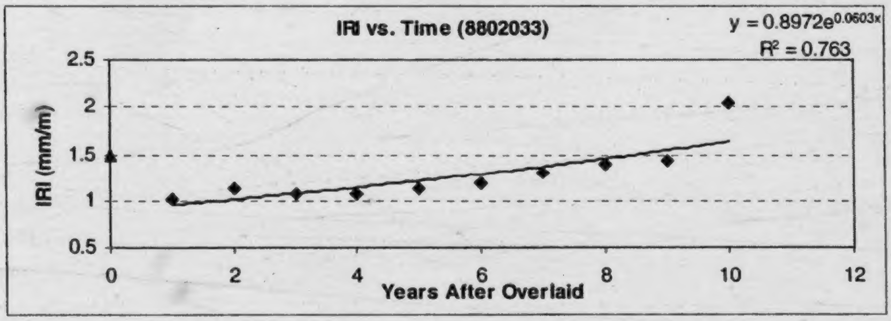
IRI vs. Time (8802033)
y = 0.8972e^0.0603x
R² = 0.763
IRI (mm/m)
2.5
2
1.5
1
0.5
0
2
4
6
8
10
12
Years After Overlaid

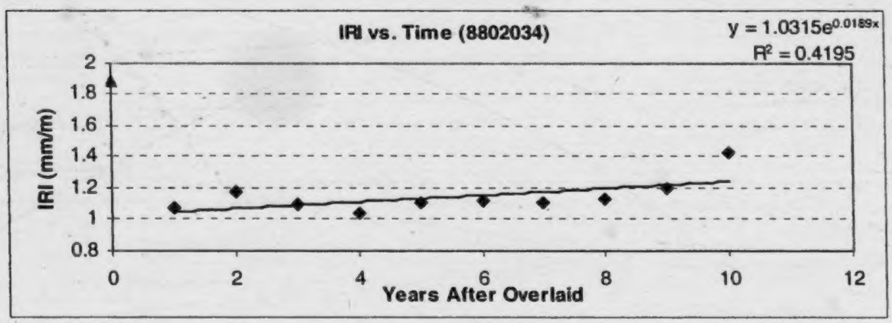
IRI vs. Time (8802034)
$y = 1.0315e^{0.0189x}$
$R^2 = 0.4195$
IRI (mm/m)
2
1.8
1.6
1.4
1.2
1
0.8
0
2
4
6
8
10
12
Years After Overlaid

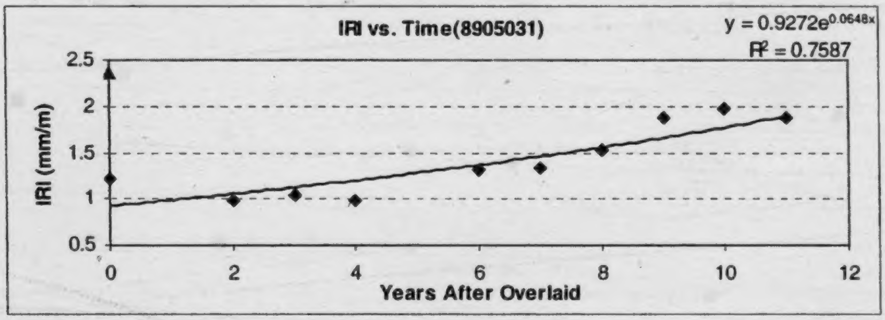
IRI vs. Time(8905031)
$y = 0.9272e^{0.0648x}$
$R^2 = 0.7587$
IRI (mm/m)
2.5
2
1.5
1
0.5
0
2
4
6
8
10
12
Years After Overlaid

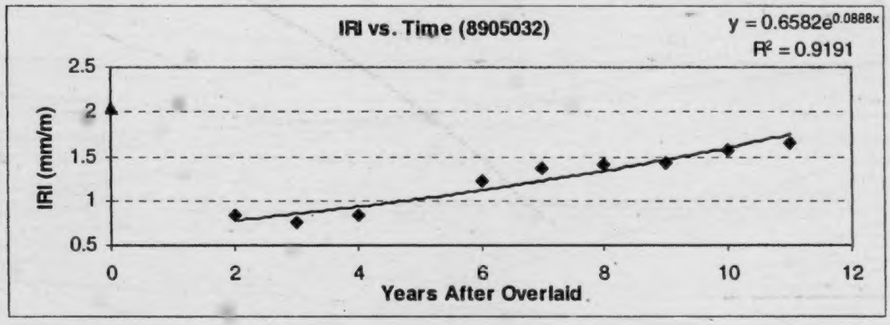
IRI vs. Time (8905032)
$y = 0.6582e^{0.0888x}$
$R^2 = 0.9191$
IRI (mm/m)
2.5
2
1.5
1
0.5
0
2
4
6
8
10
12
Years After Overlaid

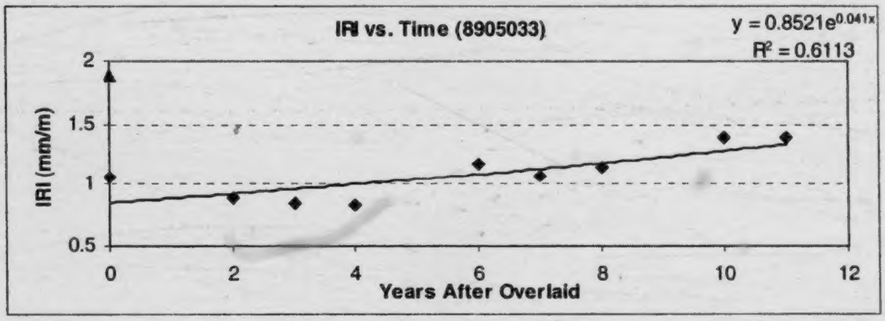
IRI vs. Time (8905033)
$y = 0.8521e^{0.041x}$
$R^2 = 0.6113$
IRI (mm/m)
2
1.5
1
0.5
0
2
4
6
8
10
12
Years After Overlaid

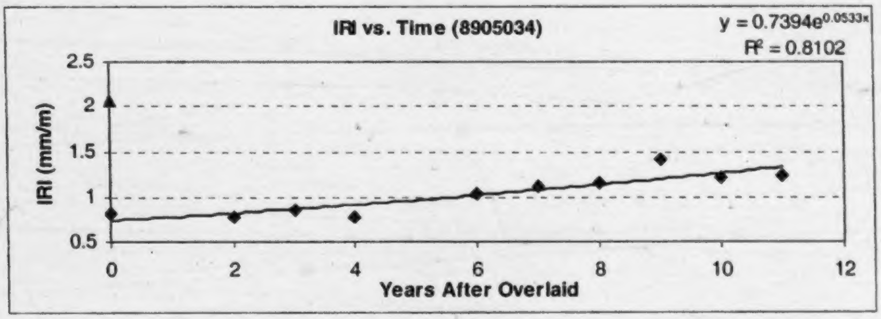
IRI vs. Time (8905034)
y = 0.7394e^0.0533x
R² = 0.8102
IRI (mm/m)
2.5
2
1.5
1
0.5
0
2
4
6
8
10
12
Years After Overlaid

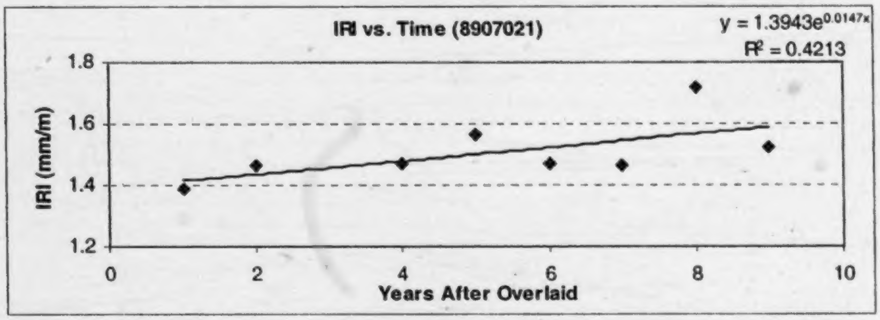
IRI vs. Time (8907021)
y = 1.3943e^0.0147x
R² = 0.4213
IRI (mm/m)
1.8
1.6
1.4
1.2
0
2
4
6
8
10
Years After Overlaid

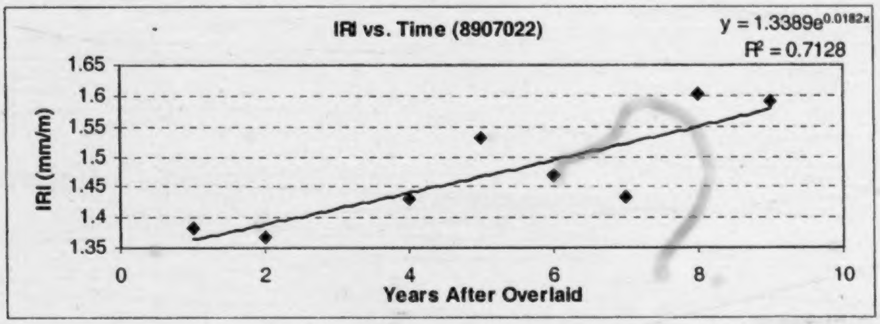
IRI vs. Time (8907022)
y = 1.3389e^0.0182x
R² = 0.7128
IRI (mm/m)
1.65
1.6
1.55
1.5
1.45
1.4
1.35
0
2
4
6
8
10
Years After Overlaid

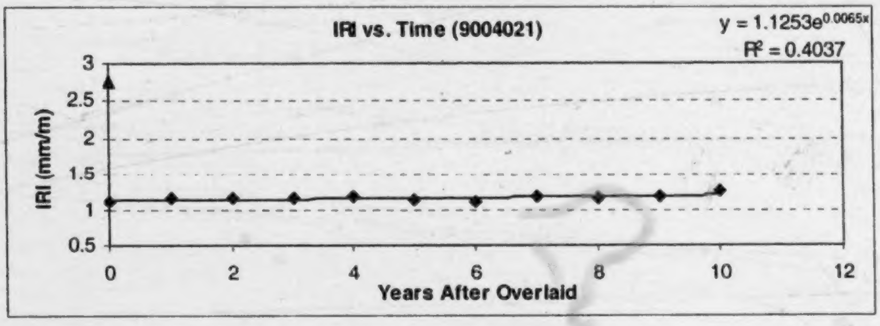
IRI vs. Time (9004021)
y = 1.1253e^0.0065x
R² = 0.4037
IRI (mm/m)
3
2.5
2
1.5
1
0.5
0
2
4
6
8
10
12
Years After Overlaid

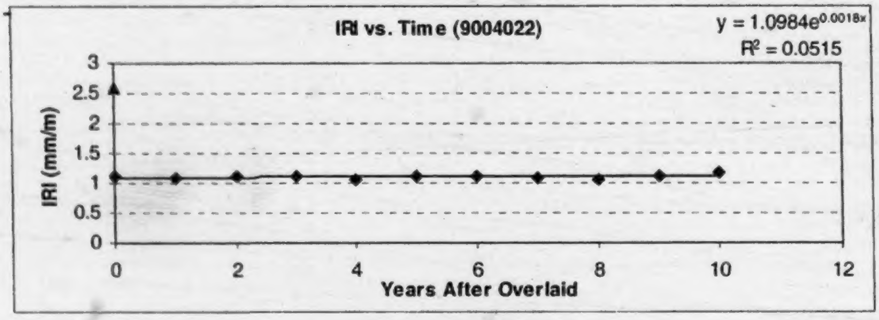
IRI vs. Time (9004022)
y = 1.0984e^0.0018x
R² = 0.0515
IRI (mm/m)
0
0.5
1
1.5
2
2.5
3
0
2
4
6
8
10
12
Years After Overlaid

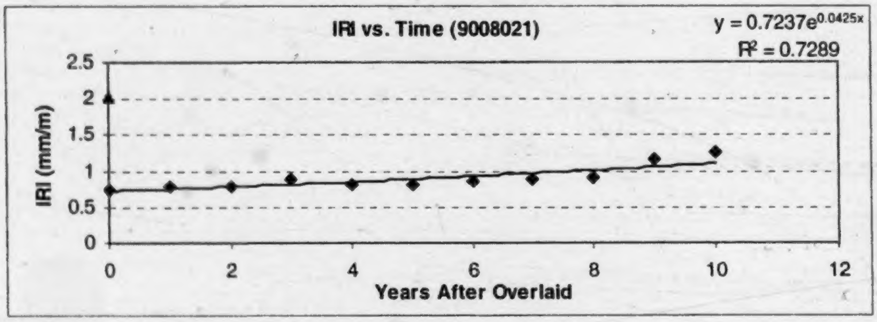
IRI vs. Time (9008021)
y = 0.7237e^0.0425x
R² = 0.7289
IRI (mm/m)
0
0.5
1
1.5
2
2.5
0
2
4
6
8
10
12
Years After Overlaid

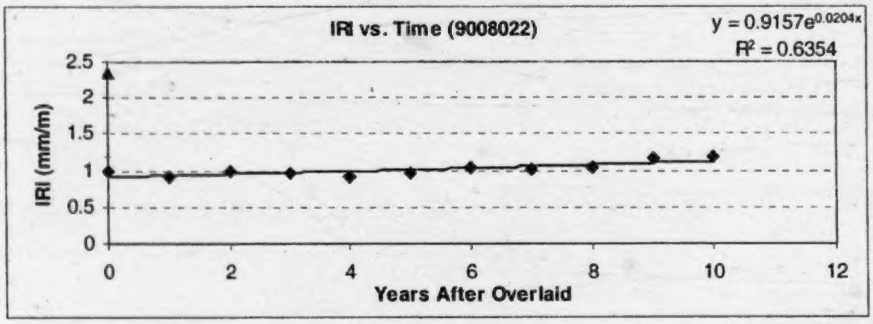
IRI vs. Time (9008022)
y = 0.9157e^0.0204x
R² = 0.6354
IRI (mm/m)
0
0.5
1
1.5
2
2.5
0
2
4
6
8
10
12
Years After Overlaid

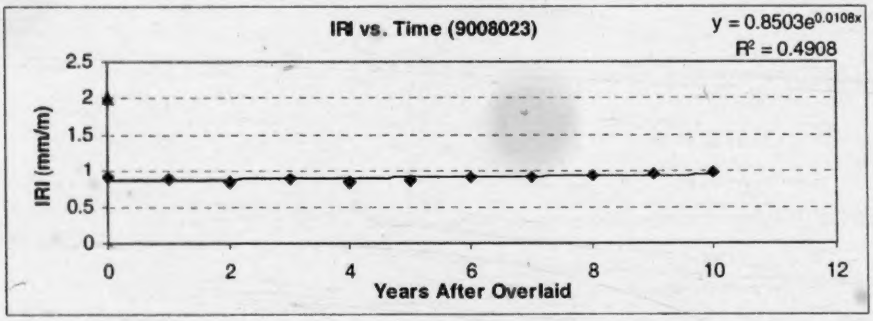
IRI vs. Time (9008023)
y = 0.8503e^0.0108x
R² = 0.4908
IRI (mm/m)
0
0.5
1
1.5
2
2.5
0
2
4
6
8
10
12
Years After Overlaid

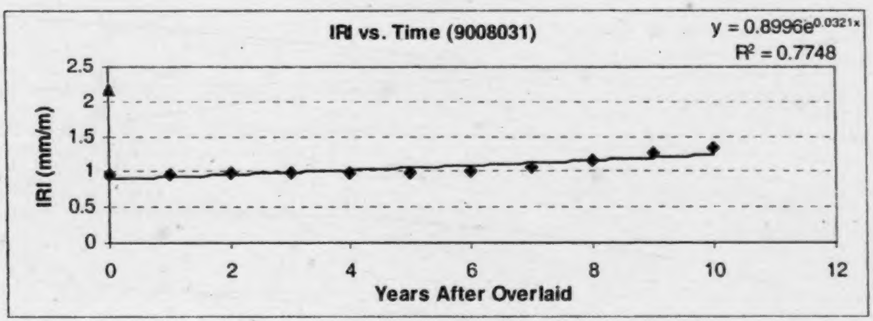
IRI vs. Time (9008031)
y = 0.8996e^0.0321x
R² = 0.7748
IRI (mm/m)
2.5
2
1.5
1
0.5
0
0
2
4
6
8
10
12
Years After Overlaid

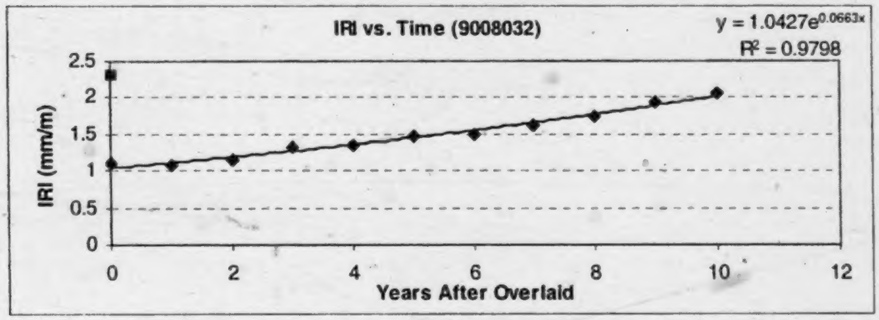
IRI vs. Time (9008032)
y = 1.0427e^0.0663x
R² = 0.9798
IRI (mm/m)
2.5
2
1.5
1
0.5
0
0
2
4
6
8
10
12
Years After Overlaid

Appendix G: Rutting trends in the C-LTPP project

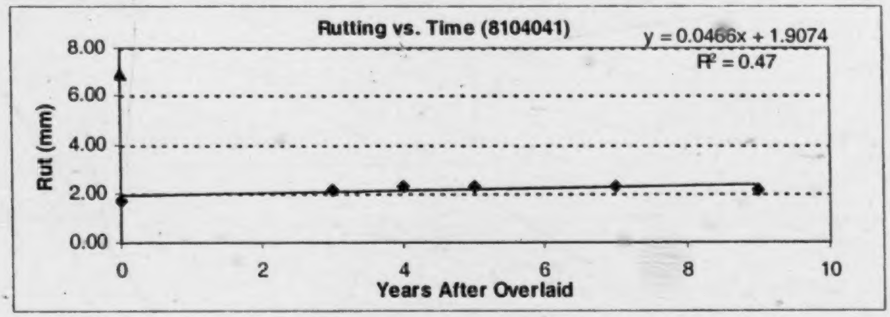

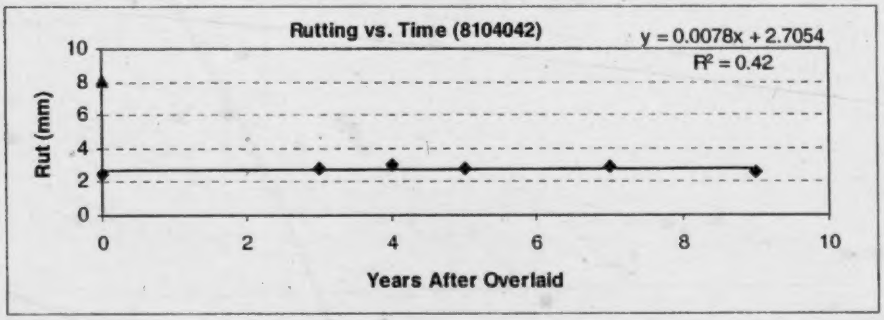

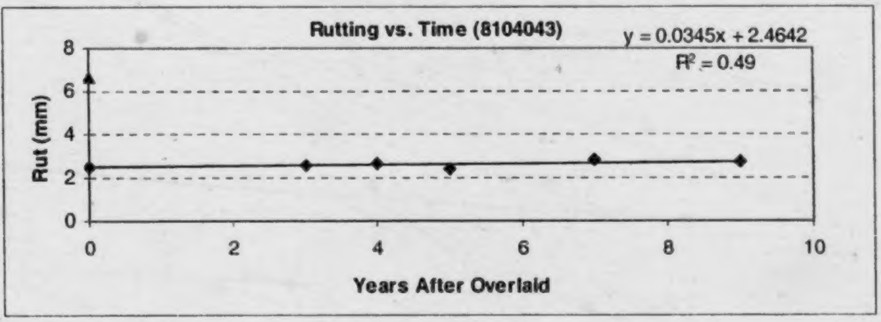

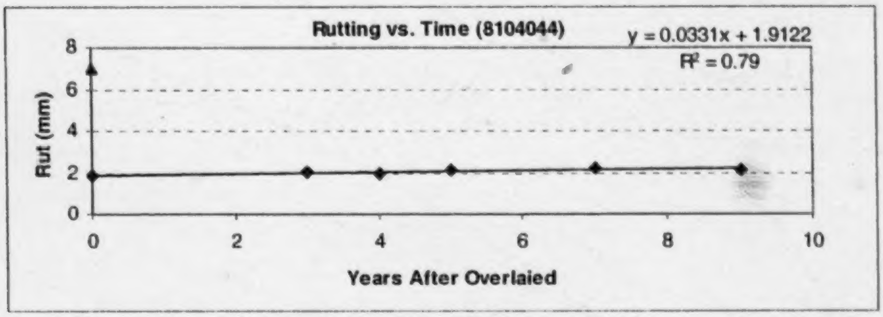
Rutting vs. Time (8104044)
y = 0.0331x + 1.9122
R^2 = 0.79
Rut (mm)
0
2
4
6
8
0
2
4
6
8
10
Years After Overlaied

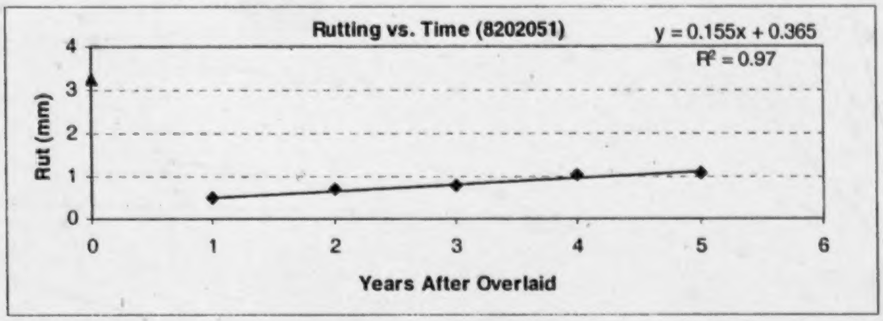
Rutting vs. Time (8202051)
y = 0.155x + 0.365
R^2 = 0.97
Rut (mm)
0
1
2
3
4
0
1
2
3
4
5
6
Years After Overlaid

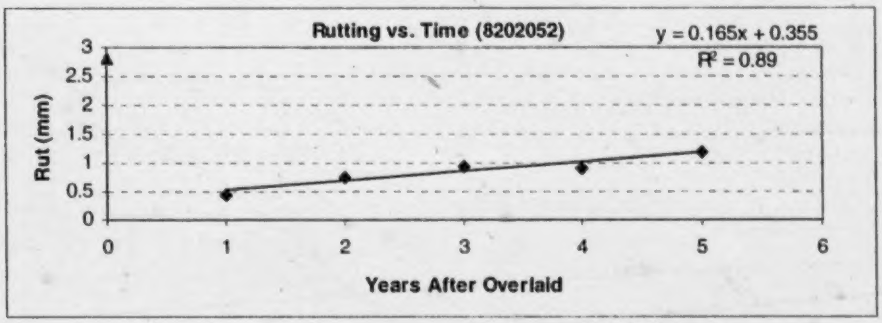
Rutting vs. Time (8202052)
y = 0.165x + 0.355
R^2 = 0.89
Rut (mm)
0
0.5
1
1.5
2
2.5
3
0
1
2
3
4
5
6
Years After Overlaid

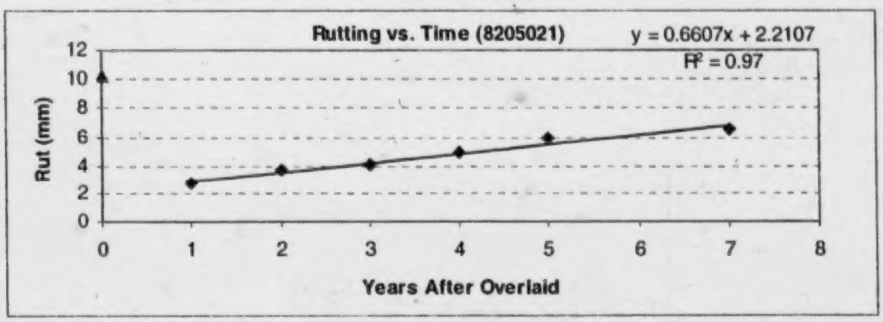
Rutting vs. Time (8205021)
y = 0.6607x + 2.2107
R^2 = 0.97
Rut (mm)
0
2
4
6
8
10
12
0
1
2
3
4
5
6
7
8
Years After Overlaid

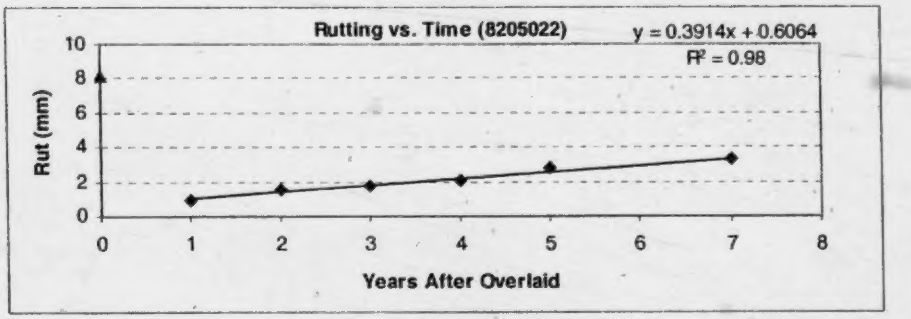
Rutting vs. Time (8205022)
y = 0.3914x + 0.6064
R² = 0.98
Rut (mm)
10
8
6
4
2
0
0
1
2
3
4
5
6
7
8
Years After Overlaid

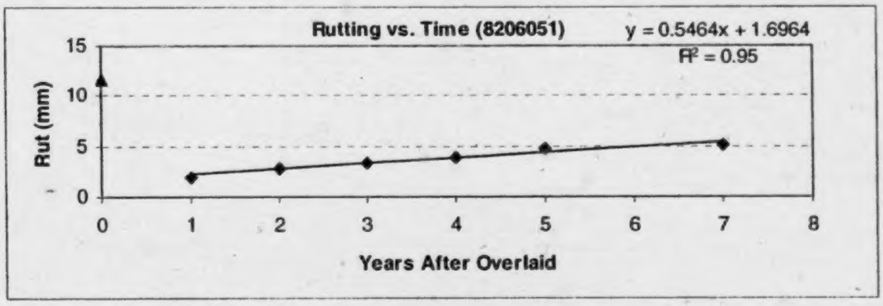
Rutting vs. Time (8206051)
y = 0.5464x + 1.6964
R² = 0.95
Rut (mm)
15
10
5
0
0
1
2
3
4
5
6
7
8
Years After Overlaid

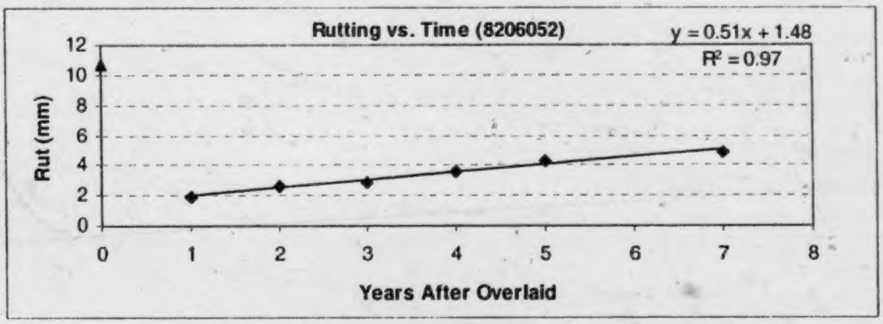
Rutting vs. Time (8206052)
y = 0.51x + 1.48
R² = 0.97
Rut (mm)
12
10
8
6
4
2
0
0
1
2
3
4
5
6
7
8
Years After Overlaid

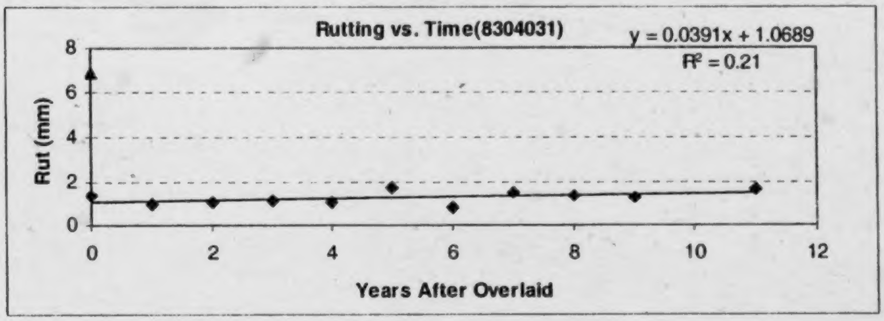
Rutting vs. Time(8304031)
y = 0.0391x + 1.0689
R² = 0.21
Rut (mm)
8
6
4
2
0
0
2
4
6
8
10
12
Years After Overlaid

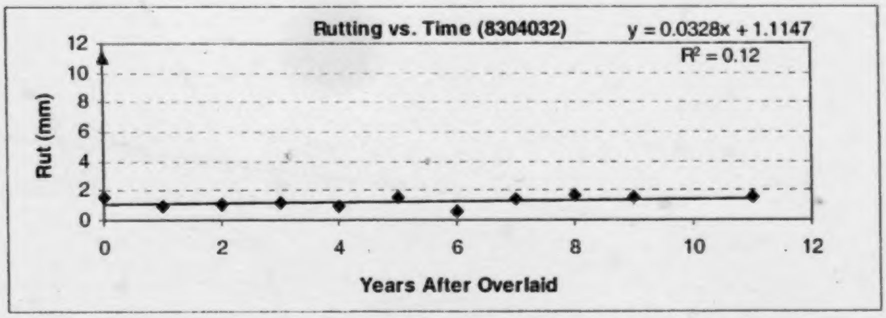
Rutting vs. Time (8304032)
y = 0.0328x + 1.1147
R² = 0.12
Rut (mm)
0
2
4
6
8
10
12
Years After Overlaid
0
2
4
6
8
10
12

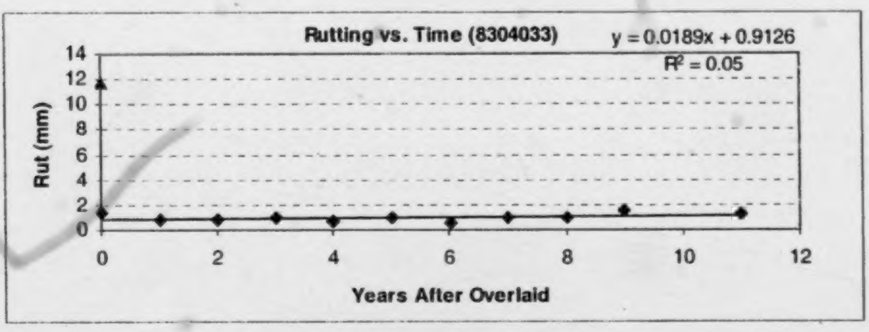
Rutting vs. Time (8304033)
y = 0.0189x + 0.9126
R² = 0.05
Rut (mm)
0
2
4
6
8
10
12
14
Years After Overlaid
0
2
4
6
8
10
12

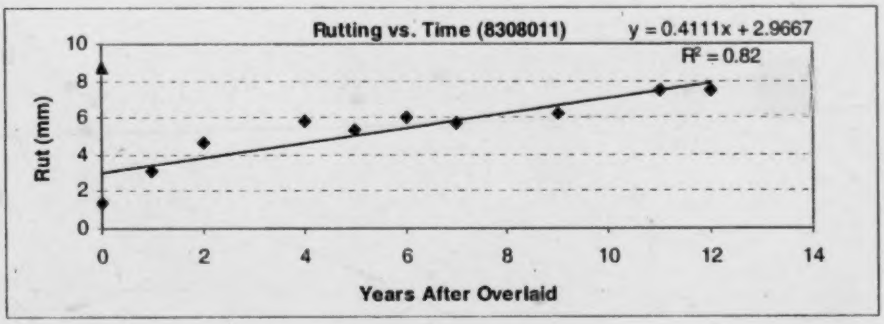
Rutting vs. Time (8308011)
y = 0.4111x + 2.9667
R² = 0.82
Rut (mm)
0
2
4
6
8
10
Years After Overlaid
0
2
4
6
8
10
12
14

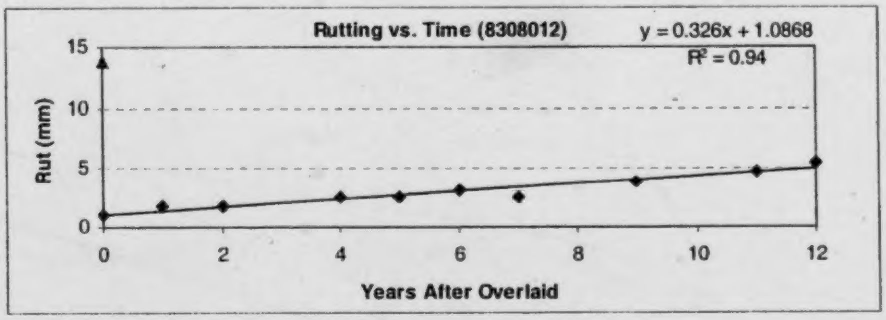
Rutting vs. Time (8308012)
y = 0.326x + 1.0868
R² = 0.94
Rut (mm)
0
5
10
15
Years After Overlaid
0
2
4
6
8
10
12

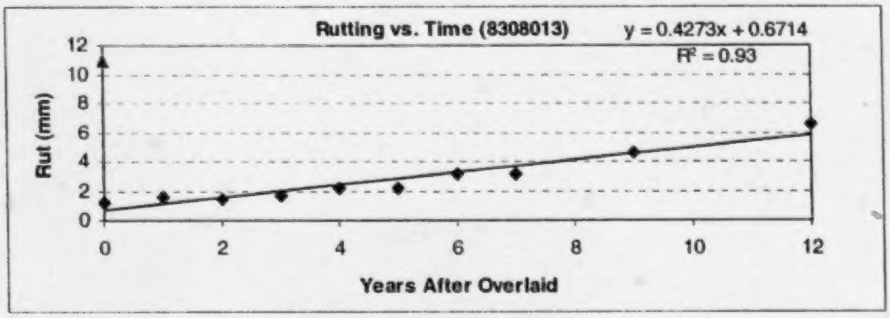
Rutting vs. Time (8308013)
y = 0.4273x + 0.6714
R² = 0.93
Rut (mm)
0
2
4
6
8
10
12
Years After Overlaid
0
2
4
6
8
10
12

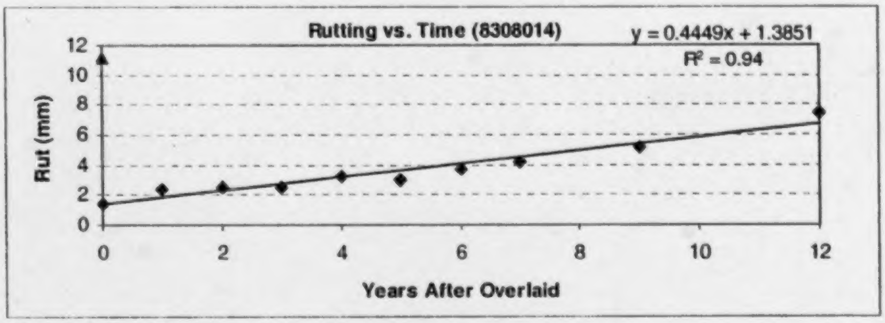
Rutting vs. Time (8308014)
y = 0.4449x + 1.3851
R² = 0.94
Rut (mm)
0
2
4
6
8
10
12
Years After Overlaid
0
2
4
6
8
10
12

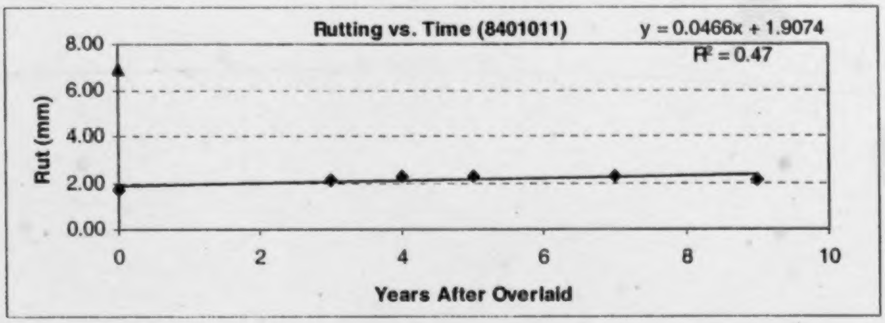
Rutting vs. Time (8401011)
y = 0.0466x + 1.9074
R² = 0.47
Rut (mm)
0.00
2.00
4.00
6.00
8.00
Years After Overlaid
0
2
4
6
8
10

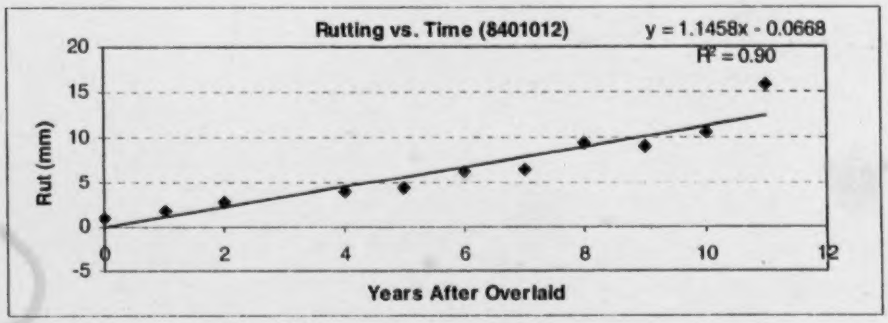
Rutting vs. Time (8401012)
y = 1.1458x - 0.0668
R² = 0.90
Rut (mm)
-5
0
5
10
15
20
Years After Overlaid
0
2
4
6
8
10
12

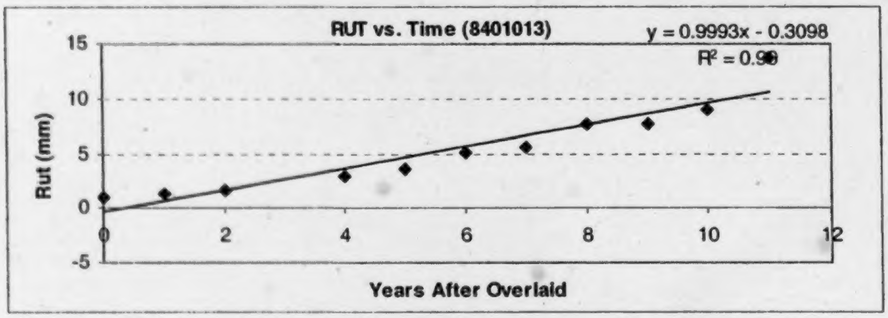
RUT vs. Time (8401013)
y = 0.9993x - 0.3098
R² = 0.96
15
10
5
0
-5
Rut (mm)
0
2
4
6
8
10
12
Years After Overlaid

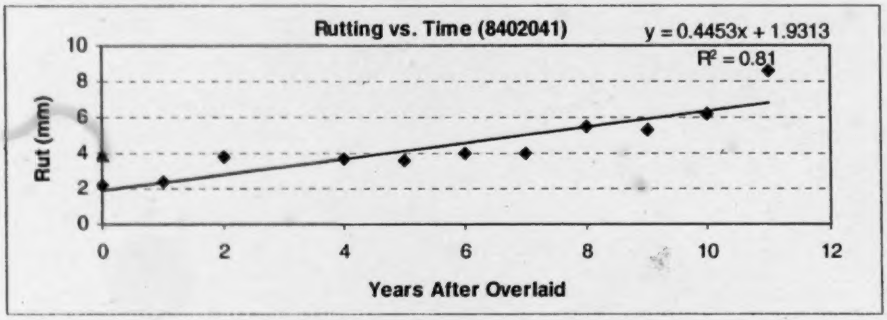
Rutting vs. Time (8402041)
y = 0.4453x + 1.9313
R² = 0.81
10
8
6
4
2
0
Rut (mm)
0
2
4
6
8
10
12
Years After Overlaid

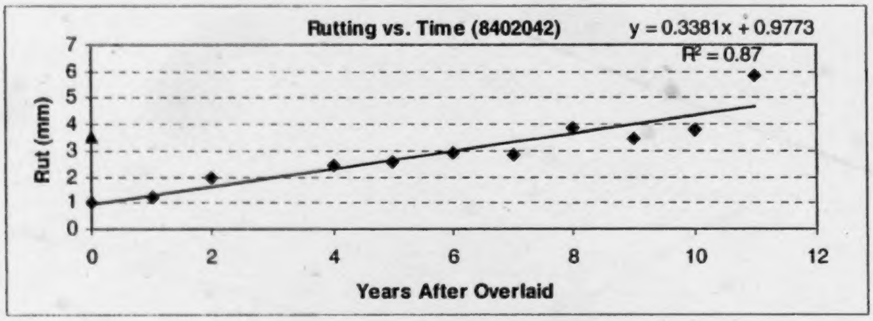
Rutting vs. Time (8402042)
y = 0.3381x + 0.9773
R² = 0.87
7
6
5
4
3
2
1
0
Rut (mm)
0
2
4
6
8
10
12
Years After Overlaid

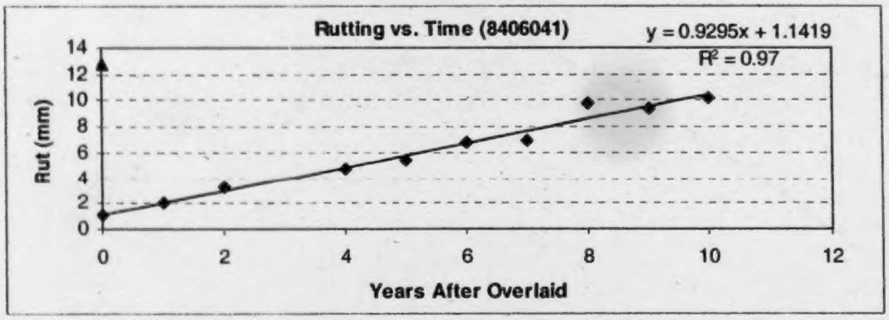
Rutting vs. Time (8406041)
y = 0.9295x + 1.1419
R² = 0.97
14
12
10
8
6
4
2
0
Rut (mm)
0
2
4
6
8
10
12
Years After Overlaid

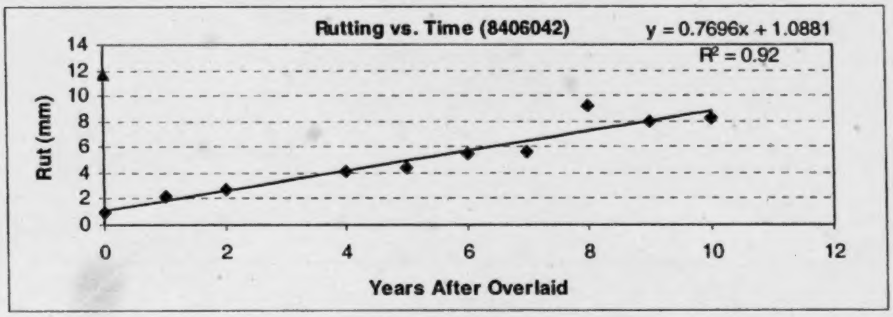
Rutting vs. Time (8406042)
y = 0.7696x + 1.0881
R² = 0.92
Rut (mm)
14
12
10
8
6
4
2
0
0
2
4
6
8
10
12
Years After Overlaid

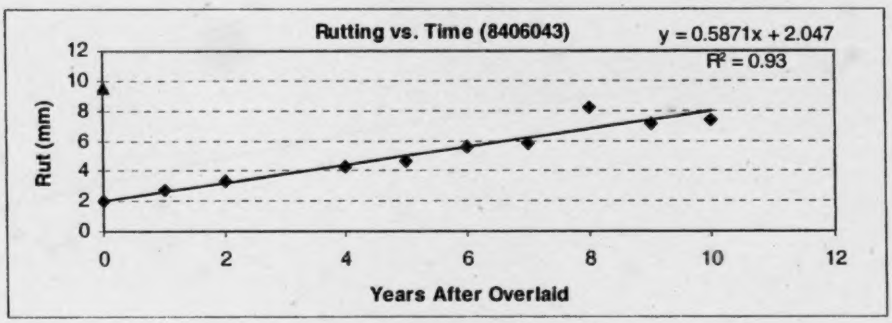
Rutting vs. Time (8406043)
y = 0.5871x + 2.047
R² = 0.93
Rut (mm)
12
10
8
6
4
2
0
0
2
4
6
8
10
12
Years After Overlaid

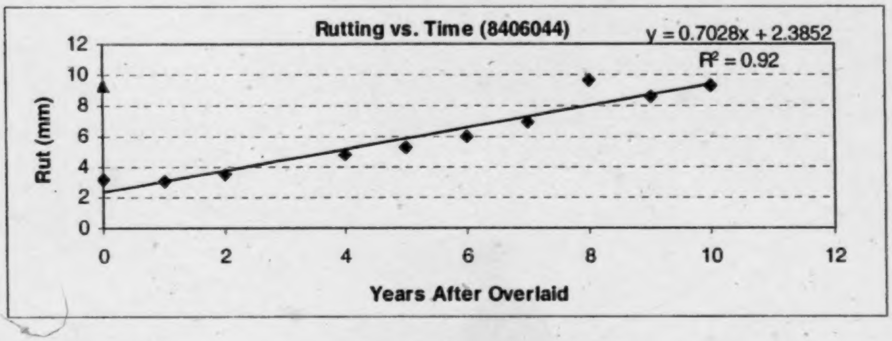
Rutting vs. Time (8406044)
y = 0.7028x + 2.3852
R² = 0.92
Rut (mm)
12
10
8
6
4
2
0
0
2
4
6
8
10
12
Years After Overlaid

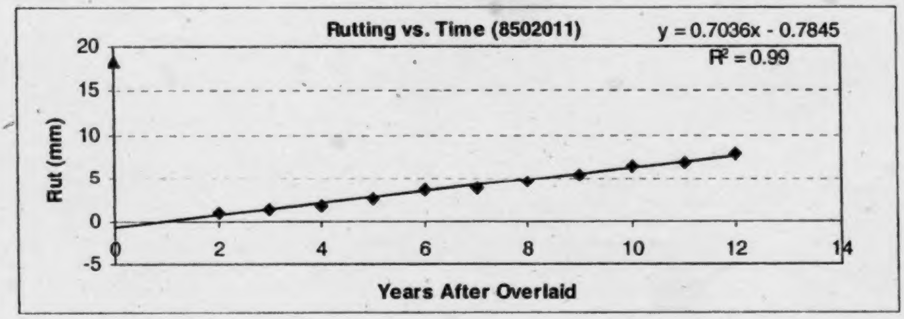
Rutting vs. Time (8502011)
y = 0.7036x - 0.7845
R² = 0.99
Rut (mm)
20
15
10
5
0
-5
0
2
4
6
8
10
12
14
Years After Overlaid

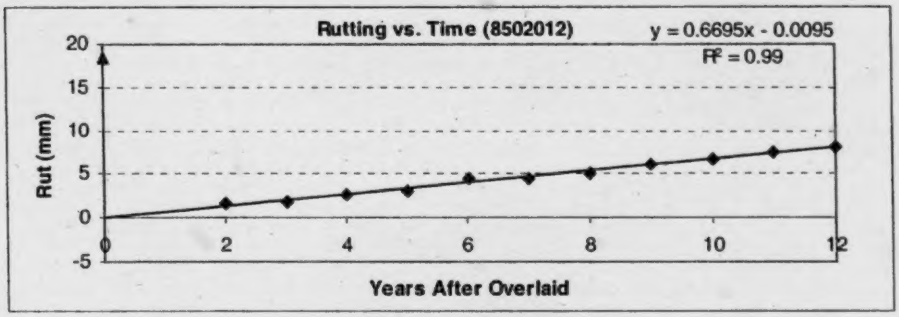
Rutting vs. Time (8502012)
y = 0.6695x - 0.0095
R² = 0.99
Rut (mm)
20
15
10
5
0
-5
0
2
4
6
8
10
12
Years After Overlaid

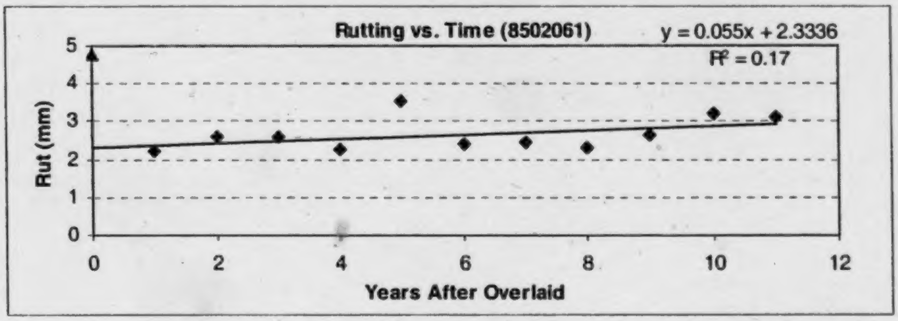
Rutting vs. Time (8502061)
y = 0.055x + 2.3336
R² = 0.17
Rut (mm)
5
4
3
2
1
0
0
2
4
6
8
10
12
Years After Overlaid

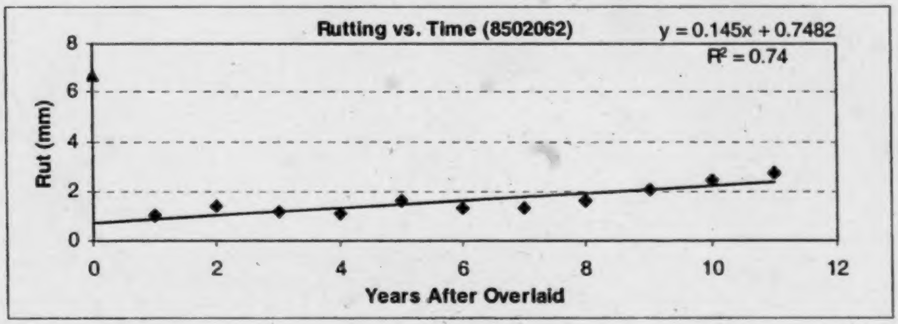
Rutting vs. Time (8502062)
y = 0.145x + 0.7482
R² = 0.74
Rut (mm)
8
6
4
2
0
0
2
4
6
8
10
12
Years After Overlaid

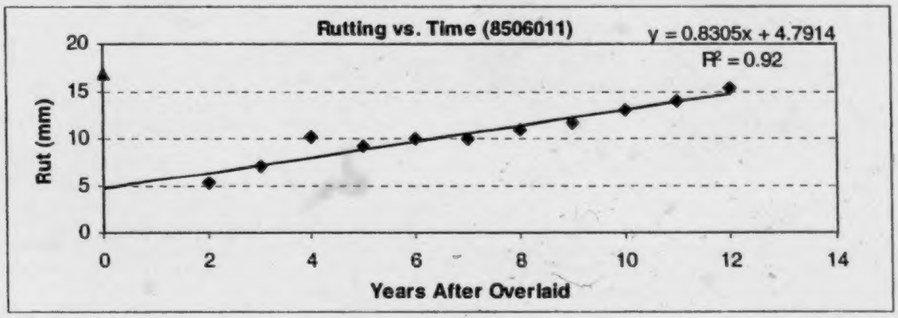
Rutting vs. Time (8506011)
y = 0.8305x + 4.7914
R² = 0.92
Rut (mm)
20
15
10
5
0
0
2
4
6
8
10
12
14
Years After Overlaid

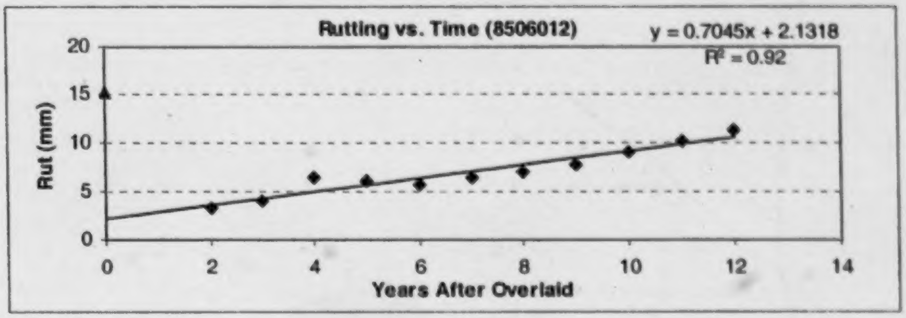
Rutting vs. Time (8506012)
y = 0.7045x + 2.1318
R^2 = 0.92
Rut (mm)
0
5
10
15
20
0
2
4
6
8
10
12
14
Years After Overlaid

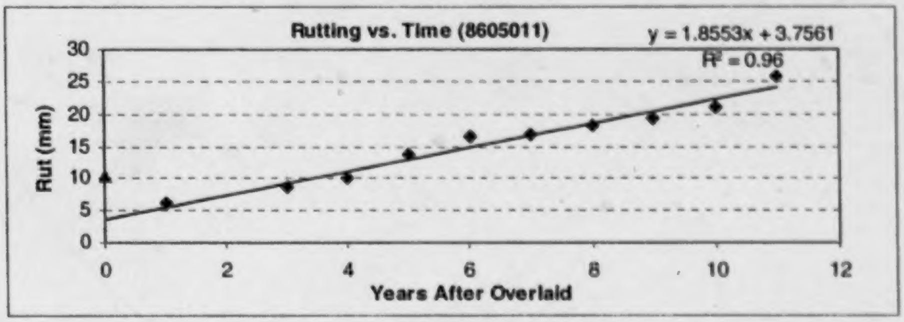
Rutting vs. Time (8605011)
y = 1.8553x + 3.7561
R^2 = 0.96
Rut (mm)
0
5
10
15
20
25
30
0
2
4
6
8
10
12
Years After Overlaid

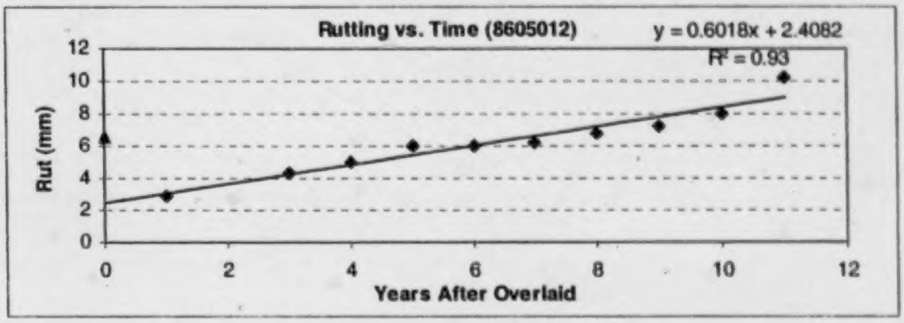
Rutting vs. Time (8605012)
y = 0.6018x + 2.4082
R^2 = 0.93
Rut (mm)
0
2
4
6
8
10
12
0
2
4
6
8
10
12
Years After Overlaid

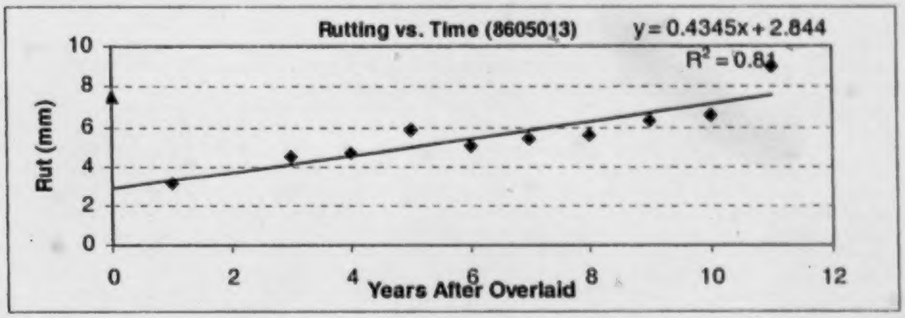
Rutting vs. Time (8605013)
y = 0.4345x + 2.844
R^2 = 0.81
Rut (mm)
0
2
4
6
8
10
0
2
4
6
8
10
12
Years After Overlaid

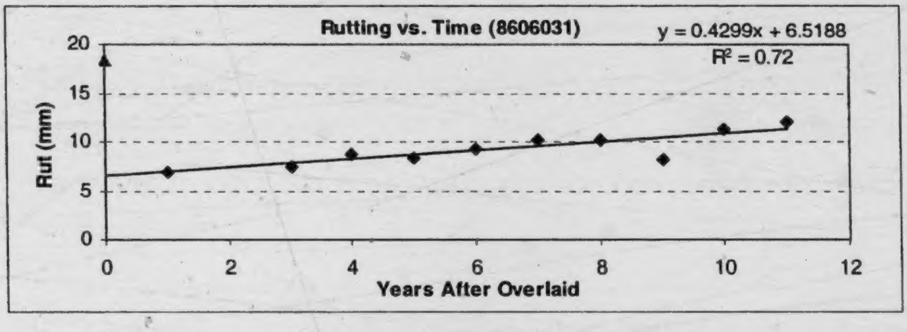
Rutting vs. Time (8606031)
y = 0.4299x + 6.5188
R² = 0.72
Rut (mm)
0
5
10
15
20
0
2
4
6
8
10
12
Years After Overlaid

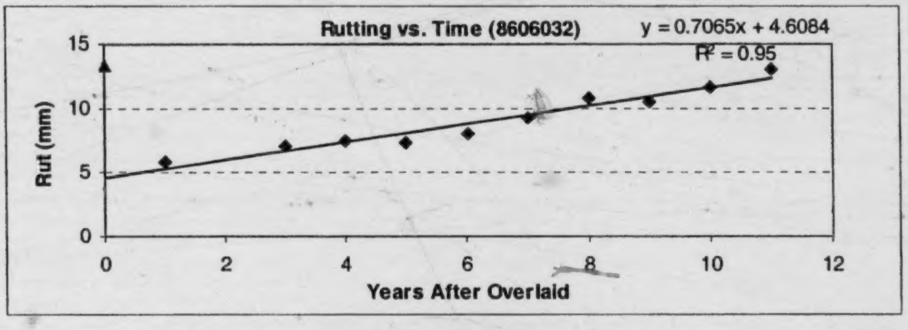
Rutting vs. Time (8606032)
y = 0.7065x + 4.6084
R² = 0.95
Rut (mm)
0
5
10
15
0
2
4
6
8
10
12
Years After Overlaid

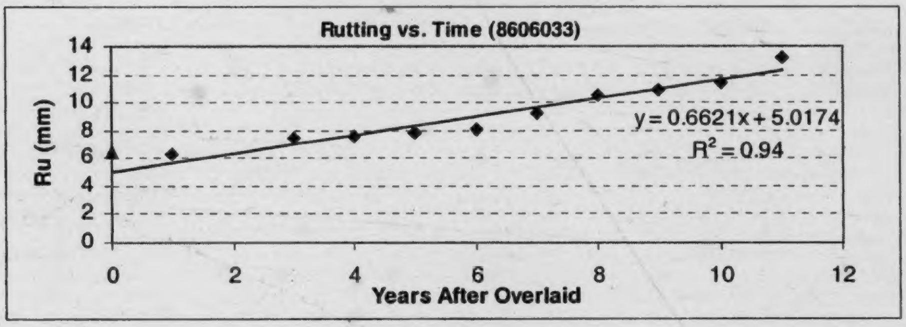
Rutting vs. Time (8606033)
y = 0.6621x + 5.0174
R² = 0.94
Ru (mm)
0
2
4
6
8
10
12
14
0
2
4
6
8
10
12
Years After Overlaid

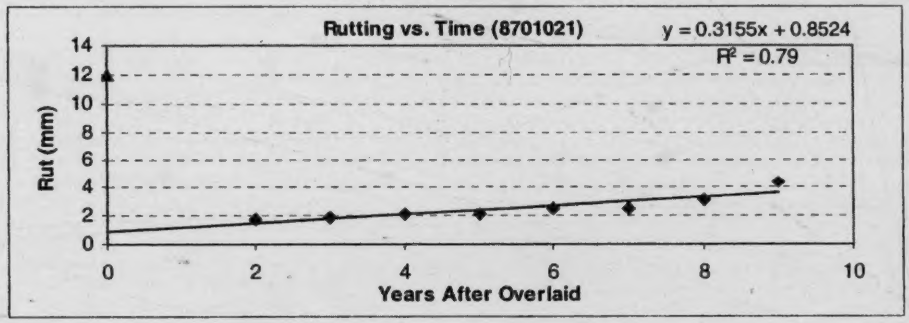
Rutting vs. Time (8701021)
y = 0.3155x + 0.8524
R² = 0.79
Rut (mm)
0
2
4
6
8
10
12
14
0
2
4
6
8
10
Years After Overlaid

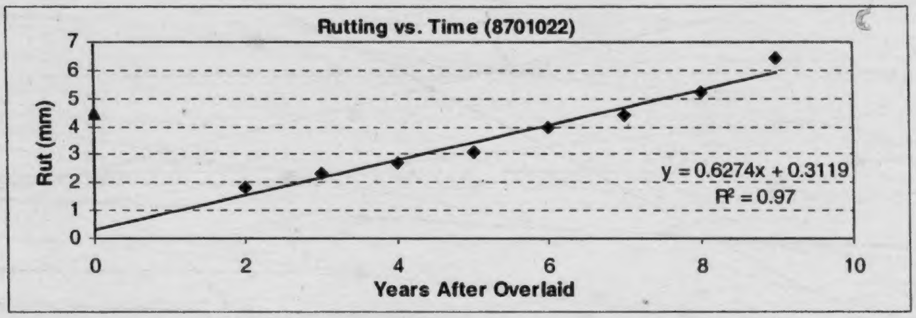
Rutting vs. Time (8701022)
Rut (mm)
0
1
2
3
4
5
6
7
y = 0.6274x + 0.3119
R² = 0.97
0
2
4
6
8
10
Years After Overlaid

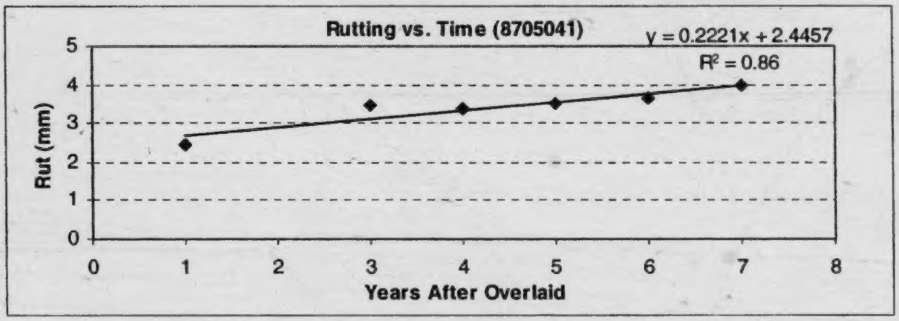
Rutting vs. Time (8705041)
y = 0.2221x + 2.4457
R² = 0.86
Rut (mm)
0
1
2
3
4
5
0
1
2
3
4
5
6
7
8
Years After Overlaid

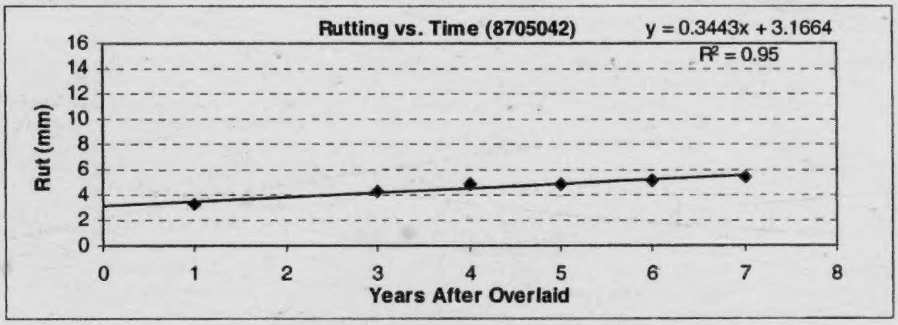
Rutting vs. Time (8705042)
y = 0.3443x + 3.1664
R² = 0.95
Rut (mm)
0
2
4
6
8
10
12
14
16
0
1
2
3
4
5
6
7
8
Years After Overlaid

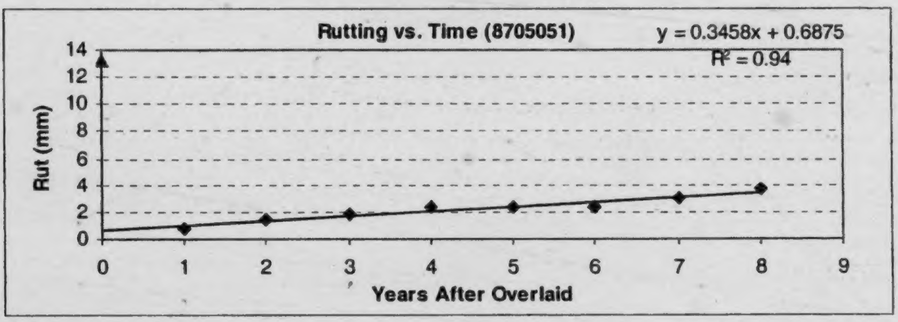
Rutting vs. Time (8705051)
y = 0.3458x + 0.6875
R² = 0.94
Rut (mm)
0
2
4
6
8
10
12
14
0
1
2
3
4
5
6
7
8
9
Years After Overlaid

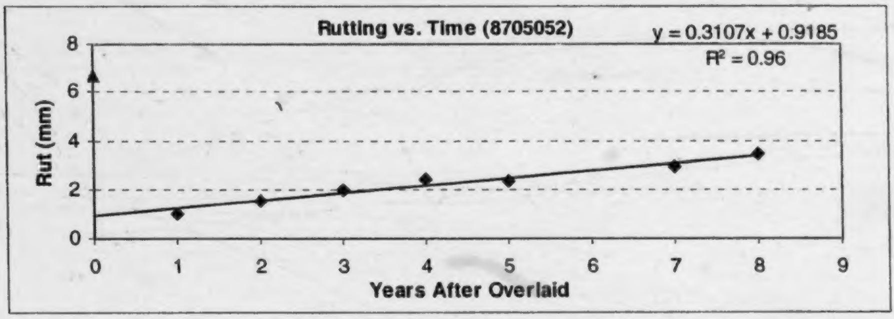
Rutting vs. Time (8705052)
y = 0.3107x + 0.9185
R^2 = 0.96
Rut (mm)
0
2
4
6
8
Years After Overlaid
0
1
2
3
4
5
6
7
8
9

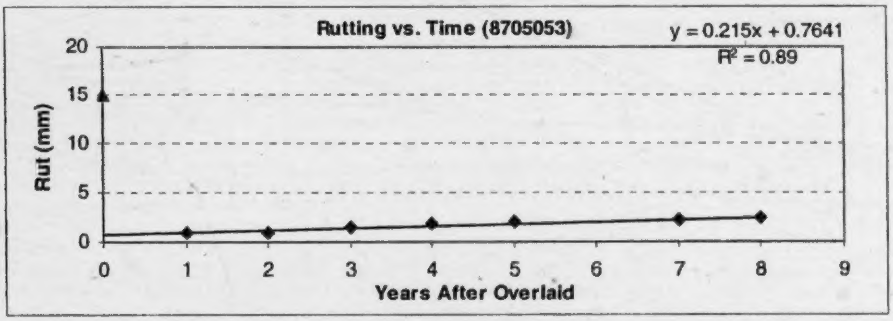
Rutting vs. Time (8705053)
y = 0.215x + 0.7641
R^2 = 0.89
Rut (mm)
0
5
10
15
20
Years After Overlaid
0
1
2
3
4
5
6
7
8
9

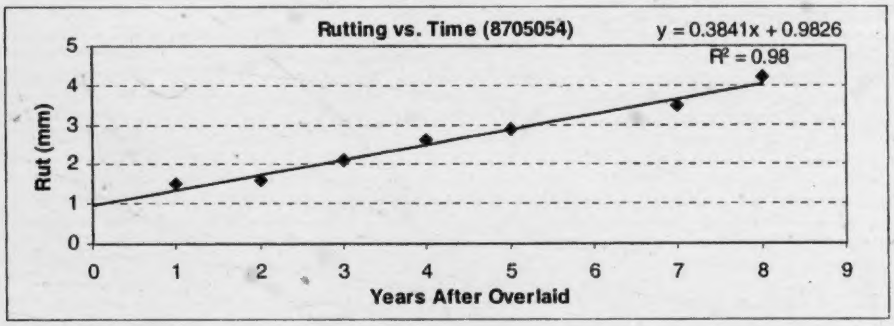
Rutting vs. Time (8705054)
y = 0.3841x + 0.9826
R^2 = 0.98
Rut (mm)
0
1
2
3
4
5
Years After Overlaid
0
1
2
3
4
5
6
7
8
9

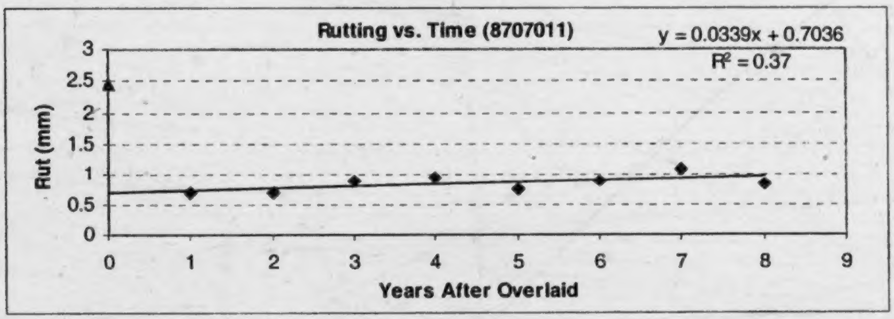
Rutting vs. Time (8707011)
y = 0.0339x + 0.7036
R^2 = 0.37
Rut (mm)
0
0.5
1
1.5
2
2.5
3
Years After Overlaid
0
1
2
3
4
5
6
7
8
9

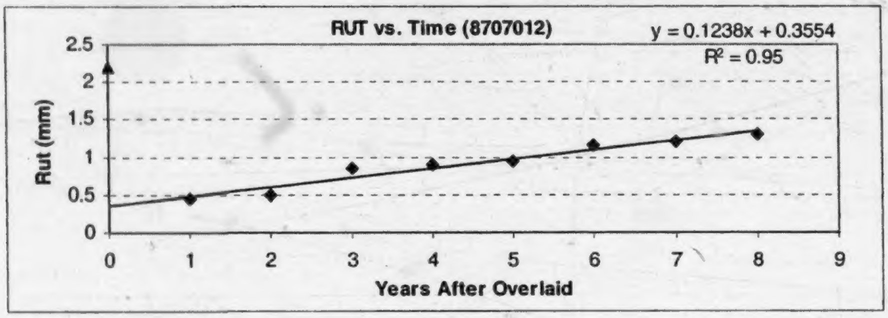
RUT vs. Time (8707012)
y = 0.1238x + 0.3554
$R^2 = 0.95$
Rut (mm)
0
0.5
1
1.5
2
2.5
Years After Overlaid
0
1
2
3
4
5
6
7
8
9

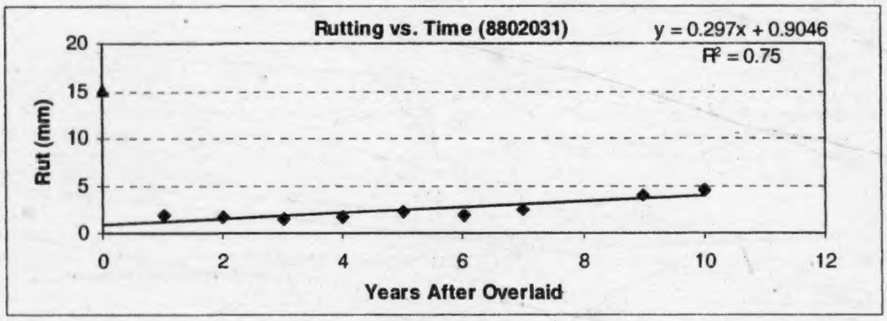
Rutting vs. Time (8802031)
y = 0.297x + 0.9046
$R^2 = 0.75$
Rut (mm)
0
5
10
15
20
Years After Overlaid
0
2
4
6
8
10
12

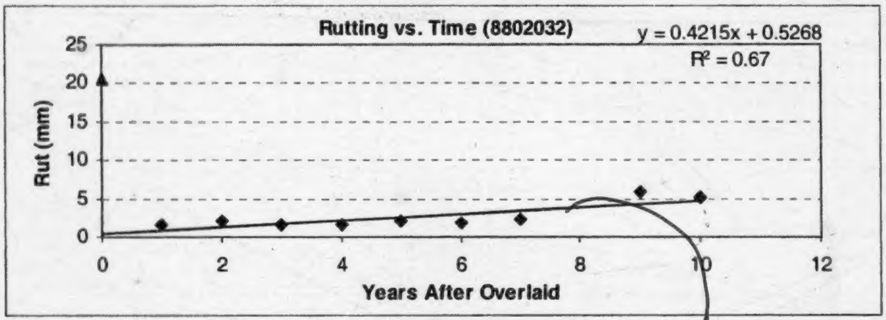
Rutting vs. Time (8802032)
y = 0.4215x + 0.5268
$R^2 = 0.67$
Rut (mm)
0
5
10
15
20
25
Years After Overlaid
0
2
4
6
8
10
12

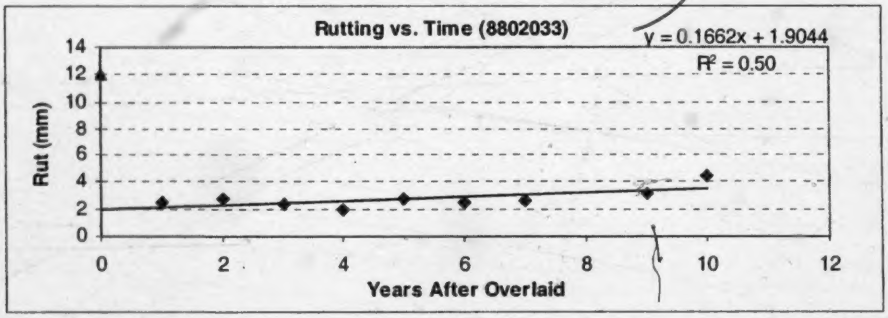
Rutting vs. Time (8802033)
y = 0.1662x + 1.9044
$R^2 = 0.50$
Rut (mm)
0
2
4
6
8
10
12
14
Years After Overlaid
0
2
4
6
8
10
12

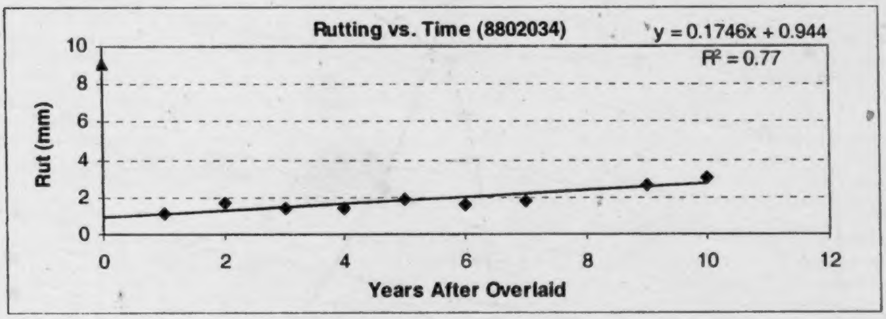
Rutting vs. Time (8802034)
y = 0.1746x + 0.944
R² = 0.77
Rut (mm)
0
2
4
6
8
10
Years After Overlaid
0
2
4
6
8
10
12

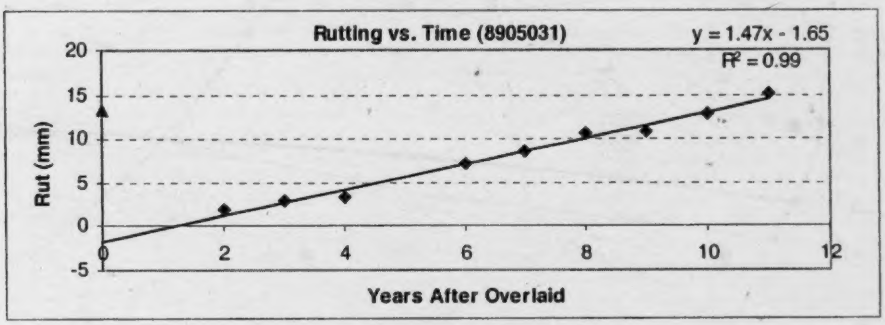
Rutting vs. Time (8905031)
y = 1.47x - 1.65
R² = 0.99
Rut (mm)
-5
0
5
10
15
20
Years After Overlaid
0
2
4
6
8
10
12

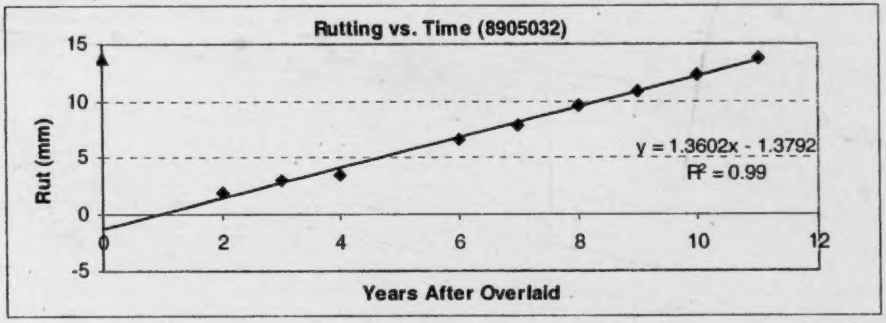
Rutting vs. Time (8905032)
y = 1.3602x - 1.3792
R² = 0.99
Rut (mm)
-5
0
5
10
15
Years After Overlaid
0
2
4
6
8
10
12

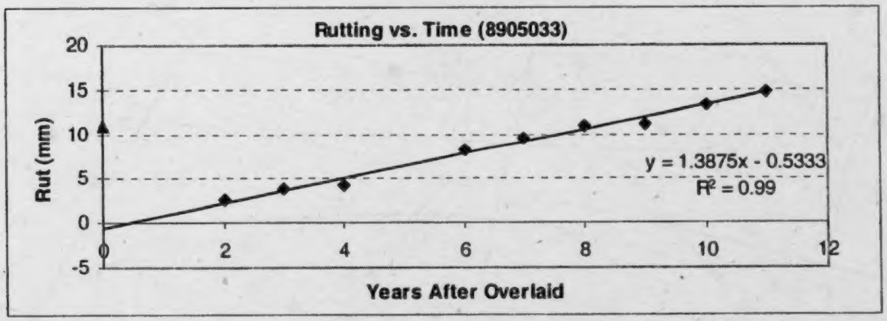
Rutting vs. Time (8905033)
y = 1.3875x - 0.5333
R² = 0.99
Rut (mm)
-5
0
5
10
15
20
Years After Overlaid
0
2
4
6
8
10
12

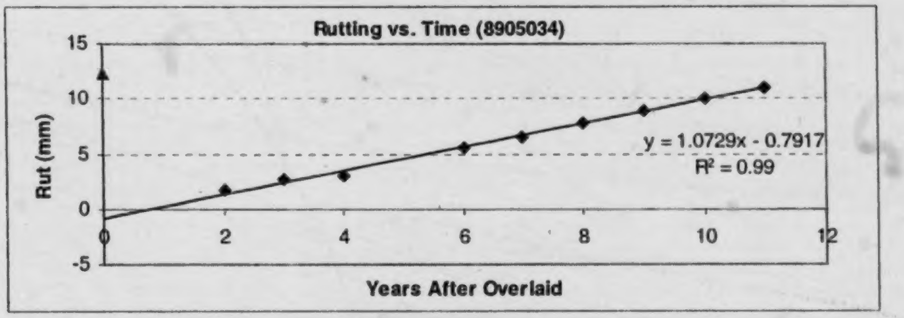
Rutting vs. Time (8905034)
Rut (mm)
15
10
5
0
-5
0
2
4
6
8
10
12
y = 1.0729x - 0.7917
R² = 0.99
Years After Overlaid

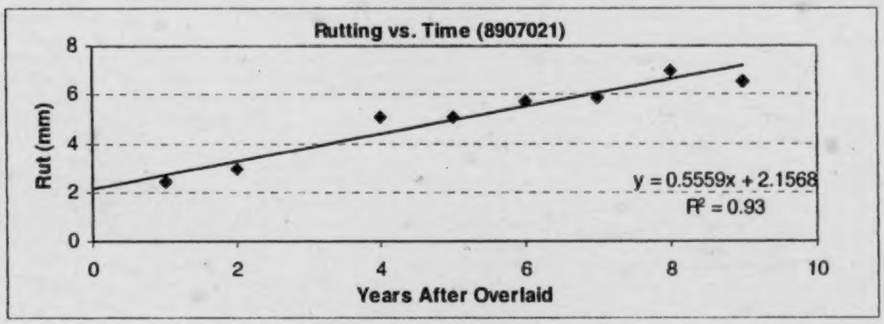
Rutting vs. Time (8907021)
Rut (mm)
8
6
4
2
0
0
2
4
6
8
10
y = 0.5559x + 2.1568
R² = 0.93
Years After Overlaid

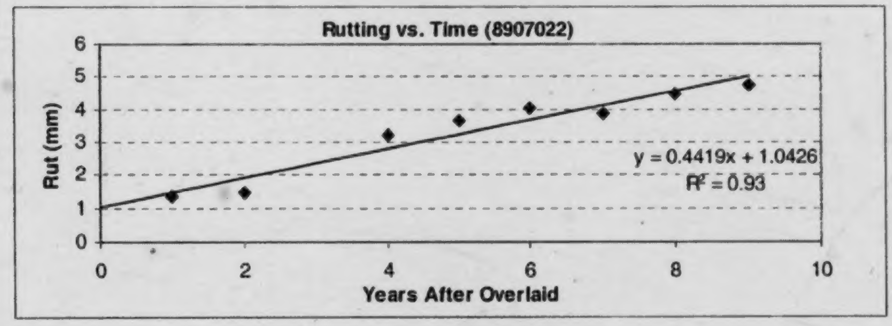
Rutting vs. Time (8907022)
Rut (mm)
6
5
4
3
2
1
0
0
2
4
6
8
10
y = 0.4419x + 1.0426
R² = 0.93
Years After Overlaid

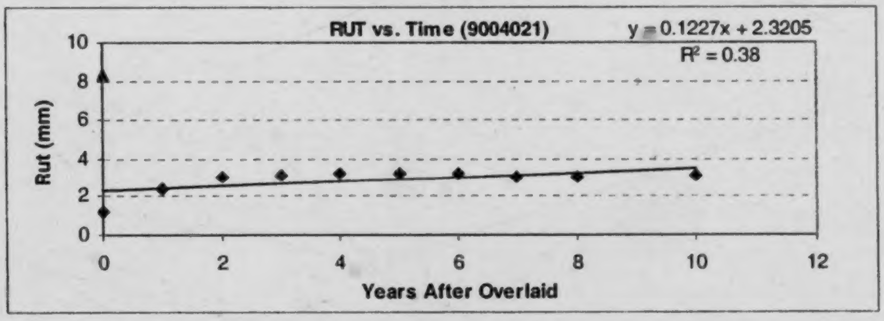
RUT vs. Time (9004021)
y = 0.1227x + 2.3205
R² = 0.38
Rut (mm)
10
8
6
4
2
0
0
2
4
6
8
10
12
Years After Overlaid

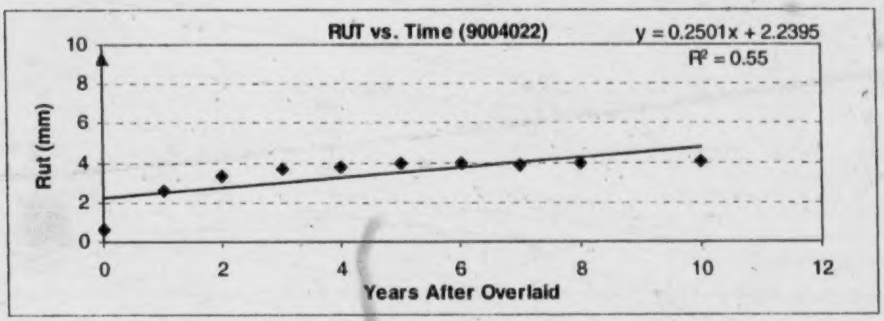
RUT vs. Time (9004022)
y = 0.2501x + 2.2395
R² = 0.55
Rut (mm)
Years After Overlaid
10
8
6
4
2
0
0
2
4
6
8
10
12

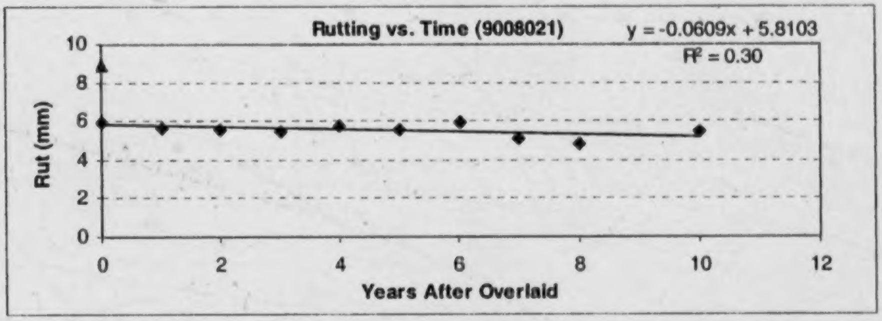
Rutting vs. Time (9008021)
y = -0.0609x + 5.8103
R² = 0.30
Rut (mm)
Years After Overlaid
10
8
6
4
2
0
0
2
4
6
8
10
12

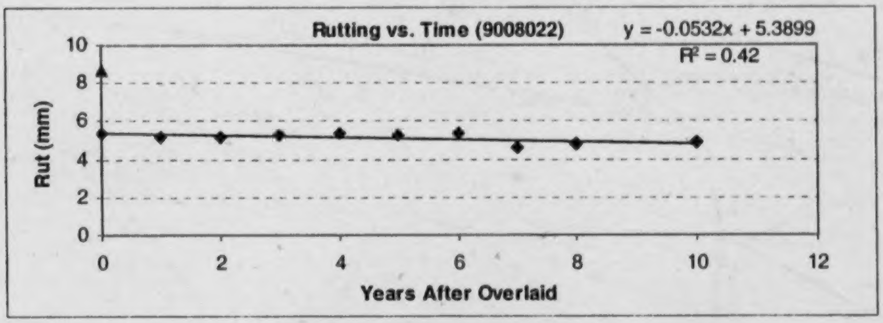
Rutting vs. Time (9008022)
y = -0.0532x + 5.3899
R² = 0.42
Rut (mm)
Years After Overlaid
10
8
6
4
2
0
0
2
4
6
8
10
12

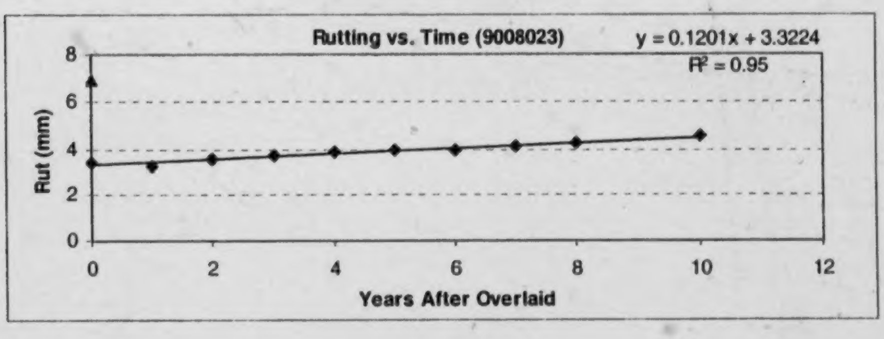
Rutting vs. Time (9008023)
y = 0.1201x + 3.3224
R² = 0.95
Rut (mm)
Years After Overlaid
8
6
4
2
0
0
2
4
6
8
10
12

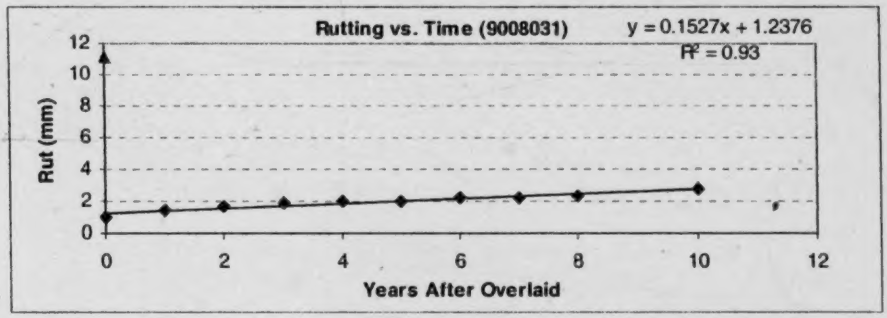
Rutting vs. Time (9008031)
y = 0.1527x + 1.2376
R² = 0.93
Rut (mm)
0
2
4
6
8
10
12
Years After Overlaid
0
2
4
6
8
10
12

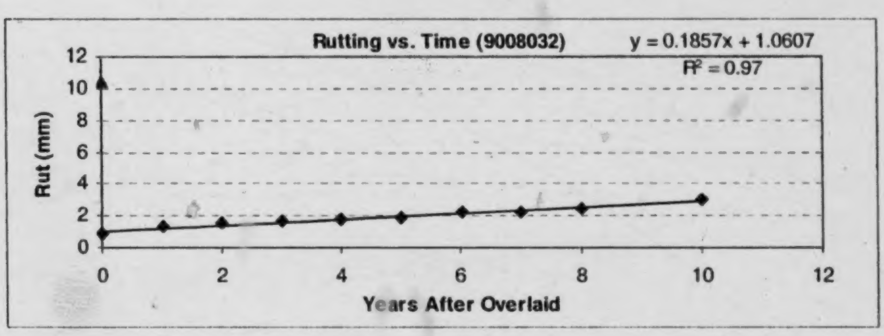
Rutting vs. Time (9008032)
y = 0.1857x + 1.0607
R² = 0.97
Rut (mm)
0
2
4
6
8
10
12
Years After Overlaid
0
2
4
6
8
10
12

Appendix H: The outputs from EVERSTRESS and ELSYM5 pavement analysis programs (Sample)

Sample of EVERSTRESS program outputs

```
CLayered Elastic Analysis by EverStress for Windows
Title: 8705051
No of Layers: 3  No of Loads:  1  No of X-Y Evaluation Points:  1
Layer   Poisson's          Thickness         Moduli(1)
*       Ratio     (in)     (ksi)
1       .35        6.600   313.00
2       .35       23.500    19.40
3       .40       *         17.00
Load NoX-Position          Y-Position        Load     Pressure Radius
*       (in)      (in)     (lbf)     (psi)   (in)
1        .00       .00     9000.0    74.53   6.200
Location No:  1  X-Position (in):   .000     Y-Position (in):   .000
cNormal Stresses
Z-Position         Layer   Sxx      Syy      Szz      Syz      Sxz      Sxy
(in)      *        (psi)   (psi)    (psi)    (psi)    (psi)    (psi)
 6.600    1         113.42  113.42  -16.57    .00      .00      .00
 30.100   3         -.03    -.03    -2.95     .00      .00      .00
cNormal Strains and Deflections
Z-Position         Layer   Exx      Eyy      Ezz      Ux       Uy       Uz
(in)      *        (10^-6) (10^-6)  (10^-6)  (mils)   (mils)   (mils)
 6.600    1         254.07  254.07  -306.60   .000     .000    15.423
 30.100   3         68.32   68.32   -171.97   .000     .000     6.873
cPrincipal Stresses and Strains
Z-Position         Layer   S1       S2       S3       E1       E2       E3
(in)      *        (psi)   (psi)    (psi)    (10^-6)  (10^-6)  (10^-6)
 6.600    1         -16.57  113.42  113.42  -306.60  254.07   254.07
 30.100   3         -2.95   -.03     -.03   -171.97  68.32    68.32

CLayered Elastic Analysis by EverStress for Windows
Title: 8705052
```

```
No of Layers: 3  No of Loads:  1  No of X-Y Evaluation Points:  1
Layer    Poisson's          Thickness          Moduli(1)
*        Ratio     (in)     (ksi)
1         .35       6.500    361.00
2         .35      23.500     27.50
3         .40      *           19.70
Load NoX-Position          Y-Position          Load        Pressure Radius
*          (in)      (in)      (lbf)      (psi)      (in)
 1          .00        .00      9000.0     74.53     6.200
Location No:  1  X-Position (in):     .000      Y-Position (in):     .000
cNormal Stresses
Z-Position          Layer   Sxx        Syy        Szz        Syz        Sxz        Sxy
(in)       *        (psi)      (psi)      (psi)      (psi)      (psi)      (psi)
  6.500   1          104.46    104.46    -18.73       .00        .00        .00
 30.000   2             .95        .95     -2.89       .00        .00        .00
cNormal Strains and Deflections
Z-Position          Layer   Exx        Eyy        Ezz        Ux         Uy         Uz
(in)       *        (10^-6)  (10^-6)  (10^-6)  (mils)     (mils)     (mils)
  6.500   1          206.25    206.25   -254.45      .000       .000     12.410
 30.000   2           59.19     59.19   -129.15      .000       .000      5.803
Line
cPrincipal Stresses and Strains
Z-Position          Layer   S1         S2         S3         E1         E2         E3
(in)       *        (psi)      (psi)      (psi)      (10^-6)  (10^-6)  (10^-6)
  6.500   1          -18.73    104.46    104.46   -254.45    206.25    206.25
 30.000   2           -2.89        .95        .95   -129.15     59.19     59.19

CLayered Elastic Analysis by EverStress for Windows
Title:  8705053
No of Layers: 3  No of Loads:  1  No of X-Y Evaluation Points:  1
Layer    Poisson's          Thickness          Moduli(1)
*        Ratio     (in)     (ksi)
1         .35       7.800    467.00
2         .35      23.500     27.20
3         .40      *           19.40
```

```
Load NoX-Position        Y-Position        Load      Pressure Radius
*          (in)      (in)      (lbf)      (psi)      (in)
1            .00      .00      9000.0    74.53    6.200
Location No:  1  X-Position (in):    .000    Y-Position (in):    .000
cNormal Stresses
Z-Position          Layer    Sxx       Syy       Szz       Syz       Sxz       Sxy
(in)       *        (psi)    (psi)     (psi)     (psi)     (psi)     (psi)
  7.800  1            96.94    96.94    -12.45      .00       .00       .00
 31.300  2              .75      .75     -2.35      .00       .00       .00
cNormal Strains and Deflections
Z-Position          Layer    Exx       Eyy       Ezz       Ux        Uy        Uz
(in)       *        (10^-6)  (10^-6)   (10^-6)   (mils)    (mils)    (mils)
  7.800  1           144.26   144.26   -171.97     .000      .000    10.177
 31.300  2            48.16    48.16   -105.74     .000      .000     5.351
cPrincipal Stresses and Strains
Z-Position          Layer    S1        S2        S3        E1        E2        E3
(in)       *        (psi)    (psi)     (psi)     (10^-6)   (10^-6)   (10^-6)
  7.800  1           -12.45    96.94     96.94   -171.97    144.26    144.26
 31.300  2            -2.35      .75       .75   -105.74     48.16     48.16

CLayered Elastic Analysis by EverStress for Windows
Title:  8705054
No of Layers:  3   No of Loads:   1   No of X-Y Evaluation Points:   1
Layer    Poisson's          Thickness        Moduli(1)
*        Ratio      (in)     (ksi)
1         .35        6.200    160.00
2         .35       23.500     19.60
3         .40       *          12.80
Load NoX-Position        Y-Position        Load      Pressure Radius
*          (in)      (in)      (lbf)      (psi)      (in)
 1           .00      .00      9000.0    74.53    6.200
Location No:  1  X-Position (in):    .000    Y-Position (in):    .000
cNormal Stresses
Z-Position          Layer    Sxx       Syy       Szz       Syz       Sxz       Sxy
```

```
(in)      *        (psi)    (psi)    (psi)    (psi)    (psi)    (psi)

 6.200  1           82.26    82.26   -24.93     .00      .00      .00
29.700  3             .05      .05    -3.12     .00      .00      .00
cNormal Strains and Deflections
Z-Position         Layer    Exx      Eyy      Ezz      Ux       Uy       Uz
(in)      *        (10^-6)  (10^-6)  (10^-6)  (mils)   (mils)   (mils)
  6.200 1           388.73   388.73  -515.72   .000     .000    20.731
 29.700 3           100.13   100.13  -247.39   .000     .000     9.221
cPrincipal Stresses and Strains
Z-Position         Layer    S1       S2       S3       E1       E2       E3
(in)      *        (psi)    (psi)    (psi)    (10^-6)  (10^-6)  (10^-6)
  6.200 1          -24.93    82.26    82.26   -515.72  388.73   388.73
 29.700 3           -3.12      .05      .05   -247.39  100.13   100.13
```

Sample of ELSYM5 program outputs

```
ELASTIC SYSTEM - 8705051
      ELASTIC   POISSONS
LAYER    MODULUS  RATIO    THICKNESS
  1     313040.   .350      6.600 IN
  2      19420.   .350     23.500 IN
  3      16980.   .400   SEMI-INFINITE
   ONE LOAD(S), EACH LOAD AS FOLLOWS
 TOTAL LOAD.....  9000.00 LBS
LOAD STRESS....    74.53 PSI
LOAD RADIUS....     6.20 IN
     LOCATED AT
LOAD    X       Y
  1   .000    .000
 RESULTS REQUESTED FOR SYSTEM LOCATION(S)
 DEPTH(S)
 Z=  6.60  30.10
 X-Y POINT(S)
  X      Y
 .00    .00

 Z=  6.60 LAYER NO, 1
 X       Y
 .00    .00

NORMAL STRESSES
SXX   .1133E+03
SYY   .1133E+03
SZZ  -.1658E+02
 SHEAR STRESSES
SXY   .0000E+00
SXZ   .0000E+00
SYZ   .0000E+00
 PRINCIPAL STRESSES
PS 1  .1133E+03
PS 2  .1133E+03
PS 3  -.1658E+02
 PRINCIPAL SHEAR STRESSES
PSS 1  .6496E+02
PSS 2  .0000E+00
PSS 3  .6496E+02
 DISPLACEMENTS
UX    .0000E+00
UY    .0000E+00
UZ    .1542E-01
 NORMAL STRAINS
EXX   .2539E-03
EYY   .2539E-03
EZZ  -.3064E-03
 SHEAR STRAINS
EXY   .0000E+00
EXZ   .0000E+00
EYZ   .0000E+00
 PRINCIPAL STRAINS
```

P

```
PE 1  .2539E-03
PE 2  .2539E-03
PE 3  -.3064E-03
 PRINCIPAL SHEAR STRAINS
PSE 1  .5603E-03
PSE 2  .0000E+00
PSE 3  .5603E-03
 Z=  30.10 LAYER NO,  2
  X        Y
  .00     .00
   NORMAL STRESSES
SXX    .4535E+00
SYY    .4535E+00
SZZ  -.2942E+01
 SHEAR STRESSES
SXY    .0000E+00
SXZ    .0000E+00
SYZ    .0000E+00
 PRINCIPAL STRESSES
PS 1   .4535E+00
PS 2   .4535E+00
PS 3  -.2942E+01
 PRINCIPAL SHEAR STRESSES
PSS 1  .1698E+01
PSS 2  .0000E+00
PSS 3  .1698E+01
 DISPLACEMENTS
UX     .0000E+00
UY     .0000E+00
UZ     .6878E-02
 NORMAL STRAINS
EXX    .6820E-04
EYY    .6820E-04
EZZ  -.1678E-03
SHEAR STRAINS
```

```
EXY   .0000E+00
EXZ   .0000E+00
EYZ   .0000E+00
 PRINCIPAL STRAINS
PE 1  .6820E-04
PE 2  .6820E-04
PE 3  -.1678E-03
 PRINCIPAL SHEAR STRAINS
PSE 1  .2360E-03
PSE 2  .0000E+00
PSE 3  .2360E-03
```

ELASTIC SYSTEM - 8705054

```
        ELASTIC   POISSONS
LAYER    MODULUS   RATIO     THICKNESS
  1      160430.    .350       6.200 IN
  2       19570.    .350      23.500 IN
  3       12720.    .400    SEMI-INFINITE
  ONE LOAD(S), EACH LOAD AS FOLLOWS
TOTAL LOAD.....   9000.00 LBS
LOAD STRESS....    74.53 PSI
LOAD RADIUS....     6.20 IN
     LOCATED AT
LOAD   X      Y
  1   .000   .000
RESULTS REQUESTED FOR SYSTEM LOCATION(S)
DEPTH(S)
Z=  6.20  29.70
X-Y POINT(S)
  X      Y
  .00      .00
     Z=   6.20 LAYER NO,  1
  X        Y
  .00     .00
```

```
 NORMAL STRESSES
SXX   .8251E+02
SYY   .8251E+02
SZZ  -.2488E+02
 SHEAR STRESSES
SXY   .0000E+00
SXZ   .0000E+00
SYZ   .0000E+00
 PRINCIPAL STRESSES
PS 1  .8251E+02
PS 2  .8251E+02
PS 3 -.2488E+02
 PRINCIPAL SHEAR STRESSES
PSS 1 .5370E+02
PSS 2 .0000E+00
PSS 3 .5370E+02
 DISPLACEMENTS
UX    .0000E+00
UY    .0000E+00
UZ    .2077E-01
 NORMAL STRAINS
EXX   .3886E-03
EYY   .3886E-03
EZZ  -.5151E-03
 SHEAR STRAINS
EXY   .0000E+00
EXZ   .0000E+00
EYZ   .0000E+00
 PRINCIPAL STRAINS
PE 1  .3886E-03
PE 2  .3886E-03
PE 3 -.5151E-03
 PRINCIPAL SHEAR STRAINS
```

```
PSE 1  .9037E-03
PSE 2  .0000E+00
PSE 3  .9037E-03
  Z=  29.70 LAYER NO,  2
  X        Y
   .00     .00
   NORMAL STRESSES
SXX   .1337E+01
SYY   .1337E+01
SZZ  -.3105E+01
 SHEAR STRESSES
SXY   .0000E+00
SXZ   .0000E+00
SYZ   .0000E+00
 PRINCIPAL STRESSES
PS 1  .1337E+01
PS 2  .1337E+01
PS 3 -.3105E+01
 PRINCIPAL SHEAR STRESSES
PSS 1 .2221E+01
PSS 2 .0000E+00
PSS 3 .2221E+01
 DISPLACEMENTS
UX    .0000E+00
UY    .0000E+00
UZ    .9269E-02
 NORMAL STRAINS
EXX   .9994E-04
EYY   .9994E-04
EZZ  -.2065E-03
 SHEAR STRAINS
EXY   .0000E+00
EXZ   .0000E+00
EYZ   .0000E+00
 PRINCIPAL STRAINS
```

```
PE 1  .9994E-04
PE 2  .9994E-04
PE 3  -.2065E-03
 PRINCIPAL SHEAR STRAINS
PSE 1  .3064E-03
PSE 2  .0000E+00
PSE 3  .3064E-03
```

Appendix I: The REPP2000 program

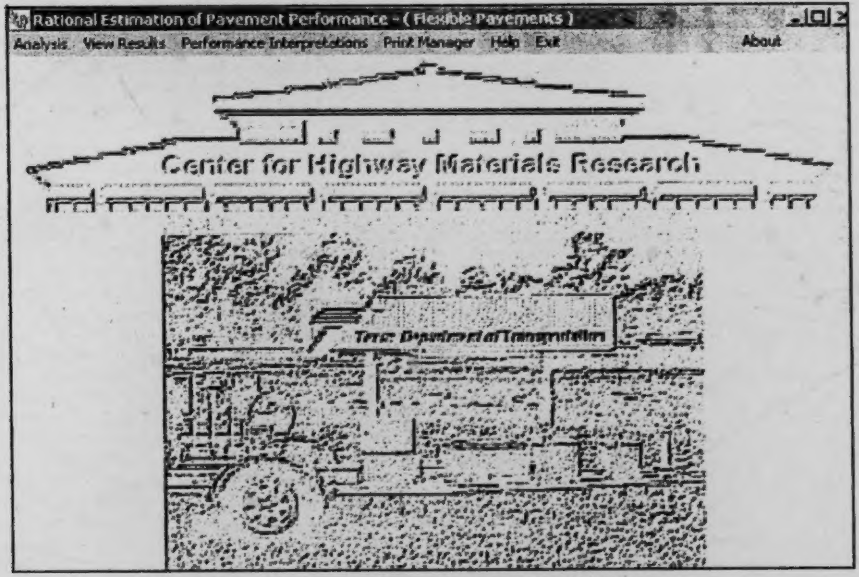
Rational Estimation of Pavement Performance - (Flexible Pavements)
Analysis
View Results
Performance Interpretations
Print Manager
Help
Exit
About
Center for Highway Materials Research
Texas Department of Transportation

Figure I-1: Main window of the REPP2000 program

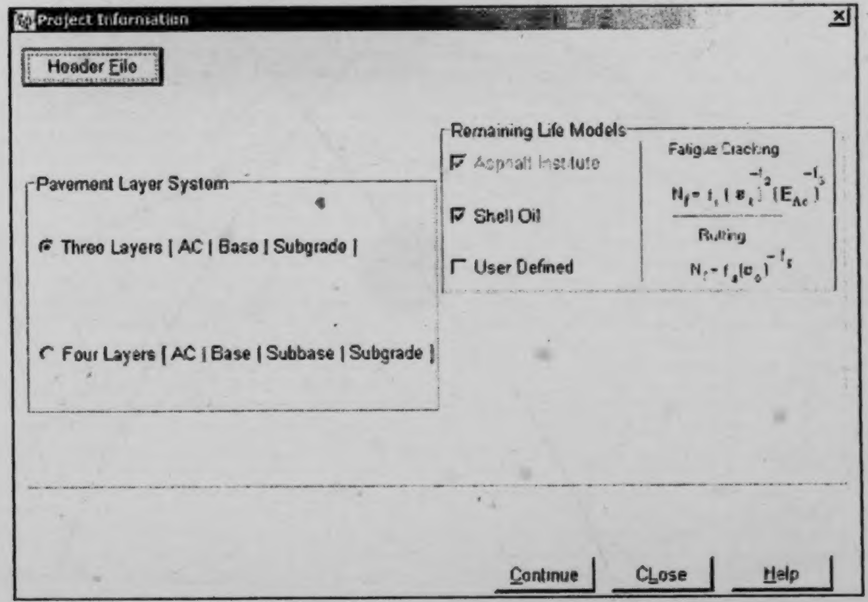
Project Information
Header File
Continue
CLose
Help

Pavement Layer System

● Three Layers | AC | Base | Subgrade |

○ Four Layers | AC | Base | Subbase | Subgrade |

Remaining Life Models

☑ Asphalt Institute

☑ Shell Oil

☐ User Defined

Fatigue Cracking

$N_f = f_1 (\varepsilon_t)^{-f_2} (E_{Ac})^{-f_3}$

Rutting

$N_r = f_4 (\varepsilon_c)^{-f_5}$

Figure I-2: Introducing pavement system to the REPP2000 program

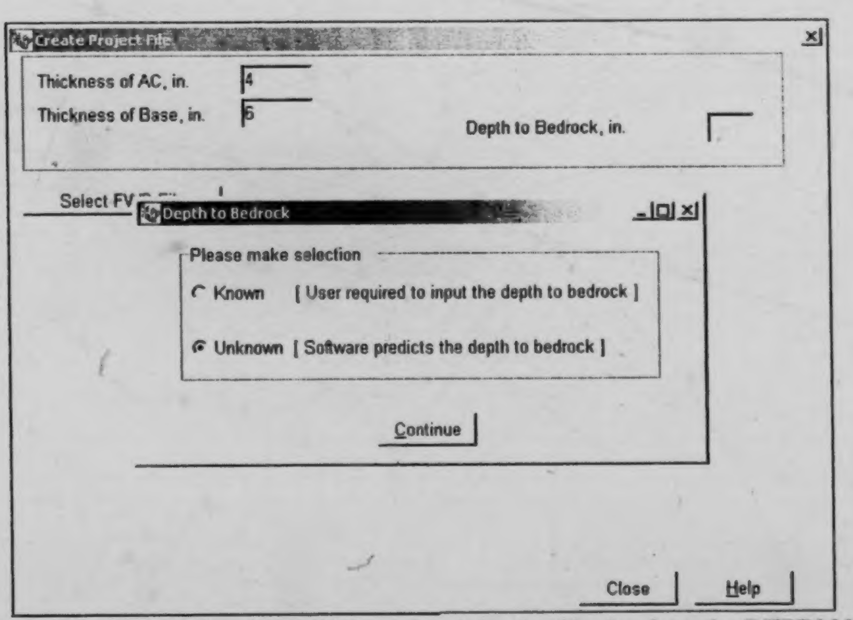
Create Project File
Select FV
Depth to Bedrock
Continue
Close
Help

Thickness of AC, in. 4

Thickness of Base, in. 6

Depth to Bedrock, in.

Please make selection

○ Known [User required to input the depth to bedrock]

● Unknown [Software predicts the depth to bedrock]

Figure I-3: Introducing layer thickness and depth of bedrock to the REPP2000 program

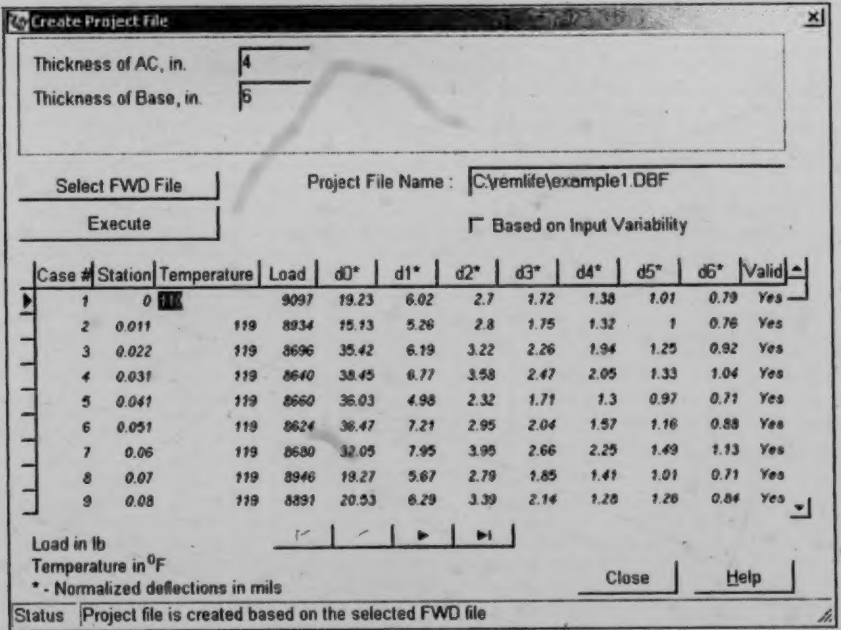
Create Project File
Select FWD File
Execute
Close
Help

Thickness of AC, in. 4

Thickness of Base, in. 6

Project File Name : C:\remlife\example1.DBF

☐ Based on Input Variability

Case #	Station	Temperature	Load	d0*	d1*	d2*	d3*	d4*	d5*	d6*	Valid
1	0	119	9097	19.23	6.02	2.7	1.72	1.38	1.01	0.79	Yes
2	0.011	119	8934	15.13	5.26	2.8	1.75	1.32	1	0.76	Yes
3	0.022	119	8696	35.42	6.19	3.22	2.26	1.94	1.25	0.92	Yes
4	0.031	119	8640	38.45	6.77	3.58	2.47	2.05	1.33	1.04	Yes
5	0.041	119	8660	36.03	4.98	2.32	1.71	1.3	0.97	0.71	Yes
6	0.051	119	8624	36.47	7.21	2.95	2.04	1.57	1.16	0.88	Yes
7	0.06	119	8680	32.05	7.95	3.95	2.66	2.25	1.49	1.13	Yes
8	0.07	119	8946	19.27	5.67	2.79	1.85	1.41	1.01	0.71	Yes
9	0.08	119	8891	20.53	6.29	3.39	2.14	1.28	1.26	0.84	Yes

Load in lb

Temperature in ^{0}F

* - Normalized deflections in mils

Status: Project file is created based on the selected FWD file

Figure I-4: Introducing FWD data to the REPP2000 program

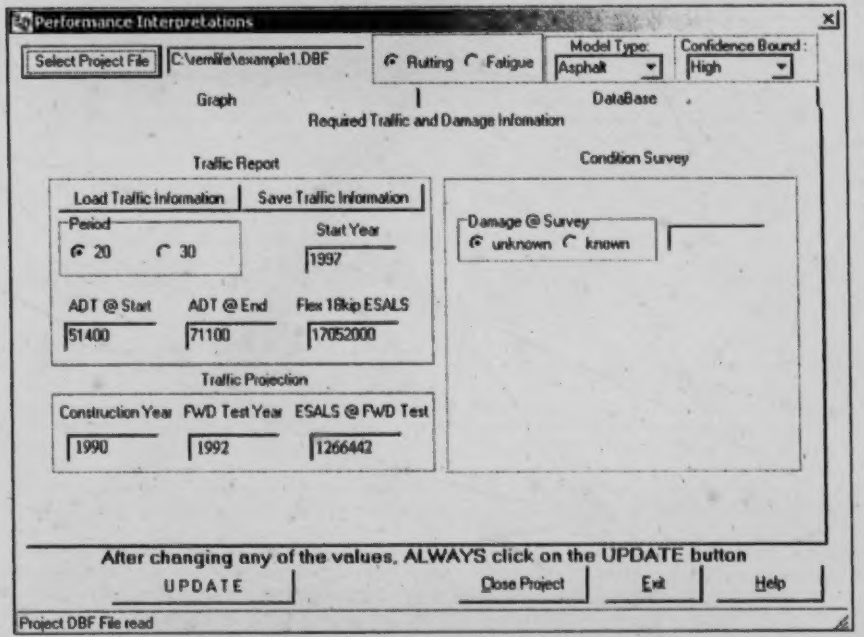
Performance Interpretations
Select Project File
Graph
DataBase
Required Traffic and Damage Infomation
Traffic Report
Condition Survey
Load Traffic Information
Save Traffic Information
UPDATE
Close Project
Exit
Help

C:\remlife\example1.DBF

● Rutting ○ Fatigue

Model Type: Asphalt

Confidence Bound : High

Period: ● 20 ○ 30

Start Year: 1997

ADT @ Start: 51400

ADT @ End: 71100

Flex 18kip ESALS: 17052000

Traffic Projection

Construction Year: 1990

FWD Test Year: 1992

ESALS @ FWD Test: 1266442

Damage @ Survey: ● unknown ○ known

After changing any of the values, ALWAYS click on the UPDATE button

Project DBF File read

Figure I-5: Introducing traffic data to the REPP2000 program

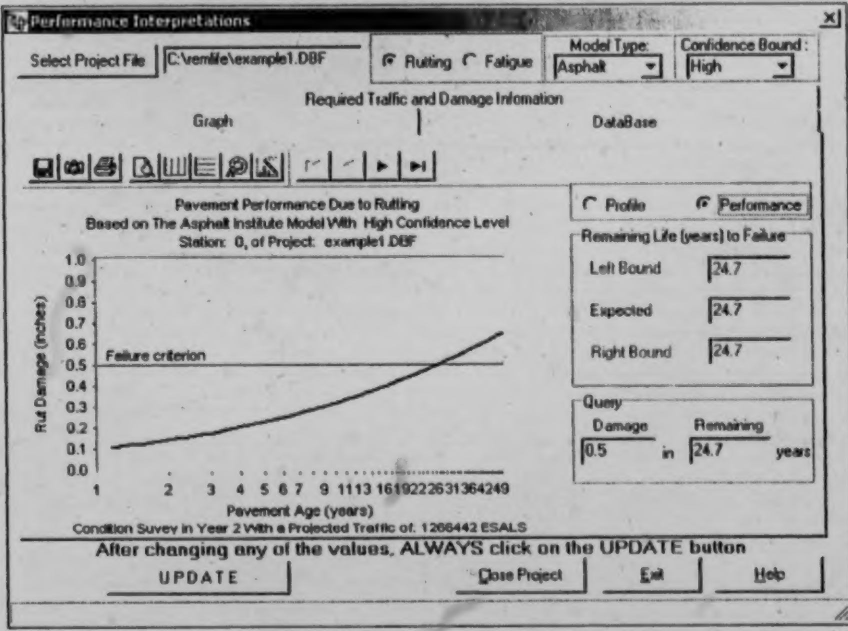
Performance Interpretations
Select Project File
Required Traffic and Damage Infomation
Graph
DataBase
Pavement Performance Due to Rutting
Based on The Asphalt Institute Model With High Confidence Level
Station: 0, of Project: example1.DBF
Rut Damage (inches)
1.0
0.9
0.8
0.7
0.6
0.5
0.4
0.3
0.2
0.1
0.0
Failure criterion
1
2
3
4
5
6
7
9
11
13
16
19
22
26
31
36
42
49
Pavement Age (years)
UPDATE
Close Project
Exit
Help

C:\remlife\example1.DBF

● Rutting ○ Fatigue

Model Type: Asphalt

Confidence Bound : High

○ Profile ● Performance

Remaining Life (years) to Failure

Left Bound: 24.7

Expected: 24.7

Right Bound: 24.7

Query

Damage 0.5 in Remaining 24.7 years

Condition Suvey in Year 2 With a Projected Traffic of: 1266442 ESALS

After changing any of the values, ALWAYS click on the UPDATE button

Figure I-6: Resulted service life and pavement performance curve from the REPP2000 program

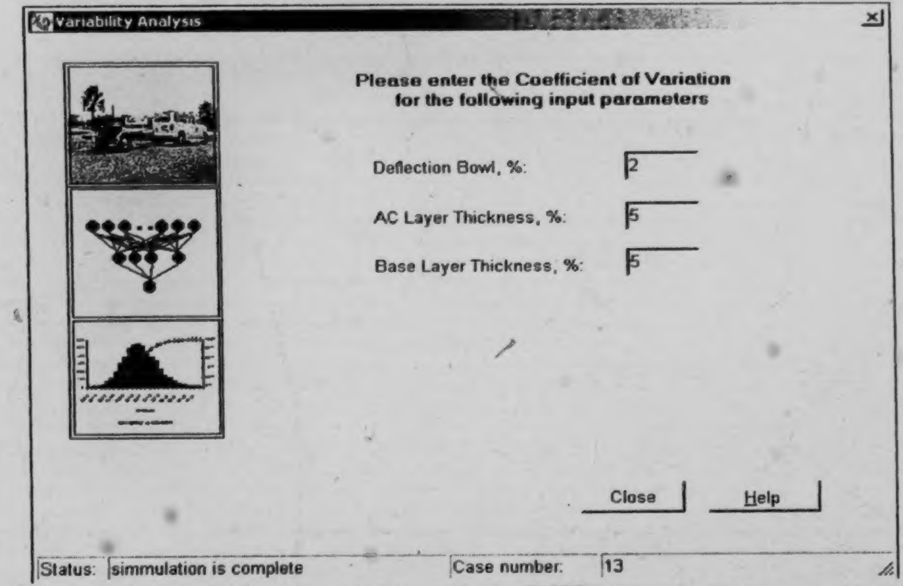
Variability Analysis
Close
Help

Please enter the Coefficient of Variation for the following input parameters

Deflection Bowl, %: 2

AC Layer Thickness, %: 5

Base Layer Thickness, %: 5

Status: simmulation is complete

Case number: 13

Figure I-7: Introducing the variations due to FWD measurements or pavement layer thicknesses to the REPP2000 program

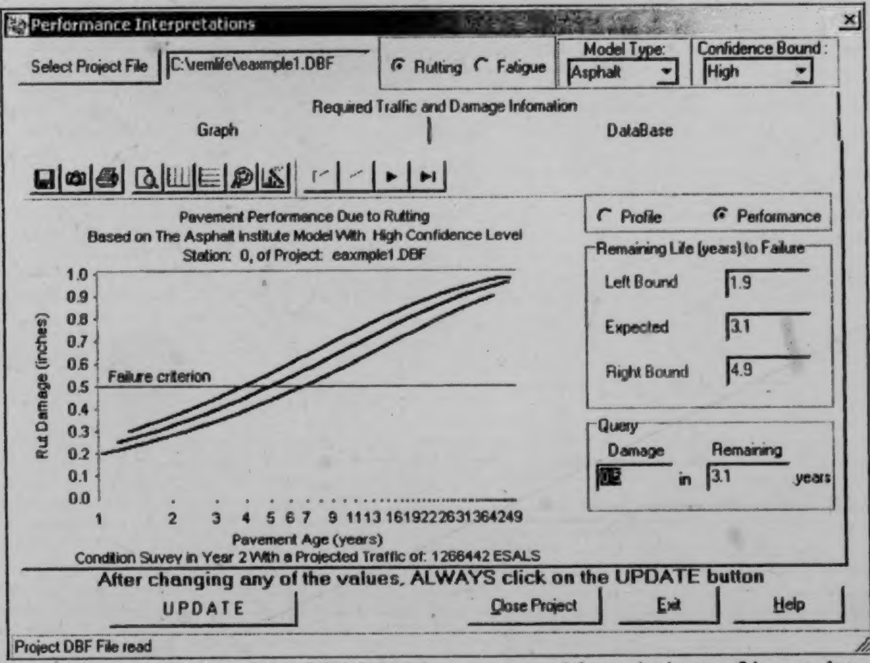
Performance Interpretations
Select Project File
Required Traffic and Damage Infomation
Graph
DataBase
Pavement Performance Due to Rutting
Based on The Asphalt Institute Model With High Confidence Level
Station: 0, of Project: eaxmple1.DBF
Rut Damage (inches)
1.0
0.9
0.8
0.7
0.6
0.5
0.4
0.3
0.2
0.1
0.0
Failure criterion
1
2
3
4
5
6
7
9
11
13
16
19
22
26
31
36
42
49
Pavement Age (years)
Condition Suvey in Year 2 With a Projected Traffic of: 1266442 ESALS
UPDATE
Close Project
Exit
Help

Project file: C:\remlife\eaxmple1.DBF

● Rutting ○ Fatigue

Model Type: Asphalt

Confidence Bound: High

○ Profile ● Performance

Remaining Life (years) to Failure

Left Bound: 1.9

Expected: 3.1

Right Bound: 4.9

Query

Damage [illegible] in Remaining 3.1 years

After changing any of the values, ALWAYS click on the UPDATE button

Project DBF File read

Figure I-8: Results of the REPP2000 program with variations of input data

Appendix J: The NEUROSHELL2 program

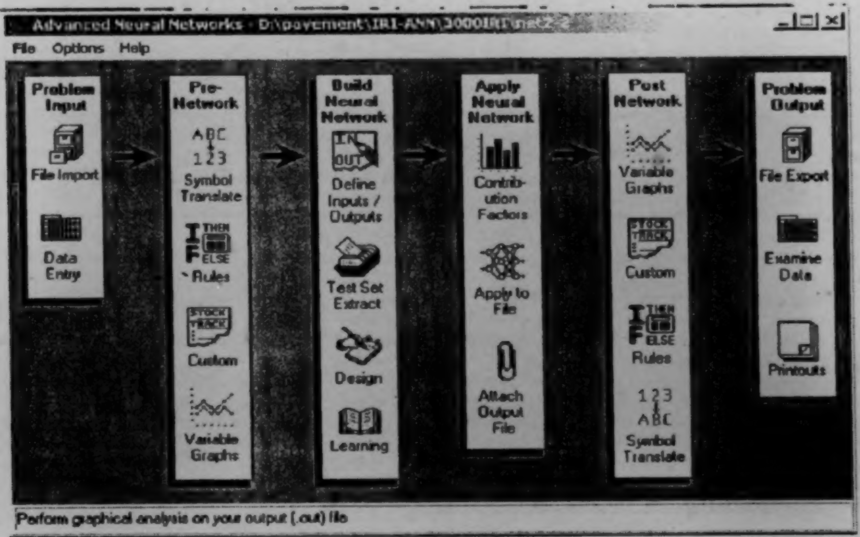
Advanced Neural Networks - D:\pavement\IRI-ANN\30001RI\net2
File Options Help
Problem Input
File Import
Data Entry
Pre-Network
Symbol Translate
Rules
Custom
Variable Graphs
Build Neural Network
Define Inputs / Outputs
Test Set Extract
Design
Learning
Apply Neural Network
Contribution Factors
Apply to File
Attach Output File
Post Network
Variable Graphs
Custom
Rules
Symbol Translate
Problem Output
File Export
Examine Data
Printouts

Perform graphical analysis on your output (.out) file

Figure J-1: The main module in NEUROSHELL2, which supports different stages for developing the neural network

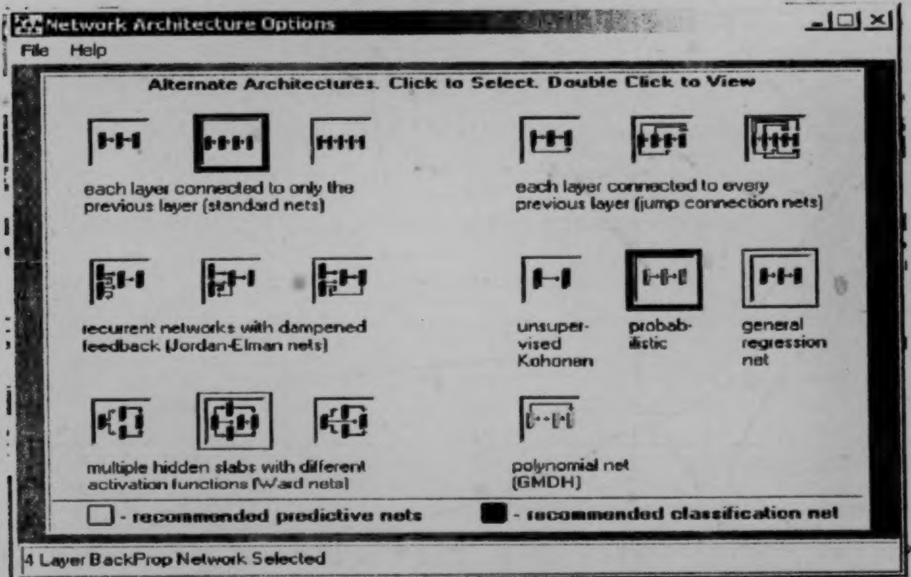
Network Architecture Options
File Help
Alternate Architectures. Click to Select. Double Click to View
each layer connected to only the previous layer (standard nets)
each layer connected to every previous layer (jump connection nets)
recurrent networks with dampened feedback (Jordan-Elman nets)
unsupervised Kohonen
probabilistic
general regression net
multiple hidden slabs with different activation functions (Ward nets)
polynomial net (GMDH)
☐ - recommended predictive nets
■ - recommended classification net

4 Layer BackProp Network Selected

Figure J-2: Different architectures for neural network, which can be employed in NEUROSHELL2 program

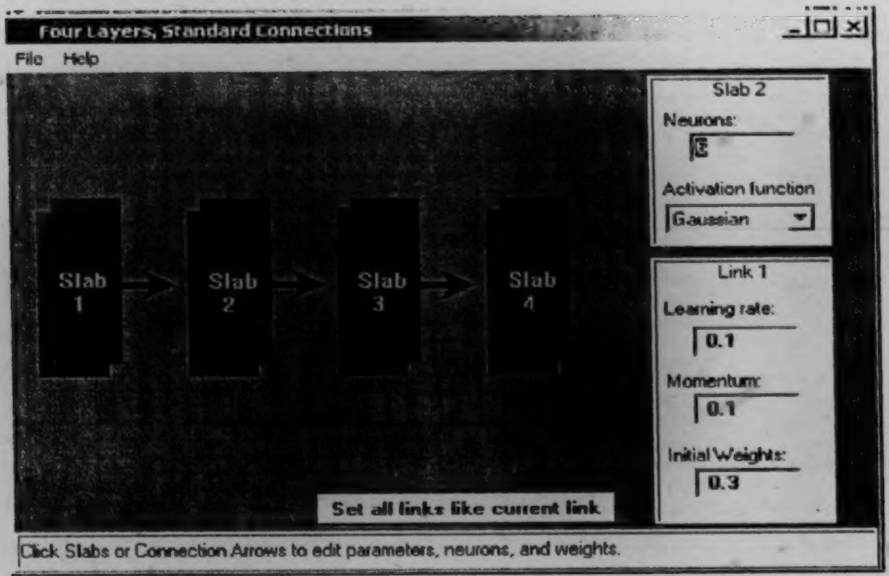
Four Layers, Standard Connections
File
Help
Slab 1
Slab 2
Slab 3
Slab 4
Set all links like current link

Slab 2

Neurons: 3

Activation function: Gaussian

Link 1

Learning rate: 0.1

Momentum: 0.1

Initial Weights: 0.3

Click Slabs or Connection Arrows to edit parameters, neurons, and weights.

Figure J-3: The input module for nodes and the required activation functions in NEUROSHELL2 program

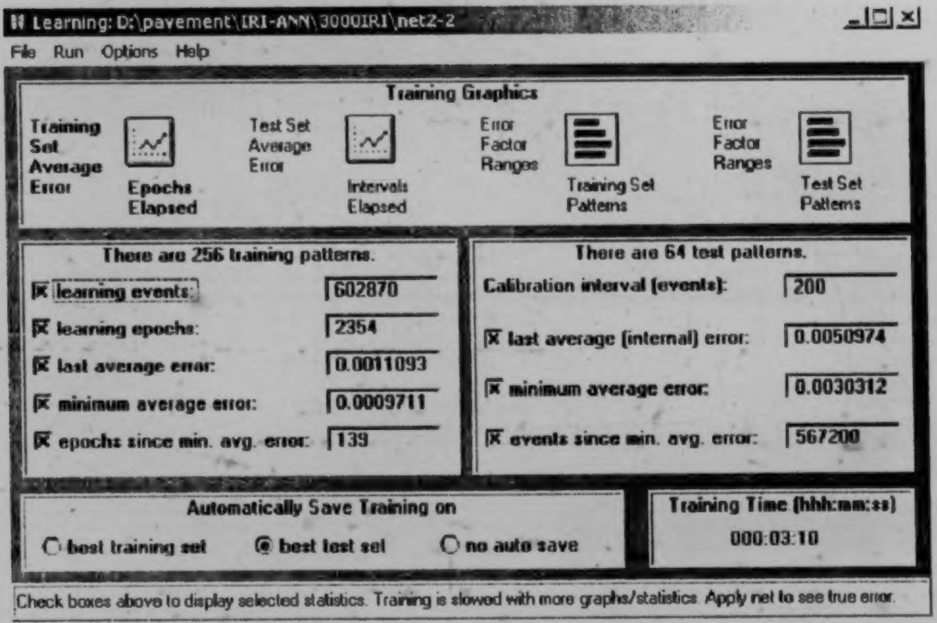
Learning: D:\pavement\IRI-ANN\3000IRI\net2-2
File
Run
Options
Help
Training Graphics
Training Set Average Error
Epochs Elapsed
Test Set Average Error
Intervals Elapsed
Error Factor Ranges
Training Set Patterns
Error Factor Ranges
Test Set Patterns

There are 256 training patterns.

☒ learning events: 602870

☒ learning epochs: 2354

☒ last average error: 0.0011093

☒ minimum average error: 0.0009711

☒ epochs since min. avg. error: 139

There are 64 test patterns.

Calibration interval (events): 200

☒ last average (internal) error: 0.0050974

☒ minimum average error: 0.0030312

☒ events since min. avg. error: 567200

Automatically Save Training on

○ best training set ● best test set ○ no auto save

Training Time (hhh:mm:ss) 000:03:10

Check boxes above to display selected statistics. Training is slowed with more graphs/statistics. Apply net to see true error.

Figure J-4: Learning window in NEUROSHELL2 program, which presents the required information about the training features and some other supportive graphs

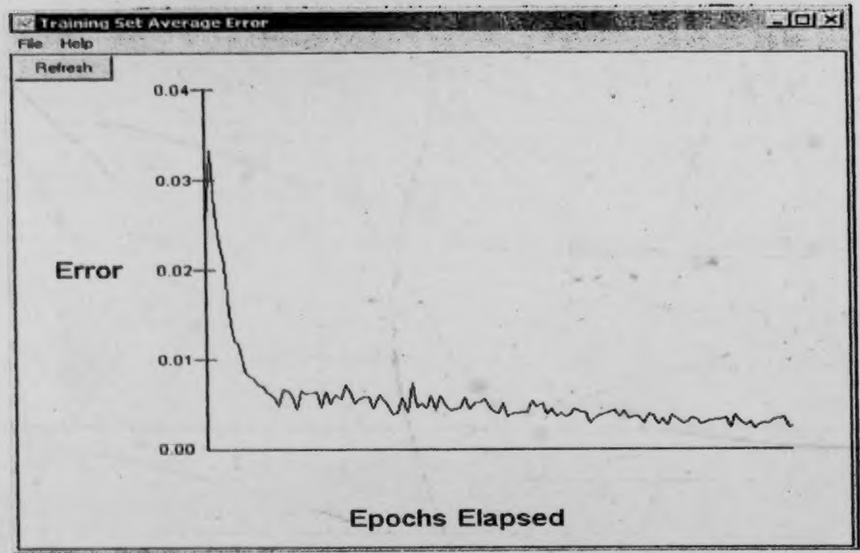

Figure J-5: Graph of reduction of error, provided by NEUROSHELL2 program during training

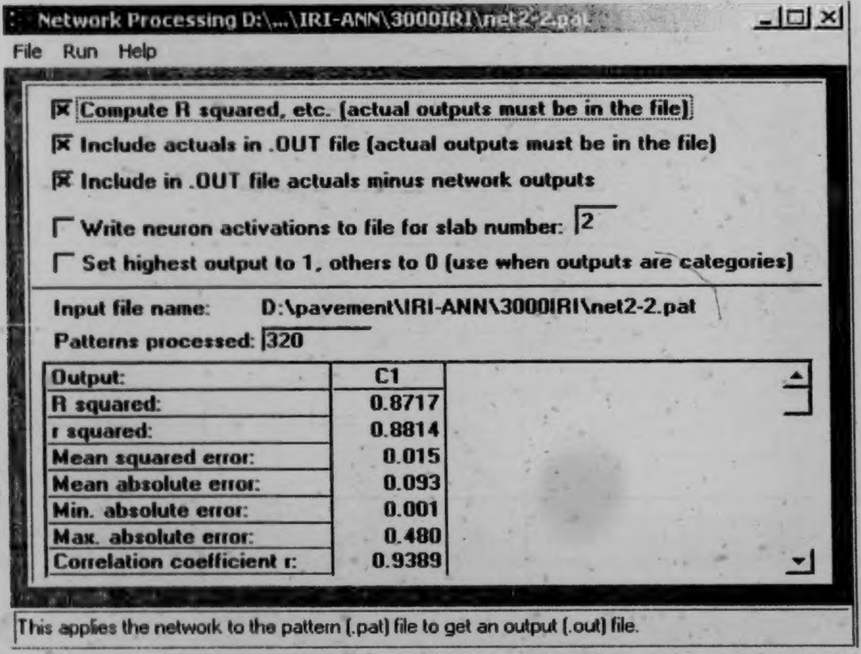

☒ Compute R squared, etc. (actual outputs must be in the file)

☒ Include actuals in .OUT file (actual outputs must be in the file)

☒ Include in .OUT file actuals minus network outputs

☐ Write neuron activations to file for slab number: 2

☐ Set highest output to 1, others to 0 (use when outputs are categories)

Input file name: D:\pavement\IRI-ANN\3000IRI\net2-2.pat

Patterns processed: 320

Output:	C1
R squared:	0.8717
r squared:	0.8814
Mean squared error:	0.015
Mean absolute error:	0.093
Min. absolute error:	0.001
Max. absolute error:	0.480
Correlation coefficient r:	0.9389

This applies the network to the pattern (.pat) file to get an output (.out) file.

Figure J-6: Final features presented by NEUROSHELL2 program after training the network including statistic R-Square